

Investigating the role of cell wall- anchored proteins during *Staphylococcus aureus* skin infection and as vaccine antigens

Keenan Lacey

B.A. (Mod) Microbiology



A thesis submitted to

Trinity College Dublin

For the degree of

Doctor of Philosophy

**Supervisor: Dr. Rachel M. McLoughlin
Host Pathogen Interactions Group
School of Biochemistry and Immunology**

**Co-supervisor: Dr. Joan A. Geoghegan
Staphylococcus Pathogenesis Group
Department of Microbiology**

February 2018

Declaration of Authorship

I declare that this thesis has not been submitted as an exercise for a degree at this or any other university and it is entirely my own work.

I agree to deposit this thesis in the University's open access institutional repository or allow the library to do so on my behalf, subject to Irish Copyright Legislation and Trinity College Library conditions of use and acknowledgement.


Keenan Lacey

Table of contents

Acknowledgements	VIII
Publications	IX
Abbreviations	X
List of figures	XIV
Abstract	XIX
1. Introduction	1
1.1 Staphylococcus aureus	2
1.2 <i>S. aureus</i> skin infection	3
1.2.1 Epidemiology	3
1.2.2 Pathology.....	4
1.3. <i>S. aureus</i> virulence factors involved in the pathogenesis of SSTIs.....	6
1.3.1 Membrane damaging toxins	6
1.3.2. Cell wall-anchored proteins	8
1.3.2.1 Clumping Factor A	13
1.3.2.2 Clumping Factor B	16
1.3.2.3 Protein A.....	17
1.4 Immune response to infection	20
1.4.2 Protective immune responses against bacterial infection.....	20
1.4.2.1 The role of antibodies in <i>S. aureus</i> infection	25
1.4.2.2 The role of neutrophils in <i>S. aureus</i> infection	25
1.4.2.3 The role of macrophages in <i>S. aureus</i> infection	27
1.4.2.4 The role of T helper 1 (Th1) cells during <i>S. aureus</i> infection.....	28
1.4.2.5 The role of T helper (Th) 17 cells during <i>S. aureus</i> infection.....	29
1.4.2.6 The role of T helper (Th) 22 cells during <i>S. aureus</i> infection.....	31
1.4.2.7 The role of $\gamma\delta^+$ T cells in <i>S. aureus</i> infection	31
1.4.2.8 The role of CD8 ⁺ T cells in <i>S. aureus</i> infection	32
1.5 Vaccines	33
1.5.1 Anti-bacterial vaccines.....	33
1.5.2 Anti- <i>S. aureus</i> vaccines	34
1.5.3 Requirements for an effective anti- <i>S. aureus</i> vaccine	36
1.7. Skin.....	39
1.6.1. Skin structure.....	39
1.6.2 Skin Immune Response	42
1.8 Project Aims	45
2. Materials and Methods	47
2.1 <i>S. aureus</i> mutant strain construction	48
2.1.1 Bacterial strains and growth conditions	48
2.1.2 DNA Manipulation.....	48
2.1.2.1 Preparation of plasmid and genomic DNA	48
2.1.2.2 Polymerase Chain Reaction	48
2.1.2.3 Sequence and ligase-independent cloning.....	49
2.1.3 Transformation of <i>S. aureus</i> and <i>E. coli</i> strains.....	49

2.1.3.1	Preparation and electroporation of <i>E. coli</i> SA08B and IM08B	49
2.1.3.2	Preparation and electroporation of <i>S. aureus</i>	50
2.1.4	<i>S. aureus</i> strain construction	50
2.1.4.1	<i>S. aureus</i> strain construction by allelic exchange mutagenesis	50
2.1.4.2	<i>S. aureus</i> strain construction using phage transduction	51
2.2	Validation of <i>S. aureus</i> mutant strains	52
2.2.1	Isolation of <i>S. aureus</i> cell-wall associated and secreted proteins for immunoblotting	52
2.2.2	Western immunoblotting	52
2.2.3	Adherence of <i>S. aureus</i> to immobilised ligands	53
2.2.4	<i>S. aureus</i> growth curve assay	53
2.2.4	Haemolytic activity of <i>S. aureus</i>	53
2.3	Protein purification	54
2.3.1	Purification of histidine-tagged recombinant proteins	54
2.3.2	Purification of GST-tagged recombinant proteins	54
2.3.3	Endotoxin removal from recombinant proteins	55
2.4	<i>In vitro</i> human T cell assay	56
2.4.1	Heat-inactivation of <i>S. aureus</i>	56
2.4.2	Isolation and stimulation of human T cells	56
2.5	<i>In vivo S. aureus</i> infection models	58
2.5.1	Mice	58
2.5.2	<i>In vivo</i> bioluminescent subcutaneous abscess model	58
2.5.2.1	Isolation of cells from murine skin	59
2.5.2	<i>In vivo S. aureus</i> peritonitis model	59
2.6	<i>In vivo</i> vaccination models	60
2.6.1	Subcutaneous vaccination with subdomains of ClfA combined with CpG for protection against systemic <i>S. aureus</i> infection	60
2.6.2	Subcutaneous vaccination with ClfA and ClfB combined with CpG or alum for protection against <i>S. aureus</i> SSTI	62
2.6.3	Measuring the cellular immune response to immunisation	64
2.6.4	Measuring the humoral immune response to immunisation	64
2.6.4.1	Antibody end point titre assay	64
2.6.4.2	Neutralising antibody assay	67
2.7	Histology	68
2.7.1	Tissue Preparation	68
2.7.2	Immunohistochemistry	68
2.7.3	Haematoxylin and eosin staining	68
2.7.4	Histological scoring	69
2.8	ELISA	71
2.9	Intracellular cytokine staining and flow cytometry	72
2.10	Statistical analysis	73
3.	Strain Construction	78
3.1	Introduction	79
3.2	Results	83
3.2.1	Validation of a <i>srtA</i> mutation in <i>S. aureus</i> LAC:: <i>lux</i>	83
3.2.2	Validation of a <i>hla</i> mutation in <i>S. aureus</i> LAC:: <i>lux</i>	86
3.2.3	Construction of <i>clfA</i> , <i>clfB</i> and <i>spa</i> null mutations in <i>S. aureus</i> LAC:: <i>lux</i>	88

3.2.4 Validation of <i>S. aureus</i> LAC:: <i>lux clfA</i>	91
3.2.5 Validation of <i>S. aureus</i> LAC:: <i>lux clfB</i>	93
3.2.5 Validation of <i>S. aureus</i> LAC:: <i>lux spa</i>	95
3.3 Discussion	97
4. Investigating cell wall-anchored proteins as T cell antigens	100
4.1 Introduction	101
4.2. Results	103
4.2.1 Human CD4 ⁺ T cells proliferate in response to heat-inactivated <i>S. aureus</i> LAC:: <i>lux</i>	103
4.2.2 Human CD4 ⁺ T cells proliferate in response to purified staphylococcal CWA proteins	111
4.2.3 Subdomains of ClfA drive antigen-specific responses in human CD4 ⁺ T cells	115
4.2.4 Immunisation of mice with individual subdomains of ClfA induces Th1 and Th17 cellular immune responses	121
4.2.5 Immunisation with individual subdomains of ClfA induces humoral immune responses	124
4.2.6 Immunisation with individual subdomains of ClfA protects against <i>S. aureus</i> systemic infection	126
4.2.7 Enhanced bacterial clearance mediated by vaccination with subdomains of ClfA is associated with increased T cell responses at site of infection	129
4.2.8 Immunisation with subdomains of ClfA enhances phagocyte activation during <i>S. aureus</i> infection	133
4.3 Discussion	136
5. Investigating the role of CWA proteins during <i>S. aureus</i> skin infection	141
5.1 Introduction	142
5.2 Results	144
5.2.1 Establishment of <i>in vivo</i> bioluminescent subcutaneous abscess model	144
5.2.2 Characterising the local cellular immune response during <i>S. aureus</i> subcutaneous abscess infection	149
5.2.3 LAC:: <i>lux srtA</i> infected mice develop smaller abscess lesions and have reduced bacterial burden than mice infected with LAC:: <i>lux</i> WT	154
5.2.4 The abscesses from LAC:: <i>lux srtA</i> infected mice are smaller and less developed than LAC:: <i>lux</i> WT infected mice	161
5.2.5 Abscesses from LAC:: <i>lux srtA</i> infected mice contain fewer neutrophils than LAC:: <i>lux</i> WT infected mice.	168
5.2.6 Mice infected with LAC:: <i>lux</i> CWA protein mutants develop smaller abscess lesions and have reduced bacterial burden	171
5.2.7 The rate of abscess formation differs between LAC:: <i>lux</i> CWA protein mutants compared to LAC:: <i>lux</i> WT infected mice in the first 72 hours post-infection	178
5.2.8 Abscesses from LAC:: <i>lux clfA</i> , <i>clfB</i> and <i>spa</i> -infected mice are less developed and the rate of abscess development is slower compared to LAC:: <i>lux</i> WT infected mice	180
5.2.9 The ClfB ligand loricrin is expressed within the skin abscess tissue in LAC:: <i>lux</i> WT infected mice.	185

5.2.10 The ClfB-licrin interaction is important for virulence during <i>S. aureus</i> SSTIs.....	187
5.2.11 Model vaccines comprising ClfB and ClfA induces antigen-specific humoral responses	191
5.2.12 Model vaccines comprising ClfB and ClfA induces antigen-specific cellular responses.....	193
5.2.13 Model vaccines comprising ClfB and ClfA protect against subsequent <i>S. aureus</i> skin infection.....	196
5.3 Discussion	203
6. General Discussion	210
7. References	220

Acknowledgements

Firstly, I would like to thank my incredible supervisor Rachel McLoughlin. Your encouragement and support has been amazing and your passion and enthusiasm for science is truly inspirational. I couldn't have asked for a better mentor!

I would also like to sincerely thank my co-supervisor Joan Geoghegan for all her guidance and support. Thank you for always having the time to help and always having a solution! Also, a special thanks to Prof. Tim Foster, was it not for him I don't think I would have ever ended up doing this PhD.

To all the McLoughlin Lab – thank you for everything, you have all made my time in the lab truly enjoyable! Michelle, thanks for all your help and always being so nice, it's been great to have a fellow microbiologist in the lab! Stephen, I really appreciate all your advice and support, from answering questions to helping plan experiments. John, thanks for all the help with experiments, all the chats and for becoming a great friend! All the other past and present members, you've all helped me at some stage and made the lab a great place to work. Thank you, Aisling, Kate, Vivienne, Tracey, Roisin, Jenny, Andrew and Alanna.

A big thank you also to all past and present members of the Geoghegan lab; Dara, Orla, Joana, Leanne, Aisling and Marta. You have all been a great help and always made me feel very welcome in the lab. Also, a special thanks to Deirdre and all the other staff in the Moyne.

Thank you to all the members of the Dunne and Stevenson Labs for all your help, advice and most importantly the entertainment! I would also like to thank Barry for his help with FACS. A special thanks to Emma for all those chats and cycles! A super special thanks to Orla and Olwyn for all the support and fun over the last few years and most importantly for the friendship!

I would also like to sincerely thank my friend, Mark, who has always been there for me.

Finally, thank you to my family for everything. Thanks Rowan for your support over the past few years. To my wonderful parents, Des and Mary, thank you for your unconditional encouragement, love and for always believing in me.

Publications

Memory Th1 cells are protective in invasive *Staphylococcus aureus* infection.

Brown AF, Murphy AG, Lalor SJ, Leech JM, O'Keeffe KM, MacAogáin M, O'Halloran DP, **Lacey KA**, Tavakol M, Hearnden CH, Fitzgerald-Hughes D, Humphreys H, Fennell JP, van Wammel WT, Foster TJ, Geoghegan JA, Lavelle EC, Rogers TR, McLoughlin RM
PloS Pathogens. 2015 Nov 5; 11(11):e1005226. doi:10.1371/journal.ppat. 1005226. eCollection 2015

The role of *Staphylococcus aureus* virulence factors in skin infection and their potential as vaccine antigens.

Lacey KA, Geoghegan JA, McLoughlin RM.
Pathogens. 2016 Feb 17; 5(1):22. doi: 10.3390/pathogens5010022.

Interleukin-10 plays opposing roles during *Staphylococcus aureus* systemic and localized infections.

Leech JM, **Lacey KA**, Mulcahy ME, Medina E, McLoughlin RM.
Journal of Immunology. 2017 Mar 15;198(6):2352-2365. doi: 10.4049/jimmunol.1601018

The *Staphylococcus aureus* cell wall-anchored protein clumping factor A is an important T cell antigen.

Lacey KA, Leech JM, Lalor JM, McCormack N, Geoghegan JA, McLoughlin RM.
Infection and Immunity. 2017 Dec. 85;12. pii: IAI.00549-17. doi: 10.1128/IAI.00549-17

Abbreviations

ADAM10	A disintegrin and metalloprotease 10
AD-HIES	Autosomal dominant hyper-IgE syndrome
Agr	Accessory gene regulator
AhR	Aryl hydrocarbon receptor
AIP	Autoinducing peptide
AMP	Antimicrobial peptide
Amp	Ampicillin
ANOVA	Analysis of Variance
APC	Antigen presenting cell
ATc	Anhydrotetracycline
BFA	Brefeldin A
C	Celsius
CA	Community acquired
CC	Clonal complex
CFU	Colony forming unit
CGD	Chronic granulomatous disease
CifA	Clumping factor A
CifB	Clumping factor B
Cm	Chloramphenicol
CoNS	Coagulase negative Staphylococci
CP	Capsular polysaccharide
CWA	Cell wall-anchored
CXCL	C-X-C motif ligand
d	Day
DC	Dendritic cell
DNA	Deoxyribonucleic acid
<i>E. coli</i>	<i>Escherichia coli</i>
ELISA	Enzyme-linked immunosorbant assay
Erm	Erythromycin

EfB	Extracellular fibrinogen-binding protein
FACS	Fluorescence-activated cell sorting
Fg	Fibrinogen
FMO	Fluorescence minus one
FnBP	Fibronectin binding protein
g	Gravity
GST	Glutathione S-Transferase
h	Hour
H ₂ O ₂	Hydrogen peroxide
HA	Hospital acquired
Hla	α-toxin (α-haemolysin)
ICAM	Intracellular adhesion molecule
i.p.	Intraperitoneal
IFN _γ	Interferon γ
Ig	Immunoglobulin
IL	Interleukin
ILN	Inguinal lymph node
iNOS	Inducible nitric oxide synthase
IRAK4	IL-1 receptor-associated kinase 4
IsdB	Iron regulated surface determinant
kDa	kilo Daltons
L2v	Loricrin loop 2 region
LPS	Lipopolysaccharide
LTA	Lipoteichoic acid
LukAB	Leukotoxin AB
LukED	Leukotoxin ED
MCS	Multiple Cloning Site
MCP-1	Monocyte chemoattractant protein-1
Mg	milligrams
MHC	Major histocompatibility complex
Min	Minutes

MI	Millilitres
MRSA	Methicillin resistant <i>Staphylococcus aureus</i>
MyD88	Myeloid differentiation primary response gene 88
NADPH	Nicotinamide adenine dinucleotide phosphate
NF- κ B	Nuclear factor- κ B
NK	Natural killer
nm	nanometer
nM	nanoMolar
NO	Nitric oxide
OD	Optical density
PAMP	Pathogen associated molecular pattern
PBP2a	Penicillin binding protein 2a
PBS	Phosphate buffered saline
PCR	Polymerase chain reaction
PFA	Paraformaldehyde
PMA	Phorbol myristate acetate
PMN	Polymorphonuclear neutrophil
PSM	Phenol soluble modulins
PVDF	Polyvinylidene fluoride
PVL	Panton-Valentine leukocidin
RNA	Ribonucleic acid
ROS	Reactive oxygen species
<i>S. aureus</i>	<i>Staphylococcus aureus</i>
s.c.	subcutaneous
SEA	Staphylococcus enterotoxin A
SDS-PAGE	Sodium Dodecyl Sulfate Poly-Acrylamide Gel Electrophoresis
SNP	Single nucleotide polymorphism
SPF	Specific Pathogen Free
SrtA	Sortase A
STAT	Signal transducer and activator of transcription
SSTI	Skin and soft tissue infection

T-bet	T box transcription factor
TCD	Trinity College Dublin
TCR	T cell receptor
TGFβ	Transforming growth factor beta
Th	T helper
TLR	Toll-like Receptor
TNF	Tumour necrosis factor
Treg	T regulatory
Trm	Resident memory T cell
TS	Temperature sensitive
TSA	Tryptic soy broth agar
TSB	Tryptic soy broth
TSST-1	Toxic shock syndrome toxin 1
V	Volts
WT	Wild-type
γδ	Gamma Delta
μg	microgram
μl	microliter

List of figures

Figure 1.1. <i>S. aureus</i> skin abscess structure	5
Figure 1.2. Mechanism of sortase-mediated surface protein anchoring to the cell wall.....	12
Figure 1.3. Staphylococcal surface proteins	15
Figure 1.4. Interaction between antigen presenting cells and T cells.....	23
Figure 1.5. CD4 ⁺ helper T cell differentiation	24
Figure 1.6. Cell differentiation in the epidermis	41
Figure 1.7. The immune responses of the skin	44
Figure 2.1. Subcutaneous vaccination with subdomains of ClfA combined with CpG.....	61
Figure 2.2. Subcutaneous vaccination with ClfA and ClfB combined with CpG or alum.....	63
Figure 2.3. Determining antibody end point titres.....	66
Figure 2.4. Histology Scoring System.....	70
Figure 3.1. Schematic representation of plasmid integration and excision	82
Figure 3.2. Validation of LAC:: <i>lux srtA</i>	85
Figure 3.3. Validation of LAC:: <i>lux hla</i>	87
Figure 3.4. Construction of pIMAY Δ <i>clfA</i>	90
Figure 3.5. Validation of LAC:: <i>lux clfA</i>	92
Figure 3.6. Validation of LAC:: <i>lux clfB</i>	94
Figure 3.7. Validation of LAC:: <i>lux spa</i>	96
Figure 4.1. Proliferation responses to heat-inactivated <i>S. aureus</i> are greatest after 10 days of stimulation.....	105
Figure 4.2. No difference in levels of proliferation of human CD4 ⁺ T cells in response to heat-inactivated <i>S. aureus</i> LAC or LAC:: <i>lux</i>	106
Figure 4.3. Human CD4 ⁺ T cell proliferation is decreased in response to <i>S. aureus</i> LAC:: <i>lux srtA</i> compared to LAC:: <i>lux</i> WT	107
Figure 4.4. Human CD4 ⁺ T cells show greater antigen-specific responses to <i>S. aureus</i> LAC:: <i>lux</i> WT compared to LAC:: <i>lux srtA</i>	109
Figure 4.5. The majority of TNF α production from human CD4 ⁺ T cells is associated with Th1 cells in responses to heat-inactivated <i>S. aureus</i>	110
Figure 4.6. No difference in levels of proliferation of human CD4 ⁺ T cells in response to media or bovine serum albumin.....	112
Figure 4.7. Human CD4 ⁺ T cells proliferate in response to purified staphylococcal cell wall-anchored proteins	113

Figure 4.8. Human CD4 ⁺ T cells have antigen-specific responses to purified staphylococcal cell wall-anchored proteins	114
Figure 4.9. Stability of subdomains of clumping factor A	117
Figure 4.10. 72.9 % of individuals possess CD4 ⁺ T cells which can recognise and proliferate in response to purified ClfA N123.....	118
Figure 4.11. Human CD4 ⁺ T cells proliferate in response to subdomains of ClfA	119
Figure 4.12. Th1 and Th17 cells proliferate in response to subdomains of ClfA	120
Figure 4.13. Immunisation with individual subdomains of ClfA induces ClfA-specific cellular immune responses.....	123
Figure 4.14 Immunisation with individual subdomains of ClfA induces ClfA-specific humoral immune responses	125
Figure 4.15. No difference in the bacterial burden of mice vaccinated with CpG+GST compared to PBS or CpG alone.....	127
Figure 4.16. Immunisation with individual subdomains of ClfA protect against <i>S. aureus</i> infection at 24 and 72 h post-infection.....	128
Figure 4.17. Immunisation with individual subdomains of ClfA with CpG increases CD4 ⁺ recruitment and cytokine production at the site of infection during <i>S. aureus</i> infection	130
Figure 4.18. Immunisation with individual subdomains of ClfA with CpG increases CD8 ⁺ T cell recruitment and cytokine production at the site of infection during <i>S. aureus</i> infection	131
Figure 4.19. Immunisation with individual subdomains of ClfA with CpG had no significant effect on the production IFN γ or IL-17 by $\gamma\delta^+$ T cells during <i>S. aureus</i> infection.....	132
Figure 4.20. Immunisation with individual subdomains of ClfA does not increase phagocyte recruitment to the peritoneal cavity	134
Figure 4.21. Immunisation with individual subdomains of ClfA enhances phagocyte ROS activity during <i>S. aureus</i> infection	135
Figure 5.1. High inoculum of <i>S. aureus</i> LAC:: <i>lux</i> WT leads to increased abscess lesion area during <i>in vivo</i> subcutaneous abscess model.....	146
Figure 5.2. Bioluminescence imaging of <i>S. aureus</i> skin infection model.....	147
Figure 5.3. C57 mice clear <i>S. aureus</i> LAC:: <i>lux</i> WT skin infection quicker than BALB/c mice	148
Figure 5.4. Cell types present within the skin of LAC:: <i>lux</i> WT infected BALB/c mice	150
Figure 5.5. T cells present within the skin of LAC:: <i>lux</i> WT infected BALB/c mice	151

Figure 5.6. Cytokine production from CD4 ⁺ T cells present within the skin of LAC:: <i>lux</i> WT infected mice	152
Figure 5.7. Cytokine production from $\gamma\delta$ ⁺ T cells present within the skin of LAC:: <i>lux</i> WT infected mice	153
Figure 5.8. LAC:: <i>lux srtA</i> infected mice develop smaller lesions than LAC:: <i>lux</i> WT infected mice	156
Figure 5.9. LAC:: <i>lux srtA</i> infected mice have lower bacterial burden compared to LAC:: <i>lux</i> WT infected mice.....	157
Figure 5.10. LAC:: <i>lux srtA</i> infected mice have reduced bacterial burden compared to LAC:: <i>lux</i> WT infected mice	158
Figure 5.11. <i>S. aureus</i> isolated from infected animals remains bioluminescent	159
Figure 5.12. Skin structure of healthy BALB/c mice	163
Figure 5.13. Skin abscess formation differs between LAC:: <i>lux</i> WT and LAC:: <i>lux srtA</i> infected mice	165
Figure 5.14. Skin abscesses from LAC:: <i>lux srtA</i> infected mice are less structurally defined and smaller than LAC:: <i>lux</i> WT infected mice	166
Figure 5.15. Bacteria present in the skin is localised within the skin abscess of LAC:: <i>lux</i> WT infected mice	167
Figure 5.16. Skin abscesses from LAC:: <i>lux srtA</i> infected mice contain fewer neutrophils than LAC:: <i>lux</i> WT infected mice.....	169
Figure 5.17. Fewer neutrophils infiltrate the surrounding tissue in LAC:: <i>lux srtA</i> infected mice compared to LAC:: <i>lux</i> WT infected mice	170
Figure 5.18. Mice infected with LAC:: <i>lux</i> CWA protein mutants develop smaller abscess lesions than LAC:: <i>lux</i> WT infected mice.....	173
Figure 5.19. Mice infected with LAC:: <i>lux</i> CWA protein mutants develop smaller abscess lesions compared to LAC:: <i>lux</i> WT infected mice.....	174
Figure 5.20. Mice infected with LAC:: <i>lux</i> CWA protein mutants have decreased bioluminescence compared to LAC:: <i>lux</i> WT infected mice	175
Figure 5.21. Mice infected with LAC:: <i>lux</i> CWA protein mutants have decreased bioluminescence compared to LAC:: <i>lux</i> WT infected mice	176
Figure 5.22. Mice infected with LAC:: <i>lux</i> CWA protein mutants have decreased bacterial burden in the skin compared to LAC:: <i>lux</i> WT infected mice.....	177
Figure 5.23. The rate of abscess formation differs between LAC:: <i>lux</i> CWA protein mutants compared to LAC:: <i>lux</i> WT infected mice in the first 72 hours post-infection.....	179
Figure 5.24. Time course of <i>S. aureus</i> skin abscess formation.....	182
Figure 5.25. Abscesses formed by LAC:: <i>lux</i> WT are more structurally defined than those of LAC:: <i>lux</i> CWA protein mutants	183

Figure 5.26. Abscesses formed by LAC:: <i>lux</i> CWA protein mutants form smaller abscesses compared to LAC:: <i>lux</i> WT	184
Figure 5.27. Loricrin is present within with the skin abscess tissue of in LAC:: <i>lux</i> WT infected animals.....	186
Figure 5.28. Blocking of the ClfB-loricrin interaction <i>in vivo</i> results in reduced abscess lesion area during subcutaneous abscess model	189
Figure 5.29. Blocking of the ClfB-loricrin interaction <i>in vivo</i> results in reduced bioluminescence during subcutaneous abscess model.....	190
Figure 5.30. Blocking of the ClfB-loricrin interaction <i>in vivo</i> results in reduced bacterial burden during subcutaneous abscess model	188
Figure 5.31. Model vaccines comprising ClfB and ClfA induce antigen-specific humoral immune responses	192
Figure 5.32. Model vaccines comprising ClfB induce humoral immune responses	194
Figure 5.33. Model vaccines comprising ClfA induce humoral immune responses	195
Figure 5.34. Model vaccines comprising ClfB in combination with CpG or alum reduces abscess lesion area.....	197
Figure 5.35. Model vaccines comprising ClfA in combination with CpG or alum reduces abscess lesion area.....	198
Figure 5.36. Model vaccines comprising ClfB in combination with CpG or alum reduces bioluminescence	199
Figure 5.37. Model vaccines comprising ClfB in combination with CpG or alum leads to a reduction in bacterial burden in the skin.....	200
Figure 5.38. Model vaccines comprising ClfA in combination with CpG or alum reduces bioluminescence	201
Figure 5.39. Model vaccines comprising ClfA leads to a reduction in bacterial burden in the skin.....	202
Figure 6.1. <i>S. aureus</i> cell wall-anchored (CWA) proteins are prime vaccine candidates for anti- <i>S. aureus</i> SSTI vaccines	219

List of tables

Table 1.1. Cell wall-anchored proteins of <i>Staphylococcus aureus</i>	10
Table 2.1. Bacterial strains and plasmids	74
Table 2.2. Primer sequences	75
Table 2.3. Antibodies.....	76
Table 2.4. FACS antibodies	77
Table 2.5. Area Scoring.....	77
Table 4.1. The percentage of donors that responded to antigen stimulation..	108
Table 5.1. No discernible dissemination to peripheral organs in <i>S. aureus</i> LAC:: <i>lux</i> subcutaneous abscess model	160

Abstract

Staphylococcus aureus has become increasingly resistant to antibiotics and community acquired methicillin resistant *S. aureus* (CA-MRSA) skin and soft tissue infections (SSTIs) are occurring with increasing frequency in healthy individuals. As skin is the most frequent site of *S. aureus* infection, a vaccine specifically targeted against SSTIs would be of great benefit. However, to date, all vaccine approaches to protect against *S. aureus* infection have failed, likely due to the inefficient induction of cellular immunity. It is now accepted that T cells are essential for promoting a successful immune response against *S. aureus* infection. However, there is a paucity of information regarding T cell antigens of *S. aureus*. *S. aureus* can express a large number of cell wall-anchored (CWA) proteins, which are covalently attached to the cell wall peptidoglycan. The virulence potential of many CWA proteins has been demonstrated in infection models, however, there is a lack of information regarding their roles during SSTIs, and whether they represent attractive T cell antigens remains to be established.

This study demonstrates the ability of *S. aureus* CWA proteins to activate human T cells, specifically, inducing antigen-specific Th1 and Th17 responses. Importantly this study has demonstrated that clumping factor A (ClfA) has the capacity to induce robust T cell responses, and that the full length ClfA N123 protein is required for maximum Th1 and Th17 activation both *in vitro* and *in vivo*. This work also supports the use of CWA proteins as vaccine antigens, as they have the ability to induce both neutralising antibodies but more importantly, are capable of driving a much-needed cellular immune response.

CWA proteins were found to be specifically important in determining abscess formation and structure, which in turn impact upon infection outcomes during subcutaneous skin infection. Most interestingly, a novel role for clumping factor B (ClfB) was discovered during SSTIs. ClfB appears to determine the abscess structure early in infection, which is dependent upon its interaction with the ligand loricrin. Consequently, a model vaccine comprising of ClfB was developed which induced humoral and cellular responses, ultimately leading to protection during subsequent *S. aureus* skin infection.

Overall, this thesis highlights an important role for CWA proteins during SSTIs, and highlights their ability to activate cellular and humoral immune responses, capable of inducing protection against *S. aureus* SSTIs. Thus, identifying them as important vaccine antigens for future SSTI vaccines.

Chapter 1

Introduction

1.1 Staphylococcus aureus

Staphylococcus aureus is a gram positive coccal bacterium that causes a wide range of illnesses from minor skin infections, such as abscesses, cellulitis, folliculitis and impetigo, to more severe life threatening diseases upon invasive entry, such as bacteraemia and septicaemia [1]. The treatment of staphylococcal infections is becoming increasingly difficult with the emergence of antibiotic resistant strains particularly in healthcare associated (HA) settings, the most notable of which is methicillin-resistant *S. aureus* (MRSA). The MRSA epidemic is an escalating problem in Western Europe and North America. In the U.S. it has been reported that invasive MRSA infections result in more deaths annually (>18,500) than HIV/AIDS, viral hepatitis and influenza combined [2, 3].

Of growing concern is the emergence of MRSA infections in young, immunocompetent individuals with no healthcare associated risk factors. These community acquired (CA) MRSA infections are characterised by distinct genotypes and distinct virulence determinants. CA-MRSA strains are considered more virulent than their representative health care associated strains [4, 5] and are also associated with rapid dissemination among particular groups including prisoners and soldiers [6]. The majority of CA-MRSA infections present as skin and soft tissue infections (SSTIs) [7]. Although many clinical manifestations of CA-MRSA are mild, severe infections leading to necrotising fasciitis and necrotising pneumonia have been associated with mortality rates of 20 % and 75 % respectively [7]. CA-MRSA is epidemic within the USA, however, its prevalence is considerably lower across Europe, although incidences are increasing [8].

1.2 S. aureus skin infection

1.2.1 Epidemiology

SSTIs are caused by microbial invasion of the layers of skin and underlying soft tissues. SSTIs have variable clinical presentations, etiology and severity. Infections may occur at sites where the skin barrier has been breached, such as a wound or surgical site. However, infections may also appear without apparent breach of the skin barrier, such as folliculitis occurring at hair follicles, or furuncles and carbuncles forming at pores [9]. The involvement of deeper layers such as the dermis and/or subcutaneous tissues leads to cellulitis [9], with the involvement of yet deeper tissues, such as underlying muscle leading to fasciitis. SSTIs are common and can affect all age groups, however, certain conditions such as trauma, immune suppression, certain skin conditions and drug use may predispose an individual to SSTIs [7]. *S. aureus* is capable of causing infections at all mentioned sites in the skin and in some instances, outbreaks of *S. aureus* SSTIs can occur. These are mainly seen in cases where there is close body contact, in groups such as prisoners, athletes and soldiers [10-13]. SSTIs caused by *S. aureus* account for over 10 million outpatient visits and almost 500,000 hospital admissions in the United States each year [14]. *S. aureus* is responsible for a third of all SSTIs within Europe [15]. Treatment of these infections is significantly hampered by the pathogen's propensity to acquire antibiotic resistance. In particular, CA-MRSA skin infections are occurring with increasing frequency and it is estimated that 90 % of CA-MRSA infections present as SSTIs [16]. CA-MRSA strains from the lineage USA300 are the most common cause of skin infections and 97 % of all MRSA SSTI cases in the USA were caused by this lineage [17].

1.2.2 Pathology

Many *S. aureus* SSTIs are self-limiting, however, complicated SSTIs can occur, and this often leads to the formation of a large abscess [18]. Abscesses can form in the dermis, epidermis and subcutaneous tissue and function primarily to contain the pathogen, preventing the spread of infection to adjacent healthy tissue [19]. Although abscess formation is part of the body's defence mechanism, they can cause significant pathology and lead to benign or malignant obstruction in tissues. They can rupture, releasing bacteria into the surrounding tissue and local inflammation at the site of the abscess can lead to painful swelling for the patient [20]. An abscess begins as an acute localised inflammatory response to the invading bacteria [19]. The abscess forms and becomes a collection of pus composed of live and necrotic neutrophils, tissue debris and live bacteria, encased in a fibrous capsule (Figure 1.1) [19]. Severe SSTIs may also lead to dermonecrosis of adjacent skin tissue. Dermonecrosis is caused by excessive inflammation in the skin and results in cell death of skin cells. Dermonecrosis is distinct from abscess formation, and is mainly caused by secreted toxins of *S. aureus* [21].

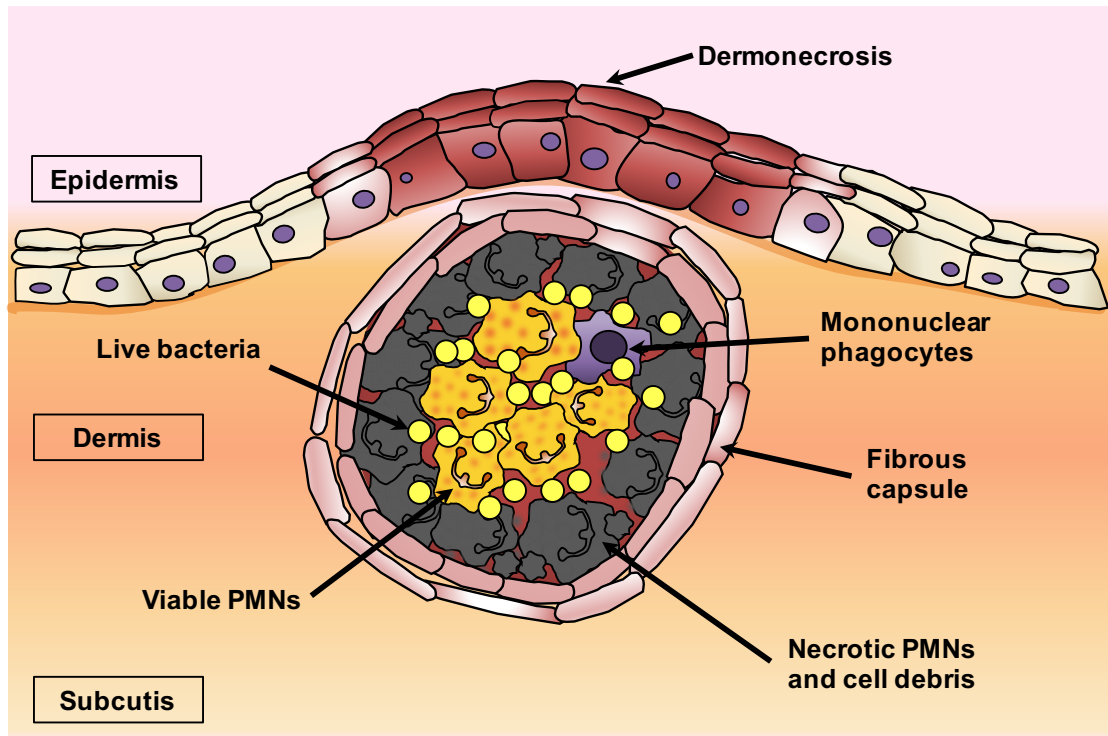


Figure 1.1. *S. aureus* skin abscess structure. *S. aureus* skin abscesses can form in the dermis, epidermis or subcutis tissue. The centre of the abscess contains an acute inflammatory exudate composed of viable and necrotic neutrophils (PMNs), tissue debris and live bacteria. The abscess is encased in a fibrous capsule structure. Dermonecrosis can occur, leading to cell death of the surrounding skin cells.

1.3. *S. aureus* virulence factors involved in the pathogenesis of SSTIs

1.3.1 Membrane damaging toxins

S. aureus secretes several membrane damaging toxins, capable of forming pores in the cytoplasmic membrane of host cells leading to cell lysis and which can contribute to dermonecrosis during SSTIs. *S. aureus* produces three classes of cytolytic toxins: (i) bi-component leukotoxins including leukocidins; (ii) small β -barrel forming toxins such as alpha hemolysin (Hla; α -toxin), and (iii) the short amphiphilic peptides including phenol soluble modulins (PSM).

Bi-component leukocidins form a β -barrel pore spanning the lipid bi-layer of the host cytoplasmic membrane resulting in cell lysis [22]. Pantone Valentine Leukocidin (PVL) is a β -barrel pore forming cytotoxin that binds to the complement receptors C5aR and C5L2 on the surface of neutrophils [22]. LukAB and LukED are bi-component leukocidins that are closely related to PVL but recognise different host cell receptors. LukAB can recognise CD11b, while LukED recognises CCR5 and CXCR1/2 [23]. Although purified LukED, LukAB and PVL induce inflammation in rabbit skin [24, 25], animal models have failed to demonstrate a clear role for bi-component leukocidins in the pathogenesis of skin infection [26-28].

The role of the small β -barrel forming alpha haemolysin (Hla) *in vivo* is much better understood. The Hla monomer binds to host cells forming a lipid bi-layer spanning β -barrel pore, which causes cell lysis. Hla has activity toward a variety of host cell types, including human keratinocytes, epithelial cells, lymphocytes and erythrocytes although it is unable to lyse neutrophils [29-32]. The receptor for Hla is A Disintegrin And Metalloprotease 10 (ADAM10) [33] which is expressed on leukocytes but also widely expressed by many cells in the liver, heart, kidney, lung, and in lymphoid tissues [34]. The Hla-ADAM10 interaction leads to the disruption of host cell membranes, and during skin infection this leads to excessive inflammation, contributing to the necrosis of the epidermis and dermis layers [33, 35]. Hla

contributes significantly to the severity of USA300 skin infections. Upon subcutaneous infection, there was a striking difference in abscess lesion phenotype between the wild-type and Hla-deficient USA300 strain infected mice [35]. Mice challenged with a Hla-deficient mutant formed significantly smaller abscess lesions with visibly less dermonecrosis than those infected with the wild-type strain. In a rabbit infection model, the Hla-deficient mutant formed smaller lesions with lower bacterial burden in the abscess compared to the wild-type strain [26]. Another recent study found that Hla contributed to the virulence of the dominant CA-MRSA strain ST93 from Australia [36]. From these studies, it is clear that Hla is an important virulence factor in SSTIs and much of the recent research has convincingly demonstrated that Hla is a major cause of dermonecrosis during SSTIs. Consistent with this, administration of monoclonal antibodies, which neutralised Hla, resulted in reduced dermonecrosis in a skin infection model [37].

In contrast to β -barrel forming toxins, Phenol-soluble Modulins (PSMs) are capable of lysing cells through non-specific and receptor-independent interactions [38]. PSMs have an exceptionally high capacity to lyse human neutrophils [39, 40]. Wang *et al.* [41], demonstrated that PSMs can activate human neutrophils, triggering inflammatory responses, leading to dermonecrosis during skin infection. Further analysis using *in vitro* assays found that PSMs can effectively lyse human neutrophils and the integrity of the plasma membrane of neutrophils was compromised after only 5 min of exposure to PSMs. A PSM-deletion strain had greatly reduced capacity to cause neutrophil lysis. [41]. PSMs cause excessive inflammation, ultimately leading to dermonecrosis of the skin during SSTIs [41]. These results suggest that the PSMs are involved in causing dermonecrosis and are responsible for destroying leukocytes and thus facilitate *S. aureus* evasion of host immune defence systems.

Taken together the evidence in the literature suggests that dermonecrosis is almost exclusively caused by secreted toxins of *S. aureus* during SSTIs. Inflammation during

SSTIs is needed to recruit leukocytes to the site of infection, ultimately leading the eradication of the infecting bacteria, however the excessive inflammation associated with dermonecrosis can lead to further damage of the skin. In addition, the cytolytic effect that these secreted proteins have upon leukocytes and other host cells acts as an immune evasion mechanism for *S. aureus*, thus facilitating persistence of the infection.

1.3.2. Cell wall-anchored proteins

S. aureus can express up to 25 different cell wall-anchored (CWA) proteins (Table 1.1). *S. aureus* CWA proteins are covalently bound to the cell wall peptidoglycan. Many of these can carry out multiple functions and there is functional redundancy between the proteins, whereby many different proteins can carry out similar roles, for example binding to the same ligands. All CWA proteins are anchored to the cell wall by transpeptidases known as sortases [42]. Proteins destined for the cell wall contain a C-terminal sorting signal with a conserved LPXTG motif, which is recognised by sortase A (Figure 1.2). Sortase A cleaves the amide bond between the threonine and glycine, and nucleophilic attack occurs with the pentaglycine chain of peptidoglycan precursor, lipid II, linking the protein to lipid II [42]. This precursor molecule can then be integrated into the cell wall during normal peptidoglycan synthesis. Sortase-deficient mutants, which lack all cell surface bound CWA proteins, have reduced virulence in murine kidney abscess infection models [43, 44]. Wild-type bacteria formed abscesses at 5 days post-challenge, whereas the sortase-deficient strain was unable to cause abscess formation and the bacteria were effectively cleared by the animal [43, 44]. Similarly, in a skin abscess model, a sortase-deficient mutant had lower bacterial burden in the skin and animals showed a significantly reduced pathology compared to wild-type infected mice [45]. These studies clearly indicate that CWA proteins are important during SSTIs and the kidney abscess models

demonstrate that CWA proteins are important during the process of abscess formation.

It is likely that CWA proteins may be particularly important for the initial attachment of bacteria to skin and in the early stages of SSTIs and abscess formation. However, there is a paucity of information regarding the role of individual surface proteins during SSTIs in the literature. Only one study to date has looked at the contribution of multiple individual CWA proteins in a murine skin infection model [45]. The study examined the contribution to pathogenesis of the surface proteins, protein A (SpA), fibronectin binding proteins (FnBPs), SasF and clumping factor A (ClfA). However, the mutants used were generated in a number of different strain backgrounds; Newman, SH1000, and LS-1, making direct comparisons between the contributions of each protein difficult. To date, the majority of research into the virulence potential of CWA proteins has been carried out in systemic invasive models of infection. Most CWA proteins have never been examined in regard to their function during skin infection, however we believe that some proteins may be of particular importance during SSTIs. For this study, we have chosen a number of CWA proteins, which we believe may have important roles during SSTIs. These proteins are discussed in the following sections.

Table 1.1. Cell wall-anchored proteins of *Staphylococcus aureus*.

Protein group	Ligand	Function	Refs
MSCRAMMs			
Clumping factor A (ClfA)	Fibrinogen γ -chain	Adhesion to fibrinogen, Immune evasion	[46, 47]
	Complement factor I	Immune evasion	[48, 49]
Clumping factor B (ClfB)	Fibrinogen α -chain, Keratin 10, Loricrin	Adhesion to epithelial cells, Nasal colonisation	[50-53]
	ClfB	Biofilm formation in absence of Ca^{2+}	[54]
Serine-aspartate repeat protein C (SdrC)	SdrC (dimerization)	Biofilm formation	[55]
	β -neurexin	Unknown	[56]
Serine-aspartate repeat protein D (SdrD)	Desquamated epithelial cells	Possibly Nasal colonisation	[57]
Serine-aspartate repeat protein E (SdrE)	Complement factor H	Immune evasion, Degrades C3b	[58]
Bone sialoprotein-binding protein	Fibrinogen α -chain	ECM adhesion	[59]
Fibronectin binding protein A (FnBPA)	Fibrinogen γ -chain, Elastin	ECM adhesion	[60]
	Fibronectin	ECM adhesion, Invasion	[61, 62]
Fibronectin binding protein B (FnBPB)	Fibrinogen	ECM adhesion	[63]
	Fibronectin	ECM adhesion, Invasion	[61, 62]
Collagen adhesin (Cna)	Collagen	Adhesion to collagen	[64]
	Complement C1q	Prevents classical pathway of complement activation	[65]
NEAT motif family			
Iron-regulated surface protein A (IsdA)	Haem, Fibrinogen, Fibronectin, Cytokeratin 10, Loricrin.	Haem uptake, Iron acquisition, Adhesion to epithelial cells, Lactoferrin resistance	[66-68]
	Unknown ligand	Resistance to antimicrobial peptides, Survival in neutrophils	[69]

Iron-regulated surface protein B (IsdB)	Haemoglobin, Haem	Haem uptake, Iron acquisition	[70, 71]
	β -3 integrins	Invasion of non-phagocytes	[72]
Iron-regulated surface protein H (IsdH)	Haem, Haemoglobin	Haem uptake, Iron acquisition	[70, 71]
	Unknown ligand	Accelerated degradation of C3b	[73]
Three-helical bundle			
Protein A	IgG, IgM, TNFR1	Inhibition of opsonophagocytosis, B-cell superantigen, Inflammation	[74-78]
	Von Willebrand factor	Endovascular infection, Endocarditis	[79]
	Unknown ligand	Inflammation	[80]
G5-E Repeat Family			
<i>S. aureus</i> surface protein G (SasG)	Unknown ligand	Adhesion to desquamated epithelial cells, Biofilm formation	[81, 82]
Serine-rich repeat glycoprotein			
Serine-rich adhesion for platelets (SraP)	L-lectin domain. Salivary agglutinin gp340, platelets.	Adhesion to cells	[83-85]
Structurally uncharacterised proteins			
Adenosine synthase A (AdsA)	No binding ligand known	Induce apoptosis in neutrophils	[86-88]
<i>S. aureus</i> surface protein X (SasX)	Unknown ligand	Biofilm formation, Cell aggregation, Adhesion to squamous cells	[89]
SasC	Unknown ligand	Biofilm formation	[90]
SasB, SasD, SasF, SasJ, SasK, SasL	Unknown ligand	No known structure or function	[91]
Biofilm-associated protein (Bap)	Gp96	Promotes biofilm, Promotes aggregation on epithelial cells. Only found in bovine strains.	[92, 93]

MSCRAMMs: Microbial surface component recognizing adhesive matrix molecule.

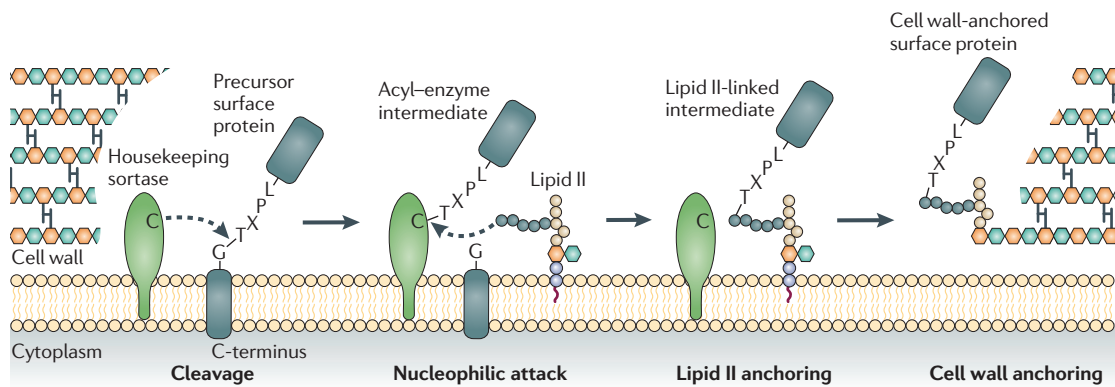


Figure 1.2. Mechanism of sortase-mediated surface protein anchoring to the cell wall. Surface proteins are synthesized in the cytoplasm as precursor proteins with an amino-terminal signal sequence and a carboxy-terminal sorting signal. The C-terminal sorting signal consists of a positively charged tail, a hydrophobic region and a LPXTG motif. Following secretion by the Sec secretion system, signal peptidases cleave the signal peptides of surface proteins, thereby producing the precursor surface proteins. The active-site Cys of the sortase cleaves the amide bond between Thr and Gly of the C-terminal pentapeptide LPXTG motif and generates an acyl–enzyme (thioester) intermediate. Nucleophilic attack by the amino group within the pentaglycine cross bridge of lipid II links the C-terminal Thr of the surface protein to lipid II. Penicillin-binding proteins incorporate the precursor into the cell wall as a mature cell wall-anchored surface protein for surface display by catalyzing a transpeptidation reaction. Figure adapted from Antoni *et al* (2011) [42].

1.3.2.1 Clumping Factor A

Clumping factor A (ClfA) was the first fibrinogen-binding protein of *S. aureus* to be discovered and characterized in detail [94]. The 92 kDa protein is primarily expressed during stationary phase growth. ClfA is the archetypal serine-aspartate dipeptide repeat (Sdr) protein, characterised by the presence of a serine-aspartate dipeptide (SD)-repeat stalk region [95]. It contains an N-terminal signal sequence, followed by a fibrinogen-binding region (A) and an SD-repeat region that varies in length between strains (Figure 1.3). The C-terminus of ClfA consists of a wall-spanning and membrane-spanning region and an LPDTG motif required for sorting and anchoring of the protein to the peptidoglycan layer. The A domain of ClfA can be further divided into three subdomains; N1, N2 and N3. The N2N3 subdomains adopt an IgG-like fold and are involved in binding fibrinogen. ClfA binds to a flexible unfolded peptide at the C-terminus of the γ -chain of fibrinogen [96]. Ten residues located at the junction between the N1 and N2 subdomains are required for protein export and cell wall localization [97]. However, a role for the remainder of the N1 subdomain remains elusive.

ClfA is the major CWA protein responsible for platelet activation by *S. aureus*. The integrin GPIIb/IIIa on platelets recognises the γ -chain of fibrinogen which is necessary for platelet aggregation [98, 99]. ClfA also recognises this same region of fibrinogen and *S. aureus* expressing ClfA can stimulate platelet activation by forming a fibrinogen bridge between the bacterium and GPIIb/IIIa. For platelet activation to occur, ClfA-specific immunoglobulin is also required to interact with the platelet immunoglobulin Fc receptor (Fc γ RIIa) [100].

ClfA is an important virulence factor of *S. aureus* and its contribution to pathogenesis has been demonstrated in several animal models of infection, including endocarditis, arthritis, and sepsis [101-103]. In a murine arthritis model, a ClfA-deficient mutant of *S. aureus* showed significantly decreased ability to cause arthritis and also

decreased mortality, when compared to the wild-type strain [101]. In this study mice were also immunized with recombinantly produced ClfA A domain which conferred some protection from subsequent *S. aureus* infection by the induction of ClfA specific antibodies [101]. In a murine kidney abscess model of *S. aureus* infection, a ClfA-deficient mutant had reduced survival in blood and caused decreased bacterial burden in the kidneys, compared to the wild-type strain. Defects in abscess formation caused by the mutant were not deemed to be significant [44]. In a murine model of septicaemia, fibrinogen-deficient mice were less susceptible to *S. aureus* infection and mice producing a mutant form of fibrinogen lacking the ClfA binding site were more resistant to challenge than wild-type mice indicating that the interaction between *S. aureus* and fibrinogen is crucial for facilitation of the infection [104]. Taken together, these findings suggest that ClfA is primarily involved in pathogen survival and dissemination in blood but may not be directly involved in forming abscesses at least in the kidneys.

ClfA may also play a role in skin infection, as mice inoculated with a ClfA-deficient mutant of *S. aureus* Newman demonstrated a lower bacterial burden in skin abscesses compared to the wild-type strain at day 2 post inoculation [45]. Another recent study using a rabbit skin infection model found that animals infected with ClfA-deficient Newman formed smaller abscesses compared to the wild-type strain, however only a modest reduction in bacterial burden was observed [105]. However, both of these studies used the laboratory strain Newman, which is not necessarily relevant to clinical SSTIs.

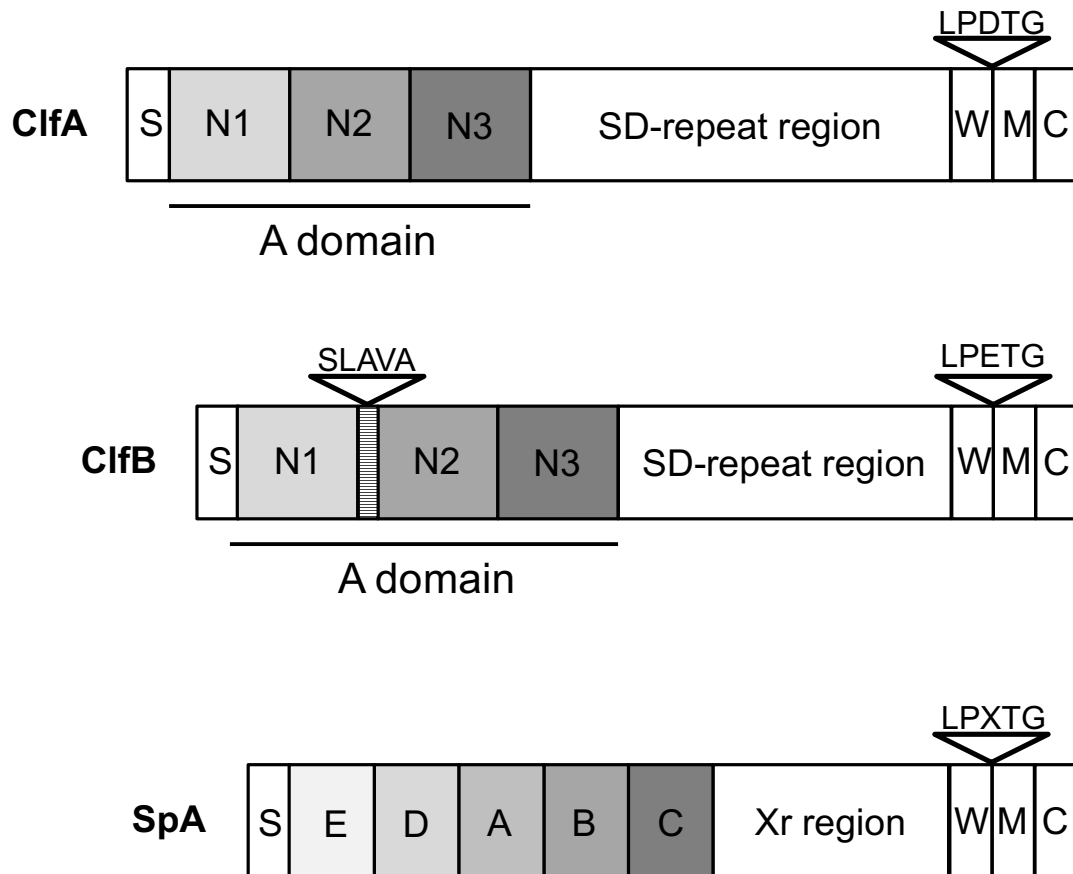


Figure 1.3. Staphylococcal surface proteins. Structural organisation of surface proteins from *S. aureus*. The A domains of ClfA and ClfB are ligand binding domains. SpA domains E, D, A, B and C are homologous ligand-binding repeats. S=Signal sequence, Xr=proline-rich regions, WMC=wall/membrane/cytoplasmic spanning regions and LPXTG sortase A recognition motifs are indicated.

1.3.2.2 Clumping Factor B

The MSCRAMM ClfB has similar structural organisation to ClfA (Figure 1.3). The signal sequence and wall anchoring domains are 36 % and 41 % identical respectively, whereas the ligand-binding regions are only 26 % identical [106]. It is expressed in the early exponential phase of growth and is absent from cells in the late exponential and stationary phase. The N-terminus of ClfB consists of a signal sequence followed by its binding domain, region A [106]. This is a 540 amino-acid-long segment containing 3 independently folded subdomains, N1, N2 and N3 [107]. N1 is separated from N2N3 by a metalloprotease recognition sequence, SLAVA [108]. Similar to ClfA, the ligand-binding region of ClfB has been localised to the N2N3 domain of region A. The N1 domain has no known binding function [107]. Following the A domain is a repeat region R, containing a variable number of SD repeats. This repeat region causes the protein to extrude from the cell wall and connects the ligand-binding region to a cell wall-spanning domain and an LPXTG motif.

ClfB can promote clumping of exponential phase cells in the presence of fibrinogen and promote *S. aureus* adherence to fibrinogen *in vitro* [106]. ClfB binds to the C-terminus of the α C-chain of fibrinogen, which contains 10 tandem repeats and ClfB binds to repeat region 5 [109]. The binding of fibrinogen by ClfB mediates platelet activation by *S. aureus*, which contributes to pathogenesis during infective endocarditis. ClfB has previously been demonstrated to contribute to virulence during experimental endocarditis in rats [110]. It has also been shown that patients recovering from endocarditis have elevated anti-ClfB antibodies titres [111].

The primary function of ClfB is, however, to promote *S. aureus* nasal colonisation. *S. aureus* attachment to the anterior nares during commensal colonisation is facilitated by ClfB through high affinity interactions with the cornified envelope. ClfB has been shown to promote nasal colonisation in both rodents and humans [50, 112, 113]. ClfB

binds to plasma fibrinogen [109], cytokeratin 10 [52], which is the dominant component of the interior of squamous cells and to loricrin which is the most abundant protein of the cornified envelope of squames [114]. Rates of *S. aureus* nasal colonisation were significantly reduced in loricrin-knockout mice compared to wild-type mice, demonstrating that loricrin is the critical ligand for ClfB *in vivo*, at least in mice [50].

In a murine kidney abscess model, a ClfB-deficient mutant had reduced bacterial burden, however, no defects in abscess formation were observed using histological methods [44]. This study suggests that ClfB is not involved in kidney abscess formation, at least during systemic infection. As ClfB is known to bind to squames in the nose it is possible that it has a role in the attachment to squames at other locations in the body, and this may be of importance for the initiation of skin infections. The contribution of ClfB to *S. aureus* skin infection and how it interacts with the immune system at this site remains to be elucidated.

1.3.2.3 Protein A

Protein A (SpA) is expressed by at least 95 % of *S. aureus* strains [115] and was the first *S. aureus* cell wall protein to be characterized [116]. The surface-exposed N-terminal region of SpA contains five homologous repeats designated as E, D, A, B and C (Figure 1.3). Each subdomain is 58-62 amino acids in length and consists of three anti-parallel α -helices that form helical bundles. Each repeat is capable of binding many ligands including the Fc region of IgG, the Fab heavy chain of V_H3 on IgM [117], TNF receptor-1 (TNFR-1) and von Willebrand factor (vWF) [79, 118]. The N-terminal domain is followed by a proline-rich repeat region (Xr domain) [119].

SpA is multifunctional and has a number of immunosuppressive traits and is one of *S. aureus*' most important mechanisms of immune evasion. SpA binds to the Fc γ portion of IgG, resulting in the bacteria becoming coated in IgG bound in the incorrect

orientation, leading to decreased recognition by neutrophils and consequently evasion of phagocytosis [120, 121]. SpA is also a B cell superantigen that binds to the V_H3^+ immunoglobulins on the surface of B cell receptors, causing clonal expansion, which results in apoptosis [122]. This depletion of B cells results in reduced antibody production and the inability to develop robust adaptive immune responses [122]. In contrast to its role in immune evasion SpA can also be proinflammatory. SpA was shown to bind to and stimulate the surface expression of TNFR1 and also its shedding from the cell [77]. TNFR1 binding leads to activation of MAPKs, which results in the expression of IL-8 and other chemoattractant cytokines, ultimately causing neutrophil recruitment. In a murine model of pneumonia, mice infected intranasally with wild-type *S. aureus* had a significantly higher incidence of pneumonia and bacteraemia than mice infected with the SpA mutant [77]. Mice lacking TNFR1 were also significantly protected from pneumonia, and bacteraemia. Thus, the lack of SpA or TNFR1 expression resulted in reduced bacterial virulence in this pneumonia model, as neutrophil recruitment to the lung, which can be detrimental to the airways, was decreased.

A murine kidney abscess model was used to determine the contribution of SpA to kidney abscess formation [44]. On day 5 post-infection, the SpA-deficient mutant infected mice had a significantly reduced number of abscesses compared to the wild-type infected mice [44]. Similarly, in an alternative study, mice infected intravenously with SpA-deficient Newman had lower bacterial load and decreased number of kidney abscesses 18 days post-inoculation compared to mice challenged with the wild-type strain [123]. This suggests that SpA is an important virulence factor for abscess formation in the kidney at least.

It is apparent that SpA has a number of functions during infection; however, its role in skin infection has yet to be fully elucidated. When mice were inoculated subcutaneously with a SpA-deficient mutant of Newman, the bacterial burden from

skin abscess was significantly lower than abscesses of mice infected with the wild-type. However, as stated previously this study used *S. aureus* Newman, which is not clinically relevant to SSTIs and only investigated virulence at one time point post-infection. The dominant role for SpA during *S. aureus* SSTI is likely immune evasion through its binding of IgG and depletion of B cells, providing the bacteria with time to establish itself and attach to ligands in the skin. It is also likely that SpA is important in driving proinflammatory responses in the skin. The TNFR1 receptor is highly expressed on human keratinocytes [124] and purified SpA was shown to up-regulate the expression of COX-2 and IL-8 in human keratinocytes by its binding to TNFR1 and triggering downstream kinases which result in the activation of Nuclear factor- κ B (NF- κ B) and AP-1, ultimately causing skin inflammation [124]. Additionally, the binding of TNFR1 may facilitate binding of *S. aureus* to the skin, which may be important for the initiation of SSTIs.

1.4 Immune response to infection

1.4.2 Protective immune responses against bacterial infection

During bacterial infection, the innate and adaptive immune responses function in concert to ultimately clear infection, while protecting the host from unwanted immunopathology. Innate immune recognition is carried out by a series of constitutively expressed receptors known as pathogen recognition receptors (PRRs), which efficiently recognise pathogen associated molecular patterns (PAMPs) conserved amongst different microbial species. However, they are incapable of distinguishing subtle differences in molecules expressed by individual species. Phagocytes such as neutrophils, macrophages and dendritic cells (DCs) recognise PAMPs, leading to their activation and recruitment to the site of infection where they can contain the infection through phagocytosis. DCs are professional antigen presenting cells (APCs) and act as a bridge linking the innate and adaptive immune systems. DCs sample antigens at peripheral sites and migrate to lymph nodes to activate antigen-specific T cells through antigen presentation by either major histocompatibility complex I (MHCI) or MHCII (Figure 1.4). All cells constitutively express MHCI and are capable of presenting intracellular bacterial or viral peptides on MHCI for recognition by CD8⁺ T cells. However, as professional APCs, DCs are also capable of phagocytosing pathogens and degrading them in order to present peptides on MHCII for recognition by CD4⁺ T cells.

The adaptive immune response involves a cellular and humoral component and develops and adapts to recognise and eliminate infection in a pathogen specific manner. Once activated, it provides a comprehensive line of defence to destroy pathogens that have overcome innate immunity. A critical aspect of the adaptive immune response is the generation of immunological memory, which is the fundamental basis of vaccination.

The humoral immune response to pathogens is mediated by antibodies produced by B cells. These antibodies are capable of recognising an infinite number of foreign antigens and can provide the host with both short- and long-term protection against the pathogen. Antibodies are important for neutralising bacterial virulence factors by binding to these factors and blocking the interaction with their target ligand. Antibodies can also enable phagocytic killing of the pathogen through opsonisation, by coating the bacterium with antibodies, which can be recognised by phagocytes.

Antigen-specific T lymphocytes are at the core of the adaptive cellular immune response. Two distinct lineages of T cells are produced and can be distinguished based on their distinct T cell receptors (TCR); $\alpha\beta$ and $\gamma\delta$. $\alpha\beta$ T cells are further classified as either $CD4^+$ T helper (Th) cells or $CD8^+$ cytotoxic T cells. $CD4^+$ Th cells function by activating and directing or “helping” the function of other effector immune cells primarily via cytokine release. The downstream effects of these cytokines enhance phagocytic and bactericidal activity of innate effector cells, induce antibody class switching, and promote activation and expansion of $CD8^+$ T cells. $CD4^+$ T cells can be divided into different effector subsets that are characterised by their expression of specific transcription factors, signal transduction pathways and cytokine secretion profiles (Figure 1.5). The primary function of $CD8^+$ T cells is to kill intracellularly infected, cancerous or abnormal host cells. Whereas the primary function of $CD4^+$ T cells is to activate effector cell functions. Innate like $\gamma\delta^+$ T cells are a distinct subset of T cells that comprise 1-5 % of circulating lymphocytes, however, they are present in much greater numbers at epithelial sites such as the skin and intestines. $\gamma\delta^+$ T cells display broad functionality and can respond rapidly to cytokine activation. In the absence of antigen, $\gamma\delta^+$ T cells were shown to secrete IL-17 in response to IL-1 and IL-23 stimulation [125]. $\gamma\delta^+$ T cells can also recognise presented antigen. Recently, antigen activation of $\gamma\delta^+$ T cells in conjunction with inflammatory cytokine stimulation was shown to stimulate increased $\gamma\delta^+$ T cell

activation compared to either stimulus alone, suggesting that $\gamma\delta^+$ T cells are capable of synergising both activation mechanisms enabling increased effector function [126]. $\gamma\delta^+$ T cells are also capable of responding to pathogen products directly via expression of their PRRs and environmental signals via AhR [127]. Activated murine $\gamma\delta^+$ T cells contribute to host resistance through production of effector cytokines such as IL-17, IL-22 and IFN γ .

Here components of both adaptive and innate immunity that are of particular importance in the immune response to *S. aureus* infection are briefly discussed.

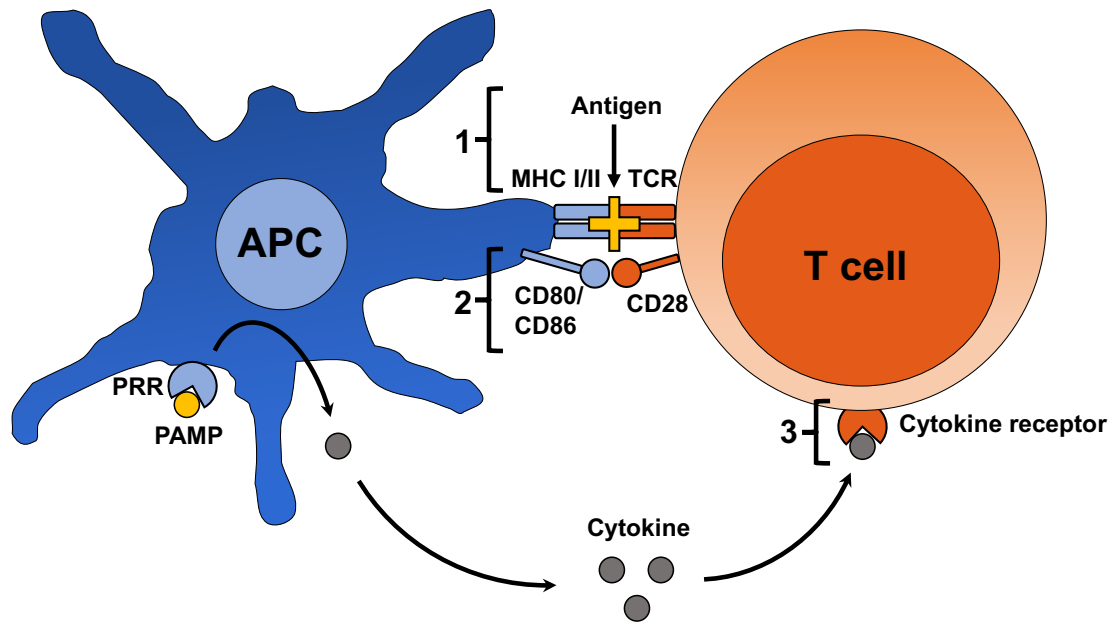


Figure 1.4. Interaction between antigen presenting cells and T cells. When APCs encounter a bacterial pathogen, they upregulate their expression of MHC I/II molecules containing pathogen derived antigenic peptides. Signal 1 is the interaction between the MHC molecule and the TCR. Signal 2 involves the interaction between the costimulatory molecules CD80/CD86 and CD28 on the T cell. Finally, signal 3 involves cytokines secreted by the APC which modulate T cell differentiation into specific subsets.

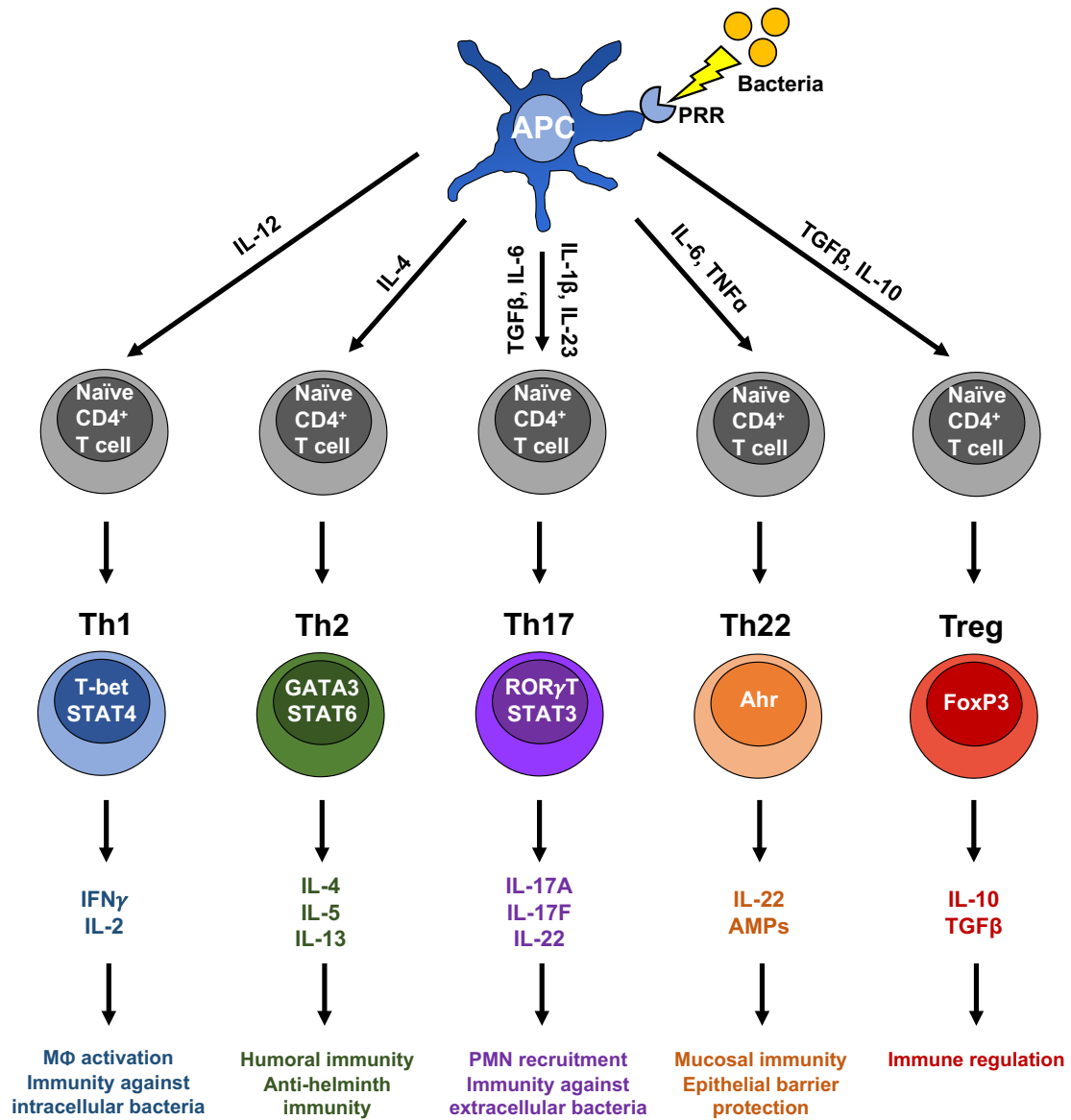


Figure 1.5. CD4⁺ helper T cell differentiation. Antigen presentation by the APC leads to the differentiation of naïve CD4⁺ T cell precursor cells. CD4⁺ T cells can differentiate into effector T cells (Th1, Th2, Th17 and Th22 cells) and T regulatory cells (Tregs). Subset differentiation is driven by distinct cytokines and transcription factors. Each subset carries out specific functions during the immune response to pathogens and the eventual resolution of infection. Adapted from Murphy et al (2012) [128] and Murphy (2014) [129].

1.4.2.1 The role of antibodies in *S. aureus* infection

Antibody responses are likely important but perhaps not critical in the immune response against *S. aureus* infection. *S. aureus*-specific antibody titres are elevated in the blood of patients after infection [130, 131] and these are important for neutralising toxins [131], inhibiting bacterial adherence to host tissue [132] and facilitating opsonisation of the bacteria to aid in opsonophagocytic clearance [133]. However, B cell deficiencies in patients or mice are not associated with increased susceptibility to *S. aureus* infection [134]. In addition, numerous studies have demonstrated that *S. aureus*-specific antibodies are produced upon exposure to the bacterium during infection and through commensal colonisation [130, 131, 135], however these antibodies do not necessarily protect against *S. aureus* infection [130, 136] and recurrence of infection is often observed in the clinic [137, 138]. Mice that received sera containing anti-staphylococcal antibodies or B cells isolated from mice vaccinated with a model anti-*S. aureus* vaccine were not protected against subsequent bacteraemia [134]. These studies suggest that induction of a humoral response alone is incapable of mediating full protection against *S. aureus* infection.

1.4.2.2 The role of neutrophils in *S. aureus* infection

Neutrophils are traditionally considered the first line in host defence against *S. aureus* infection. The importance of neutrophils in *S. aureus* infection is demonstrated by patients with deficiencies in neutrophil activity. These patients are susceptible to increased pyrogenic bacterial infections, often caused by *S. aureus*. For example, patients who suffer from Chronic Granulomatous Disease (CGD) are deficient in NADPH oxidase, an enzyme critical for the generation of reactive oxygen species (ROS), required for oxygen-dependent killing in neutrophils. These patients suffer from recurrent *S. aureus* infections [139]. Patients suffering from Chédiak-Higashi syndrome have reduced neutrophil chemotaxis and phagolysosome activity, leading to an increased occurrence of *S. aureus* infection [140]. Additionally, mice

depleted of neutrophils had elevated mortality in response to *S. aureus* pulmonary challenge compared to immunocompetent mice [141]. This demonstrates the importance of an effective neutrophil response for protection against *S. aureus* infection

Neutrophils are a hallmark of acute infection due to their rapid recruitment to the site of infection. Upon *S. aureus* infection, endothelial cells and resident macrophages in the affected tissue release the chemokine CXCL8 (IL-8) in response to secreted and surface associated molecules of *S. aureus*. These include capsular polysaccharide [142], lipoteichoic acid (LTA) [143] and secreted toxins such as enterotoxin A and B and toxic shock syndrome toxin 1 (TSST-1) [144]. The production of CXCL8 stimulates granulopoiesis and the release of neutrophils from the bone marrow, expanding the number of neutrophils in circulation available to control infection. It also generates a chemotactic gradient, which directs neutrophils to the site of *S. aureus* infection and allows them to enter infected tissue from the bloodstream, through a process known as extravasation [128].

Neutrophils recognise *S. aureus* through the recognition of PAMPs including LTA and CpG DNA which interact with TLRs on the neutrophil to promote phagocytosis. Neutrophils also express Fc receptors and complement receptors that bind the Fc region of antibody-coated bacteria and complement-opsonised bacteria respectively [145].

Although neutrophils are clearly important in the clearance of *S. aureus*, some reports however suggest that high numbers of neutrophils may have a negative effect on *S. aureus* clearance. A previous study has demonstrated that reducing but not ablating neutrophil numbers during *S. aureus* induced peritonitis led to enhanced bacterial clearance, whereas increasing neutrophil influx by administration of recombinant CXC chemokines increased bacterial burden, leading to decreased

survival [146]. Administration of recombinant CXCL2 during *S. aureus* surgical wound infection also led to an increase in bacterial burden at the infection site and this was shown to be due to enhanced intracellular survival of *S. aureus* within the neutrophil [147]. *S. aureus* uses its ability to survive within the neutrophil as a means of protecting itself from the host immune response and a means of dissemination to other tissues [148]. These studies suggest that whilst neutrophils are an essential component of anti-*S. aureus* immunity, an “appropriate” neutrophil response is required, whereby neutrophils are rapidly recruited for phagocytosis and after sufficient clearance of the bacterium undergo apoptosis allowing for a timely resolution of the inflammatory response.

1.4.2.3 The role of macrophages in *S. aureus* infection

Macrophages are mononuclear cells that circulate in the blood as monocytes and they have been shown to be important in the immune response to *S. aureus* [149]. Macrophages are recruited to the infection site by chemokines such as CCL2 (MCP-1) [150]. When monocytes encounter a chemotactic gradient or other signalling mechanism, they pass through the endothelium into the tissue where they differentiate to become macrophages [151].

Macrophages recognise pathogens through the ligation of PRRs by PAMPS on the bacterial surface resulting in phagocytosis [152]. Macrophages also express receptors such as Fc, complement and scavenger receptors that recognise opsonins or ligands present on the surface of bacteria [153-155].

The importance of macrophages in the immune response to *S. aureus* was demonstrated by the depletion of macrophages in mice with systemic *S. aureus* infection which led to increased bacterial burden both locally and systemically [156]. Furthermore, inhibition of nitric oxide synthase (NOS) activity caused increased

severity of *S. aureus* bacteraemia and septic arthritis, alongside reduced bactericidal activity by the macrophages *in vitro* [157].

1.4.2.4 The role of T helper 1 (Th1) cells during *S. aureus* infection

Th1 cells are characterised by the production of IFN γ and are crucial for the cellular immune response to *S. aureus* infection. IL-12 and IFN γ produced by innate immune cells upon PRR activation and NK cells respectively, polarise naïve CD4⁺ T cells towards Th1 differentiation through the activation of T box transcription factor (T-bet) and signal transducer and activator of transcription (STAT) 1 and STAT 4 (Figure 1.5) [158, 159].

During bacterial infection, antigen-specific Th1 responses are crucial for enhancing macrophage effector functions and converting them into potent anti-bacterial effector cells. IFN γ increases the activation of macrophages in response to proinflammatory cytokines and bacterial products [160]. IFN γ signalling enhances respiratory burst and the formation of ROS by upregulating gp91phox, a subunit of NADPH oxidase in both macrophages and neutrophils [161]. IFN γ also upregulates NOS in macrophages, which enhances reactive nitric oxide (NO) [162], which is involved in the formation of bactericidal NO [163]. Furthermore, in response to IFN γ signalling, macrophages can upregulate the expression of Fc γ R1, a receptor involved in binding opsonised bacteria or their components [164].

Th1 cells are expanded during *S. aureus* infection [156] and the production of IFN γ from Th1 cells has been shown to drive macrophage and neutrophil recruitment and activation [147, 165]. However, the role of IFN γ during *S. aureus* infection is not fully understood. It has been demonstrated that IFN γ signalling is dispensable for protection against *S. aureus* SSTIs, with IFN γ R^{-/-} and WT mice displaying similar pathologies upon cutaneous staphylococcal infection [166]. While other studies have shown a detrimental effect for IFN γ , as deficiency in IFN γ was associated with

protection in a model of surgical site infection [147]. It appears that the role of IFN γ is dependent on the site of infection, as significant evidence suggests that IFN γ plays a crucial protective role during systemic infections. Studies have shown that administration of recombinant IFN γ led to increased phagocyte recruitment and bacterial clearance during intravenous infection, suggesting a protective function for IFN γ in this systemic model [167]. In addition, a recent study reports that memory Th1 cells protect against systemic *S. aureus* infection in mice and importantly are expanded in the circulating blood of patients recovering from *S. aureus* bloodstream infections [156], suggesting Th1 cells play a crucial role during systemic infection. Furthermore, adoptive transfer of *S. aureus* antigen-specific Th1 cells were protective in naïve mice, by promoting macrophage activation during *S. aureus* peritonitis [156]. Taken together, these results indicate that Th1 cells play a crucial role in protection against systemic *S. aureus* infection.

1.4.2.5 The role of T helper (Th) 17 cells during *S. aureus* infection

Th17 cells are characterised by the production of IL-17A, IL-17F and IL-22 and are crucial for protection against extracellular bacteria, particularly at mucosal sites. Th17 cells can induce neutrophil recruitment to sites of infection through the regulation of CXC chemokines. Th17 cells have also been associated with the generation of IgA, an important antibody for mucosal defences [168]. TGF β , IL-6, IL-21 and IL-23 produced by activated innate immune cells polarises naïve CD4⁺ T cells towards Th17 differentiation through the activation of transcription factor retinoid-related orphan receptor (ROR) γ T and STAT3 signalling (Figure 1.5) [168-172].

Th17 cells are crucial for controlling neutrophil responses. IL-17A promotes granulopoiesis by inducing CSF and G-CSF production by epithelial cells which in turn signals to bone marrow stimulating the proliferation of hemopoietic stem cells. IL-17A is also a potent activator of CXC chemokine secretion by epithelial cells, endothelial cells and keratinocytes which acts to attract neutrophils to the site of

infection [173-176]. The upregulation of ICAM-1 expression by keratinocytes is induced by IL-17A which also facilitates neutrophil migration [177]. Not only does IL-17A induce neutrophil recruitment, it also enhances bacterial killing by neutrophils [178]. Furthermore, it can stimulate other innate immune responses to induce the production of antimicrobial peptides (AMPs) by epithelial cells [179, 180].

Patients with autosomal dominant hyper-IgE syndrome (AD-HIES) are susceptible to recurrent staphylococcal skin and lung abscesses [181]. AD-HIES results in impaired Th17 cell development; however, CD4⁺ T cells retain the ability to differentiate into other subsets of Th cells [182]. Interestingly, these patients are not more susceptible to *S. aureus* bloodstream infection, suggesting that Th17 responses are particularly important during skin and respiratory site infections, but may be less important during systemic infection. Similar to patients with T cell deficiencies, T lymphocyte deficient mice demonstrate increased susceptibility to *S. aureus* infection compared to wild-type mice [134]. Studies using mice deficient in T cell derived cytokines have revealed further insights into immune mechanisms important in *S. aureus* infections. Sub-epithelial infections of IL-17A^{-/-}IL-17F^{-/-} double knock-out mice [183] and subcutaneous [166] or surgical site [184] infections of IL-17R deficient mice resulted in increased bacterial burden and disease pathology. However, IL-17A^{-/-}IL-17F^{-/-} mice were not significantly impaired in their ability to clear systemic *S. aureus* infection suggesting a site-specific role for IL-17 in anti-*S. aureus* immunity [183]. Therefore, in contrast to IFN γ , IL-17 may play a more protective role at mucosal sites of *S. aureus* infection.

1.4.2.6 The role of T helper (Th) 22 cells during *S. aureus* infection

Th22 cells are characterised by the production of large amounts of IL-22 but little or no IL-17 or IFN γ and their expression of the skin homing chemokine receptors CCR4 and CCR10 in conjunction with CCR6 (characteristic of Th17 cells) [185, 186]. The presence of IL-6, TNF α and vitamin D3 metabolites are thought to polarise naïve CD4⁺ T cells towards a Th22 phenotype through the activation of the transcription factor for the aryl hydrocarbon receptor (AhR) (figure 1.5) [185, 186].

As Th22 cells home to the skin, it is unsurprising that IL-22 has been shown to be protective against infections at barrier sites (e.g. skin, respiratory tract) where it promotes AMP production in the epithelium [187, 188]. In the skin, IL-22 induces AMPs, such as defensins, but also plays a role in wound healing and tissue remodelling, as it promotes keratinocyte proliferation and inhibits differentiation [189, 190]. Recently, IL-22 produced by Th22, Th17 and $\gamma\delta^+$ T cells was shown to be protective during a *S. aureus* induced pneumonia model [191]. During *S. aureus* pneumonia, neutralisation of IL-22 with an anti-IL-22 antibody prior to challenge with *S. aureus* led to increased susceptibility while conversely, intra-nasal administration of IL-22 at the time of infection with *S. aureus* renders mice more resistant to infection, suggesting that IL-22 is protective against *S. aureus* pneumonia [191]. During *S. aureus* subcutaneous infection, IL-22 was shown to play a non-redundant role in host protection by promoting the expression of AMPs [192]. Similar to the role of IL-17, IL-22 appears to have its most profound affect at mucosal sites.

1.4.2.7 The role of $\gamma\delta^+$ T cells in *S. aureus* infection

In the context of *S. aureus* infection, $\gamma\delta^+$ T cells have been identified as a potent source of innate IL-17. In a cutaneous infection model, $\gamma\delta^+$ T cell deficient mice were found to have reduced neutrophil recruitment to the site of infection and impaired bacterial clearance compared to WT controls [166]. $\gamma\delta^+$ T cells were also shown to have a protective role during surgical site infection through their capacity to induce

IL-17 [184]. In addition, it has been demonstrated that systemic *S. aureus* infection expands a population of memory $\gamma\delta^+$ T cells which provide IL-17-mediated protection against subsequent infection [193]. Most recently, using WT and IL-22^{-/-} mice, IL-22 from $\gamma\delta^+$ T cells was found to be important for limiting the growth of *S. aureus* on mechanically injured skin [194].

1.4.2.8 The role of CD8⁺ T cells in *S. aureus* infection

There is a paucity of information regarding the role of CD8⁺ T cells during *S. aureus* infection. However, given *S. aureus* is capable of invading and persisting within a variety of nonprofessional phagocytic host cells [4, 146, 195-198], it is likely that CD8⁺ T cells play a currently underappreciated role during *S. aureus* infection.

1.5 Vaccines

1.5.1 Anti-bacterial vaccines

Vaccination is the administration of antigenic material to stimulate an individual's immune system to establish long-term adaptive immunological memory. Vaccines are one of the most effective and sustainable ways of preventing infectious disease. To date, the majority of successful anti-bacterial vaccines are based on the induction of memory B cells capable of producing antigen-specific antibodies. These pre-existing antibodies generated in vaccinated hosts allow for quick resolution of subsequent infection [199].

There are five main types of vaccines: attenuated (live) vaccines, inactivated vaccines, toxoid vaccines, subunit vaccines and conjugate vaccines. Traditionally, anti-bacterial vaccines consisted of live, attenuated (e.g. *Bacillus anthracis*) or inactivated, whole cell bacteria (e.g. *B. pertussis*) [200]. Toxoid vaccines induce protective immune responses against a specific toxin by generating antibodies against bacterial exotoxins. Toxoid vaccines are used against tetanus and diphtheria. Subunit vaccines contain purified bacterial components, often combined with an adjuvant to increase their immunogenicity, e.g. acellular *B. pertussis* vaccine [201]. Conjugate vaccines are created by covalently attaching bacterial polysaccharides to a protein carrier, enabling peptide recognition by T cells which generates a T cell dependent anti-polysaccharide antibody response. Conjugate vaccines are used against encapsulated bacteria such as pneumococci and meningococci and generate antibodies specific for carbohydrates present on the surface of the pathogen [202, 203]. Reverse vaccinology has allowed for the rational selection of antigens by screening the genomes of pathogens for potential immunogenic targets and was first implemented in a conjugate vaccine against Serogroup B meningococcus [204]. To date, most licensed anti-bacterial vaccine strategies generate antibody mediated protection and this form of vaccination has been hugely successful in controlling and

even eradicating a number of infectious diseases. However, these vaccination strategies are not without limitations as considerable efforts have been employed to develop anti-*S. aureus* vaccines with no success to date [205].

1.5.2 Anti-*S. aureus* vaccines

There is currently a major unmet clinical need for an anti-*S. aureus* vaccine. The emergence of *S. aureus* strains resistant to vancomycin [206], linezolid [207] and daptomycin [208] reveals the rapid ability of this bacterium to become resistant to the newest forms of antibiotics. Alternative approaches to standard antibiotic therapies are therefore urgently required. It is likely that future success will lie in our ability to prevent severe MRSA infections with the use of immunomodulatory therapies and the development of anti-*S. aureus* vaccines would prevent the bacteria from developing direct resistance. Consequently in recent years there have been numerous attempts to develop active and passive vaccination strategies, all of which have been unsuccessful to date.

The first anti-*S. aureus* vaccines focused on the induction of antibodies against capsular polysaccharides, as previous successful vaccines against other encapsulated bacteria (meningococci and pneumococci) used this strategy. The conjugate vaccine StaphVAX, developed by NABI pharmaceuticals was one of the first vaccines developed against *S. aureus*. The bivalent vaccine was composed of CP5 and CP8 conjugated to the protein carrier *Pseudomonas* exotoxin A. The vaccine induced high antibody titres during phase II clinical trials that were maintained for approximately 6 months [209]. However, despite these encouraging results, the vaccine did not reduce the incidence of invasive *S. aureus* infections in a large phase III trial. This lack of efficacy occurred despite the induction of opsonophagocytic, anti-capsular antibodies in immunised patients [210].

More recently, Merck developed a vaccine targeted against the CWA protein IsdB, which interfered with iron uptake by *S. aureus*, leading to reduced bacterial growth [211]. During a murine model of *S. aureus* induced sepsis, mice immunised with IsdB adjuvanted with alum, had increased survival rates compared to mice immunised with alum alone [212]. However when this IsdB based vaccine underwent clinical trials in humans, it failed to elicit the desired responses and phase IIb trial were terminated in 2011 [213], despite the vaccine showing promising antibody responses in its phase I trials.

In addition to active immunisation, passive vaccination strategies have also been attempted targeting staphylococcal CWA proteins. The Aurexis vaccine consisted of anti-staphylococcal monoclonal antibody raised against the ligand-binding domain of ClfA. There was a non-significant trend towards improved outcomes in patients suffering from *S. aureus* bacteraemia who received this antibody treatment [214]. However a subsequent study found that high anti-ClfA polyclonal antibody titres did not correlate with protection among high risk neonates and the trials were subsequently halted [215]. The Veronate vaccine also targeted ClfA in addition to SdrG, a *Staphylococcus epidermidis* adhesin, and consisted of an anti-ClfA and anti-SdrG immunoglobulin preparation. Elevated antibody titres were observed against both proteins, however the treatment was unsuccessful in Phase III trials in 2000 patients due to insufficient protection [216].

S. aureus nasal carriage has previously been targeted by vaccination in an attempt to lower the incidence of *S. aureus* infection. Intranasal vaccination with killed *S. aureus* significantly reduced the bacterial burden present in murine nares after staphylococcal challenge [112]. Furthermore, intranasal and systemic vaccination with ClfB significantly reduced the bacterial burden in the murine nares following subsequent challenge [112]. A preclinical trial using a conjugate vaccine containing capsular polysaccharides was attempted to protect against nasal colonisation in

humans, however immunisation did not significantly reduce nasal colonisation compared to pre-colonisation rates [217]. This was observed despite an increase in antibody titres against CP5 and CP8 [217]. Interestingly, natural antibody responses detected in infants against staphylococcal surface proteins have been reported to provide no protection against subsequent carriage a year later [218].

1.5.3 Requirements for an effective anti-*S. aureus* vaccine

The development of an effective anti-*S. aureus* vaccine has been unachievable to date and numerous challenges have been encountered. Many of the vaccines which have undergone clinical trials failed to elicit protection in humans, despite demonstrating significant efficacy in murine models. This may be due to the fact that rodents are not natural hosts for *S. aureus* and are therefore naturally more resistant to the bacteria than humans. In addition, unlike humans, mice do not possess pre-existing antibodies and immune memory to *S. aureus* which may significantly impact upon the outcome of treatments when translated from mice to humans. The number and functional redundancy of *S. aureus* virulence factors capable of interacting with the host immune response also hinders vaccine development, as it makes the selection of specific antigens for inclusion in a vaccine increasingly complex. The failure of human vaccination strategies tested to date to confer protection also suggests that antibodies alone are not sufficient to provide protection against *S. aureus*. All of the *S. aureus* vaccines that have reached clinical trial, were designed to induce neutralising and opsonising antibodies [219], and although these vaccines produced robust humoral immunity, and proved to be efficacious in preclinical models, they did not prevent or attenuate infection in humans [220]. It is now widely accepted that protection against *S. aureus* requires a robust T cell response, in particular Th1 and Th17 cells which are critical for controlling phagocytic cell responses and thus facilitating bacterial clearance [205, 219]. Evidence is now indicating that certain T cell subsets are of greater importance at specific sites of infection [21]. Th1 mediated

immunity appears to be of particular importance during systemic infections [156, 221]. In contrast, IL-17 responses seem to be of utmost importance during skin infections [166]. Interestingly, it has been shown in mice at least, that model vaccines can actually confer protection against *S. aureus* infection in the complete absence of antibodies provided there is a robust T cell response [134, 222]. Lin *et al.* demonstrated that both Th1 and Th17 cells are important in mediating vaccine induced protective immunity against intravenous *S. aureus* infections [223]. In this study researchers vaccinated mice with Candidal Als3p adhesion molecule, which is a homologue of ClfA, prior to intravenous challenge with *S. aureus*. Vaccine induced protective immunity required CD4⁺ T cell derived IFN γ and IL-17, both of which enhanced effective phagocyte recruitment [223], demonstrating the powerful upstream control of CD4⁺ T cells on downstream effector cells. Antibodies were not found to be necessary in subsequent protection using this vaccination model [223]. In a separate study, vaccination with targeted nanoparticles, loaded with purified ClfA A domain, led to a Th1 and Th17 cellular immune response in the absence of any humoral response, and was capable of protecting against systemic *S. aureus* infection [222]. These studies demonstrate that protection against acute *S. aureus* infection can be achieved purely with a cellular response.

As specific immune responses may be of greater importance at distinct sites of infection, the requirements for a vaccine may need to be tailored to the type of infection that it is aimed at preventing. A universal anti-*S. aureus* vaccine may never be realised [224] and instead, a vaccine targeting specific clinical manifestations may need to be pursued. As skin is the most frequent site of *S. aureus* infection [225], a vaccine specifically against SSTIs would be of great benefit. A recent study demonstrated that a model vaccine, consisting of Als3p combined with alum, targeted against skin infection specifically drove IL-17 and IL-22 mediated immunity and was able to reduce bacterial burden in the skin during *S. aureus* SSTIs [226]. If

prophylactic vaccines or other forms of immunotherapy to treat *S. aureus* SSTIs are to be developed, we first need a greater understanding of the specific roles of individual virulence factors during infection at this site, as they may be important antigens for inclusion in future vaccine therapies.

1.7. Skin

1.6.1. Skin structure

The skin is the largest organ of the body and with the underlying fat layers, fascia, and muscle, represents the majority of the tissue in the body [227]. The corneal layer is the outermost layer of the skin and it is composed of terminally differentiated keratinocytes, which have highly cross-linked keratin fibrils (Figure 1.6 D) [228]. This corneal layer is composed of a layer of crosslinked proteins coated with covalently bound lipids. The proteins include loricrin and involucrin, keratins such as cytokeratin 10 (K10), and other structural proteins such as filaggrin and small proline-rich proteins which are highly crosslinked and act as the physical barrier of skin [228]. Loricrin is the most abundant protein in the cornified envelope, accounting for about 80 % of the protein mass [114]. The 26 kDa protein is expressed in keratohyalin granules from where it is released to the granular layer. Here they become crosslinked to other proteins and become the main protein re-enforcement on the cytoplasmic side of the cell [229].

The granular, spinous and basal layers lie below the corneal layer, and together with the corneal layer they make up the epidermis. Keratinocytes migrate from the basal layer up to the corneal layer from where they are eventually shed. This process of migration occurs constantly, allowing the epidermis to be continuously renewed. As epidermal differentiation begins, the proliferating basal keratinocytes, which contain a keratin 5 and 14 network (Figure 1.6 A), begins to change and keratins 1 and 10, alongside fatty acids, structural proteins, and ceramides are synthesised in the spinous layers (Figure 1.6 B). Keratins 1 and 10 begin to aggregate in the granular layer (Figure 1.6 C), and filaggrin helps promote the collapse of the cell into the typical flattened morphology of the corneocyte present in the cornified envelope (Figure 1.6 D). Beneath the epidermis resides the dermis layer, which is subdivided into the papillary dermis and the reticular dermis. The dermis is mainly composed of

collagen and elastin fibres, but there are a number of skin structures which span the layers, such as hair follicles, sweat glands and sebaceous glands [227].

Although the skin is an important physical barrier to the invasion of pathogens, it is colonised with a normal microbiome, the species of which vary depending on the location, and other factors such as the temperature, pH, the presence of moisture, sebum, salt and fatty acids. The normal flora includes various species of staphylococci, propionibacteria, corynebacteria and yeasts. It is thought that the normal flora acts as a competitive inhibitor of non-commensal pathogenic microbes [228]. Some skin colonizing microorganisms, in particular *S. aureus*, and β -haemolytic group A streptococci but also Gram-negative bacteria, viruses and fungi, have the potential to cause infection, particularly when the skin barrier is breached [230].

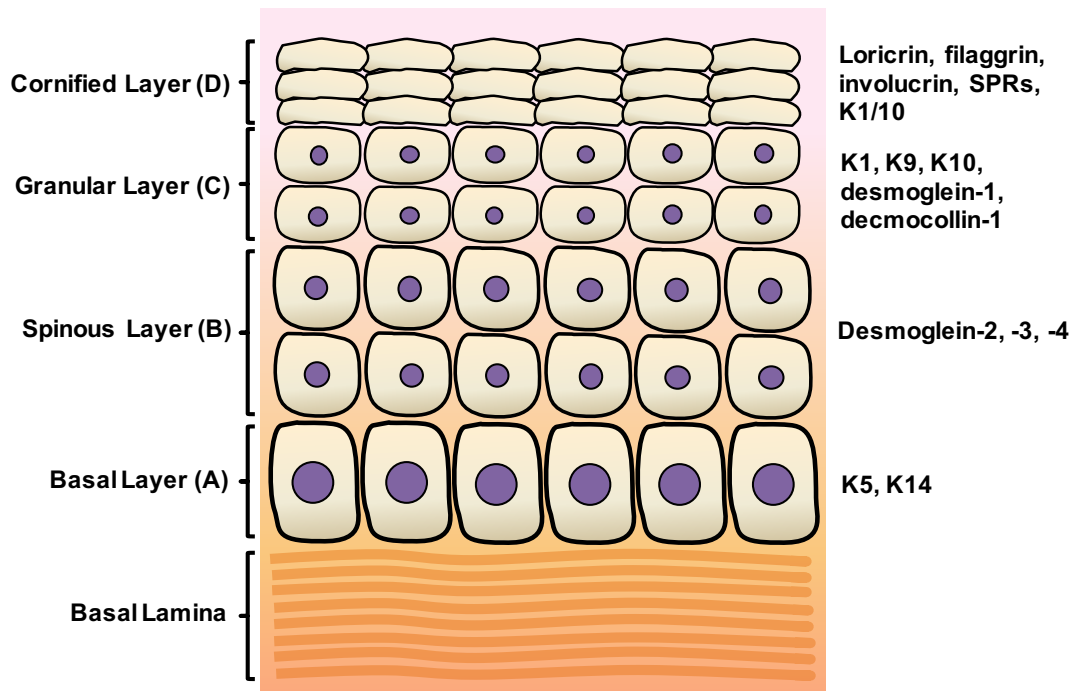


Figure 1.6. Cell differentiation in the epidermis. The proteins that are expressed in the cell membrane/wall in each layer are listed. Cell differentiation begins as cells migrate from the basal layer (A) to the spinous layer (B) and to the granular layer (C). Cells in the cornified layer (D) are terminally differentiated and are sloughed off the surface of the epithelium. K=Keratin, SPR=small proline-rich protein. Adapted from Candi *et al.* 2005 [229].

1.6.2 Skin Immune Response

The skin possesses a robust innate and adaptive immune system to tackle infection if the skin barrier is breached (Figure 1.7). There are many resident immune cells in the skin including specialised dendritic cells known as Langerhans cells which are resident in the epidermis [228]. In the dermis, there are dendritic cells, macrophages, mast cells, T and B cells, plasma cells, and NK cells and their contribution to the cutaneous immune response has been the subject of a number of reviews [228, 231]. Keratinocytes are also very important in the cutaneous immune responses. They produce large quantities of IL-1 α , TNF α and AMPs such as β -defensins in response to various stimuli, including the presence of bacteria [231]. Keratinocytes also produce a large number of chemokines and other immunoregulatory cytokines in response to stimulation and these products in turn activate the resident innate immune cells in the skin, further up-regulating expression of other inducible mediators and facilitating the recruitment of additional immune cells from the blood (Figure 1.6) [231]. Keratinocytes recognise the presence of *S. aureus* using PRRs. TLR-2 present on keratinocytes recognise *S. aureus* PAMPs including peptidoglycan and lipopeptides [232]. Keratinocytes also express IL-1R, which is activated by both autocrine and paracrine produced IL-1 α and IL-1 β [225]. Both IL-1R and TLR-2 signal through MyD88 to activate downstream signalling, through NF- κ B and mitogen-activating protein kinase (MAPK) signalling pathways, leading to the transcription of proinflammatory genes, such as TNF α and IL-6 and CXCL8, which recruit neutrophils during *S. aureus* skin infections [233, 234]. *S. aureus* subcutaneous infection of MyD88-deficient mice found that these mice had a reduced capacity for neutrophil recruitment and cytokine production, resulting in increased susceptibility to infection. Further study identified the IL-1R-MyD88 signalling axis, but not TLR2/MyD88 signalling, as being primarily important for recruitment of neutrophils and protection against *S. aureus* SSTIs [235].

Clinical studies have highlighted the importance of the IL-1–IL-17 axis in cutaneous host defence against *S. aureus* [225]. Patients with IL-1 receptor-associated kinase 4 (IRAK4) deficiency, where IL-1R and TLR signalling is impaired, and AD-HIES patients who have defective IL-17 responses, suffer from recurrent *S. aureus* SSTIs [182, 233, 236]. IL-1 functions to promote the production of IL-17 and related cytokines from Th17 cells but also from subpopulations of $\gamma\delta^+$ T cells [125]. These IL-17 producing cells, comprising both Th17 cells and $\gamma\delta^+$ T cells, have an important role in epithelial site immune responses. Through the production of IL-17A and IL-17F, they induce the expression of neutrophil-attracting chemokines and granulopoiesis factors thus promoting neutrophil recruitment and abscess formation [166, 237, 238]. In murine studies, resident epidermal $\gamma\delta^+$ T cells were required for neutrophil recruitment during *S. aureus* skin infection. IL-17 production by $\gamma\delta^+$ T cells was shown to be TLR2- and IL-23-dependent [166]. In addition, IL-17 can also induce keratinocytes to produce antimicrobial peptides [180]. Murine models have shown that the related Th17 cytokine IL-22 is also involved in protection against SSTIs [166, 226]. In a murine skin abscess model, the inhibition of either IL-17A or IL-22 alone resulted in significantly larger lesion size, indicating that both IL-17A and IL-22 are necessary for local control of SSTIs [192]. A recent study demonstrated that a model vaccine containing Als3p with alum, specifically drove Th17 (IL-17 and IL-22) immunity that was able to contain *S. aureus* SSTIs [226]. Overall, it is clear that the skin possesses a unique immune response to infection, and vaccines targeting *S. aureus* SSTIs may need to be tailored to specifically drive the relevant responses.

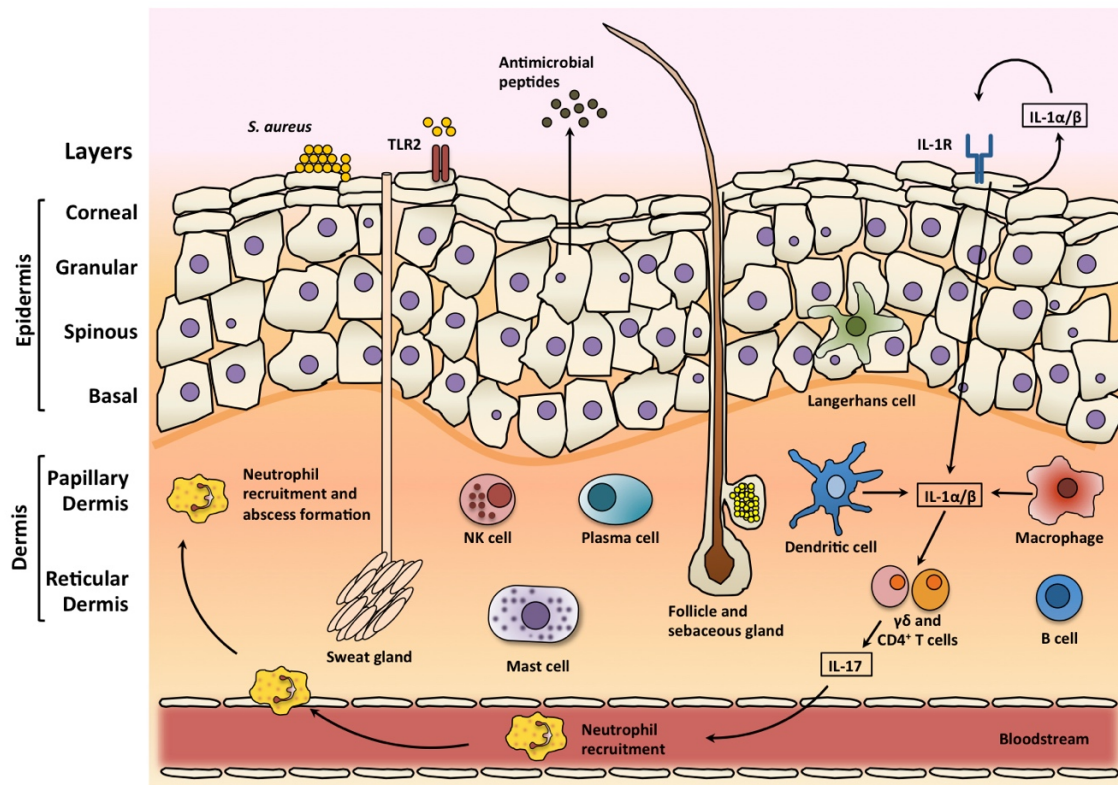


Figure 1.7. The immune responses of the skin. There are resident skin immune cells including Langerhans cells in the epidermis and dendritic cells, macrophages, mast cells, B and T cells, plasma cells and natural killer (NK) cells in the dermis. During a *S. aureus* skin infection, these cells produce proinflammatory cytokines, chemokines and adhesion molecules, which can promote the recruitment of neutrophils from the bloodstream. Proinflammatory cytokines also induce the production of antimicrobial peptides that have bacteriostatic or bactericidal activity against *S. aureus*. Toll-like receptor 2 (TLR2) is activated by *S. aureus* lipoproteins and lipoteichoic acid, and interleukin-1 receptor (IL-1R) is activated by IL-1 α and IL-1 β . IL-1 promotes the production of IL-17 and related cytokines from T cells. Through the production of IL-17, $\gamma\delta^+$ and $CD4^+$ T cells induce the expression of neutrophil-attracting chemokines and granulopoiesis factors thus promoting neutrophil recruitment and abscess formation. Figure from Lacey KA, *et al.* (2016) [21].

1.8 Project Aims

S. aureus causes the vast majority of SSTIs in humans. *S. aureus* has become increasingly resistant to antibiotics and CA-MRSA skin infections are occurring with increasing frequency in healthy individuals. There is an urgent need for new strategies to tackle *S. aureus* infections and vaccines offer a potential solution to this epidemic of antimicrobial resistance. However, to date, vaccine approaches have failed to protect against *S. aureus* infection, likely due to the inefficient induction of cellular immunity. It is now accepted that T cells are essential for promoting a successful immune response against *S. aureus* infection. However, there is a paucity of information regarding T cell antigens expressed by *S. aureus*. In addition, it is likely that site specific vaccines for skin infection will need to be developed. *S. aureus* can express a large number of CWA proteins, which are covalently attached to the cell wall peptidoglycan. The virulence potential of many CWA proteins has been demonstrated in other infection models, however, there is a lack of information regarding their roles during SSTIs and whether they might represent attractive T cell antigens remains to be established.

Therefore, this project aims to initially investigate if these proteins are capable of inducing T cell activation and then to establish the role of CWA proteins during SSTI infection, with the ultimate goal of advancing knowledge towards the development of a vaccine capable of protecting against *S. aureus* SSTIs.

To achieve this, the following specific aims will be addressed:

1. Create CWA protein null mutants in the CA-MRSA USA300 strain, LAC::*lux*, enabling in depth analysis of CWA protein function during SSTI and as T cell antigens.
2. Investigate the ability of purified CWA proteins and specifically subdomains of ClfA to activate human T cells.

3. Investigate ClfA's potential as a candidate vaccine antigen by establishing if vaccines composed of sub-domains of ClfA are capable of eliciting Th1 and Th17-mediated protection against systemic *S. aureus* infection.
4. Characterise the contribution of CWA proteins to virulence and specifically abscess formation in a murine model of *S. aureus* skin infection.
5. Establish if CWA proteins are capable of offering protection against *S. aureus* SSTIs when used as vaccine antigens.

Chapter 2

Materials and Methods

2.1 *S. aureus* mutant strain construction

2.1.1 Bacterial strains and growth conditions

All bacterial strains, plasmids and oligonucleotides are listed in Table 2.1. *S. aureus* strains were grown on trypticase soy agar (TSA) or trypticase soy broth (TSB). *E. coli* was grown in Luria broth (L-broth) or agar (L-agar). Unless otherwise stated, cultures were grown at 37 °C and broth cultures were shaken at 200 r.p.m. Antibiotics were added as follows: ampicillin (Amp) at 100 µg/ml, chloramphenicol (Cm) at 10 µg/ml, erythromycin (Erm) at 10 µg/ml and anhydrotetracycline (ATc) at 1 µg/ml.

2.1.2 DNA Manipulation

2.1.2.1 Preparation of plasmid and genomic DNA

Plasmid DNA was isolated using the Wizard® Plus SV Miniprep kit (Promega) or Qiagen® Plasmid *Plus* Midi kit according to the manufacturer's recommendations. DNA purification was carried out using PCR Clean-up System (Promega). Genomic DNA was prepared using Bacterial Genomic DNA purification kit (Edge BioSystems). Plasmids and genomic DNA extracts from *S. aureus* required the addition of 200 µg/ml of lysostaphin to digest cell wall peptidoglycan. The concentration of isolated DNA was measured using a nanodrop spectrophotometer (NanoDrop 1000, Thermo Scientific). DNA samples were run on gels containing 1 % agarose in Tris-acetate-EDTA (TAE) buffer. Electrophoresis of samples was routinely performed at 100 V. Gels were bathed in ethidium bromide for 10 min, washed and viewed under UV light. Gel images were imaged using an Alpha Imager.

2.1.2.2 Polymerase Chain Reaction

Polymerase Chain Reaction (PCR) amplification was carried out in a DNA thermal cycler (Techne or PIKO). Reactions were typically carried out using Velocity DNA polymerase (Bioline) or Phire Hot Start DNA polymerase (Finnzymes) according to the manufacturer's instructions. Plasmid DNA (1-10 ng) or genomic DNA (20-150 ng)

were used as templates for PCR. Primers were purchased from Integrated DNA Technologies and are listed in Table 2.2. Initial denaturation was carried out at 98 °C (30 s) followed by 30 cycles of denaturation (10 s) at 98 °C, 20 s annealing at 52-58 °C and extension at 72 °C. When amplifying plasmid DNA, a 15 s extension time per 1kb DNA was used. For genomic DNA a longer extension time was used (30 s per kb). A final extension step was carried out at 72 °C for 5 min. PCR products were purified using PCR clean-up system (Promega).

2.1.2.3 Sequence and ligase-independent cloning

Cloning was carried out using the sequence and ligase-independent cloning (SLIC) procedure as described by Li and Elledge [239]. Both vector and insert were amplified by PCR. Primers for amplification of insert were designed with 5' extensions, typically 24 bp in length that possessed sequence homology to the end regions on the amplified vector. Both vector and insert DNA were incubated with T4 polymerase (3 U; NEB), NEB Buffer 2, molecular grade BSA (NEB), Dithiothreitol (DTT; 5 mM) and urea (200 mM). The reaction mix was incubated at 23 °C for 20 min and stopped by the addition of EDTA (25 mM), followed by further incubation at 75 °C for 20 min. 5 µl each of vector and insert with single-stranded ends were mixed and were allowed to anneal. This reaction was incubated at 65 °C for 10 min followed by a slow decrease in temperature from 65 - 25 °C with 1 min hold for each degree. The entire reaction volume was used for transformation of *E. coli* SA08B or IM08B.

2.1.3 Transformation of *S. aureus* and *E. coli* strains

2.1.3.1 Preparation and electroporation of *E. coli* SA08B and IM08B

The pIMAY plasmid was introduced into the *E. coli* strains SA08B or IM08B by electroporation [240]. Electrocompetent cells were prepared by growing *E. coli* to an optical density of 600 nm (OD₆₀₀) of 0.7. Cells were harvested at 7,000 x g for 10 min at 4 °C and washed three times with sterile 10 % (v/v) glycerol. Aliquots were stored at -80 °C.

Plasmid DNA was added to cells and transferred to electroporation cuvettes (Bio-Rad) and pulsed at 1.8 kV/cm, 200 Ω and 25 μ F. Cells were immediately resuspended in 1 ml L-broth and incubated for 1 h. Cells were then plated on L-agar containing the appropriate antibiotic. Transformants were screened by PCR and restriction mapping.

2.1.3.2 Preparation and electroporation of *S. aureus*

Plasmids isolated from *E. coli* SA08B or IM08B were introduced into *S. aureus* by electroporation. Electrocompetent cells were prepared as described by Löfblom *et al.* [241]. Prior to electroporation, cells were centrifuged and resuspended in 10 % glycerol and 500 mM sucrose. Up to 5 μ g of plasmid DNA was added to the cells and transferred into a cuvette. Electroporation was carried out at 2.1 kV, 100 Ω and 25 μ F. Immediately after electroporation, TSB supplemented with 500 mM sucrose was added to the cells and these were incubated for 1.5 h. Cells were plated on TSA containing Cm and incubated at 28 °C. Transformants were screened by PCR, restriction mapping, adhesion assay and Western Immunoblotting.

2.1.4 *S. aureus* strain construction

2.1.4.1 *S. aureus* strain construction by allelic exchange mutagenesis

LAC::*lux clfA*, LAC::*lux clfB* and LAC::*lux spa* were constructed by allelic exchange using plasmid pIMAY [242]. Primers were designed to amplify a 500-600 bp region of DNA located upstream and downstream of the gene to be deleted. Genomic DNA from *S. aureus* LAC::*lux* was used as template and the resulting PCR products were denatured and allowed to reanneal via the complementary sequences in primers B and C and then amplified using primers A and D, resulting in a 1000-1200 bp fragment consisting of linked upstream and downstream sequences of the gene (the cassette). The cassette was joined to pIMAY between *EcoRI* and *SalI* restriction sites using SLIC.

The resulting plasmid was transformed into *E. coli* SA08B or IM08B and verified by DNA sequencing. The plasmid was then transformed into electrocompetent LAC::*lux*. Cells were plated on TSA containing Cm and incubated at 28 °C for 48 h. Putative positive colonies were streaked on TSA containing Cm and grown at 28 °C. Colonies were screened by PCR to confirm the presence of replicating plasmid. In order to select for plasmid integrants, a single colony was vortexed in TSB and dilutions were plated on TSA containing Cm and incubated at 37 °C. Plasmid integration was confirmed by colony PCR using MCS primers. Positive integrants were screened with a second set of primers (OUT F/D, OUT R/A, Table 2.2) to ascertain the side of integration.

To encourage plasmid excision, one colony was grown in broth at 28 °C. The broth was plated onto TSA containing ATc. Plates were incubated at 28 °C for 48 h. Large colonies were streaked onto TSA containing ATc and TSA Cm and incubated at 37 °C. Cm sensitive colonies were screened by colony PCR with the OUT primers, with the PCR extension time allowing for the amplification of the wild-type product. Genomic DNA was isolated from putative mutants and the OUT PCR was repeated.

2.1.4.2 *S. aureus* strain construction using phage transduction

Mutations marked with antibiotic resistance were moved between *S. aureus* strains by generalised bacteriophage 85-mediated transduction [243]. Bacteriophage were propagated on the donor strain and used to infect the recipient strain. To select for recipient bacteria carrying the desired mutation, antibiotic selection was used. Putative transductant colonies were single colony purified three times on TSA plates containing the appropriate antibiotic and 0.05 % sodium citrate (w/v) to eliminate contaminating phage particles. Strains LAC::*lux srtA* and LAC::*lux hla* were constructed by transduction of *srtA*::Erm^r [244] or *hla*::Erm^r [245] respectively into strain LAC::*lux*.

2.2 Validation of *S. aureus* mutant strains

2.2.1 Isolation of *S. aureus* cell-wall associated and secreted proteins for immunoblotting

To extract cell wall-associated proteins, cultures of *S. aureus* were harvested, washed twice in PBS and resuspended in lysis buffer (50 mM Tris-HCl, 20 mM MgCl₂, pH 7.5) supplemented with raffinose (30 % w/v) and complete protease inhibitors (40 µl/ml, Roche). Cell wall proteins were solubilised by incubation with lysostaphin (100 µg/ml; AMBI) for 8 min at 37 °C. Protoplasts were removed by centrifugation at 16,000 x g for 5 min. Both protoplasts and the supernatant (containing solubilised cell wall proteins) were boiled for 10 min in Laemmli sample buffer.

To isolate secreted proteins, cultures were harvested and the supernatant was passed through a 0.2 µm filter (Whatman). Filtered supernatants were concentrated using a centrifugal filter (Millipore) with a molecular weight cut off of 30000 before Laemmli sample buffer was added. Samples were used for SDS-PAGE or stored at -20 °C.

2.2.2 Western immunoblotting

Proteins samples were diluted 2-fold in Laemmli sample buffer and boiled for 5-10 min before separation by SDS-PAGE. Electrophoresis was carried out at 120 V. Proteins were electroblotted onto PVDF membranes (Roche) for 1 h at 100 V using a wet transfer cell (Bio Rad). Membranes were incubated for 1 h at 4 °C in TS buffer (10 nM Tris-HCL, pH 7.4, 150 nM NaCl) containing 10 % (w/v) skimmed milk (Marvel). Primary antibodies diluted in 10 % (w/v) Marvel/TS buffer were incubated with the membranes for 1 h at room temperature. Antibodies are described in Table 2.3. Unbound antibody was removed by three 10 min washes with TS buffer. When necessary, secondary antibodies diluted in 10 % (w/v) Marvel/TS buffer were incubated with the membranes for 1 h at room temperature. Unbound secondary

antibody was removed by washing with TS buffer. Chemiluminescent substrate LumiGlo and peroxidase detection system (Cell Signalling Technology) was used according to manufacturer's instructions. Blots were developed and visualised using ImageQuant TL software (GE).

2.2.3 Adherence of *S. aureus* to immobilised ligands

Microtiter plates (Nunc) were coated with protein ligand in PBS or sodium carbonate buffer (15 mM Na₂CO₃, 35 mM NaHCO₃, pH 9.6) and incubated overnight at 4 °C. Wells were washed with PBS and blocked with 5 % (w/v) BSA for 2 h at 37 °C. The plates were washed with PBS and a *S. aureus* cell suspension (OD₆₀₀ = 1.0) was added and the plates were incubated for 2 h at 37 °C. After washing, bound cells were fixed with formaldehyde (25 % v/v) and stained with crystal violet (0.5 % v/v). Following washing with PBS, acetic acid (5 % v/v) was added to each well and incubated for 5 min at room temperature with shaking. The absorbance was measured at 570 nm in an ELISA plate reader (Labsystems).

2.2.4 *S. aureus* growth curve assay

Overnight cultures of *S. aureus* were diluted to an OD₆₀₀ of 0.05 in TSB. 200 µl of bacterial culture was added to triplicate wells in a flat-bottomed 96 well microtiter plate. The plate was incubated at 37 °C for 12 h in a plate reader (Synergy H1 Plate Reader, BioTek). Absorbance values at 570 nm were recorded at 15 min intervals.

2.2.4 Haemolytic activity of *S. aureus*

Alpha (α) and delta (δ)-haemolysin production by *S. aureus* strains was tested on sheep blood agar plates. Wild-type strains and the corresponding mutant strains were streaked perpendicular to the strain RN4220. The production of α-haemolysin can be visualized as a zone of clearance surrounding the streaked bacteria. At the intersection of the wild-type or mutant and RN4220 the β-toxin (from RN4220) and δ-haemolysin (from test strain) synergise to produce a zone of clear haemolysis.

2.3 Protein purification

2.3.1 Purification of histidine-tagged recombinant proteins

Recombinant proteins (ClfA N123, ClfA N23 and ClfB N123) were expressed from pQE30 with an N-terminal hexa-histidine affinity tag to allow purification by nickel affinity chromatography. The pQE30 vector contains an IPTG-inducible promoter for controlled expression of recombinant proteins. Cultures of *E. coli* XL1-Blue containing pQE30 were grown to OD₆₀₀ of 0.5 and then induced with 1 nM IPTG for 3 h at 37 °C. Cells were harvested and resuspended in PBS containing protease inhibitors (Roche) prior to breakage in a French pressure cell. The lysate was centrifuged at 17,000 x g for 20 min. DNase was added to the supernatant followed by filtration through a 0.45 µm filter.

A HiTrap™ Chelating HP column (5 ml; GE Healthcare) was used according to the manufacturer's instructions with the flow rate controlled using a peristaltic pump. The filtered, cleared cell lysate was applied to the column and bound protein was eluted from the column with a continuous linear gradient of imidazole (5-100 mM) in 0.5 M NaCl and 20 mM Tris-HCL (pH 7.9). Elution was monitored by measuring the OD₂₈₀ of the eluate. Positive fractions were analysed by SDS-PAGE and visualised by Coomassie blue staining. Fractions containing the recombinant protein were dialysed against PBS for 16 h at 4 °C. Protein concentrations were determined by measuring absorbance at 280 nm.

2.3.2 Purification of GST-tagged recombinant proteins

Recombinant proteins (ClfA N1 and GST) were expressed from pGEX-4T2 with an N-terminal glutathione-S-transferase (GST) IPTG-inducible affinity tag in *E. coli* TOPP3. Cultures were induced with 1 mM IPTG for 3 h at 37 °C. Cells were harvested and resuspended in 40 ml PBS containing protease inhibitors (EDTA-free; Roche) prior to lysis in a French pressure cell. The lysate was centrifuged and

DNase (1 mg/ml) was added to the supernatant followed by filtration through a 0.45 µm filter.

A GStap™ FF column (5 ml; GE Healthcare) was equilibrated using PBS. The filtered, cleared cell lysate was applied to the column. Bound protein was eluted from the column. Positive fractions were analysed by SDS-PAGE after which proteins were visualized by Coomassie blue staining. Fractions containing the recombinant protein were dialysed against PBS for 16 h at 4 °C. Protein concentrations were determined by measuring absorbance at 280 nm.

2.3.3 Endotoxin removal from recombinant proteins

Endotoxins were removed from recombinantly produced proteins using Detoxi-Gel™ Endotoxin Removing Columns (Thermo Scientific). Protein samples were applied to the column and incubated for 30 min. Samples were eluted and collected in fractions. Protein concentrations were determined by measuring absorbance at 280 nm.

2.4 In vitro human T cell assay

2.4.1 Heat-inactivation of *S. aureus*

Overnight cultures of *S. aureus* were resuspended in PBS to an OD₆₀₀ of 1.0. The bacterial suspensions were incubated at 90 °C for 45 min and then washed 3 times. Protein concentration was determined by Pierce BCA Protein Assay (Thermo Scientific) kit. Bacterial killing was verified by plating on TSA and incubating at 37 °C for 5 d. The bacteria was stored at 4 °C for up to 4 weeks.

2.4.2 Isolation and stimulation of human T cells

Blood donor buffy coats were obtained from the Irish Blood Transfusion Service, St. James Hospital, Dublin. To isolate peripheral blood mononuclear cells, buffy coats were mixed with PBS (1:1 ratio) and layered over a Lymphoprep gradient (Axis-Shield) for density centrifugation at 900 x g for 20 min. The plasma layer was discarded and the buffy coat layer was removed and centrifuged at 650 x g for 10 min. The cells were resuspended in PBS and centrifuged at 250 x g for 7 min to remove platelets. Cells were resuspended in complete RPMI (cRPMI) and enumerated by Trypan blue staining. cRPMI comprised RPMI (Sigma), 10 % (vol/vol) fetal calf serum (Biosera), 100 mM L-glutamine (Gibco) and 100 µg/ml penicillin-streptomycin (Gibco).

CD4⁺ T cells were purified using CD4⁺ T cell Isolation Kit (Miltenyi Biotec) according to manufacturer's instructions. Purified CD4⁺ cells were labelled with 5 µM carboxyfluorescein diacetate succinimidyl ester (CFSE), enumerated and resuspended in cRPMI at 1x10⁶ cells/ml. PBMCs were gamma-irradiated at 30 Gy with a ¹³⁷Cs source (Gammacell 3000, Best Theratronics) for 9 min. Cells were enumerated and resuspended in cRPMI at 1x10⁶ cells/ml.

CFSE-labelled CD4⁺ cells (1x10⁵) were co-cultured with irradiated PBMCs (1x10⁵) in 96-well round-bottomed plates at 37 °C with 5 % CO₂. Cells were cultured in cRPMI

alone (negative control), staphylococcal enterotoxin A (100 ng/ml, positive control), heat-inactivated *S. aureus* (1 µg/ml) or purified *S. aureus* antigens (0.88 µM). T cell proliferation was assessed on day 10 by flow cytometry.

2.5 *In vivo S. aureus* infection models

2.5.1 Mice

Wild-type BALB/c mice were purchased from Charles River Laboratories at 6-8 weeks old. Wild-type C57BL/6 mice were bred in-house. Mice were housed 5 per cage under specific pathogen free (SPF) conditions in the TCD Comparative Medicines facility. All animal experiments were conducted under licence (AE19136/P006) in accordance with the recommendations and guidelines of the Health Products Regulatory Authority (HPRA), the competent authority in Ireland.

2.5.2. *In vivo* bioluminescent subcutaneous abscess model

BALB/c mice were anaesthetized with an intraperitoneal (i.p.) injection of ketamine/xylazine (75 µl per mouse) and their backs were shaved. The skin at the injection site was disinfected with 70 % ethanol. Mice were injected subcutaneously (s.c.) with 100 µl of LAC::*lux* WT, *srtA*, *spa*, *clfA*, *clfB* or *hla* containing 2×10^7 CFU. For *in vivo* bioluminescence imaging, mice were anaesthetized via inhalation of 2 % isoflurane and imaged using a PhotonIMAGER (Biospace Lab). Data are presented on colour scale overlaid on a greyscale photograph of mice and were quantified as total photon flux (photons/second/steradian, ph/s/sr) within a circular region (1.3 cm²) of interest using M3 Vision™ software (Biospace Lab). Measurements of total lesion size (cm²) were computed using the M3 Vision™ software. Digital photographs (Canon PowerShot SX710 HS) of mice were taken daily.

Mice were euthanized at specific time points and tissues were harvested. Skin abscesses were collected using an 8 mm punch biopsy for analyses of bacterial burden, histology or immune response. The liver, kidneys and spleens were isolated to assess bacteria burden. Skin abscess punch biopsies were weighed and homogenized using a homogenizer (Kinematica Polytron PT 2500E) with a 7 mm blade. Organs were also homogenized. The homogenizer was cleaned between samples using 1 M NaOH, H₂O, 70 % (v/v) EtOH and PBS. Serial dilutions of the

homogenate were prepared in PBS and spread on TSA plates and incubated for 24 h at 37 °C.

For *in vivo* inhibition of the ClfB-loricrin interaction during *S. aureus* skin infection, LAC::*lux* WT (2×10^7 CFU) was pre-incubated with recombinant GST, GST-tagged loricrin region 2v (L2v; 24 μ M) or PBS for 30 min at RT. The bacterial cell-peptide mixture was administered s.c. as described in section 2.18.1 and bioluminescence imaging was used to monitor the infection over a 72 h time period.

2.5.2.1 Isolation of cells from murine skin

To isolate cells from murine skin, the skin was cut into pieces and added to 2 ml of digestion cocktail (2 mg/ml collagenase XI, 0.5 mg/ml hyaluronidase, 0.1 mg/ml DNase in cRPMI) and incubated at 37 °C at 255 r.p.m. for 45 min. After incubation, 15 ml of cRPMI was added to the digested skin and the mixture was passed through a 40 μ M filter to obtain single cell suspensions.

2.18.2 *In vivo S. aureus* peritonitis model

Mice were infected by intraperitoneal injection of 5×10^8 CFU of *S. aureus* PS80 in 100 μ l PBS. Mice were euthanised at specific time points post-infection and the peritoneum was lavaged with 2 ml PBS and the liver, kidneys and spleens were isolated to assess bacteria burden.

2.6 In vivo vaccination models

2.6.1 Subcutaneous vaccination with subdomains of ClfA combined with CpG for protection against systemic *S. aureus* infection

To investigate if subdomains of ClfA were capable of driving protective immune responses against systemic *S. aureus* infection, naïve C57 mice were vaccinated via s.c. injection with CpG (50 µg/mouse, Hycult Biotech) alone; CpG in combination with ClfA N123, N23, N1 or GST (1 µg/mouse); or vehicle (PBS) on d 0, 14, and 28 (Figure 2.1). At 5 weeks post final boost (d 63), and prior to challenge with *S. aureus*, mice were sacrificed to analyse immune responses. Peritoneal exudate cells (PECs) were recovered from the peritoneal cavity following lavage with sterile PBS (2 ml) and analysed by flow cytometry. Vaccinated mice were then challenged with *S. aureus* PS80 via i.p. injection (5×10^8 CFU). At specific time points post-challenge, mice were sacrificed and bacterial burdens and immune responses were assessed.

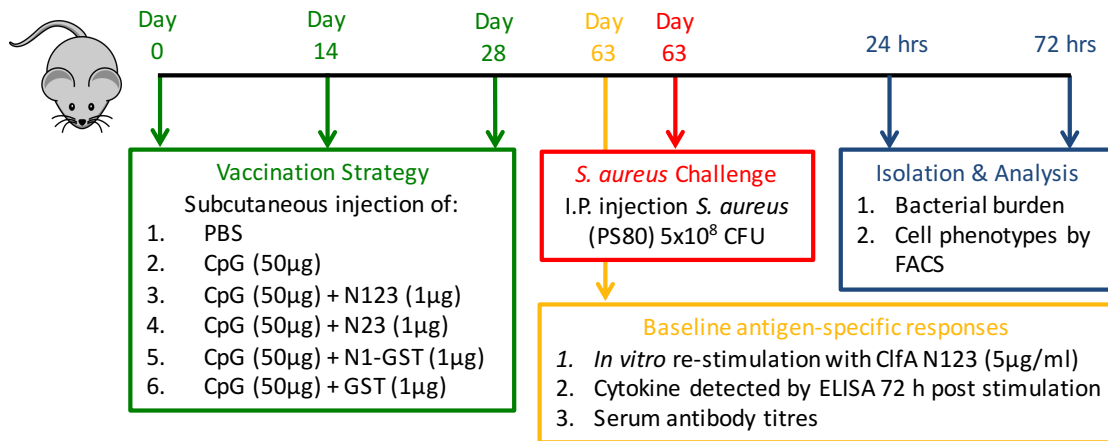


Figure 2.1. Subcutaneous vaccination with subdomains of ClfA combined with CpG. Mice were vaccinated via s.c. injection with PBS, CpG (50 µg/mouse) alone or in combination with ClfA N123, N23, N1 or GST (1µg/mouse) on d 0, 14 and 28. On d 63 cells from vaccinated mice were stimulated *in vitro* with ClfA N123 for 72 h to assess baseline T cell responses via cytokine production. Sera was also isolated to assess antigen-specific antibody titres. On d 63 another group of vaccinated mice were challenged with *S. aureus* PS80 (5×10^8 CFU) via i.p injection. At 24 and 72 h post-infection the bacterial burden, T cell responses and phagocyte influx were assessed and compared between the groups.

2.6.2 Subcutaneous vaccination with ClfA and ClfB combined with CpG or alum for protection against *S. aureus* SSTI

To investigate if ClfA and ClfB were capable of driving protective immune responses against *S. aureus skin* infection, naïve BALB/c mice were vaccinated via s.c. injection with CpG (50 µg/mouse, Hycult Biotech) or alum (0.5 mg/ml, Brenntag) alone, or in combination with ClfA or ClfB (5 µg/mouse) on d 0, 14, and 28 (Figure 2.2). At 2 weeks post final boost (d 42), and prior to challenge with *S. aureus*, mice were sacrificed to analyse immune responses. Vaccinated mice were then challenged with *S. aureus* LAC::*lux* WT via s.c. injection (2×10^7 CFU) and bioluminescent imaging was performed to monitor the infection. Mice were sacrificed at d 6 post-infection and bacterial burden was assessed.

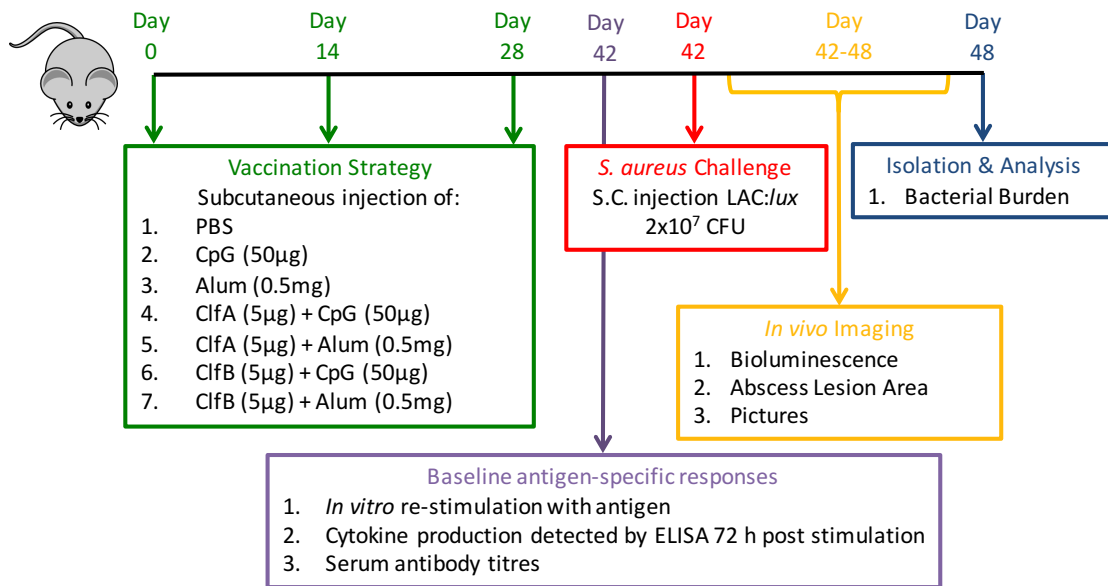


Figure 2.2. Subcutaneous vaccination with ClfA and ClfB combined with CpG or alum. Mice were vaccinated via s.c. injection with PBS, CpG (50 µg/mouse) or alum (0.5 mg/mouse) alone or in combination with ClfA N123 or ClfB N123 (5 µg/mouse) on d 0, 14 and 28. On d 42 cells from vaccinated mice were stimulated *in vitro* with ClfA or ClfB for 72 h to assess baseline T cell responses via cytokine production. Sera was also isolated to assess antigen-specific antibody titres. On d 42 another group of vaccinated mice were challenged with *S. aureus* LAC::*lux* WT (2x10⁷ CFU) via s.c. injection. The infection was monitored by *in vivo* bioluminescence imaging. At d 48, the bacterial burden was assessed and compared between the groups.

2.6.3 Measuring the cellular immune response to immunisation

To investigate if cells exposed *in vivo* to *S. aureus* antigens could respond to *in vitro* stimulation with *S. aureus* antigens, antigen recall experiments were used. Cells were isolated from ILN and spleens of vaccinated mice. ILN and spleen cells were disrupted in cRPMI using 40 µM filters to obtain single cell suspensions. Cell samples were resuspended at 2×10^6 cells/ml in cRPMI and 200 µl was transferred into wells of a 96-well round-bottomed plate. Cells were stimulated with the relevant antigen (5 µg/ml). Cells were also stimulated with anti-CD3 (1 µg/ml), PMA (10 ng/ml) as a positive control. After 72 h incubation at 37 °C and 5 % CO₂, the cell supernatants were collected for cytokine analysis by ELISA.

2.6.4 Measuring the humoral immune response to immunisation

To measure humoral immune responses, blood was collected from vaccinated animals by cardiac puncture or tail vein bleeding. Collected blood was allowed to settle at room temperature for 1 h, centrifuged at 750 x g for 5 min and sera contained in the supernatant was stored at -20 °C until further analysis.

2.6.4.1 Antibody end point titre assay

Medium binding 96-well plates were coated with ClfA N123 or ClfB N123 (1 µg/ml, 50 µl/well) and incubated for 2 h at 37°C. Plates were washed 3 times in ELISA wash buffer and blocked with 10 % (w/v) milk powder (Sigma Aldrich) in PBS (100 µl/well) for 2 h at RT. After blocking, plates were washed and coated with doubling dilutions of serum samples in PBS (50 µl/well) (starting concentration: 1 in 400 dilution for ClfA, 1 in 50 for ClfB). Samples were incubated over night at 4 °C. Plates were washed and anti-mouse IgG-HRP (1 in 4000, SouthernBiotech; 50 µl/well) was added and incubated at 37°C for 1 h. The plates were washed and incubated at RT in the dark with TMB substrate solution. The reaction was stopped by the addition of 25 µl of 1M H₂SO₄. Absorbance was then measured at 450 nm on a microplate reader.

To determine the end point antibody titres, best fit linear regression curves were calculated for the absorbance values obtained for each serum titration. These curves were extrapolated against titrations of naïve sera to find the intersection point between the two. These intersection points were used to find the corresponding dilution at which the absorbance values reached PBS control levels. This intersection revealed the Log_{10} value of the antibody titres (Figure 2.3).

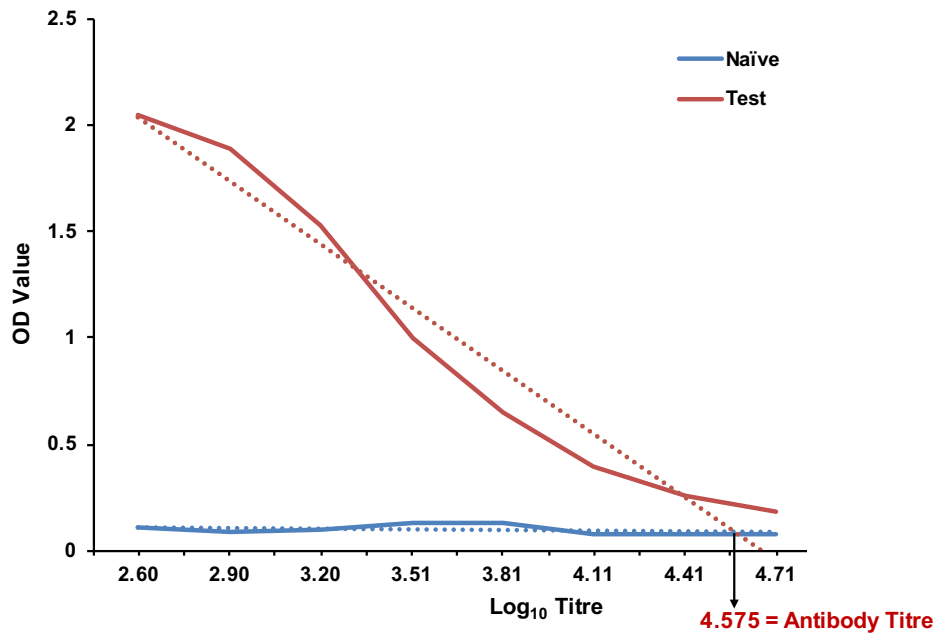


Figure 2.3. Determining antibody end point titres. The OD values for each serum titration were plotted on a curve and a best fit linear regression curve was calculated for both naïve sera (control) and the experimental (test) sera. A standard curve (dotted line) was calculated for the test and naïve samples. The intersection of these curves was used to find the corresponding dilution at which the absorbance values reached naïve control levels. The intersection revealed the Log₁₀ value of the antibody titres.

2.6.4.2 Neutralising antibody assay

A flat-bottomed 96-well plate was coated with 2 µg/ml fibrinogen in PBS and incubated at 4°C overnight. Plates were washed with PBS and blocked with 5 % (w/v) BSA for 2 h at 37 °C. Stationary phase cultures of PS80 were washed and adjusted to an OD_{600nm} of 1 in PBS. Sera (1 in 60 dilution) were incubated with bacteria on a shaker for 30 min at RT.

After blocking, the plate was washed 3 times in PBS and 100 µl of sera: bacteria solution was transferred to the fibrinogen coated plate. The plate was incubated for 90 min at 37 °C. Following incubation, the plate was washed and bound cells were fixed with formaldehyde (25 % v/v) and stained with crystal violet (0.5 % v/v). Following washing with PBS, acetic acid (5 % v/v) was added to each well and incubated for 5 min at room temperature with shaking. The absorbance was measured at 570 nm in an ELISA plate reader (Labsystems).

The presence of neutralising antibodies was determined by testing the ability of serum to inhibit the adherence of *S. aureus* to fibrinogen. Adherence was expressed as a percentage of bacterial adherence in the absence of serum. Percentage inhibition was determined by subtracting the percentage adherence values from 100.

2.7 Histology

2.7.1 Tissue Preparation

Skin abscess tissue was fixed in 10 % formalin for 48 h at room temperature. Tissue was dehydrated through ethanol and underwent clearing through xylene and infiltrated with paraffin wax using a tissue processor (Leica TP1020). Tissue was embedded in paraffin wax using a Tissue Embedding Center (Leica EG1150). Embedded sections were sliced horizontally at 5-10 μM using a microtome (Leica RM2235) and placed on positively charged microscope slides (VWR). Slides were incubated at 60 °C over night.

2.7.2 Immunohistochemistry

Tissue samples were deparaffinised and hydrated to water through changes of 100 %, 90 %, and 70 % ethanol and then rinsed in PBS. Antigen retrieval was carried out by heating slides in sodium citrate buffer (10 mM sodium citrate, 0.05 % Tween 20, pH 6.0). The samples were blocked (1 % BSA, 10 % goat serum) for 1 h. Primary antibody (Table 2.3) was added to the samples and incubated at 4 °C overnight. Slides were washed three times in PBS and secondary antibody (Table 2.3) was added and incubated at RT for 1 h. Slides stained for confocal microscopy were washed with PBS and coverslips were mounted using fluorescent mounting medium (Fluoroshield with DAPI, Sigma). Slides were visualised using a Leica SP8 scanning confocal microscope. Loricrin stained slides were developed by adding DAB peroxidase substrate (Vector Labs), before rinsing with cold running water. Slides were dehydrated through 100 % EtOH, soaked in xylene and cover slips were mounted using Sub-X mounting medium (Leica) and samples were visualised by bright field microscopy.

2.7.3 Haematoxylin and eosin staining

Tissue samples were deparaffinised through two changes of xylene. Samples were rehydrated to water. Slides were stained in haematoxylin for 5 min washed in water.

Slides were then stained in eosin for 2 min. The samples were dehydrated through 70 %, 90 % and 100% ethanol and cleared through two changes of xylene. Cover slips were mounted onto the slides using Sub-X mounting medium and samples were visualised by bright field microscopy using an Olympus BX51 microscope.

2.7.4 Histological scoring

H&E stained samples were inspected by two observers blinded in respect to the injected strains and the grade of abscess structure was scored using a histological score of 0-5 (Figure 2.4). Abscess images were analysed using ImageJ software to calculate the area of the abscess and scores were calculated accordingly (Table 2.5).

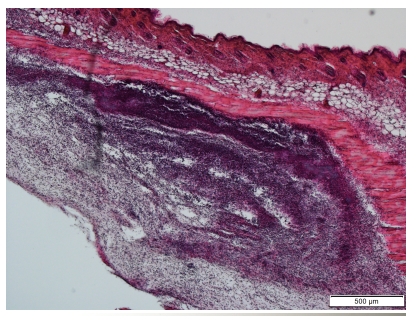
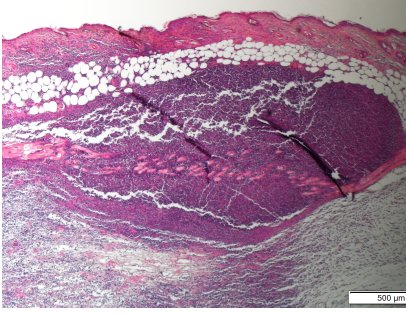
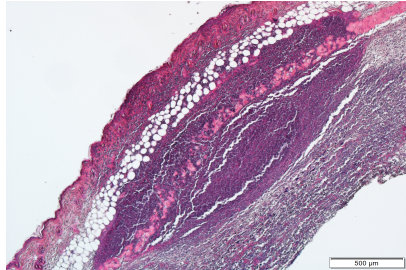
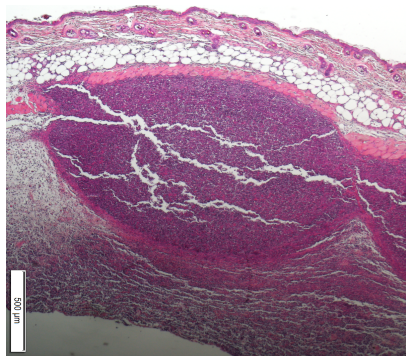
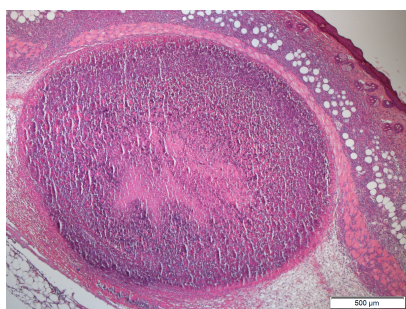
Histology Score		Defining features
1		<ul style="list-style-type: none"> • No defined Structure • Spread out • No abscess wall • Bacteria in surrounding tissue
2		<ul style="list-style-type: none"> • Partially defined structure • Spread out • No abscess wall • Bacteria in surrounding tissue
3		<ul style="list-style-type: none"> • Partially defined structure • Spread out • No clear abscess wall • Bacteria in surrounding tissue
4		<ul style="list-style-type: none"> • Defined structure • Oval/round • Visible abscess wall • Some bacteria in surrounding tissue
5		<ul style="list-style-type: none"> • Very defined structure • Round/oval • Clear abscess wall • All bacteria are inside the abscess

Figure 2.4. Histology Scoring System. The histology score differentiates abscess according to their structure. The score is indicated with a number from 1-5. Defining features of each score are listed.

2.8 ELISA

ELISAs for murine IFN γ , and IL-17A (R&D) were performed on cell culture supernatants, as per the manufacturer's instructions. A high binding 96-well plate was coated with capture antibody (diluted to a working concentration in PBS, 50 μ l/well) and was incubated at RT overnight. Wells were washed in ELISA wash buffer (PBS with 0.05 % Tween 20) 3 times and incubated with 1 % (w/v) BSA (200 μ l/well) for 1 h at RT. Wells were again washed and cytokine standards and samples (50 μ l) were added to the appropriate wells overnight at 4°C. Following sample incubation wells were washed and detection antibody solution (50 μ l/well), was added for 2 h at RT. After washing, 50 μ l streptavidin-horse radish peroxidase (HRP) solution was added to the wells for 20 min at RT in the dark. After washing, TMB substrate solution (50 μ l/well) was added for 20 min at RT in the dark. The reaction was stopped using 1M H $_2$ SO $_4$ (25 μ l/well). Absorbance was measured at 450nm using a micro-plate reader and Softmax Pro software.

2.9 Intracellular cytokine staining and flow cytometry

Brefeldin A (BFA, 5 µg/ml) was added to human T cells co-cultures for the final 16 h of culture at 37 °C with 5 % CO₂. Murine T cell cultures were incubated in the presence of phorbol myristate acetate (PMA, 50 ng/ml), ionomycin (500 ng/ml) and BFA (5 µg/ml) for 4 h 37 °C with 5 % CO₂. Cells were centrifuged and resuspended in Fixable Viability dye (diluted 1:1000 in PBS) for 20 min at 4 °C. Cells were then washed and resuspended in specific cell surface antibodies (Table 2.4, diluted 1:100 in PBS) and incubated at room temperature. Intracellular cytokines were stained with antibodies (Table 2.4) using the Fix & Perm Cell Permeabilization Kit (Life Technologies). Samples were washed and transferred to FACs tubes.

Flow cytometry analysis was acquired with a BD LSRFortessa or BD FACSCanto II using FACS DIVA and FlowJo software (Treestar, Inc). Gating for analysis was set on respective Fluorescence Minus One (FMOs).

To investigate ROS activity within phagocytes 123-dihydrorhodamine (DHR) assays were carried out as previously described [246]. ROS breaks down 123-DHR to rhodamine within the cell. Rhodamine fluoresces on the FL1 channel allowing rhodamine positive cells to be identified by flow cytometry. After surface staining, cells were re-suspended in 100 µl cRPMI containing 25 µl of 5 µM 123-DHR solution. Cells were incubated for 7 min at 37 °C, after which cells were washed in PBS, spun down and resuspended in 1 % paraformaldehyde. Stained cells were then immediately analysed by flow cytometry.

2.10 Statistical analysis

Statistical analysis was performed using GraphPad Prism statistical analysis software. Differences between normally distributed groups were analysed using unpaired Student's t-test, one-way ANOVA with Tukey's comparison post-test or two-way ANOVA with a Bonferroni post-test where appropriate. Differences between non-normally distributed groups were analysed using a Mann-Whitney U test or Kruskal-Wallis test with Dunn's multiple-comparison post-test. Categorical differences between groups were analysed using Fisher's exact test. A p value ≤ 0.05 was considered significant.

Table 2.1. Bacterial strains and plasmids.

Strain or Plasmid	Relevant characteristics	Source or reference
<i>S. aureus</i> strains		
LAC	CA-MRSA strain of USA300 lineage. CC8	[247]
LAC:: <i>lux</i>	Erm ^r derivative of LAC. Contains the luciferase gene.	[248]
LAC:: <i>lux srtA</i> ::Erm ^r	LAC:: <i>lux</i> derivative with a <i>srtA</i> mutation	This study
LAC:: <i>lux clfA</i>	LAC:: <i>lux</i> derivative deficient in ClfA	This study
LAC:: <i>lux clfB</i>	LAC:: <i>lux</i> derivative deficient in ClfB	This study
LAC:: <i>lux spa</i>	LAC:: <i>lux</i> derivative deficient in SpA	This study
LAC:: <i>lux hla</i> ::Erm ^r	LAC:: <i>lux</i> derivative with a Hla mutation	This study
RN4220	CC8; derivative of 8325-4	[249]
PS80	CC30	[250]
<i>E. coli</i> strains		
SA08B	<i>dam</i> ⁺ Δ <i>dcm hsdMS</i> ^{CC30}	[251]
IM08B	<i>dam</i> ⁺ Δ <i>dcm hsdMS</i> ^{CC8-1}	[252]
XL1-Blue	<i>E. coli</i> cloning host	Stratagene
Topp3	<i>E. coli</i> expression host	Stratagene
Plasmids		
pQE30	<i>E. coli</i> expression vector for expression of proteins with N-terminal polyhistadine-tags. Amp ^r	Qiagen
pGEX-4T2	<i>E. coli</i> expression vector, GST-tagged. Amp ^r	GE
pIMAY	Thermosensitive plasmid for allelic exchange. Cm ^r	[240]
pIMAY Δ <i>clfA</i>	pIMAY carrying <i>clfA</i> deletion construct consisting of 567 bp upstream and 513 bp downstream of <i>clfA</i> .	This study
pIMAY Δ <i>clfB</i>	pIMAY carrying <i>clfB</i> deletion construct consisting of 500 bp upstream and downstream of <i>clfB</i> .	[50]
pIMAY Δ <i>spa</i>	pIMAY carrying <i>spa</i> deletion construct consisting of <i>spa</i> bp upstream and downstream of <i>clfA</i> .	JG Lab

Table 2.2. Primer sequences.

Primer	5' - 3' sequence
pIMAY MCS F	TACATGTCAAGAATAAACTGCCAAAGC
pIMAY MCS R	AATACCTGTGACGGAAGATCACTTCG
clfA OUT F	GTAGGGCACGGTTTACTAAG
clfA OUT R	CGCACTTTAATTGCTCCTCTTC
clfA-A	CCTCACTAAAGGGAACAAAAGCTGGGTACCGGTATTGGGAAG CGATTGATTC
clfA-B	CTTCATATTCATTTTATTCCCTC
clfA-C	GAGGGAATAAAATGAATATGAAGGGATTATTAGCATCAATAG GTTC
clfA-D	CGACTCACTATAGGGCGAATTGGAGCTCGCT TCTTTATATTCAGGATTATC
clfB OUT F	ATACGATCAAGATGAATTTTATGAAATCAA
clfB OUT R	CCTTGTGTTAATGCAAATTTAATTGTG
clfB-A	CCCGTCGACACAGTTTTTAACTATTCAACTCATGAG
clfB-B	CAAAAATATTACTCCATTTCAATTTCTAGA
clfB-C	AATTGAAATGGAGTAATATTTTTGTAAATACTTTTTTAGGCCGA ATAC
clfB-D	CCCGAATTCCCATATCCTCCCATAGAGTGACCT
spa OUT F	TAATTGAAAGAATCCACCATAAATACC
spa OUT R	ATTGGTAAAGTTATGACATACGGTGG
spa-A	ATATGTCGACAATTCATATGGATGACGCGCAGC
spa-B	CATAATATAACGAATTATGTATTGCAATAC
spa-C	TGCAATACATAATTCGTTATATTATGTAAAAACAAACAATACAC AACGATAGATATC
spa-D	ATATGAATTCATTAATTGTGGCAGCTAACACTGC

Table 2.3. Antibodies

Antibody	Dilution	Supplier/Reference
<i>Western blotting antibodies</i>		
Rabbit anti-sortase A	1 in 1000	Abcam
Murine anti-ClfA A region IgG	1 in 1000	[100]
Rabbit anti-ClfB A region IgG	1 in 1000	[50]
Rabbit anti-Hla IgG	1 in 1000	[253]
Rabbit anti-murine IgG HRP-conjugated	1 in 1000	Dako
Protein A-peroxidase HRP-conjugated	1 in 500	Sigma
<i>Immunohistochemistry antibodies</i>		
Rat anti-mouse Ly6G/C (GR1)	1 in 100	Invitrogen
Rabbit anti-murine loricrin IgG	1 in 100	Covance
Goat anti-rabbit IgG HRP-conjugated	1 in 200	Dako
<i>Antibody titre assay</i>		
Goat anti-murine IgG HRP-conjugated	1 in 4000	SouthernBiotech

Table 2.4. FACS antibodies

Antibody	Fluorochrome	Clone	Supplier
<i>Anti-human</i>			
CD4	Pe-Cyanine 7	RPA-T4	eBiosciences
IFN γ	APC-eFluor 780	4S.B3	eBiosciences
IL-17AF	eFluor 450	20LJS09	eBiosciences
TNF α	Alexa Fluor 700	Mab11	eBiosciences
Fixable Visibility Dye	eFluor 506 / APC-eFluor 780	N/A	eBiosciences
<i>Anti-mouse</i>			
CD3	BV510	17A2	BioLegend
CD4	eFluor 450	GK1.5	eBiosciences
CD8	APC-eFluor 780	53-6.7	eBiosciences
CD45	Pe-Cyanine 7 / FITC	30-F11	eBiosciences
V δ TCR	APC	eBioGL3	eBiosciences
CD11b	BV510	M1/70	BioLegend
F4/80	APC	BM8	eBiosciences
Ly6G	PE	1A8	BD Bioscience
IFN γ	PerCp 5.5	XMG1.2	eBiosciences
IL-17A	PE	IH8PWSR	eBiosciences
IL-22	Pe-Cyanine 7	eBio17B7	eBiosciences

Table 2.5. Area Scoring

Score	Area
1	< 0.7 mm ²
2	0.7 mm ² – 1.4 mm ²
3	1.4 mm ² – 2.1 mm ²
4	2.1 mm ² – 2.8 mm ²
5	> 2.8 mm ²

Chapter 3

Strain Construction

3.1 Introduction

Staphylococcal genetic manipulation techniques have been essential for the study of virulence and pathogenesis in *S. aureus*. The isolation of mutations in staphylococcal genes and the comparison to their wild-type parental strains has led to the discovery of numerous factors involved in infection by *S. aureus*. The construction of isogenic mutants can be achieved using a number techniques and these can include, directed plasmid integration and allelic replacement. In this project, allelic replacement and generalised transduction of mutations marked with antibiotic resistance cassettes were used to isolate mutants.

Site-specific mutations can be generated using directed plasmid integration and allelic replacement. A deletion cassette can be constructed which contains gene sequences upstream and downstream of the target gene to be deleted. Temperature-sensitive (TS) plasmids are conditionally replicating vectors that contain a temperature-controlled origin of replication. Thermosensitive replicons derived from pC194 [254] and pT181 [255] are used in *S. aureus* TS plasmids. In *S. aureus*, these can replicate at a permissive growth temperature (typically 28 °C), but replication is inhibited at higher restrictive temperatures (typically 37-42 °C). These vectors allow for the production of unmarked, in-frame deletion mutants which carry no extraneous DNA. The TS plasmid containing the relevant deletion cassette is transformed into the *S. aureus* host (Figure 3.1). The transformed cells are grown at the permissive temperature for plasmid replication with selection for the plasmid. Next, incubation at the restrictive temperature in selective medium selects for single cross-over integrants. Single-crossover integrants are then incubated at the permissive temperature for plasmid replication in non-selective media to induce a double-crossover event by homologous recombination (Figure 3.1 B) [256]. Finally, growth at the restrictive temperature leads to plasmid excision from the chromosome, resulting in a wild-type or mutant genotype, depending on where the second cross-over event

occurred (Figure 3.1 C). TS plasmid constructs can be transferred at the permissive growth temperature between strains, allowing for allelic exchange in different *S. aureus* strain backgrounds using the same method.

The TS plasmid used in this project was pIMAY, which was specifically developed for use in *S. aureus*. The pIMAY plasmid employs inducible *secY* antisense-RNA counter-selection [240, 257]. SecY is a component of the SecYEG translocase which is involved in the transportation of proteins containing a Sec signal peptide across the cytoplasmic membrane [258]. SecY expression and protein secretion are both essential for bacterial growth. *S. aureus* growth is inhibited by the expression of *secY* antisense RNA [259]. Agar plates containing anhydrotetracycline are used, as anhydrotetracycline induces the expression of antisense *secY* RNA, thus, selecting for plasmid loss and excision.

The TS plasmid pIMAY was made by combining the vector pIMts with the tetracycline-inducible antisense *secY* region of pKOR1 [240]. It contains the chloramphenicol resistance gene (*cat*) from pIMC, the low copy *E. coli* origin of replication (p15A) and the pBluescript multiple cloning site [260] with the TS Gram-positive bacterial replication genes from pVE6007 [261]. The 5742bp plasmid, pIMAY, is highly temperature-sensitive in *S. aureus*. Its permissive temperature for replication is 28 °C, while its restrictive temperature is 37 °C. This restrictive temperature is lower than other TS plasmids, which reduces the risk of secondary mutations from occurring at higher temperatures.

Staphylococcal strains contain strong restriction barriers, which inhibit the uptake of foreign DNA, and transformation into many *S. aureus* strains has therefore been impossible [262-264]. Previously, DNA from wild-type *E. coli* required passage through *S. aureus* RN4220, which is a restriction-deficient mutant, before subsequent transformation into closely related *S. aureus* isolates [249]. The inability to take up

foreign DNA is due to the activity of Type I restriction-modification system and the Type IV restriction endonuclease, SauUSI [262, 264, 265]. SauUSI recognises cytosine methylated DNA. Plasmids isolated from strains of *E. coli* containing a *dcm* mutation are capable of bypassing the staphylococcal Type IV restriction barrier. The high-efficiency cloning strain *E. coli* DH10B has been engineered to contain a *dcm* mutation [240]. The resulting strain, known as DC10B, has been further modified by the addition of the *hsdMS* genes derived from a clonal complex 8 (CC8) *S. aureus* strain, to give rise to the cloning strains SA08B and IM08B used in this project. Plasmids isolated from either of these strains can be used to transfer plasmid DNA directly into *S. aureus* [240, 252].

This chapter describes the construction and validation of a series of *S. aureus* mutants which will be used to investigate the role of CWA proteins during SSTIs and as T cell antigens. These mutants were all generated in the CA-MRSA USA300 LAC::*lux* strain. Strains from the USA300 lineage are the most common cause of skin infections, 97 % of all MRSA SSTI cases in the USA were caused by this lineage [17]. The LAC::*lux srtA* and LAC::*lux hla* mutant were generated by generalised transduction of existing mutations. The LAC::*lux clfA*, LAC::*lux clfB* and LAC::*lux spa* mutants were generated by allelic replacement using the TS plasmid pIMAY.

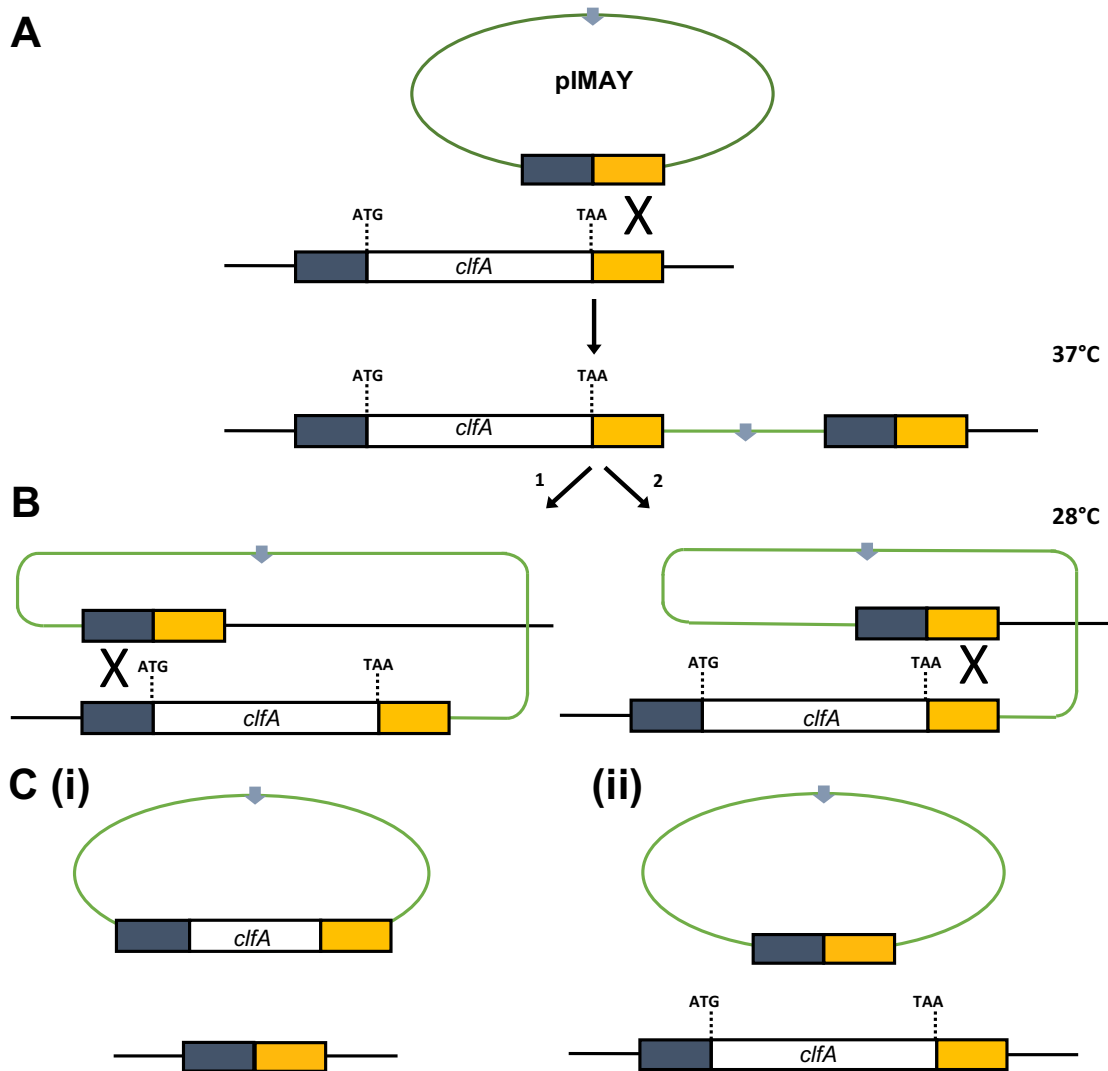


Figure 3.1. Schematic representation of plasmid integration and excision. (A) Plasmid integration can occur upstream or downstream of the chromosomal locus by a single cross-over event. (B) To induce a second recombination event, single cross-over variants are incubated at the permissive temperature for replication, allowing for plasmid excision. (C) (i) A second cross-over on the opposite side to the first event causes removal of the wild-type gene, resulting in successful allelic replacement. (ii) A second cross-over on the same side of the mutation as the first event causes removal of the mutation to the plasmid.

3.2 Results

3.2.1 Validation of a *srtA* mutation in *S. aureus* LAC::*lux*

A *srtA* mutant was constructed by generalised transduction of *srtA*::Erm^r [244] into strain LAC::*lux* using phage 85. The resulting strain was validated in a number of ways to ensure that the *srtA* gene was disrupted and that no secondary mutations had occurred during the mutagenesis process. The strain was tested for δ -haemolysin production in order to assess *agr* function (Figure 3.2 A). The accessory gene regulator (Agr) is a two-component quorum-sensing system, which controls many virulence factors of *S. aureus*. Spontaneous *agr* mutations are known to occur at high frequency in bacteria under stress [266, 267]. These mutations may affect expression of virulence factors and alter fitness due to lower growth rate. δ -haemolysin is a short peptide that is encoded within RNAIII, a transcript from the Agr two-component system. It has weak activity on sheep blood agar but is strongly synergistic with β -haemolysin, producing a zone of clear haemolysis where they interact. LAC::*lux srtA* and its LAC::*lux* WT were cross-streaked against RN4220, which produces only β -haemolysin [268]. A similar zone of clear haemolysis was observed for each strain, indicating significant δ -haemolysin activity and by extension confirming normal *agr* function (Figure 3.2 A). Bioluminescence activity of LAC::*lux srtA* was tested to confirm that the luciferase genes were intact after the mutagenesis (Figure 3.2 B). The growth of LAC::*lux srtA* was examined and it displayed a similar growth profile and reached a similar final OD₆₀₀ to LAC::*lux* WT (Figure 3.2 C). Lack of SrtA expression was verified by Western immunoblotting using an anti-SrtA IgG (Figure 3.2 D).

Since the ability of *S. aureus* to adhere to fibrinogen depends entirely on CWA proteins, the functionality of SrtA in LAC::*lux srtA* was assayed by testing this strain's ability to adhere to human fibrinogen (Figure 3.2 E) and recombinant human loricrin loop 2 (L2v) (Figure 3.2 F). LAC::*lux srtA* displayed a reduced ability to adhere to

fibrinogen and loricrin compared to LAC::*lux* WT, indicating that surface proteins that facilitate binding were defective in the mutant strain, indicative of a lack of SrtA activity.

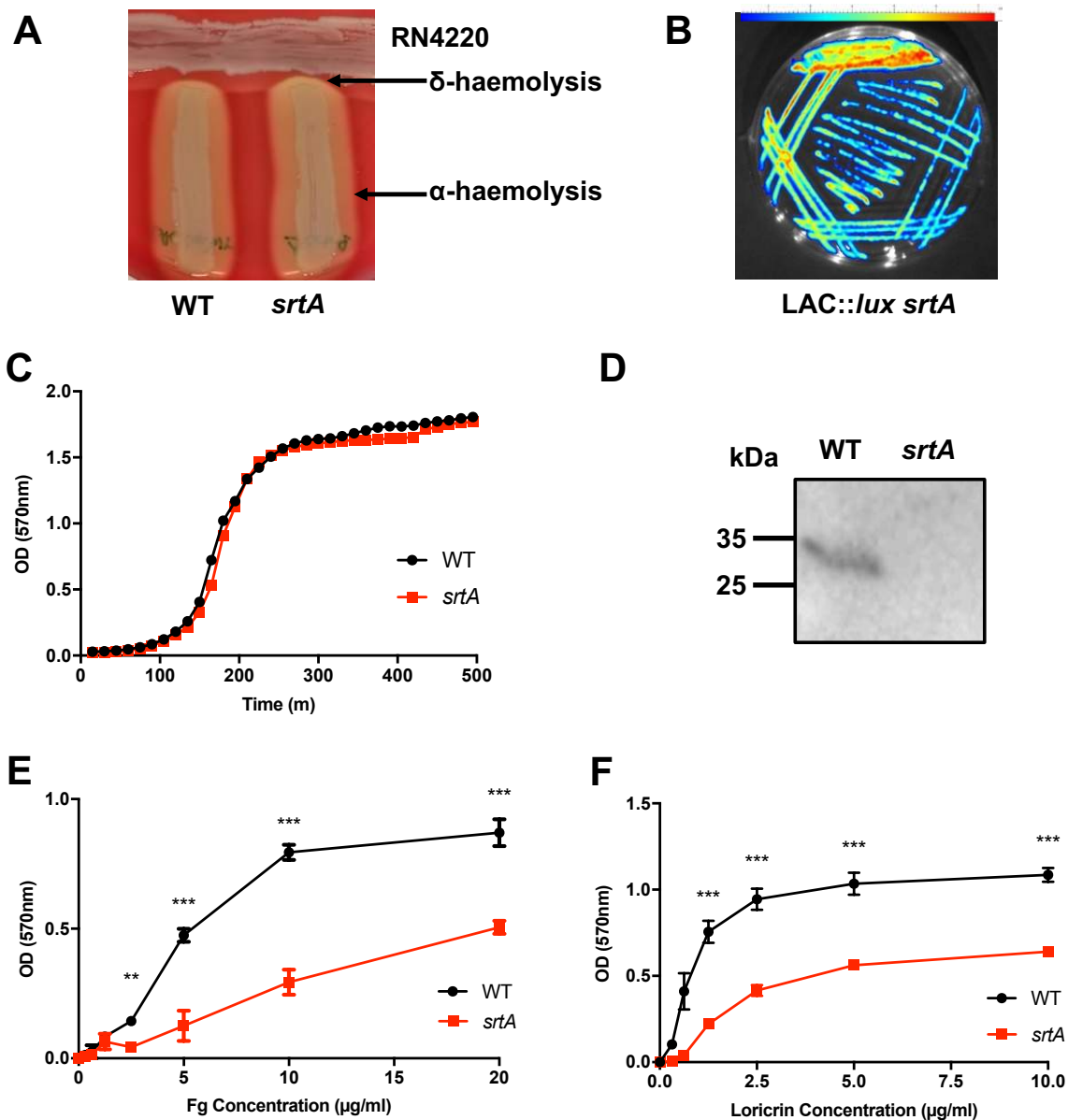


Figure 3.2. Validation of LAC::lux *srtA*. LAC::lux *srtA* and LAC::lux WT were cross-streaked against RN4220 in order to compare the haemolytic pattern (A). Haemolysis is indicated by arrows. Bioluminescence of LAC::lux *srtA* was confirmed by bioluminescence imaging (B). The growth profile of LAC::lux *srtA* was compared to LAC::lux WT (C). Expression of SrtA was analysed by Western immunoblotting of lysed protoplasts, separated on 10 % SDS-PAGE gel and probed with anti-SrtA IgG (D). The ability of LAC::lux *srtA* to adhere to human fibrinogen (Fg) (E) and loricrin L2v (F) was assessed. The results shown are representative of 3 independent experiments (C, D). Results expressed as mean \pm SEM with data pooled from 3 independent experiments (E, F). Two-way ANOVA with Bonferroni post-test was performed to compare variances between groups (E, F). ** $P < 0.01$, *** $P < 0.001$.

3.2.2 Validation of a *hla* mutation in *S. aureus* LAC::*lux*

A *hla* mutant was constructed by generalised transduction of *hla*::Erm^r [245] into strain LAC::*lux* using phage 85. The resulting strain was validated to ensure that the *hla* gene was disrupted and that no secondary mutations had occurred during the mutagenesis process. The strain was tested for α -haemolysin production in order to confirm Hla function had been disrupted (Figure 3.3 A). LAC::*lux hla* and its parental strain were cross-streaked against RN4220 on sheep blood agar. A zone of haemolysis was observed surrounding LAC::*lux* WT, however this zone of haemolysis was absent from LAC::*lux hla*. Hla is known to cause lysis of erythrocytes [269], and this absence of lysis surrounding the *hla* mutant strain can be attributed to the absence of Hla. δ -haemolysin activity remains intact in LAC::*lux hla*, suggesting no secondary mutations have occurred. The bioluminescent activity of LAC::*lux hla* was tested to confirm that the luciferase genes were intact after the mutagenesis (Figure 3.3 B). The growth of LAC::*lux hla* was also examined and it displayed a similar growth profile and reached a similar final OD₆₀₀ compared to LAC::*lux* WT (Figure 3.2 C). Lack of Hla expression was verified by Western immunoblotting of supernatants using an anti-Hla antibody (Figure 3.2 D). A band corresponding to ~33 kDa is present in supernatants from LAC::*lux* WT but absent from LAC::*lux srtA* supernatants.

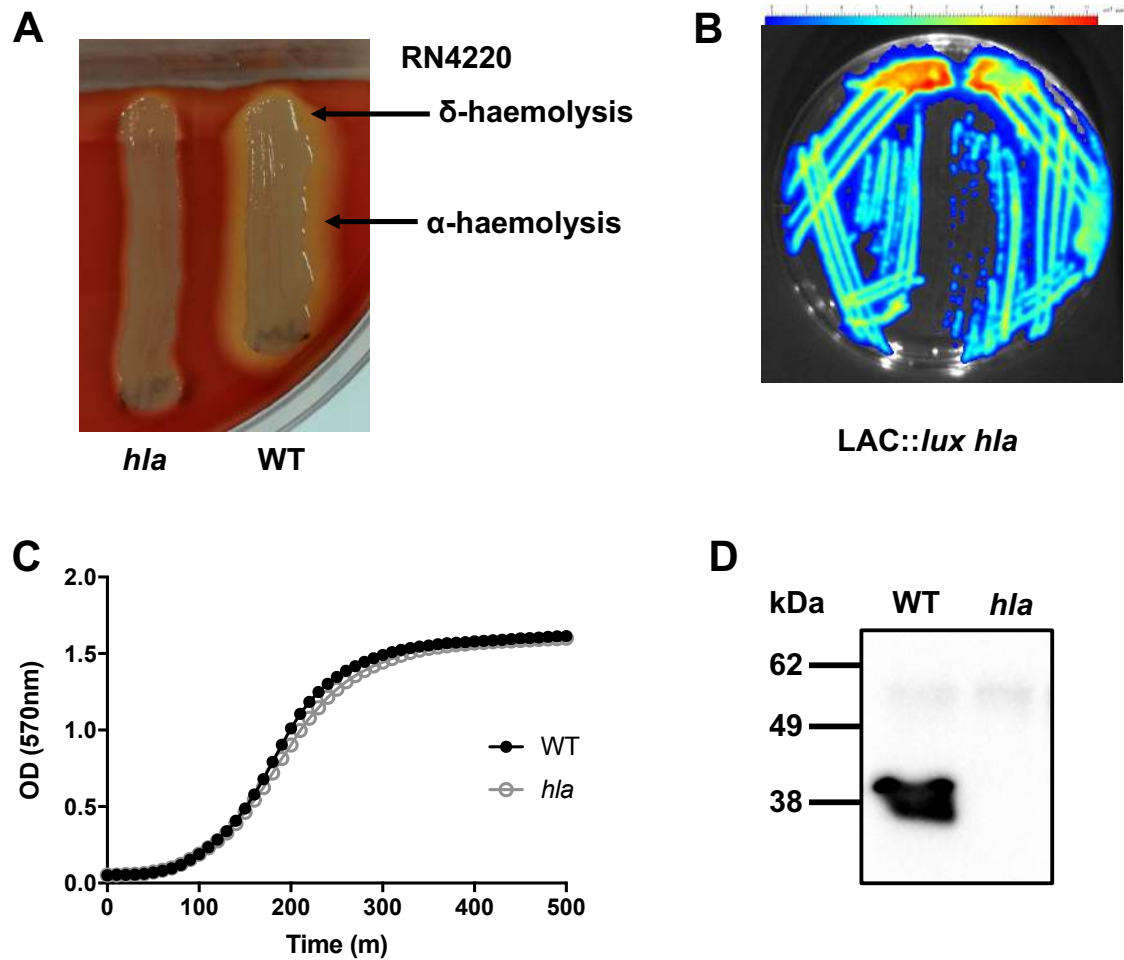


Figure 3.3. Validation of LAC::lux *hla*. LAC::lux *hla* and LAC::lux WT were cross-streaked against RN4220 in order to compare the haemolytic pattern (A). Haemolysis is indicated by arrows. Bioluminescence of LAC::lux *hla* was confirmed by bioluminescence imaging (B). The growth profile of LAC::lux *hla* was compared to LAC::lux WT (C). Expression of Hla was analysed by Western immunoblotting of supernatants, separated on 15 % SDS-PAGE gel and probed with anti-*hla* IgG (D). The results shown are representative of 3 independent experiments (C, D).

3.2.3 Construction of *clfA*, *clfB* and *spa* null mutations in *S. aureus* LAC::*lux*

S. aureus LAC::*lux clfA*, LAC::*lux clfB* and LAC::*lux spa* were all constructed by allelic exchange using pIMAY. Two sets of primers were designed to amplify 600 bp of DNA located upstream and downstream of the *clfA* gene (Figure 3.4 A). Primers A and B were used to amplify the 600 bp upstream region of the *clfA* gene. Primers C and D amplified the 600 bp downstream region of the gene. Restriction sites *EcoRI* and *Sall* were incorporated into primers A and D, respectively, to allow for directional insertion into pIMAY. Primer C was designed to include a 5' extension complementary to the nucleotide sequence of primer B. Genomic DNA was isolated from LAC::*lux* and used as template for PCR. The resulting PCR products were denatured, allowed to reanneal via the complementary sequences in primer B and C and then amplified using primers A and D, resulting in a 1200 bp fragment consisting of linked sequences upstream and downstream of the *clfA* gene (Δ *clfA* cassette, Figure 3.4 B). The cassette was cloned into pIMAY between *EcoRI* and *Sall* restriction sites. Deletion of the *clfA* gene was achieved by allelic exchange. To allow for allelic exchange, pIMAY containing the Δ *clfA* cassette was transferred to electrocompetent LAC::*lux*. Following a temperature shift to the restrictive temperature (37 °C), cells were plated onto TSA containing chloramphenicol to select for a single crossover event leading to integration. The side of integration was determined by PCR screening using primers designed to recognise ~650 bp sequences upstream and downstream of the deletion construct (OUT primers, Figure 3.4 C). In order to induce plasmid excision, successful integrants were grown at the permissive temperature (28 °C).

The deletion was confirmed by amplification across the *clfA* gene (Figure 3.4 D). The same OUT primers were used to screen genomic DNA isolated from possible mutants and their parental strain. If the mutation construct was retained in the chromosome then PCR-amplification would yield ~1300 bp product from LAC::*lux*

clfA, but not the parental strain. As predicted, a 1300 bp product was amplified from mutants of LAC::*lux clfA*, whereas the parental strain yielded the wild-type product.

The same allelic exchange process was carried out to create the LAC::*lux clfB* and LAC::*lux spa* mutants.

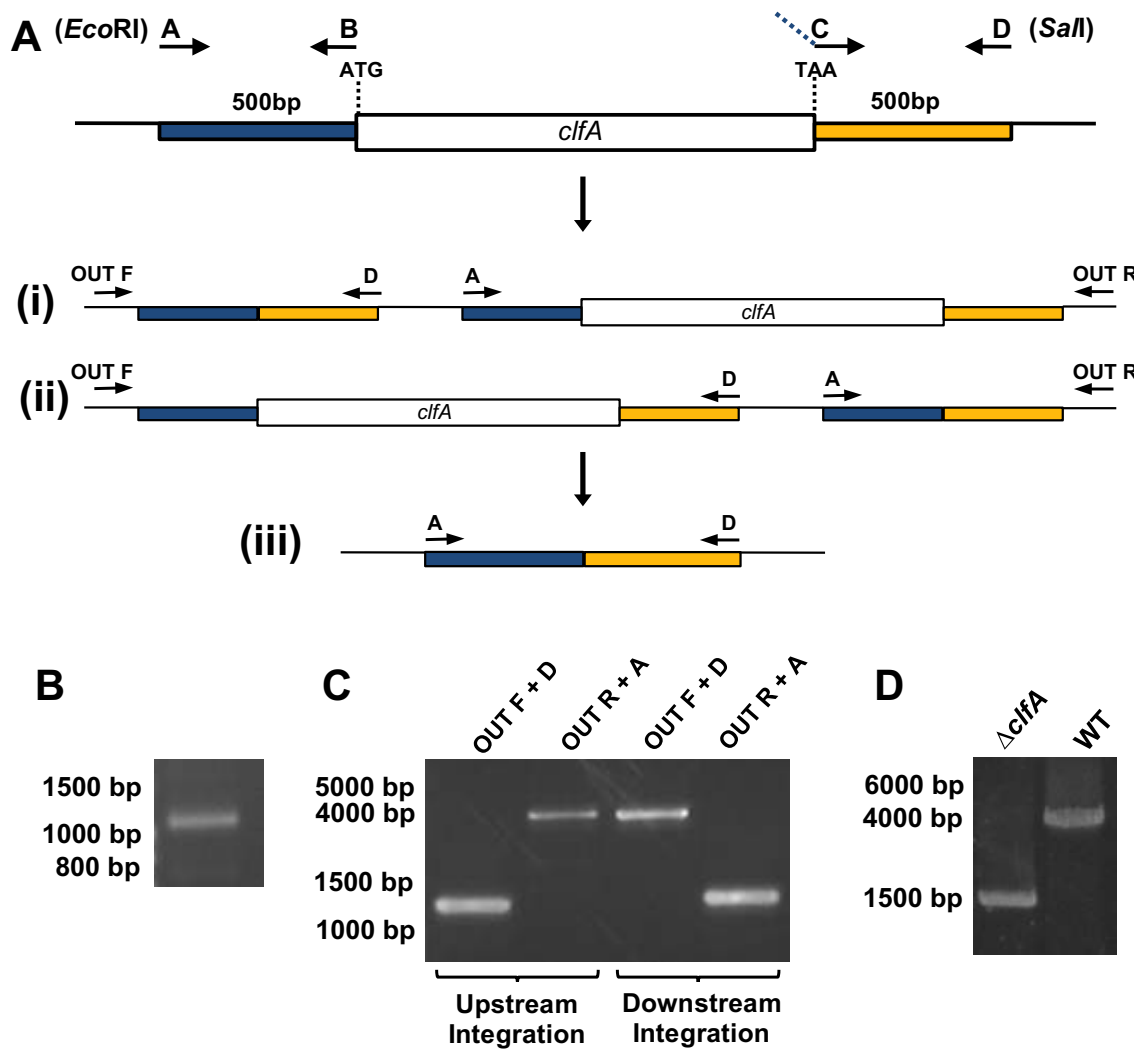


Figure 3.4. Construction of pIMAY Δ *clfA*. Schematic representation of the *clfB* mutation (A). 500–600 bp regions upstream and downstream of the *clfB* gene were amplified by PCR and were joined to form a *clfA* mutation construct. The construct was cloned into pIMAY and was then introduced into *S. aureus* LAC::*lux*. The side of integration on the chromosome can be determined by PCR amplification of the regions using OUT primers to determine upstream (i) or downstream (ii) integration. The plasmid is then excised, leaving the deletion construct on the chromosome (iii). PCR amplification of the 1000 bp *clfA* deletion construct (B). PCR amplification to determine the side of integration (C). The deletion was confirmed by PCR-amplifying genomic DNA from the deletion mutant and comparing it to the wild-type product (D).

3.2.4 Validation of *S. aureus* LAC::*lux clfA*

The resulting ClfA-deficient strain was validated *in vitro* for the loss of ClfA. LAC::*lux clfA* was compared to LAC::*lux* WT for expression of δ -haemolysin in order to assess *agr* function (Figure 3.5 A). The δ -haemolysis profile of LAC::*lux clfA* compared to LAC::*lux* WT suggests a normally functioning Agr system in the mutant strain. The bioluminescence of LAC::*lux clfA* was investigated and was confirmed to produce bioluminescent signal (Figure 3.5 B). LAC::*lux clfA* displayed a similar growth profile and reached a similar final OD₆₀₀ compared to LAC::*lux* WT (Figure 3.5 C). Lack of ClfA expression was verified by Western immunoblotting of cell wall extracts (Figure 3.5 D). A band of 170 kDa is present in cell wall extracts from LAC::*lux* WT and this corresponds to ClfA, a smaller band of 130 kDa is visible due to breakdown of the ClfA protein. Cell wall extracts from LAC::*lux clfA* do not contain any bands, confirming the absence of ClfA.

Genomic DNA was isolated from LAC::*lux clfA* and the *clfA* gene was amplified using the OUT primers (Table 2.2). The PCR product was sent for sequencing, which confirmed that the *clfA* gene was absent.

The functionality of ClfA was assessed using a bacterial fibrinogen adherence assay (Figure 3.4 E). LAC::*lux clfA* grown to stationary phase displayed a reduced ability to adhere to human fibrinogen compared to LAC::*lux* WT, indicating that ClfA-mediated adherence to the ligand had been abolished.

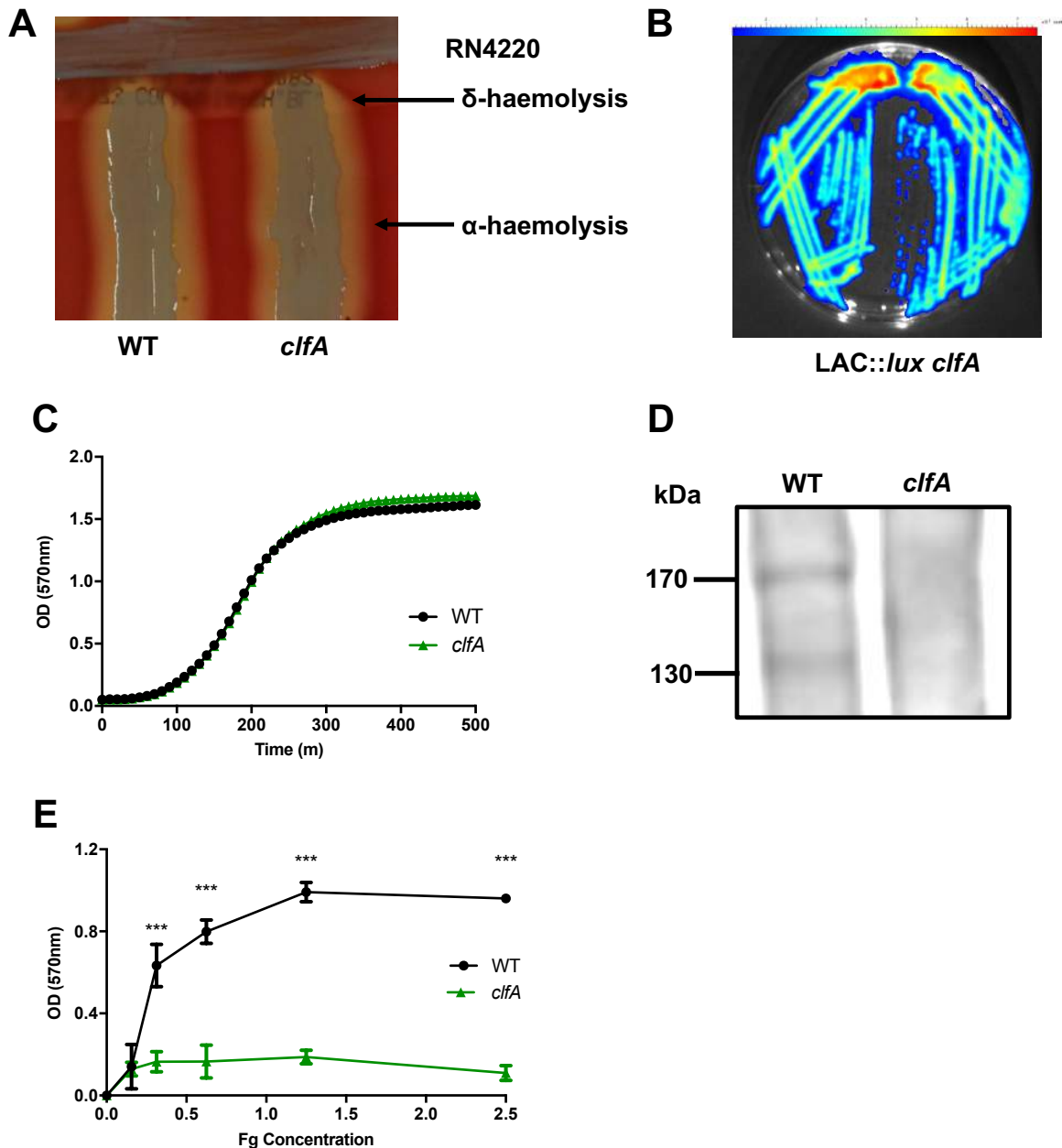


Figure 3.5. Validation of LAC::lux *clfA*. LAC::lux *clfA* and LAC::lux WT were cross-streaked against RN4220 in order to compare the haemolytic pattern (A). Haemolysis is indicated by arrows. Bioluminescence of LAC::lux *clfA* was confirmed by bioluminescence imaging (B). The growth profile of LAC::lux *clfA* was compared to LAC::lux WT (C). Expression of ClfA was analysed by Western immunoblotting of cell wall proteins that had been solubilized by lysostaphin digest during protoplast formation, separated on 10 % SDS-PAGE gel and probed with anti-ClfA igG (D). Adherence of LAC::lux *clfA* to human fibrinogen (Fg) was assessed (E). The results shown are representative of 3 independent experiments (C, D). Results expressed as mean \pm SEM with data pooled from 3 independent experiments and two-way ANOVA with Bonferroni post-test used to compare variances (E). *** $P < 0.001$.

3.2.5 Validation of *S. aureus* LAC::*lux clfB*

The ClfB-deficient strain was created by allelic exchange and validated *in vitro* for the loss of ClfB. LAC::*lux clfB* expression of δ -haemolysin was compared to LAC::*lux* WT in order to assess *agr* function (Figure 3.6 A). The δ -haemolytic profile of LAC::*lux clfB* compared to LAC::*lux* WT suggests a normally functioning Agr system in the mutant strain. The bioluminescent activity of LAC::*lux clfB* was investigated to confirm that the luciferase genes were intact after the mutagenesis process (Figure 3.6 B). LAC::*lux clfB* displayed a similar growth profile and reached a similar final OD₆₀₀ compared to the wild-type strain (Figure 3.6 C). Lack of ClfB expression was verified by Western immunoblotting (Figure 3.6 D). No bands corresponding to ClfB were present in cell wall extracts isolated from LAC::*lux clfB*, in contrast to the band corresponding to ~170 kDa in LAC::*lux* WT. A smaller breakdown product is also visible at ~80 kDa.

Genomic DNA was isolated from LAC::*lux clfB* and the *clfB* gene was amplified using the OUT primers (Table 2.2). The PCR product was sent for sequencing, which confirmed the absence of the *clfB* gene.

The functionality of LAC::*lux clfB* was assessed using an adherence assay (Figure 3.6 E). LAC::*lux clfB* was unable to adhere to recombinant human loricrin loop 2v (L2v) compared to LAC::*lux* WT, demonstrating that ClfB-mediated adherence has been abolished.

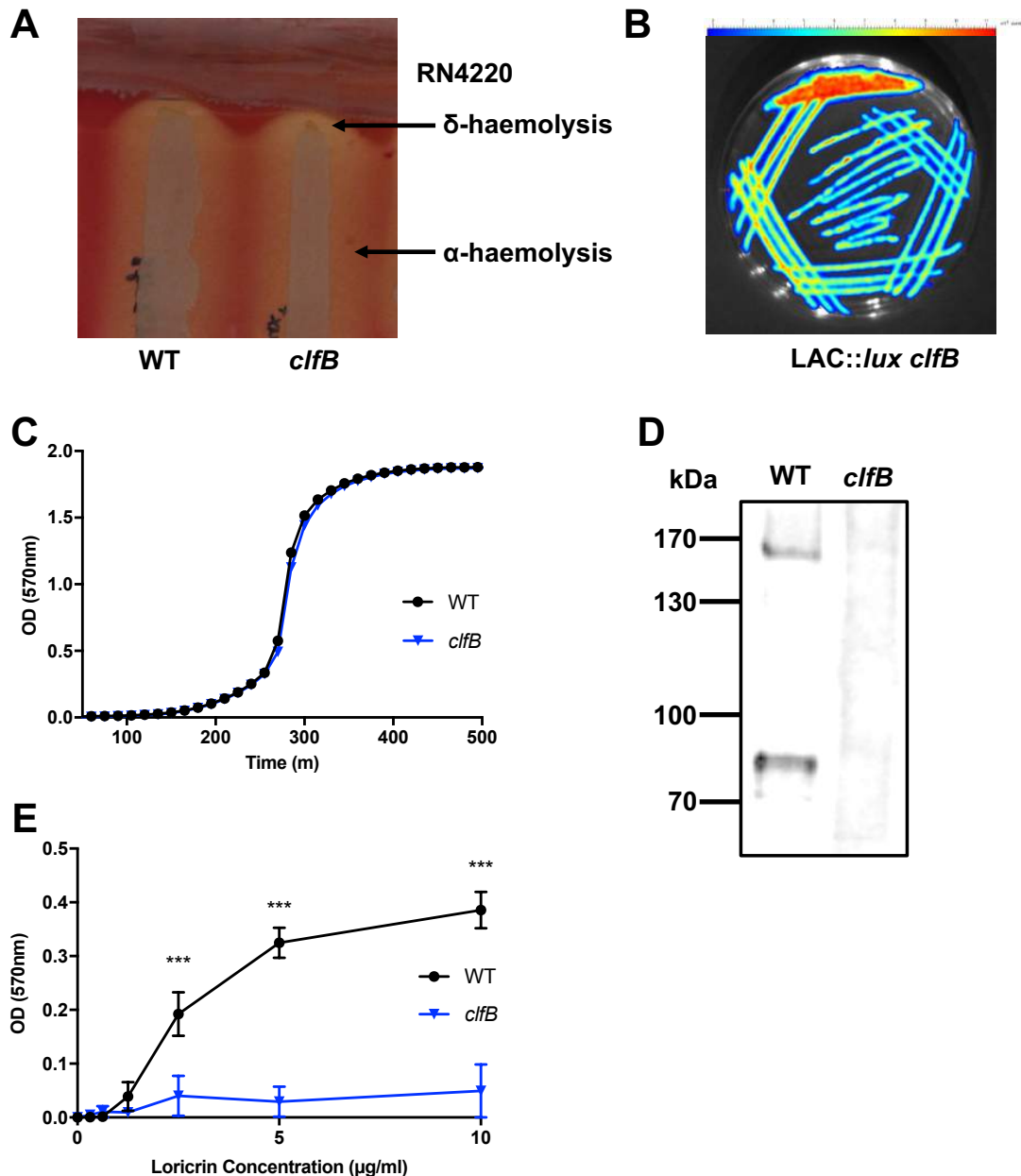


Figure 3.6. Validation of LAC::lux *clfB*. LAC::lux *clfB* and LAC::lux WT were cross-streaked against RN4220 to compare the haemolytic pattern (A). Haemolysis is indicated by arrows. Bioluminescence of LAC::lux *clfB* was confirmed by bioluminescence imaging (B). The growth profile of LAC::lux *clfB* was compared to LAC::lux WT (C). Expression of ClfB was analysed by Western immunoblotting of cell wall proteins that had been solubilized by lysostaphin digest during protoplast formation, separated on 10 % SDS-PAGE gel and probed with anti-clfB IgG (D). Adherence of LAC::lux *clfB* to recombinant human loricrin loop 2v was assessed (E). Results are representative of 3 independent experiments (C, D). Results expressed as mean \pm SEM with data pooled from 3 independent experiments (E). Two-way ANOVA with Bonferroni post-test performed to compare variances (E). *** $P < 0.001$.

3.2.5 Validation of *S. aureus* LAC::*lux spa*

The SpA-deficient strain was created by allelic exchange and validated *in vitro* for the loss of SpA. LAC::*lux spa* was compared to LAC::*lux* WT for expression of δ -haemolysin in order to assess *agr* function (Figure 3.7 A). The δ -haemolytic profile of LAC::*lux spa* compared to LAC::*lux* WT suggests a normally functioning Agr system in the mutant strain. The bioluminescence of LAC::*lux spa* was investigated and confirmed to produce bioluminescent signal (Figure 3.7 B). LAC::*lux spa* displayed a similar growth profile and reached a similar final OD₆₀₀ compared to LAC::*lux* WT (Figure 3.6 C).

Lack of SpA expression was verified by Western immunoblotting (Figure 3.6 D). Cell wall extracts were probed with rabbit IgG. As SpA can bind IgG in a non-immune manner, this Western immunoblotting acts as the functional assay for SpA.

Genomic DNA was isolated from LAC::*lux spa* and the *spa* gene was amplified using the OUT primers (Table 2.2). Sequencing of the PCR product confirmed the absence of the *spa* gene.

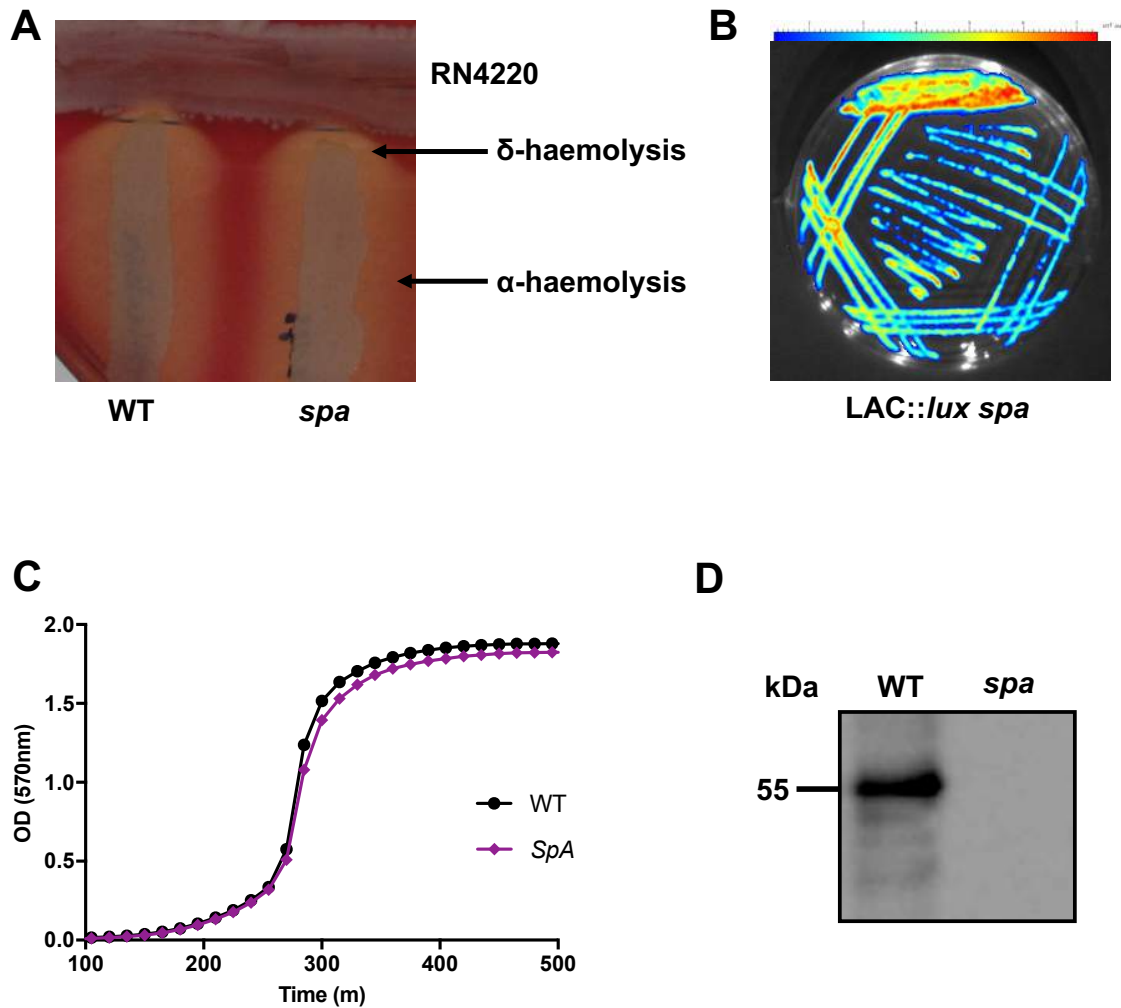


Figure 3.7. Validation of LAC::lux spa. LAC::lux spa and LAC::lux WT were cross-streaked against RN4220 in order to compare the haemolytic pattern (A). Haemolysis is indicated by black arrows. Bioluminescence of LAC::lux spa was confirmed by bioluminescence imaging (B). The growth profile of LAC lux spa was compared to LAC::lux WT (C). Expression of SpA was analysed by Western immunoblotting of cell wall proteins that had been solubilized by lysostaphin digest during protoplast formation, separated on 10 % SDS-PAGE gel and probed with HRP-conjugated rabbit IgG (D). The results shown are representative of 3 independent experiments (C, D).

3.3 Discussion

Surface proteins have previously been implicated as virulence factors in *S. aureus* skin infections [45]. In order to further investigate the role of these CWA proteins during skin infections and also investigate their ability to activate T cells, a *srtA* mutant which lacked all cell surface bound CWA proteins was created. Mutations in individual proteins were also created to investigate the specific roles played by individual CWA proteins during SSTIs.

The study of *S. aureus* virulence mechanisms requires the generation of isogenic mutations in chromosomal genes in order to identify important virulence factors. To facilitate investigations into the bacterial factors involved in SSTIs, and their contribution to abscess formation, it was important that isogenic mutants were created in the same strain background of *S. aureus* enabling direct comparisons to be made between the strains. These mutants were created in a clinically relevant USA300 strain, which is known to cause severe skin infections [17]. The LAC::*lux* strain of the USA300 lineage was chosen as it contains the bioluminescent luciferase genes, enabling live *in vivo* imaging during the murine skin infection model (Chapter 5). LAC::*lux srtA* and LAC::*lux hla* were created by generalised transduction of existing mutations, while allelic replacement was used to remove the genes encoding the individual CWA proteins ClfA, ClfB and SpA.

The Agr system is a global regulator of proteins associated with virulence in *S. aureus*. It is activated in the late-exponential phase of growth. The *agr* locus produces two divergent transcripts known as RNA II and RNA III, initiated from the P2 and P3 promoters, respectively [270, 271]. RNA III functions as the regulatory signal of the Agr system and regulates the transcripts of many target genes. It also encodes δ -haemolysin. When bacteria are subjected to stressful conditions, such as temperature shift during mutagenesis, spontaneous mutations in the *agr* locus may occur. If secondary mutations occur in the system during mutagenesis, then the

mutants cannot be used. Fortunately, this can be detected by assessing the production of δ -haemolysin by *S. aureus*, by lysis of red blood cells in sheep blood agar. *S. aureus* can produce four types of haemolysin; α -, β -, γ - and δ -haemolysins. As δ -haemolysin is strongly upregulated by the Agr system, it can indirectly be used to assess Agr function. On sheep blood agar, δ -haemolysin produces a weak zone of haemolysis, however, it is highly synergistic with β -haemolysin. The mutant strains constructed in this chapter, alongside LAC::*lux* WT, were cross-streaked against *S. aureus* RN4220 to assess δ -haemolysin production. RN4220 only produces β -haemolysin. Due to the synergistic effect of δ -haemolysin and β -haemolysin, a zone of clear haemolysis was observed where these two toxins interact. LAC::*lux srtA*, *hla*, *clfA*, *clfB* and *spa* produced similar levels of δ -haemolysin as the parental strain, indicating that no secondary *agr* mutations occurred during the mutagenesis process.

The growth profile of all the mutants was confirmed to be the same as LAC::*lux* WT, and all of them remained bioluminescent after the mutagenesis process. The absence of the SrtA, Hla, ClfA, ClfB and SpA proteins was confirmed by western blotting and sequencing results confirmed the absence of the *clfA*, *clfB* and *spa* genes in the chromosome. The functionality of the mutants was assessed, and LAC::*lux srtA* had reduced adherence to fibrinogen and loricrin, indicating that surface proteins were absent from its surface. Low level adherence was observed and this can be attributed to some retention of CWA proteins in the cell membrane following secretion. The LAC::*lux clfA* failed to bind to fibrinogen, which is the main ligand for ClfA, similarly, LAC::*lux clfB* was unable to bind to loricrin, the major ClfB ligand.

Complementation, whereby the gene of interest is reintroduced into the mutant strain, either on a plasmid or reinstated on the chromosome could be carried out to restore phenotypes to wild-type levels. This would act to further verify the mutant phenotypes. Whole genome sequencing of the wild-type and mutant strains could

also be carried out, followed by computational analysis, to fully establish if the gene of interest is absent and that no secondary mutations occur between the mutants and the wild-type strains.

The creation of *S. aureus* LAC::*lux srtA* will enable research into the ability of CWA proteins to activate human T cells (Chapter 4). All of the CWA protein mutants will be used to investigate the specific role of CWA proteins and how they contribute to abscess formation during *S. aureus* SSTIs using a bioluminescent murine skin infection model (Chapter 5).

Chapter 4

Investigating cell wall-anchored proteins as T cell antigens

4.1 Introduction

Targeting individual T cell subsets is now considered an important strategy for next generation anti-*S. aureus* vaccines [21]. However, to-date no well-established *S. aureus* T cell epitopes have been identified. It has recently been shown that an average of 3.6 % of circulating T cells in healthy adults are *S. aureus* specific, indicative of their previous exposure to *S. aureus* either through commensal colonisation or previous sub-clinical infection [272]. Given that the normal healthy population have multiple prior exposures to *S. aureus*, immune recall responses to staphylococcal antigens will likely vary significantly depending on individuals' exposure histories. However, the use of buffy coats from healthy blood donors presents a valuable opportunity to screen antigens for their human T cell-activating capacity. Kolata *et al.* demonstrated that extracellular proteins, composed of both secreted proteins and surface bound proteins, elicited greater T cell responses than intracellular proteins [272]. Browne *et al.* have also been demonstrated that heat-inactivated *S. aureus*, washed to remove all secreted factors, elicits a robust T cell response, suggesting surface-located factors of *S. aureus* are important for T cell activation [156]. Indeed, surface exposed capsular polysaccharide and wall teichoic acid of *S. aureus* have previously been shown to activate T cells [147, 250, 273-275], however, *S. aureus* cell wall-anchored (CWA) protein T cell epitopes have yet to be identified. As CWA proteins are present on the surface of the bacteria, they are in direct contact with the host's immune system and as such represent attractive targets for vaccine strategies. Previous studies have demonstrated that CWA proteins can drive antibody responses in vaccinated animals [66, 101, 212, 276-278] and humans [279-283]. However, if these CWA proteins are ever to be considered for use as vaccine antigens, it is imperative that their ability to activate human T cells be specifically examined, as ultimately anti-*S. aureus* vaccines will have to drive cellular immune responses in humans.

Many CWA proteins are multifunctional and involved in adhesion, invasion, biofilm formation and/or evasion of host immune responses [95]. However, for the most part, there is a lack of understanding into how these CWA proteins interact with immune pathways and their capacity to activate T cells remains to be fully established. The CWA protein ClfA contains a ligand-binding A domain composed of three subdomains; N1, N2 and N3. The N23 subdomains are involved in ligand binding [94], however, a role for the N1 subdomain remains unknown, with the exception of ten residues located at the junction between the N1 and N2 subdomains which are required for protein export and cell wall localization [97]. ClfA is considered a good vaccine candidate because it is expressed ubiquitously across strains and is a major virulence factor contributing to pathogenesis [101-103]. Consequently ClfA is a vaccine antigen included in multivalent vaccines in development by Pfizer and GSK [280, 281, 284].

The goal of this current study is to investigate the potential of *S. aureus* CWA proteins to activate human T cells using buffy coats from healthy individuals and to specifically investigate the ability of ClfA and its subdomains to activate human Th1 and Th17 cell subsets. In addition, the efficacy of model vaccines developed using subdomains of ClfA will be investigated to establish if these subdomains can drive protective cellular and humoral immune responses against *S. aureus* infection *in vivo*.

4.2. Results

4.2.1 Human CD4⁺ T cells proliferate in response to heat-inactivated *S. aureus* LAC::*lux*

To investigate if CWA proteins have the capacity for human T cell activation, heat-inactivated *S. aureus* was incubated with CD4⁺ T cells purified from buffy coats isolated from healthy adults and co-cultured with autologous irradiated APCs. Proliferation and cytokine production was assessed on day 10. Day 10 was chosen as optimisation experiments had identified this as the peak of CD4⁺ T cell proliferation (Figure 4.1). For consistency LAC::*lux* was selected as the parental wild-type strain (this strain is used in the skin infection model (Chapter 5)), and we initially confirmed that it performed the same as LAC in our assay system. The proportion of proliferating CD4⁺ T cells was assessed in cells stimulated with heat-inactivated LAC or LAC::*lux* and no difference in T cell activating capability was observed (Figure 4.2), confirming that the presence of the luciferase genes does not affect T cell activation.

To investigate the capacity of CWA proteins to activate T cells, LAC::*lux srtA* was created (Chapter 3), which lacked all surface bound CWA proteins and the ability of T cells to respond to this was compared to LAC::*lux* WT. The proportion of proliferating CD4⁺ T cells was significantly elevated in cells stimulated with the heat-inactivated LAC::*lux* WT strain compared to LAC::*lux srtA* (Figure 4.3). There was a wide spread in the proportion of CD4⁺ T cells proliferating in response to heat-inactivated *S. aureus*. The WT strain induced proliferation in 90 % of individuals as compared to the *srtA* mutant which induced proliferation in only 77 % of individuals (Table 4.1). To further investigate which specific T cell subsets were responding, intracellular staining for the cytokines IFN γ , TNF α and IL-17 was carried out. The proportions of CD4⁺ T cells proliferating and producing IFN γ (Figure 4.4 A), TNF α (Figure 4.4 B) and IL-17 (Figure 4.4 C) were significantly higher in WT stimulated cells compared to *srtA* stimulated. The CD4⁺ T cells producing IL-17 were not found to be producing

either IFN γ (Figure 4.5 A) or TNF α (Figure 4.5 B), suggesting these cells are bona fide Th17 cells. The CD4⁺IFN γ ⁺ cells are indicative of Th1 cells, and a subset of these cells were dual producers of both IFN γ and TNF α (Figure 4.5 C). Interestingly, a proportion of the TNF α produced was from a distinct population of CD4⁺TNF α ⁺IFN γ ⁻ cells, however these were not activated by CWA proteins. As the majority of the TNF α is originating from Th1 cells, TNF α was not studied going forward. Overall, these studies suggest that CWA proteins are capable of driving human Th1 and Th17 cell expansion.

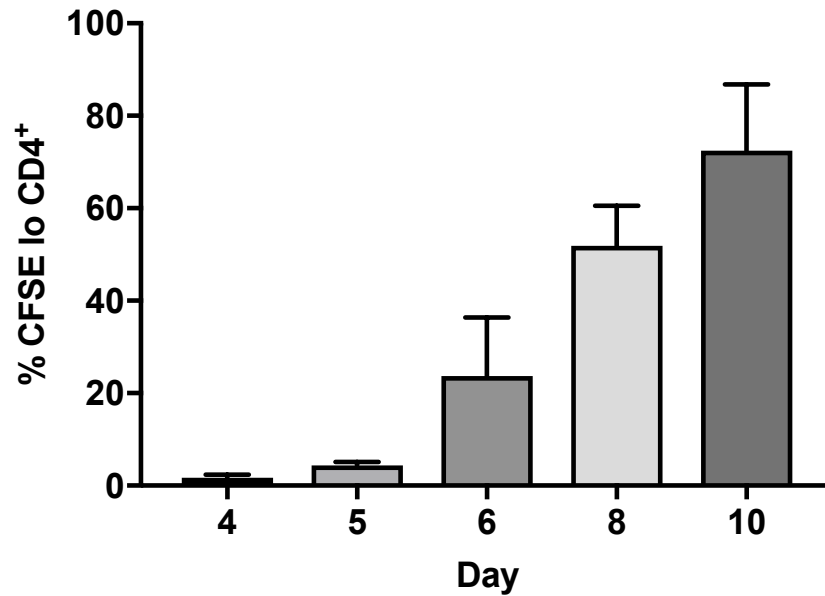


Figure 4.1. Proliferation responses to heat-inactivated *S. aureus* are greatest after 10 days of stimulation. Human PBMCs from healthy blood donors were CFSE-labelled and incubated with heat-inactivated *S. aureus* (1 μ g/ml) or media alone. PMA (50 ng/ml) and ionomycin (5 ng/ml) were added for the final 4 h of culture. On day 4, 5, 6, 8 and 10 proliferation was assessed by gating on CFSE₁₀ cells in the CD4⁺ population. For each patient, media only responses were subtracted from responses to heat-inactivated *S. aureus* to determine antigen-specific response. Results expressed as mean \pm SEM. n=4-7 per group. **Experiment performed by Tracey Claxton.**

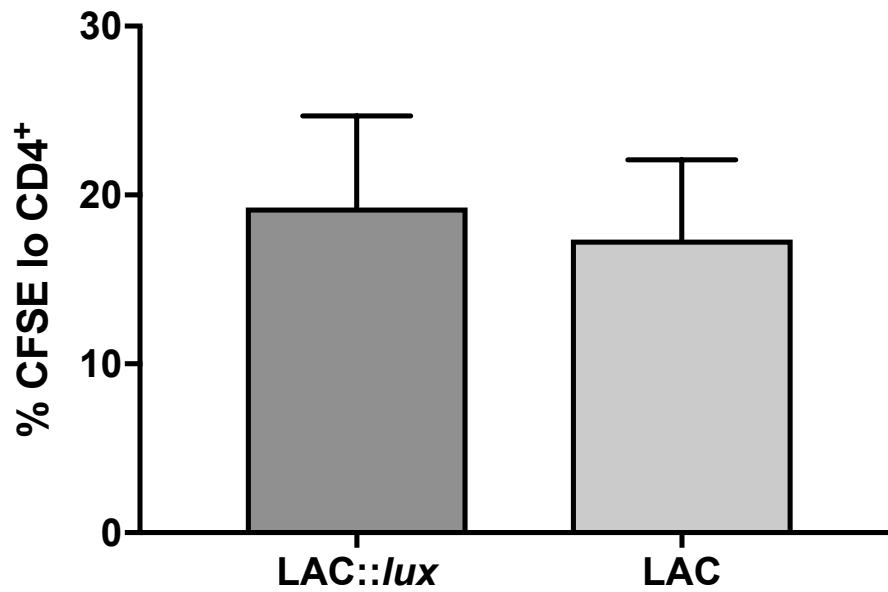


Figure 4.2. No difference in levels of proliferation of human CD4⁺ T cells in response to heat-inactivated *S. aureus* LAC or LAC::lux. Human PBMCs from healthy blood donors were CFSE-labelled and incubated with heat-inactivated LAC or LAC::lux (1 μ g/ml) or media alone. On day 10, proliferation was assessed by gating on CFSE^{lo} cells in the CD4⁺ population. For each patient, media only responses were subtracted from responses to heat-inactivated *S. aureus* to determine antigen-specific response. Results expressed as mean \pm SEM. n=3 per group.

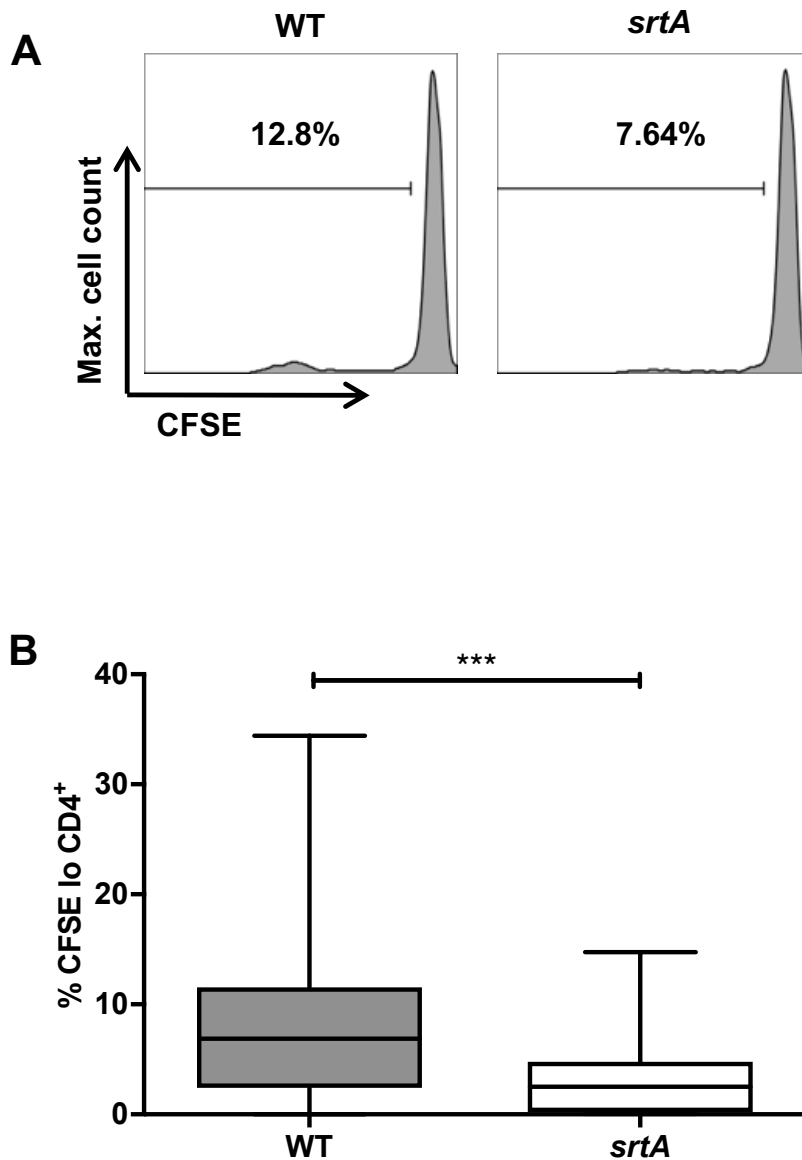


Figure 4.3. Human CD4⁺ T cell proliferation is decreased in response to *S. aureus* LAC::lux *srtA* compared to LAC::lux WT. Purified CD4⁺ T cells were CFSE-labelled and co-cultured with autologous irradiated APCs from healthy blood donors and incubated with heat-inactivated LAC::lux WT, LAC::lux *srtA* (1 μ g/ml) or media alone. On d 10, proliferation was assessed by gating on CFSE^{lo} cells in the CD4⁺ population. For each donor, media only responses were subtracted from responses to heat-inactivated *S. aureus* to determine antigen-specific T cell responses. Results shown as box-and-whiskers plots where the horizontal line indicate the median, boundaries of the box the IQR, and whiskers indicate the highest and lowest values of the results (B). Representative FACS plots of proliferating CD4⁺ cells are shown (A). n=40 per group. A nonparametric Mann-Whitney U test was used to analyse variances between groups. *** $p < 0.001$.

Antigen	% of Responders	p-value
HI LAC:: <i>lux</i> WT	90 %	
HI LAC:: <i>lux srtA</i>	77.5 %	$p=0.224$ vs. HI LAC:: <i>lux</i> WT
CifA N123	72.9 %	
CifA N23	62.5 %	$p=0.421$ vs. CifA N123
CifA N1	42.9 %	$p=0.0283$ vs. CifA N123
CifB	40 %	$p=0.0034$ vs. CifA N123
SdrC	57.7 %	$p=0.202$ vs. CifA N123

Table 4.1. The percentage of donors that responded to antigen stimulation.

Purified CD4⁺ T cells were CFSE-labelled and combined with autologous irradiated APCs from healthy blood donor buffy coats and stimulated with antigens of *S. aureus* or media alone. After 10 d, proliferation was assessed by gating on CFSE^{lo} cells in the CD4⁺ population. Antigen-specific T cell responses were calculated by subtracting any proliferation of media only treated cells. Donors with antigen-specific proliferation >0 % were designated a responder to the relevant antigen. HI=Heat-inactivated. *P* values were calculated using Fisher's exact test.

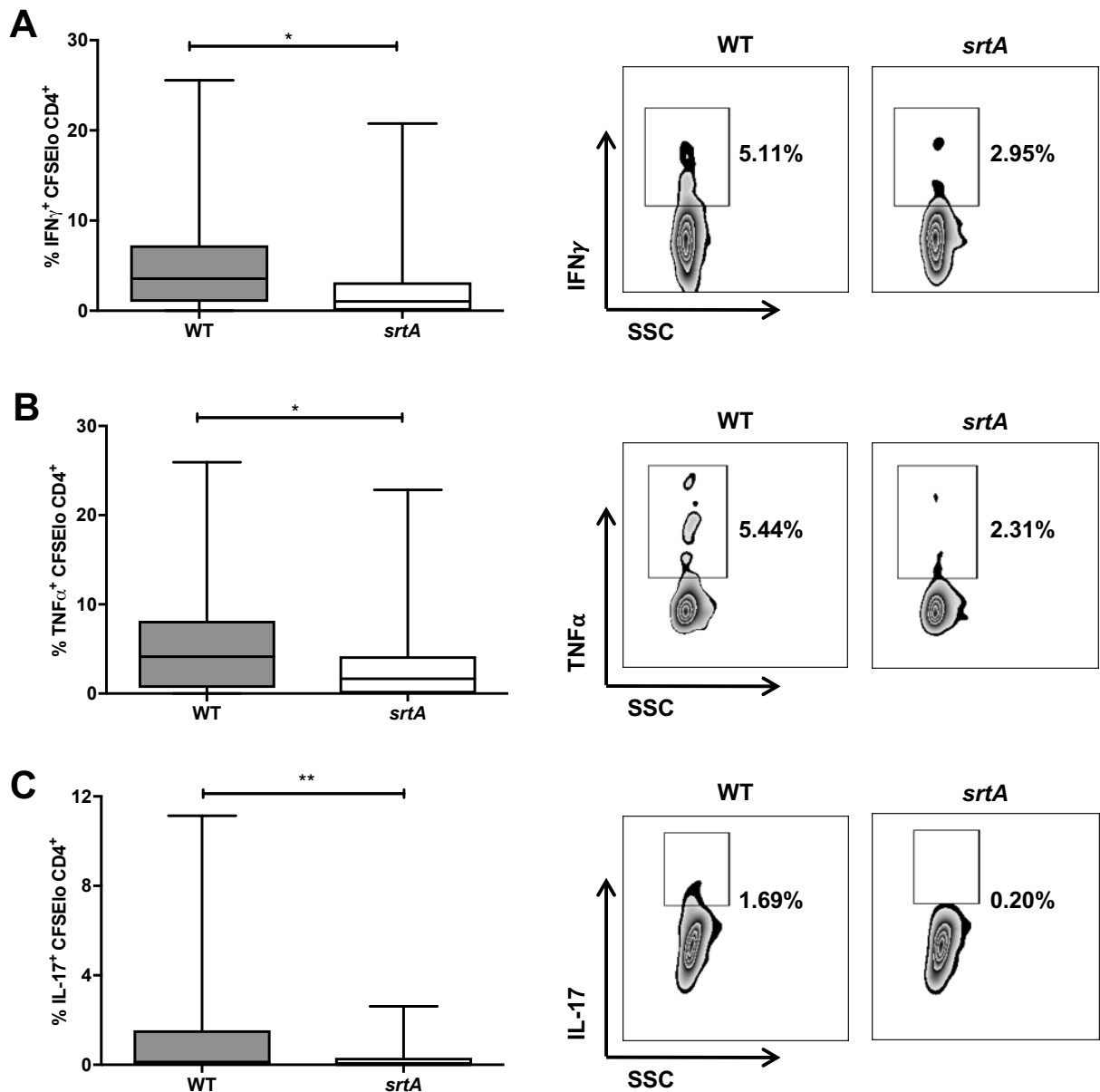


Figure 4.4. Human CD4⁺ T cells show greater antigen-specific responses to *S. aureus* LAC::lux WT compared to LAC::lux *srtA*. Purified CD4⁺ T cells were CFSE-labelled and co-cultured with autologous irradiated APCs from healthy blood donors and incubated with heat-inactivated LAC::lux WT, LAC::lux *srtA* (1 μ g/ml) or media alone. On d 10 *S. aureus*-specific IFN γ (A), TNF α (B), and IL-17 (C) responses were assessed by gating on IFN γ^+ , TNF α^+ or IL-17⁺ cells within the CFSE $_{lo}$ CD4⁺ population. For each donor, media only responses were subtracted from responses to heat-inactivated *S. aureus* to determine antigen-specific response. Results shown as box-and-whiskers plots where the horizontal line indicate the median, boundaries of the box the IQR, and whiskers indicate the highest and lowest values of the results (B). Representative FACS plots of proliferating CD4⁺ cells are shown (A). n=34-40 per group. A nonparametric Mann-Whitney U test was used to analyse variances between groups. * $p < 0.05$, ** $p < 0.01$.

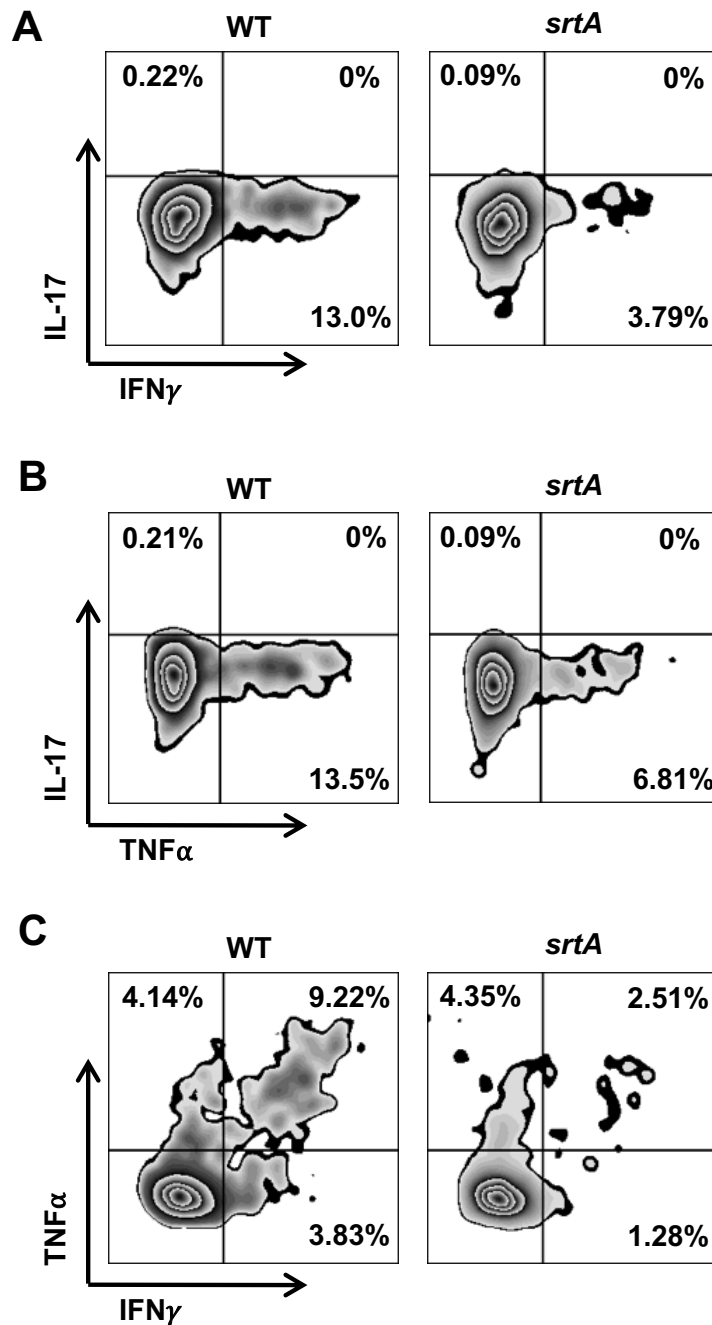


Figure 4.5. The majority of TNF α production from human CD4⁺ T cells is associated with Th1 cells in responses to heat-inactivated *S. aureus*. Purified CD4⁺ T cells were CFSE-labelled and co-cultured with autologous irradiated APCs from healthy blood donors and incubated with heat-inactivated LAC::lux WT, LAC::lux *srtA* (1 μ g/ml) or media alone. On d 10 *S. aureus*-specific IFN γ ⁺IL-17⁺ (A), IL-17⁺TNF α ⁺ (B) and TNF α ⁺IFN γ ⁺ (C) responses were assessed by gating within the CFSElo CD4⁺ population. Representative FACS plots of proliferating CD4⁺ cells are shown.

4.2.2 Human CD4⁺ T cells proliferate in response to purified staphylococcal CWA proteins

As human T cell proliferation was reduced in response to heat-inactivated *S. aureus* LAC::*lux srtA*, this indicated that human T cells were capable of responding to CWA proteins of *S. aureus*. The ability of selected staphylococcal CWA proteins; ClfA, ClfB and SdrC, to induce CD4⁺ T cell proliferation was then investigated. ClfA was chosen as it has been used as a vaccine antigen in human clinical trials by both Pfizer and GSK [280, 281, 284]. However its ability to activate T cells has not previously been examined. ClfB and SdrC were chosen as they are structurally similar to ClfA and all belong to the MSCRAMM family of CWA proteins, which are characterised by their IgG-folded domains [95].

CD4⁺ T cells were co-cultured with irradiated APCs and stimulated with recombinant *S. aureus* proteins purified from *E. coli*. Antigen-specific proliferation and cytokine production was assessed on day 10 and responses to media alone were deducted. Of note, no difference in CD4⁺ T cell proliferation following stimulation with media alone or an irrelevant control antigen (bovine serum albumin) was observed (Figure 4.6).

73 % of individuals were in possession of CD4⁺ T cells capable of responding to ClfA, while 58 % of individuals responded to SdrC and 40 % responded to ClfB (Table 4.1). The levels of CD4⁺ T cell proliferation were significantly higher in ClfA stimulated cells compared to cells stimulated with ClfB or SdrC (Figure 4.7). All three of the proteins had the ability to induce the production of IFN γ and IL-17 from CD4⁺ T cells (Figure 4.8), with a trend towards ClfA inducing a greater response compared to ClfB and SdrC. These results indicate that individual CWA proteins have the potential to activate Th1 and Th17 cells, however some proteins, such as ClfA, may be more potent at activating specific T cell subsets than others.

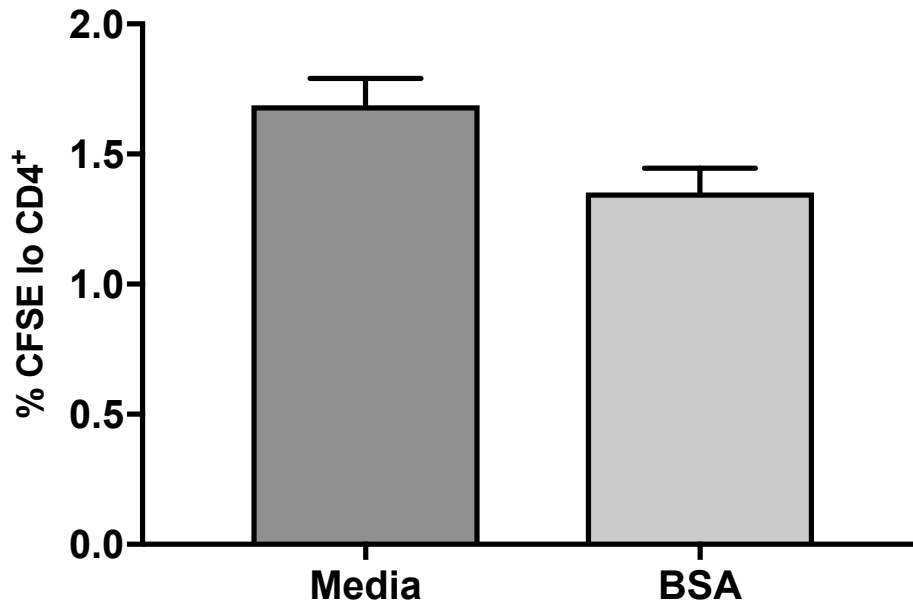


Figure 4.6. No difference in levels of proliferation of human CD4⁺ T cells in response to media or bovine serum albumin. Human PBMCs from healthy blood donors were CFSE-labelled and incubated with media alone or bovine serum albumin (1 μ g/ml). On day 10, proliferation was assessed by gating on CFSE^{lo} cells in the CD4⁺ population. Results expressed as mean \pm SEM. n=3 per group.

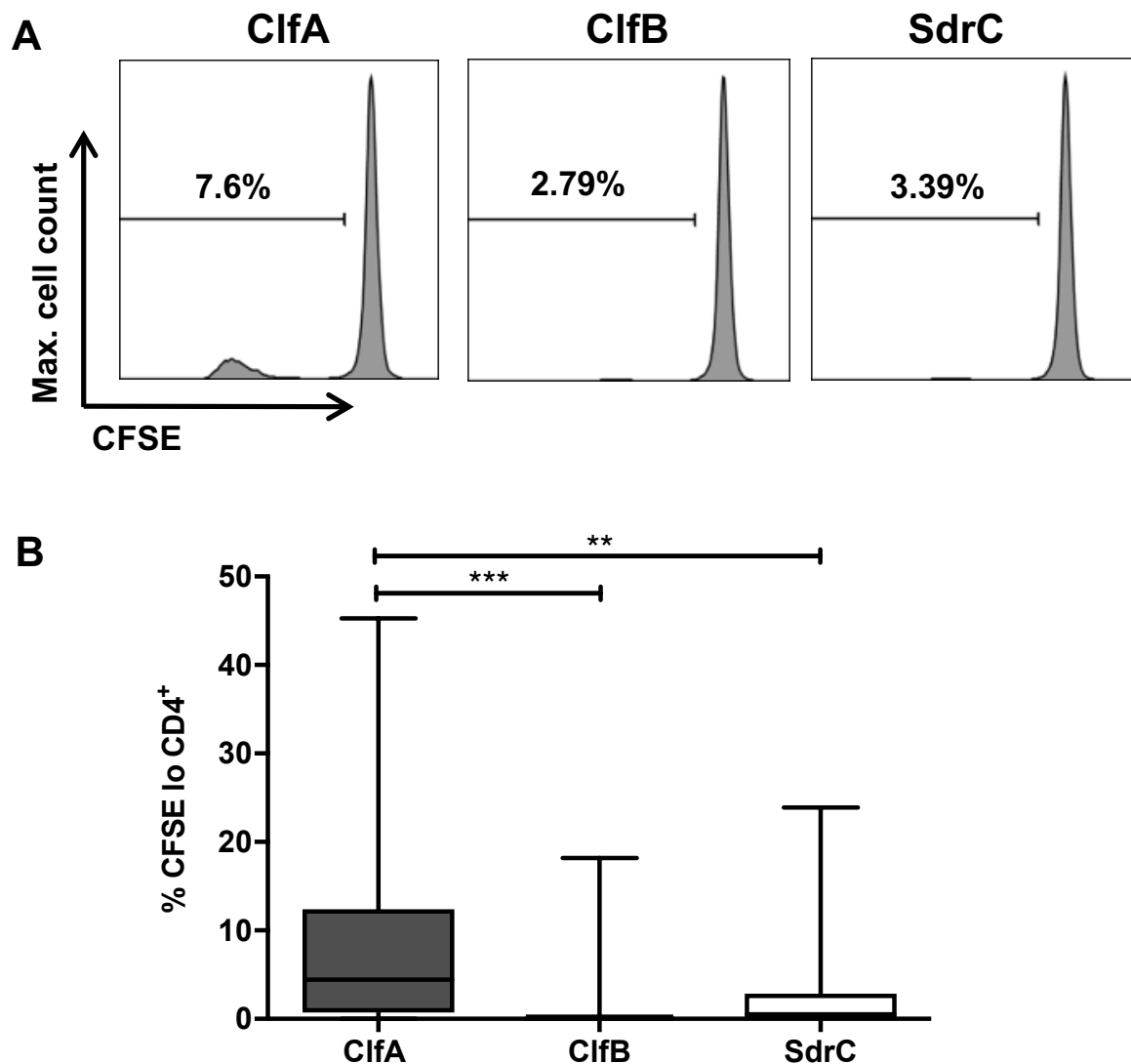


Figure 4.7. Human CD4⁺ T cells proliferate in response to purified staphylococcal cell wall-anchored proteins. Purified CD4⁺ T cells were CFSE-labelled and co-cultured with autologous irradiated APCs from healthy blood donors and stimulated with ClfA, ClfB, SdrC (0.88 μ M) or media alone. On d 10, proliferation was assessed by gating on CFSE^{lo} cells in the CD4⁺ population. For each patient, media only responses were subtracted from responses to purified *S. aureus* proteins to determine antigen-specific response. Results shown as box-and-whiskers plots where the horizontal line indicated the median, boundaries of the box the IQR, and whiskers indicate the highest and lowest values of the results (B). Representative FACS plots of CD4⁺ cells are shown (A). n=39 for ClfA, n=35 for ClfB, n=26 for SdrC. Kruskal-Wallis test with Dunn's multiple comparison post-test was used to compare variances between groups. ** $p < 0.01$, *** $p < 0.001$.

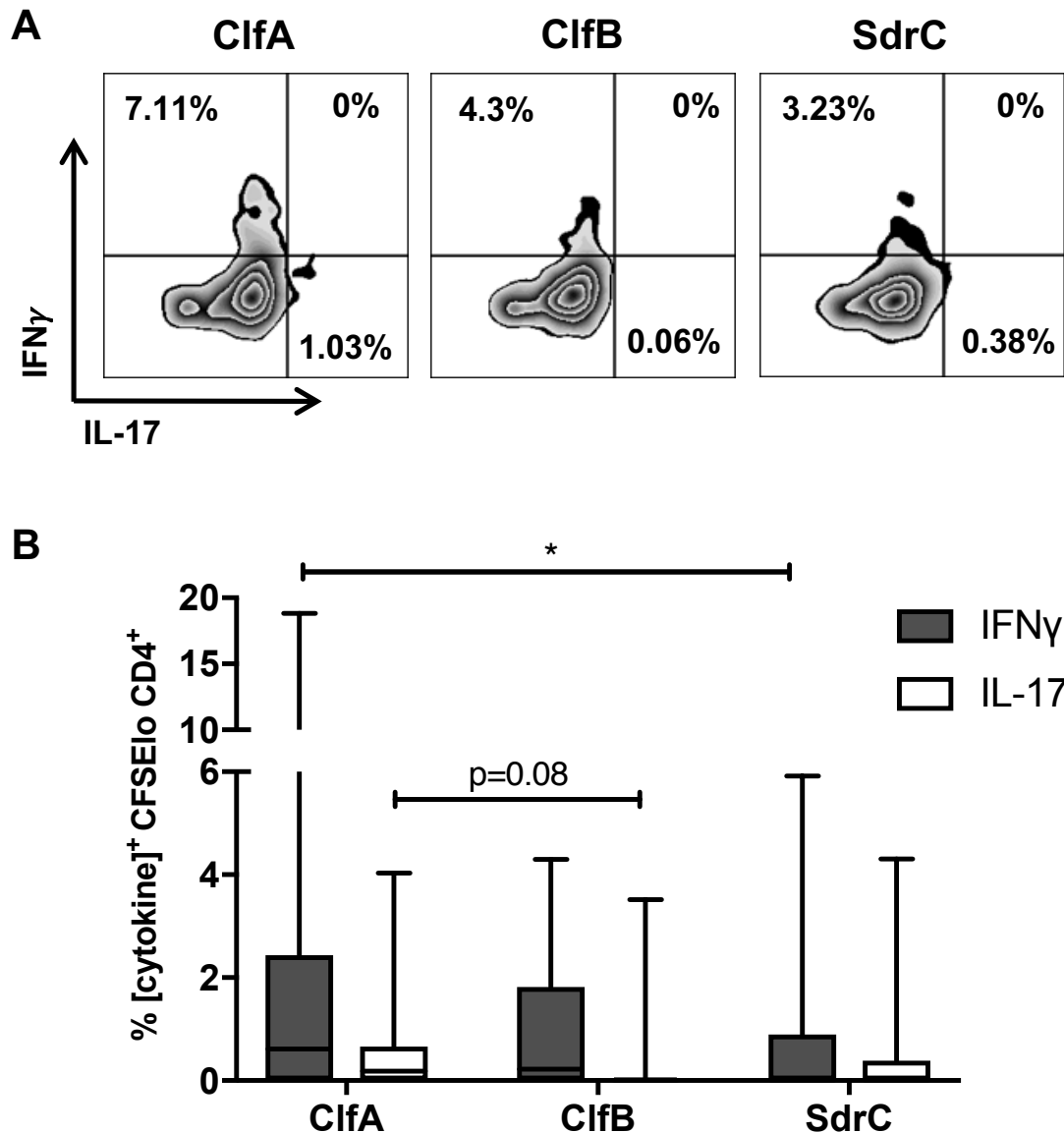


Figure 4.8. Human CD4⁺ T cells have antigen-specific responses to purified staphylococcal cell wall-anchored proteins. Purified CD4⁺ T cells were CFSE-labelled and co-cultured with autologous irradiated APCs from healthy blood donors and stimulated with CifA, CifB, SdrC (0.88 μ M) or media alone for 10 d. *S. aureus* antigen-specific Th1 and Th17 proportions were compared by gating on IFN γ ⁺ and IL-17⁺ cells within in the CFSE^{lo} CD4⁺ population. For each donor, media only responses were subtracted from responses to purified protein to determine antigen-specific response. Results shown as box-and-whiskers plots where the horizontal line indicated the median, boundaries of the box the IQR, and whiskers indicate the highest and lowest values of the results (B). n=39 for CifA, n=35 for CifB, n=26 for SdrC. Representative FACS plots of dividing CD4⁺ cells are shown (A). Kruskal-Wallis test with Dunn's multiple comparison post-test was used to compare variances between groups. * $p < 0.05$, ** $p < 0.01$, *** $p < 0.001$.

4.2.3 Subdomains of ClfA drive antigen-specific responses in human CD4⁺ T cells

Having demonstrated that ClfA is a potent T cell activator, we investigated which subdomains of the protein may be involved in T cell activation. Full length ClfA A domain (ClfA N123) alongside two truncated proteins, ClfA N23 and ClfA N1 were expressed and purified from *E. coli*. Subdomains N2 and N3 were expressed as a single polypeptide since together they represent a functional subunit, the minimum fibrinogen binding region. ClfA N1 was highly unstable and prone to degradation. To increase the protein's stability, it was bound to glutathione S-transferase (GST). The stability of these proteins was assessed by running the proteins on an SDS-PAGE gel (Figure 4.9). To control for the presence of GST, cells were also treated with purified GST and responses for N1 were corrected by subtracting any proliferation or cytokine production caused by GST alone. To most accurately assess which subdomain of ClfA was involved in T cell activation, only T cells from individuals who could respond to full length ClfA N123 (i.e. the donors were in possession of ClfA specific T cells) (Figure 4.10) were selected to accurately assess the subdomains involved in T cell activation.

CD4⁺ T cells were isolated from buffy coats of healthy adult blood donors and co-cultured with autologous irradiated APCs in the presence of purified ClfA N123, ClfA N23, ClfA N1 or GST for 10 days. The percentage of CD4⁺ T cells dividing in response to N123 was significantly greater compared to cells treated with either the N23 or N1 subdomains (Figure 4.11), suggesting that the full length protein is needed for the highest levels of CD4⁺ T cell proliferation. All three subdomains were capable of activating Th1 cells to a similar extent (Figure 4.12). Full length ClfA N123 and N23 domains induced almost equivalent levels of Th17 cell activation (Figure 4.12). In contrast however, it appears that the N1 domain was not required for Th17 cell

expansion. These results indicate that the N23 domain possess both Th1 and Th17 cell activating abilities however the N1 domain can exclusively activate Th1 cells.

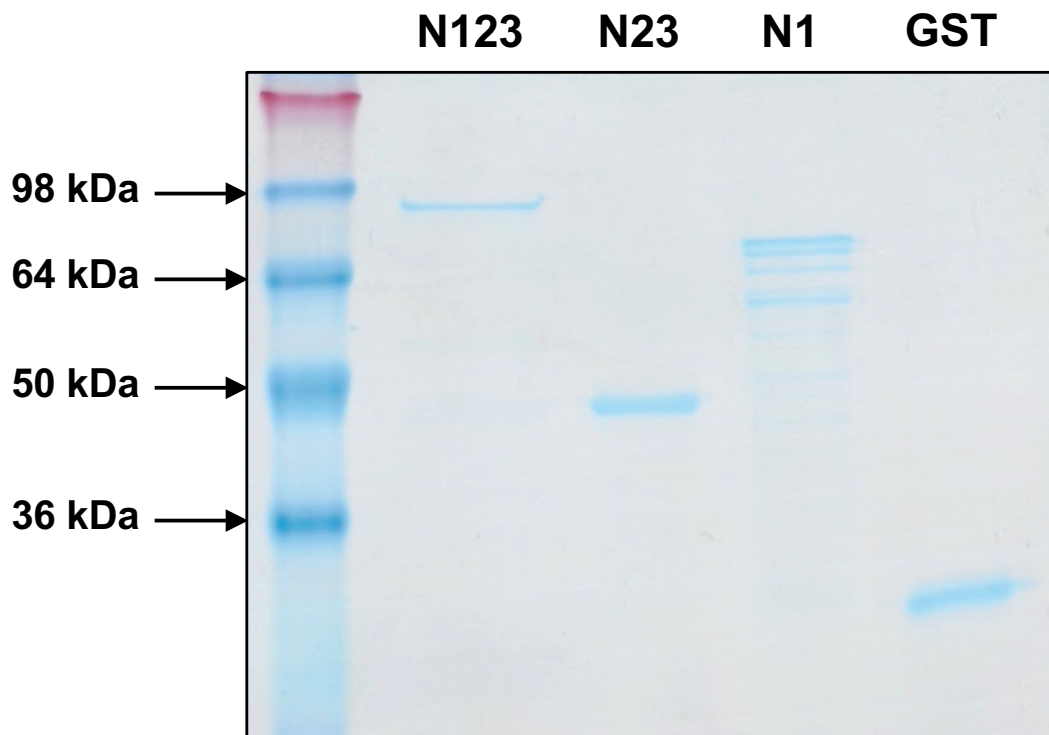


Figure 4.9. Stability of subdomains of clumping factor A. ClfA N123, ClfA N23, ClfA N1 and GST were run on a 12 % SDS-PAGE gel and stained with Instant Blue (Expedeon). Slight breakdown of the ClfA N1 subdomain is observed. The results shown are representative of 3 independent experiments.

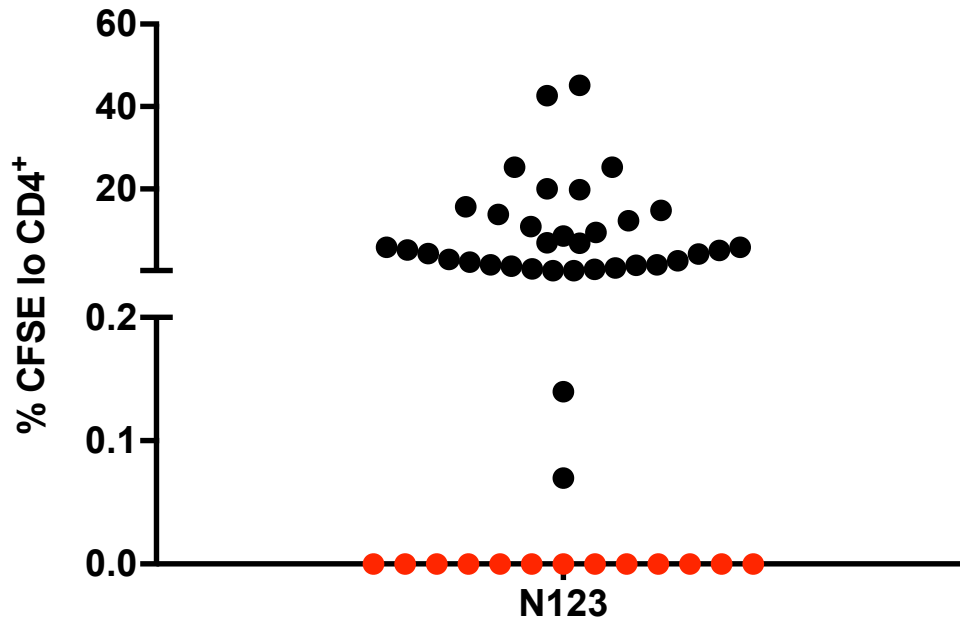


Figure 4.10. 72.9 % of individuals possess CD4⁺ T cells which can recognise and proliferate in response to purified ClfA N123. Purified CD4⁺ T cells and irradiated APCs from healthy blood donor buffy coats were CFSE-labelled and stimulated with ClfA N123 (0.88 μ M) or media alone. On 10 d, proliferation was assessed by gating on CFSElo cells in the CD4⁺ population. Donor cells which failed to respond to ClfA N123 stimulation (indicated as red dots) were excluded from further study.

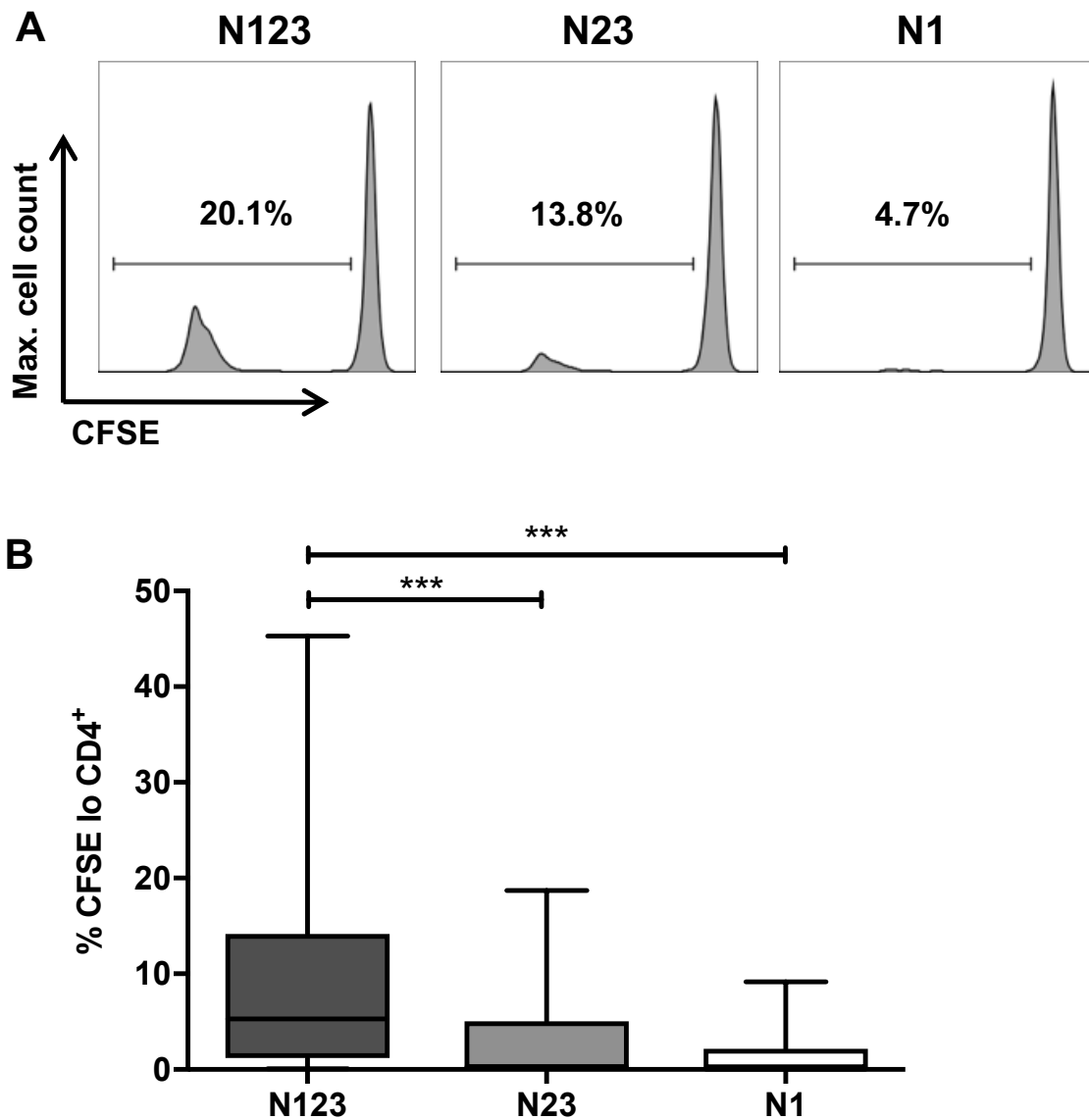


Figure 4.11. Human CD4⁺ T cells proliferate in response to subdomains of ClfA. Purified CD4⁺ T cells were CFSE-labelled and co-cultured with autologous irradiated APCs from healthy blood donors and stimulated with ClfA N123, N23, N1, GST (0.88 μ M) or media alone. On d 10, proliferation was assessed by gating on CFSE^{lo} cells in the CD4⁺ population. For each donor, media only responses were subtracted from responses to purified protein to determine antigen-specific response. ClfA N1 results were corrected for the presence of GST by subtracting proliferation values in GST treated cells. Results shown as box-and-whiskers plots where the horizontal line indicated the median, boundaries of the box the IQR, and whiskers indicate the highest and lowest values of the results (B). Representative FACS plots of proliferating CD4⁺ cells are shown (A). n=30 for N123, n=25 for N23, n=21 for N1. Kruskal-Wallis test with Dunn's multiple comparison post-test was used to compare variances between groups. *** p<0.001.

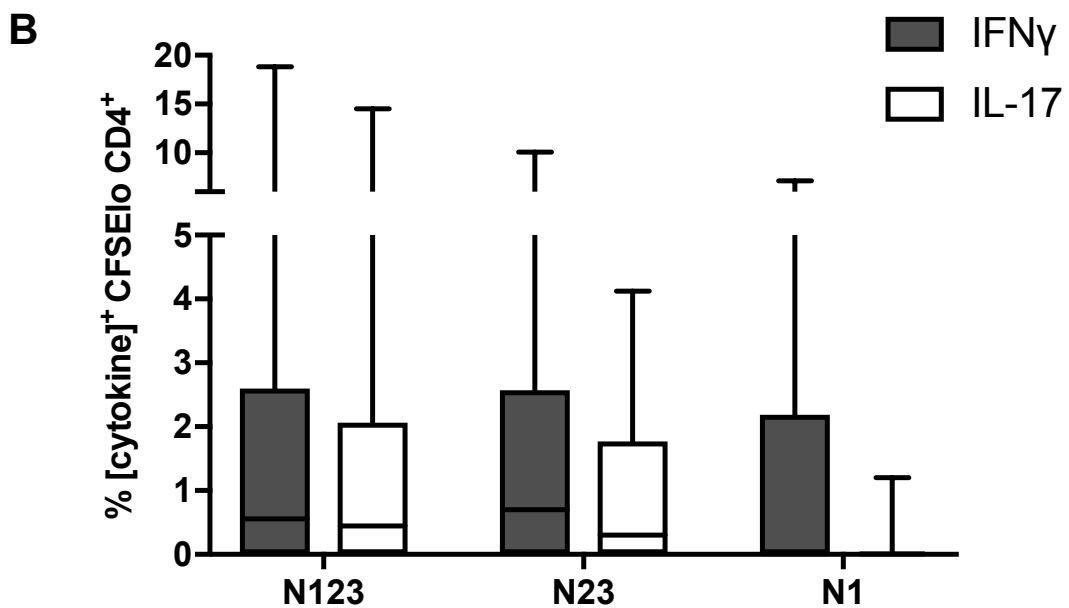
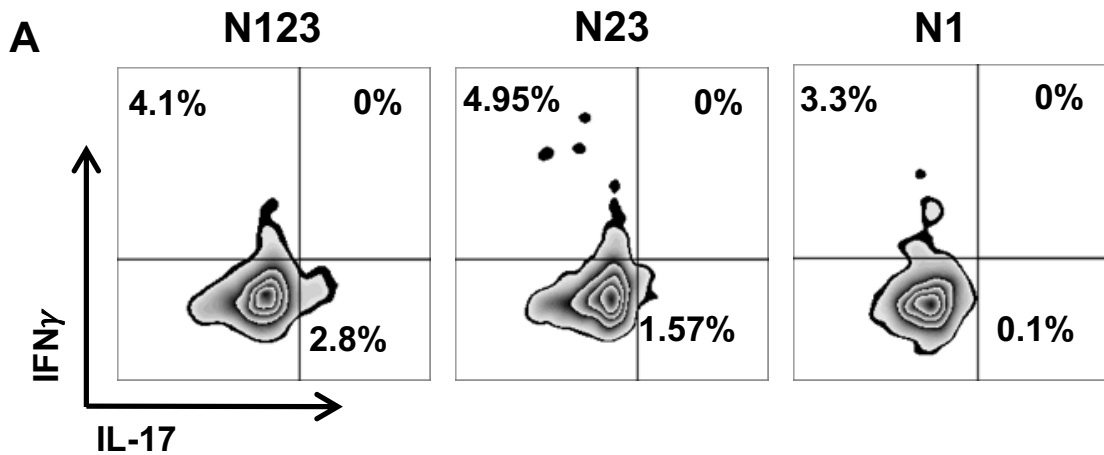


Figure 4.12. Th1 and Th17 cells proliferate in response to subdomains of ClfA.

Purified CD4⁺ T cells were CFSE-labelled and co-cultured with autologous irradiated APCs from healthy blood donors and co-cultured with ClfA N123, N23, N1, GST (0.88 μM) or media alone. On d 10, *S. aureus* antigen-specific Th1 and Th17 proportions were compared by gating on IFNγ⁺ or IL-17⁺ cells within in the CFSElo CD4⁺ population. For each donor, media only responses were subtracted from responses to purified protein to determine antigen-specific response. ClfA N1 results were corrected for the presence of GST by subtracting proliferation values in GST treated cells. Results shown as box-and-whiskers plots where the horizontal line indicated the median, boundaries of the box the IQR, and whiskers indicate the highest and lowest values of the results (B). Representative FACS plots of proliferating CD4⁺ cells are shown (A). n=30 for N123, n=25 for N23, n=21 for N1.

4.2.4 Immunisation of mice with individual subdomains of ClfA induces Th1 and Th17 cellular immune responses

Having confirmed that ClfA N123, N23 and N1 can promote human Th1 and Th17 responses *in vitro*, albeit to differing extents, we investigated if these domains could promote T cell responses *in vivo* when used in model vaccines. A model *S. aureus* vaccine previously described [156] was utilised, composed of ClfA N123 or its individual subdomains formulated with the TLR9 agonist CpG as an adjuvant. Groups of naïve mice were vaccinated via the s.c. route with CpG (50 µg/mouse) alone, CpG combined with either ClfA N123, N23, N1 (1 µg/mouse) or PBS alone on d 0, 14 and 28. To account for the presence of GST bound N1, mice were also vaccinated with CpG+GST. On d 63 (5 weeks after final immunisation) the inguinal lymph nodes (ILN) and spleens were isolated. Total isolated cells were stimulated *in vitro* with ClfA N123 (5 µg/ml) or anti-CD3 and PMA as a positive control. Cell supernatants were collected 72 h post-stimulation for analysis of secreted cytokines by ELISA to assess antigen-specific cellular responses prior to challenge. There was no difference in IFN γ and IL-17 production by ILN or splenic cells between GST vaccinated mice and PBS or CpG vaccinated mice (Data not shown).

Immunisation with CpG+N123 drove a significant increase in IFN γ production by ILN cells compared to control groups (PBS alone or CpG alone), whereas vaccination with CpG+N23 and CpG+N1 resulted in a modest increase (Figure 4.13 A). IL-17 production by ILN cells was significantly increased in all vaccinated groups compared to controls (Figure 4.13 B), however, the levels of IL-17 were relatively low compared to the IFN γ response, consistent with the use of the Th1 inducing adjuvant CpG. Cells isolated from the spleens of mice vaccinated with CpG+N123, CpG+N23 and CpG+N1 produced increased amounts of IFN γ (Figure 4.13 C) and IL-17 (Figure 4.13 D) upon restimulation with ClfA N123 *in vitro*, compared to splenic cells from control groups. These results demonstrate that vaccination with subdomains of ClfA

can drive antigen specific T cell responses resulting in the production of both IFN γ and IL-17.

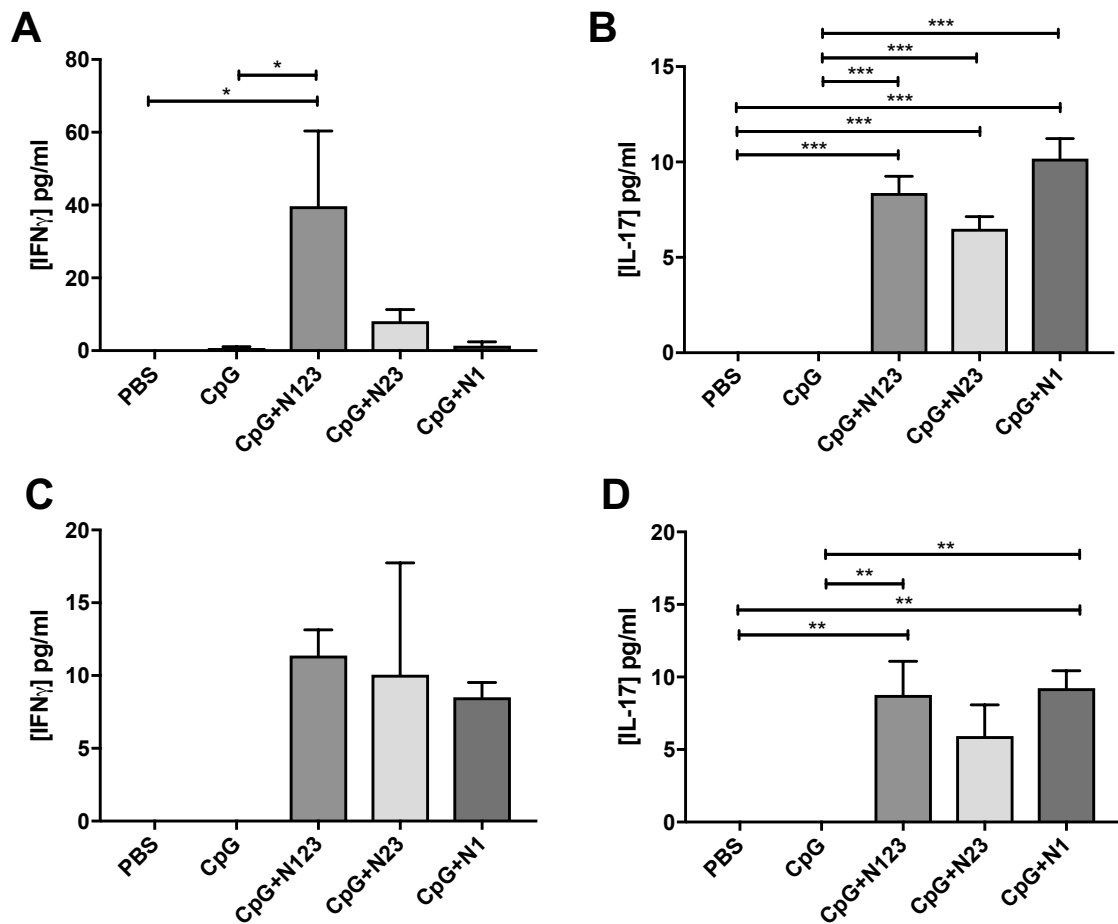


Figure 4.13. Immunisation with individual subdomains of ClfA induces ClfA-specific cellular immune responses. Mice were vaccinated with CpG (50 μ g/mouse)+ClfA N123, N23 or N1 (1 μ g/mouse) via s.c. injection on d 0, 14 and 28. Antigen-specific responses by cells isolated from the inguinal lymph nodes (A, B) and spleens (C, D) were determined on d 63, by ex vivo stimulation with media or ClfA N123 (5 μ g/ml) for 72 h, and subsequent ELISA to determine levels of IFN γ (A, C) and IL-17 (B, D). Antigen-specific responses were determined by subtracting responses to media alone. Results expressed as mean \pm SEM. n=5 per group. One-way ANOVA with Tukey post-test was performed to compare variances. * p <0.05, ** p <0.01, *** p <0.001.

4.2.5 Immunisation with individual subdomains of ClfA induces humoral immune responses

Having confirmed that vaccination could induce cellular immunity, humoral immune responses were measured in these vaccinated mice. Serum was isolated from vaccinated mice and antibody titres were assessed by ELISA. Anti-ClfA N123 IgG titres were significantly elevated in the sera of all immunised mice compared to control groups (Figure 4.14 A). Critically these antibodies were functional, as sera from all vaccinated mice effectively inhibited the binding of *S. aureus* PS80 to fibrinogen via ClfA (Figure 4.14 B), thus confirming that antibodies present were specifically ClfA neutralising. These results, taken together with the previous data, confirm that vaccination with subdomains of ClfA can drive both cellular humoral immune responses *in vivo*.

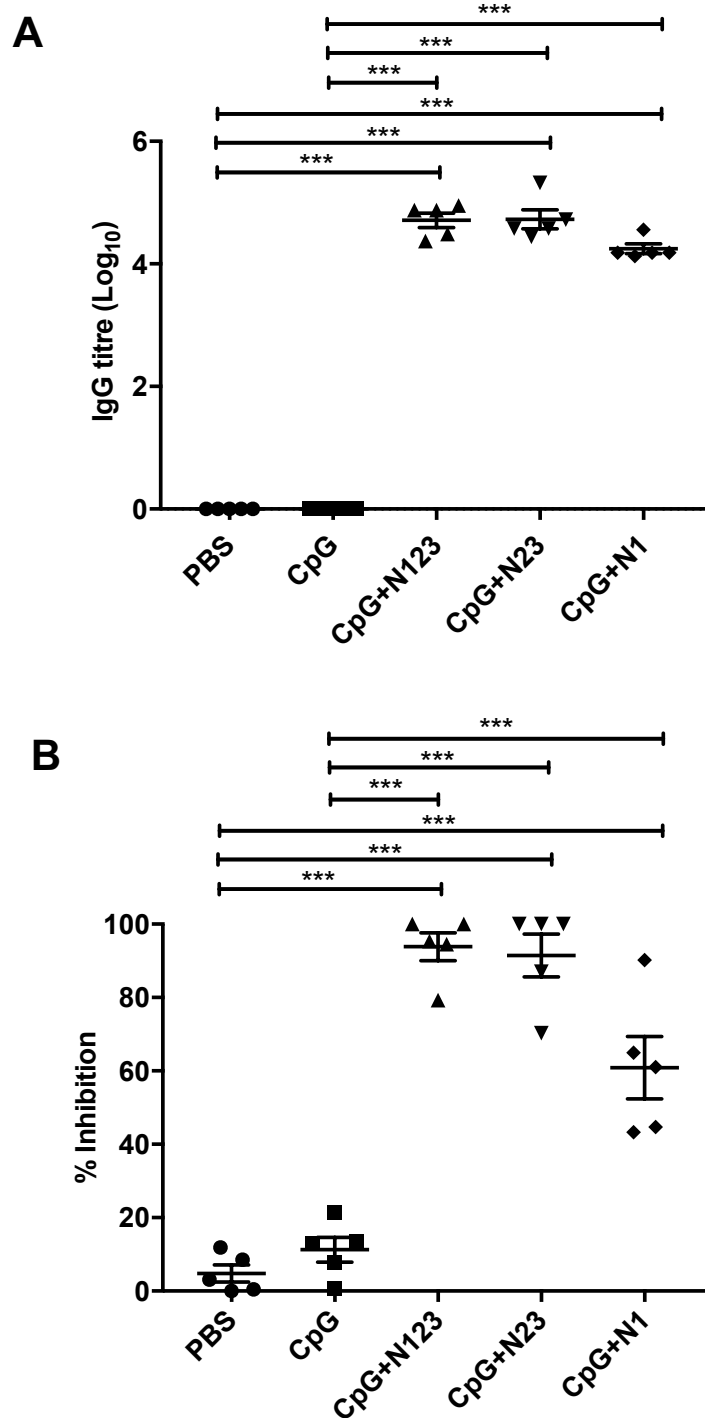


Figure 4.14 Immunisation with individual subdomains of ClfA induces ClfA-specific humoral immune responses. Mice were vaccinated with CpG (50 $\mu\text{g}/\text{mouse}$)+ClfA N123, N23 or N1 (1 $\mu\text{g}/\text{mouse}$) via s.c. injection on d 0, 14 and 28. On d 63, sera was collected from vaccinated mice. ClfA N123-specific IgG titres were determined using ELISA (A). Neutralising antibodies were determined by measuring the ability of serum to inhibit staphylococcal adherence to fibrinogen via ClfA (B). Results expressed as mean \pm SEM. $n=5$ per group. One-way ANOVA with Bonferroni post-test was performed to compare variances. * $p<0.05$, *** $p<0.001$.

4.2.6 Immunisation with individual subdomains of ClfA protects against *S. aureus* systemic infection

Having demonstrated that immunisation with ClfA N123, N23 and N1 could induce antigen-specific cellular and humoral immune responses, the ability of these vaccines to offer protection in mice against systemic infection was assessed. Groups of mice were immunized s.c. with CpG (50 µg/mouse) alone, CpG combined with either ClfA N123, N23, N1 (1 µg/mouse) or PBS alone on d 0, 14 and 28. On d 63 (5 weeks post final immunisation) mice received an i.p. injection of *S. aureus* PS80 (5×10^8 CFU). An i.p. challenge with PS80 was used as it has previously been used in this vaccination model [156]. At 24h and 72 h post-infection the peritoneal cavity was lavaged to determine the bacterial burden and the organs isolated to assess the dissemination of infection. To account for the presence of GST bound N1, mice were also vaccinated with CpG+GST. There was no difference in bacterial burden between GST vaccinated mice and PBS and CpG vaccinated mice in the peritoneal cavity (Figure 4.15 A, B), liver (Figure 4.15 C, D) and kidneys (Figure 4.15 E, F) at 24 h and 72 h respectively.

Vaccination with CpG+N123 significantly enhanced the clearance of *S. aureus* infection from the peritoneal infection site at 24 h ($\sim 4 \log_{10}$ reduction) (4.16 A) and 72 h ($\sim 3 \log_{10}$ reduction) (Figure 4.16 B) post-infection compared to control groups (PBS and CpG). Vaccination with ClfA N23 or N1 did not reduce the bacterial burden to appreciable levels in the peritoneal cavity at 24 h or 72 h post-infection. Interestingly however, vaccination with CpG+N23 or CpG+N1 conferred systemic protection at comparable levels to full length ClfA N123 by significantly reducing bacterial burden in the liver at 24 h (Figure 4.16 C) and 72 h (Figure 4.16 D) and the kidneys at 72 h (Figure 4.16 F).

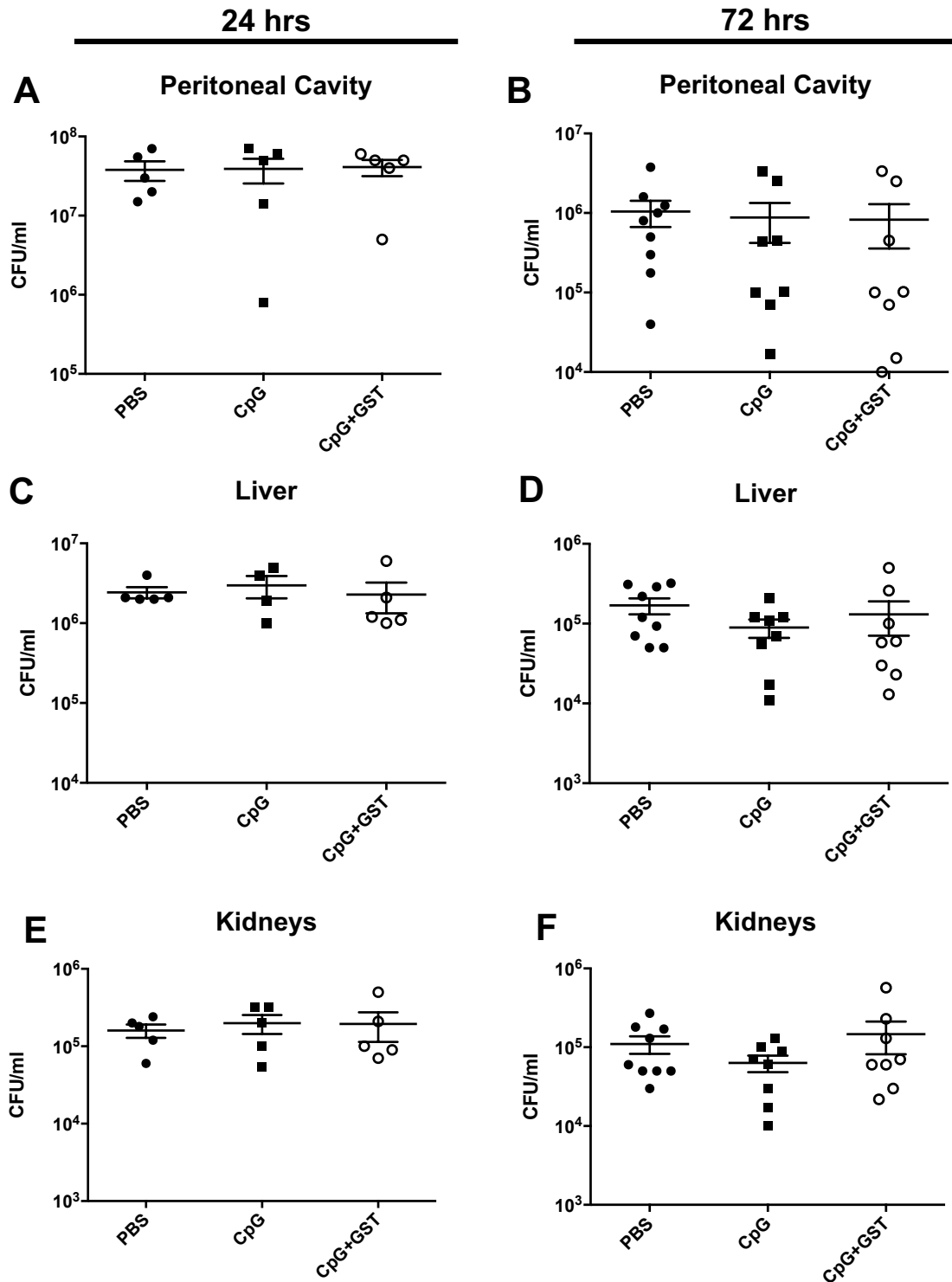


Figure 4.15. No difference in the bacterial burden of mice vaccinated with CpG+GST compared to PBS or CpG alone. Mice were vaccinated with PBS, CpG (50 $\mu\text{g}/\text{mouse}$) or CpG+GST (1 $\mu\text{g}/\text{mouse}$) via s.c. injection on d 0, 14 and 28. On d 63, mice were challenged with PS80 (5×10^8 CFU) via i.p. injection alongside a control group of sham-immunised (with PBS) mice. At 24 and 72 h post-infection, bacterial burden was assessed in the peritoneal cavity (A, B), liver (C, D) and kidneys (E, F). Results expressed as \log_{10} CFU/ml with means indicated by bars. $n=5$ per group (24h), $n=8-9$ (72h).

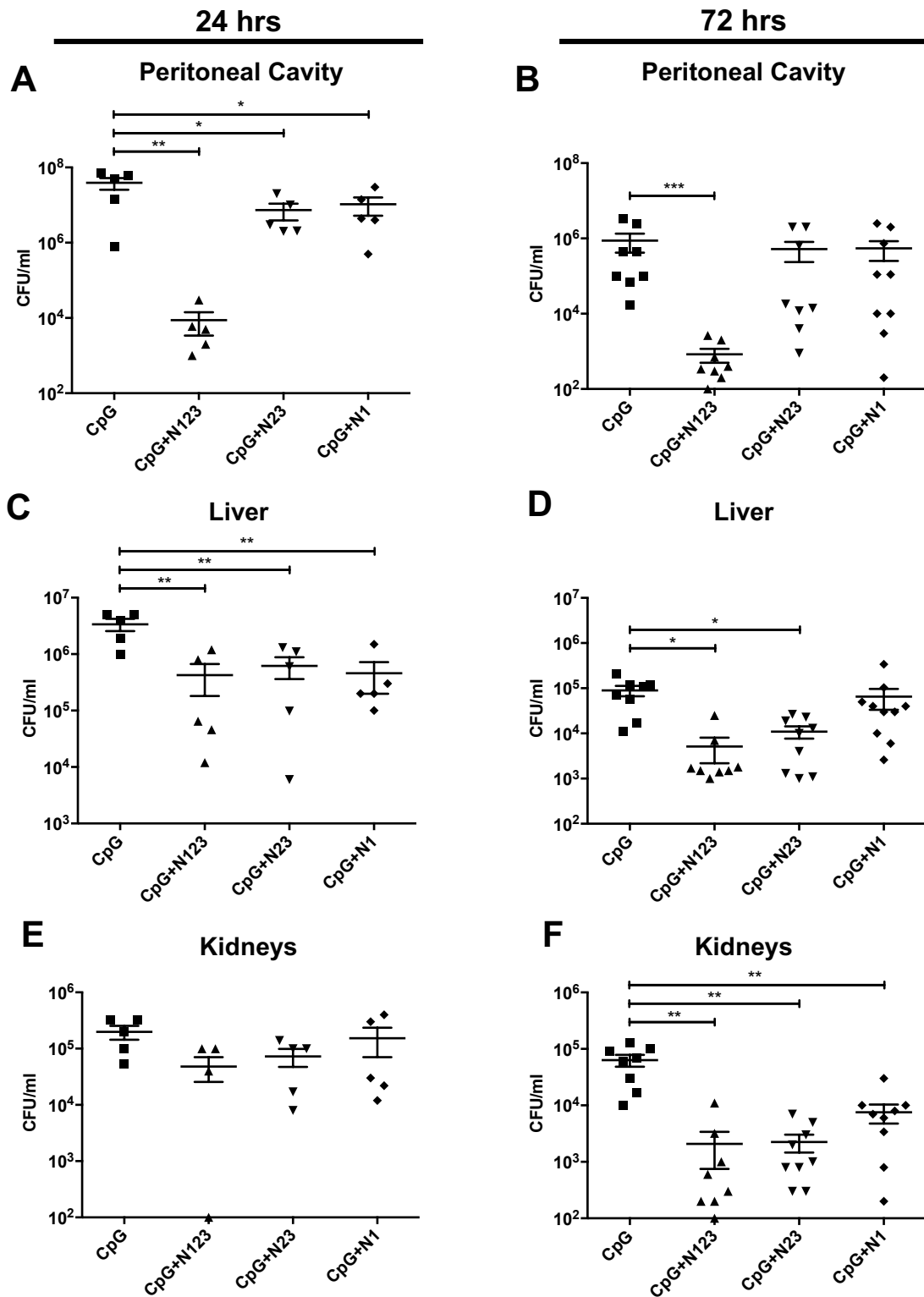


Figure 4.16. Immunisation with subdomains of ClfA protects against *S. aureus* infection at 24 and 72 h post-infection. Mice were vaccinated with CpG (50 μ g/mouse)+ClfA N123, N23 or N1 (1 μ g/mouse) via s.c. injection on d 0, 14 and 28. On d 63, mice were challenged with PS80 (5×10^8 CFU) via i.p. injection. At 24 and 72 h post-infection, bacterial burden was assessed in the peritoneal cavity (A, B), liver (C, D) and kidneys (E, F). Results expressed as \log_{10} CFU/ml with means indicated by bars. $n=5$ per group (24h), $n=8-10$ (72h). One-way ANOVA with Tukey post-test was performed. * $p < 0.05$, ** $p < 0.01$, *** $p < 0.001$.

4.2.7 Enhanced bacterial clearance mediated by vaccination with subdomains of ClfA is associated with increased T cell responses at site of infection

As vaccination with subdomains of ClfA enhanced bacterial clearance during *S. aureus* infection, the type of immune response induced by immunisation was investigated. To determine if the vaccine-induced protection was associated with an enhanced T cell response, the cells infiltrating the peritoneal cavity at 72 h post-infection were assessed. The total number of infiltrating CD4⁺ T cells was elevated in all vaccinated groups compared to control groups (Figure 4.17 A). The number of CD4⁺ T cells producing IFN γ (Figure 4.17 B) was also increased in the peritoneal cavities of CpG+N123, CpG+N23 and CpG+N1 immunised mice compared to control groups. IL-17 production by CD4⁺ T cells was also increased in all vaccinated groups compared to control groups (Figure 4.17 C).

There was also elevated levels of CD8⁺ T cells infiltrating the peritoneal cavity in all vaccinated groups compared to control animals (Figure 4.18 A). IFN γ (Figure 4.18 B) and IL-17 (Figure 4.18 C) production by these CD8⁺ T cells was increased in CpG+N123, CpG+N23 and CpG+N1 vaccinated groups compared to controls.

Overall, these results reveal that vaccination with full length N123, N23 or N1 in combination with the adjuvant CpG significantly increased IFN γ and IL-17 production by both CD4⁺ and CD8⁺ T cells at the site of infection. Of note, vaccination with either full length N123 or subdomains N23 or N1 had no significant effect on the number of $\gamma\delta$ ⁺ T cells in the peritoneal cavity (Figure 4.19 A) or their production of IFN γ (Figure 4.19 B) or IL-17 (Figure 4.19 C) at 72 h post-infection. However, there was a slight increase in $\gamma\delta$ ⁺ T cell responses to CpG+N23 vaccinated mice. To fully investigate the contribution of these $\gamma\delta$ ⁺ T cells during this infection model, an earlier time point of 3 hours would be desirable, as $\gamma\delta$ ⁺ T cell responses have previously been shown to peak at this time point during peritoneal infection [193].

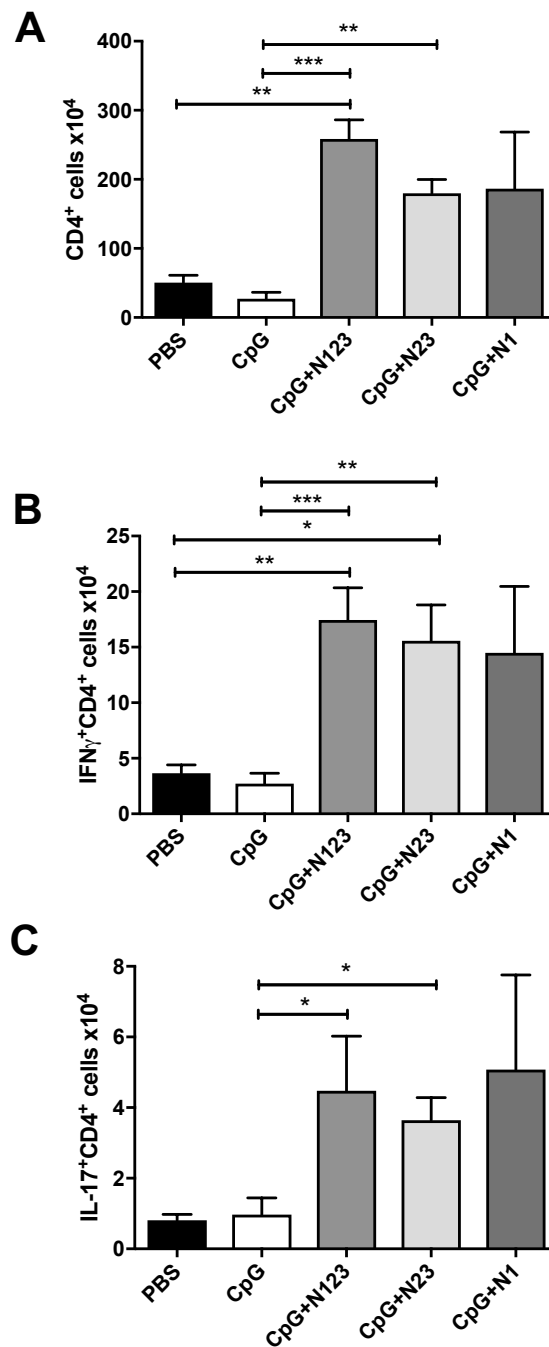


Figure 4.17. Immunisation with individual subdomains of ClfA with CpG increases CD4⁺ recruitment and cytokine production at the site of infection during *S. aureus* infection. Mice were vaccinated with PBS, CpG (50 μ g/mouse), CpG+ClfA N123, N23 or N1 (1 μ g/mouse) via s.c. injection on d 0, 14 and 28. On d 63, mice were challenged with PS80 (5×10^8 CFU) via i.p. injection. At 72 h post-infection cells were isolated from the peritoneal cavity to assess the number of CD4⁺ T cells (A). The number of IFN γ ⁺CD4⁺ (B) and IL-17⁺CD4⁺ (C) cells in the peritoneum was assessed by flow cytometry. Results expressed as mean \pm SEM. n=8-10 per group. One-way ANOVA with Tukey post-test was performed to compare variances. * $p < 0.05$, ** $p < 0.01$, *** $p < 0.001$.

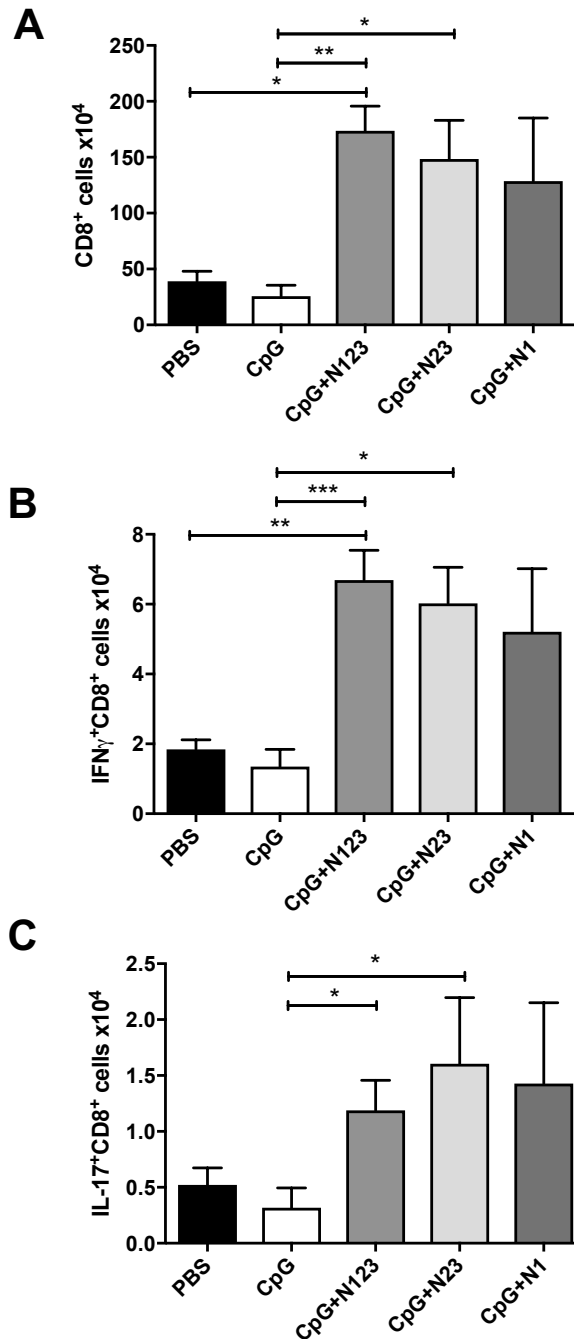


Figure 4.18. Immunisation with individual subdomains of ClfA with CpG increases CD8⁺ T cell recruitment and cytokine production at the site of infection during *S. aureus* infection. Mice were vaccinated with PBS, CpG (50 μ g/mouse), CpG+ClfA N123, N23 or N1 (1 μ g/mouse) via s.c. injection on d 0, 14 and 28. On d 63, mice were challenged with *S. aureus* PS80 (5×10^8 CFU) via i.p. injection. At 72 h post-infection cells were isolated from the peritoneal cavity to assess the number of CD8⁺ T cells (A). The number of IFN γ ⁺CD8⁺ (B) and IL-17⁺CD8⁺ (C) cells in the peritoneum was assessed by flow cytometry. Results expressed as mean \pm SEM. n=8-10 per group. One-way ANOVA with Tukey post-test was performed to compare variances. * $p < 0.05$, ** $p < 0.01$, *** $p < 0.001$.

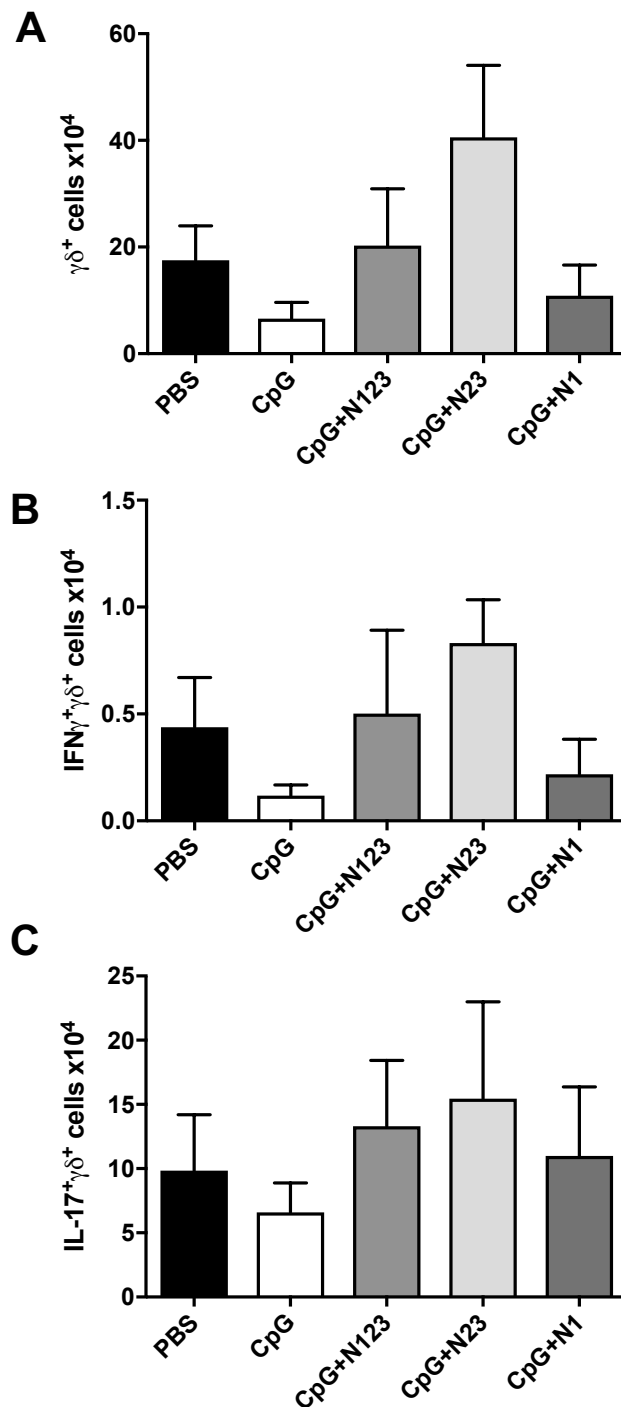


Figure 4.19. Immunisation with individual subdomains of ClfA with CpG had no significant effect on the production of $\text{IFN}\gamma$ or IL-17 by $\gamma\delta^+$ T cells during *S. aureus* infection. Mice were vaccinated with PBS, CpG (50 $\mu\text{g}/\text{mouse}$), CpG+ClfA N123, N23 or N1 (1 $\mu\text{g}/\text{mouse}$) via s.c. injection on d 0, 14 and 28. On d 63, mice were challenged with *S. aureus* PS80 (5×10^8 CFU) via i.p. injection. At 72 h post-infection, cells were isolated from the peritoneal cavity to assess the number of $\text{IFN}\gamma^+\gamma\delta^+$ (A) and $\text{IL-17}^+\gamma\delta^+$ (B) cells by flow cytometry. Results expressed as mean \pm SEM. n=8-10 per group.

4.2.8 Immunisation with subdomains of ClfA enhances phagocyte activation during *S. aureus* infection

Enhanced bacterial clearance induced by vaccination with subdomains of ClfA in combination with CpG was associated with the induction of T cell responses locally within the peritoneal cavity during *S. aureus* infection. To establish the downstream effects of this ClfA induced protective T cell response, phagocyte influx and activity at the infection site was examined 72 h post-infection.

Vaccination with subdomains of ClfA in combination with CpG did not affect the total numbers of neutrophils (Figure 4.20 A) or macrophages (Figure 4.20 B) recruited to the peritoneal cavity during *S. aureus* infection. However the phagocytes in vaccinated mice displayed increased activation. 123-Dihydrorhodamine staining was used to measure ROS activity within cells [246]. Significantly elevated ROS activity was observed in neutrophils (Figure 4.21 A) in all vaccinated groups compared to control groups at 72 h post-infection. Similarly, a significant increase in the ROS activity of macrophages was detected in vaccinated groups compared to controls and macrophages (Figure 4.21 B).

Taken together, these results demonstrate that vaccination with full length N123, N23 or N1 can drive Th1 and Th17 responses, which in turn enhance neutrophil and macrophage effector functions to prevent *S. aureus* systemic dissemination.

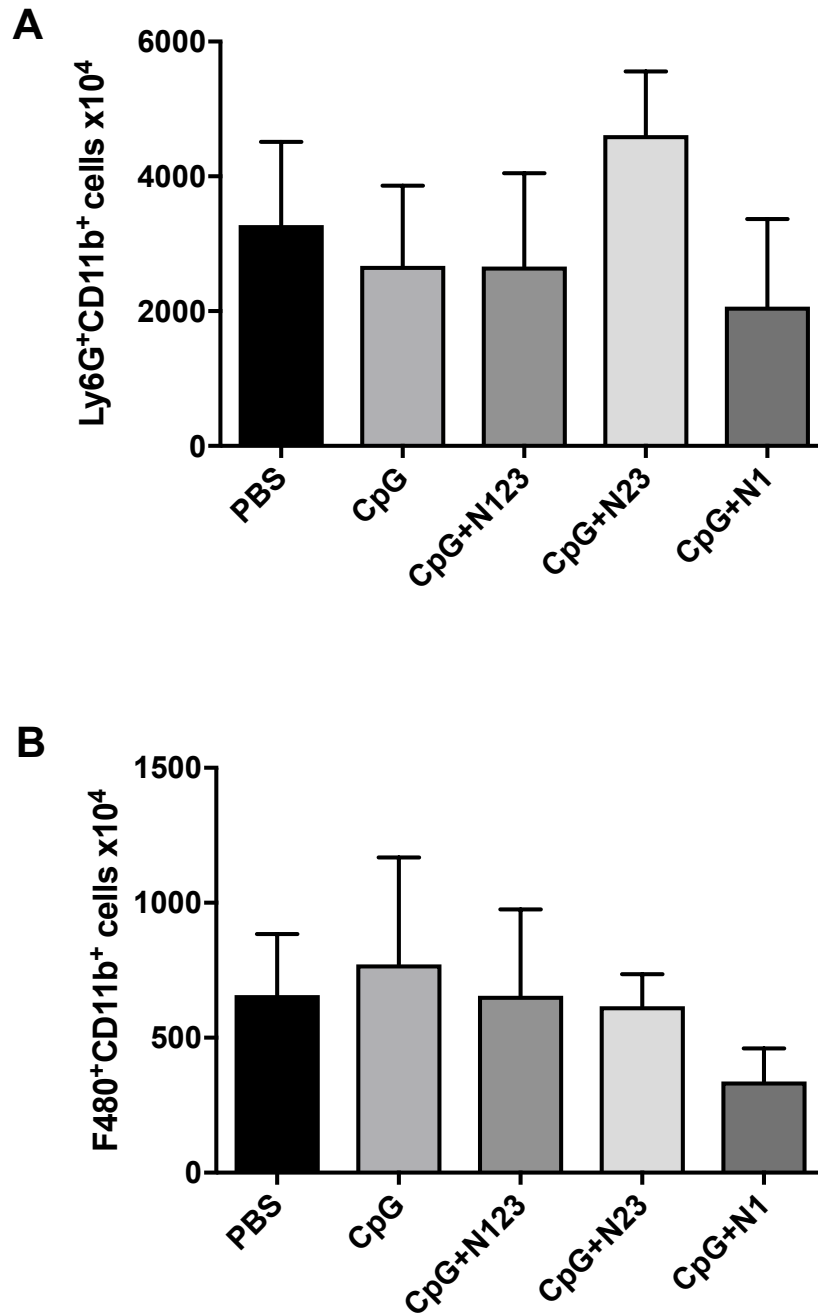


Figure 4.20. Immunisation with individual subdomains of ClfA does not increase phagocyte recruitment to the peritoneal cavity. Mice were vaccinated with PBS, CpG (50 $\mu\text{g}/\text{mouse}$)+ClfA N123, N23 or N1 (1 $\mu\text{g}/\text{mouse}$) via s.c. injection on d 0, 14 and 28. On d 63 mice were challenged with *S. aureus* PS80 (5×10^8 CFU) via i.p. injection. At 72 h post-infection, the number of neutrophils [Ly6G⁺F480⁺] (A) and macrophages [F480⁺Ly6G⁺] (B) infiltrating the peritoneal cavity was assessed. Results expressed as mean \pm SEM. n=5 per group.

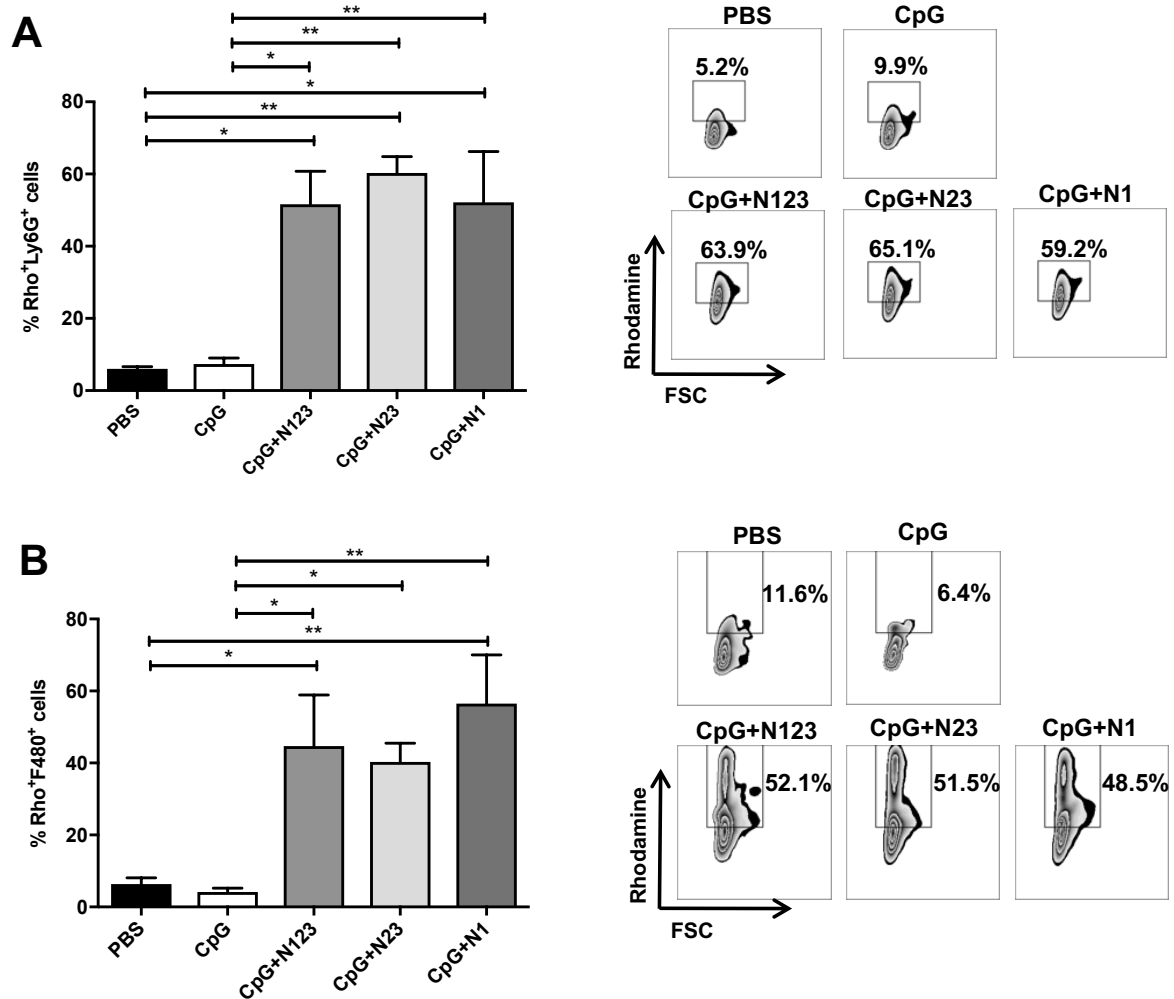


Figure 4.21. Immunisation with individual subdomains of ClfA enhances phagocyte ROS activity during *S. aureus* infection. Mice were vaccinated with CpG (50 $\mu\text{g}/\text{mouse}$)+ClfA N123, N23 or N1 (1 $\mu\text{g}/\text{mouse}$) via s.c. injection on d 0, 14 and 28. On d 63, mice were challenged with *S. aureus* PS80 (5×10^8 CFU) via i.p. injection alongside a control group of sham-immunised (with PBS) mice. At 72 h post-infection neutrophils [Ly6G⁺F480⁻] (A) and macrophages [F480⁺Ly6G⁻] (B) were assessed for reactive oxygen species (ROS) activity, detected by rhodamine (Rho) positive cells. Results expressed as mean \pm SEM and representative FACS plots of neutrophils (A) and macrophages (B) are shown. $n=5$ per group. One-way ANOVA with Tukey post-test was performed to compare variances. * $p < 0.05$, ** $p < 0.01$.

4.3 Discussion

The activation of cellular immune responses is considered an important strategy for next generation anti-*S. aureus* vaccines and the major challenge now facing vaccine companies is identifying appropriate antigens (and adjuvants) capable of inducing cellular immune responses in humans. It is now accepted that next-generation anti-*S. aureus* vaccines will likely be comprised of multiple staphylococcal antigens capable of inducing humoral and cellular immunity. An ideal vaccine against *S. aureus* should be able to induce antibodies to neutralise secreted toxins, antibodies to inhibit CWA proteins, which may be important for attachment of bacteria to host ligands and finally be capable of inducing a robust T cell response.

Phase I/Ib clinical trials of NDV-3A by NovaDigm [285] and phase I trials of four-component *S. aureus* vaccine by GSK [281] have demonstrated T cell responses and associated cytokine production in vaccinated individuals. However, in the case of the GSK vaccine, T cell responses were very low [281]. The NDV-3A vaccine is composed of a single antigen which is structurally similar to ClfA [285], while the GSK anti-*S. aureus* vaccine is multivalent, composed of ClfA N123, capsular polysaccharide type 5 and 8 and alpha toxin [281]. This current study highlights the importance of CWA proteins and in particular ClfA, as T cell activators, specifically capable of driving Th1 and Th17 immune responses *in vivo* but also crucially using human *in vitro* T cell cultures.

As the normal healthy population possess significant levels of circulating *S. aureus*-specific T cells [272], this enables human blood from healthy volunteers to be used to screen antigens for their human T cell activating capabilities. An approach such as this could be utilised in advance of clinical trials to direct research towards specific antigens that may be useful T cell activators. As humans are exposed to *S. aureus* throughout their lifetime, this leads to imprints on their adaptive immune system which varies considerably between individuals depending on their level of exposure.

This variation is highlighted in this study, as there is a broad range of responses associated with different *S. aureus* antigens. This may be a very important consideration for the design of future vaccines, as an individual's baseline level of antigen-specific T cells may impact the vaccine induced response achievable in distinct individuals.

Heat-inactivated *S. aureus* (which represents a pool of *S. aureus* cell associated antigens) was a potent human CD4⁺ T cell activator, however when CWA proteins were absent in the SrtA-deficient mutant, CD4⁺ T cell activation (proliferation and cytokine production) was significantly reduced. Subsequently, it was demonstrated that purified ClfA, ClfB and SdrC were all capable of driving antigen-specific proliferation of human CD4⁺ T cells and had the ability to induce significant levels of both IFN γ and IL-17 production by these CD4⁺ T cells indicating their capacity to drive Th1 and Th17 cell activation. Although ClfA was the most potent T cell activator, all proteins were capable of inducing responses, highlighting that CWA proteins represent an important pool of T cell antigens. The subdomains of ClfA were then further investigated for their involvement in T cell activation and it was found that the full length ClfA N123 and N23 were potent Th1 and Th17 activators. Interestingly however the N1 subdomain was capable of activating Th1 cells, but it was not a potent Th17 activator. This suggests that the Th17 activating region of ClfA is located within the N23 domain, whereas there is redundancy in the part of ClfA that can activate Th1 cells. Importantly, this work highlights the need for a systematic screen of all staphylococcal CWA proteins to identify the most potent T cell activators and furthermore indicates that unique epitopes may be present in such molecules which are recognised by distinct T cell subsets .

To investigate whether subdomains of ClfA have differing capabilities to activate T cells *in vivo*, a model anti-staphylococcal vaccine combining either ClfA N123, N23 or N1 with the adjuvant CpG was produced to investigate how the N23 and N1

subdomains would compare to the full length ClfA N123 protein as vaccine antigens. Adjuvants play an important role in directing the nature of the immune response elicited by a vaccine, and distinct T cell subsets may be targeted by careful adjuvant selection. CpG is a TLR9 agonist, which is a potent inducer of Th1 responses [286]. When alum was replaced with CpG in the acellular pertussis vaccine, it drove an antigen-specific Th1/Th17 response instead of a Th2/Th17 response, leading to greater protection against pertussis challenge [287]. In a recent study, vaccination with ClfA N23 combined with alum did not induce a Th1 or Th17 response in mice [277], however when Sigma Adjuvant System (SAS), which is an oil-in-water emulsion, was added to the adjuvant this did elicit both a Th1 and a Th17 response. Despite this however, the vaccine strategy used in the study failed to confer protection in the specific infection models used. The difference in *S. aureus* strains and vaccine formulations used by Li X. *et al.* [277] and this current study may account for the differing results.

In the current study, vaccination with CpG+N123, CpG+N23 and CpG+N1 induced antigen-specific IFN γ and IL-17 responses from ILN and spleen cells upon *ex vivo* restimulation, and this was associated with protection upon systemic challenge. In contrast to the human studies, vaccination of mice with CpG+N1 induced appreciable levels of IL-17, highlighting that the N1 domain may be capable of inducing IL-17 activation in mice but not in humans. All vaccines were capable of driving significant levels of ClfA-specific neutralising antibodies

Importantly all three vaccine antigens were capable of conferring protection upon systemic challenge. Vaccination with CpG+N123 offered protection locally at the site of infection and in the peripheral organs which complements previous findings [156]. Although vaccination with the subdomains N23 and N1 caused only a modest reduction in bacterial burden at the peritoneal infection site, bacterial dissemination to the peripheral organs was reduced to similar levels as ClfA N123 vaccinated mice.

Although the reduction in bacterial burden in the vaccinated mice did not equate to sterilising immunity, translated to humans however, it would almost equate to just that. Bloodstream infections in adults have much lower bacterial burden than that required to establish infection in mice. In fact, the number of microorganisms present in the blood is typically less than 10 CFU/ml [288]. Even high-burden endovascular infections tend to have counts less than 500 CFU/ml [289]. While the pursuit of sterilising immunity is the 'holy grail' of immunisation, a vaccine that could achieve even a 1 log reduction in bacterial load could immeasurably improve prognosis of *S. aureus* infection.

The protection against systemic dissemination appears to be associated with increased T cell responses. Mice immunised with subdomains of ClfA had elevated levels of Th1 and IFN γ ⁺CD8⁺ T cells. Although CpG is classically thought to induce a Th1 phenotype, it has also been reported to polarise Th17 responses alongside Th1 [287, 290]. In this study, vaccination with subdomains of ClfA combined with CpG also drove IL-17 responses from CD4⁺ and CD8⁺ T cells, albeit to a lesser extent than vaccine induced IFN γ responses, with IFN γ producing T cells dominating the cellular immune response. The increase in IFN γ and IL-17 producing CD4⁺ and CD8⁺ T cells in vaccinated groups was associated with a resultant increase in phagocyte responses. Vaccine induced type I immunity was associated with enhanced ROS accumulation in both macrophages and neutrophils. IFN γ signalling is known to enhance respiratory burst and the formation of ROS within phagocytes [161]. Vaccine-induced IL-17 is also likely to contribute to the increased ROS accumulation, as production of IL-17 from CD4⁺ memory T cells has previously been demonstrated to enhance the phagocytic activity of neutrophils [291]. To further confirm that T cell responses generated by these vaccines were contributing to overall protection against *S. aureus* infection, T cell deficient mice could be utilised to investigate whether the same level of protection occurred in these mice. Similarly, B cell deficient

mice could be used to determine the importance of the antibody responses generated by these vaccine formulations.

An antigen alone control group was not included in this experiment, as it has previously been demonstrated that vaccination with ClfA N123 alone did not confer protection or induce immune responses [156]. However, as there can be batch to batch variability between antigens, the inclusion of such controls would further strengthen these data.

Previously, the only role attributed to the N1 subdomain of ClfA was 10 residues known to be crucial for export and cell wall localization of ClfA [97]. For the first time, this study demonstrates that the N1 subdomain contains T cell epitopes capable of activating Th1 cells. Interestingly, antibodies from CpG+N1 vaccinated mice were also capable of inhibiting binding to fibrinogen, despite the fact that the N1 domain is not involved in fibrinogen binding. This inhibition of binding may be due to N1 antibodies sterically blocking the binding of ClfA to fibrinogen. The ClfA N1 domain is highly unstable and prone to degradation, making it costly and time-consuming to manufacture, thus, it is in the interest of vaccine producers to use a truncated version of the protein (i.e. N23 only) in their vaccine formulation. Importantly, these results support the inclusion of the full length ClfA N123 protein as an antigen in multicomponent anti-*S. aureus* vaccines.

This work supports the use of CWA proteins as vaccine antigens, as they have the ability to both induce neutralising antibodies but more importantly, are capable of driving a much-needed cellular response. Importantly, this study demonstrates that ClfA has the capacity to induce robust T cell responses, and that the full length ClfA N123 protein is required for maximum Th1 and Th17 activation *in vitro* and *in vivo*.

Chapter 5

Investigating the role of CWA proteins during *S. aureus* skin infection

5.1 Introduction

Sortase-deficient mutants, which lack all surface bound CWA proteins, have been shown to have reduced virulence in murine kidney abscess infection models [43, 44]. Similarly, in a skin abscess model, a sortase-deficient mutant had lower bacterial burden in the skin and animals showed a significantly reduced pathology compared to wild-type infected mice [45]. These studies suggest that CWA proteins are important during SSTIs and contribute to abscess formation, however, no study to date has thoroughly investigated the role of individual proteins involved in this process.

As discussed previously there is currently an urgent unmet clinical need for an anti-*S. aureus* vaccine. However, a universal anti-*S. aureus* vaccine may never be realised [224], and instead, a vaccine targeting specific clinical manifestations may need to be pursued. As skin is the most frequent site of *S. aureus* infection [225], a vaccine specifically targeted to SSTIs would be of great benefit. If prophylactic vaccines or other forms of immunotherapy to treat *S. aureus* SSTIs are to be developed as an alternative to antibiotics, a greater understanding of the specific role of individual virulence factors during infection at this site is needed, as they may be important targets of future therapy.

Typically, *S. aureus* skin infections manifest as pyogenic abscesses which form in the epidermis, dermis or subcutaneous tissue [19]. The epidermis is composed of a number of layers, of which the cornified envelope within the outermost layer, the corneal layer, acts as the physical barrier of the skin. The protein loricrin accounts for the majority of the protein mass within the cornified envelope [114]. Abscess formation within these layers begins as an acute proinflammatory response to *S. aureus* and it develops several characteristic features. The centre of the abscess is composed of live and necrotic neutrophils, live *S. aureus*, tissue debris, and fibrin

and a fibrous capsule forms at the periphery, which functions to contain the pathogen [19].

No information on factors that govern the rate of abscess formation, or the factors that are involved in forming the abscess structure during *S. aureus* skin infection are known. It is likely that CWA proteins may be particularly important in this process as they may be crucial for the initial attachment of bacteria to the skin. However, there is a lack of information regarding the role of individual CWA proteins during SSTIs. If the role of these proteins were known, then future therapies against SSTIs could target these functions. The aim of this study therefore, was to investigate the role of CWA proteins during SSTIs and identify specific proteins contributing to the pathogenesis and subsequently use these proteins in model vaccines to establish if they could offer protection against *S. aureus* skin infection.

To examine the roles of CWA proteins during SSTIs, an *in vivo* bioluminescent subcutaneous abscess model was utilised with mutants lacking CWA proteins that were created in the clinically relevant USA300 strain LAC::*lux* (Chapter 3). The skin infection model was initially optimized for this study and then used to examine the contribution of CWA proteins to abscess formation and virulence during SSTIs. Subsequently, specific CWA were investigated as vaccine antigens to assess their ability to protect against *S. aureus* SSTIs.

5.2 Results

5.2.1 Establishment of *in vivo* bioluminescent subcutaneous abscess model

An *in vivo* model of *S. aureus* skin infection was established using the bioluminescent LAC::*lux* strain. Initially it was important to assess the optimal inoculum and mouse strain to establish reproducible and robust skin infections.

Groups of BALB/c mice were inoculated subcutaneously with *S. aureus* LAC::*lux* WT at two different concentrations (2×10^7 and 2×10^8 CFU) and abscess lesion area was measured and bioluminescence imaging of mice was recorded at 24 h intervals during the infection period. *In vivo* bioluminescence of live, actively metabolizing bacteria is represented as total flux measurements in photons/second. The photon flux from the bacteria is proportional to the number of light emitting cells and the signal can be measured to monitor bacteria present at the site of infection.

Mice infected with the higher inoculum (2×10^8 CFU) developed significantly larger abscess lesions compared to mice infected with the lower inoculum (Figure 5.1). Abscess lesion area was quantified by measuring the area using the Photon Imager software. Lesions from mice infected with the higher inoculum had large areas of dermonecrosis, which were absent in the lesions of mice infected with the lower inoculum (Figure 5.1 A). The bioluminescence signal from mice infected with the higher inoculum is approximately 1 log higher than from those infected with the lower inoculum, which is to be expected, as there was a single log difference between the two inoculums (Figure 5.2 B). From the bioluminescent images, it is clear that the higher inoculum created an increased bioluminescent signal (Figure 5.2 A).

As dermonecrosis caused by *S. aureus* during SSTIs is almost exclusively caused by secreted toxins [21], the lower inoculum was chosen as the preferred inoculum to investigate the virulence potential of CWA proteins during skin infection.

Having optimized the inoculum for the model, the appropriate mouse strain best suited for use with this model was investigated. Groups of BALB/c and C57 mice were given a s.c. injection of LAC::*lux* WT (2×10^7 CFU). *In vivo* bioluminescence was monitored over a 10-day infection period. The bioluminescence signal was increased in BALB/c mice compared to C57 mice across all time points (Figure 5.3 A and B). These results indicate that C57 mice are capable of clearing *S. aureus* skin infection more rapidly than BALB/c mice. BALB/c mice were therefore chosen as the mouse strain for our model because the prolonged rate of infection clearance may afford a better opportunity to identify the specific contribution of CWA proteins.

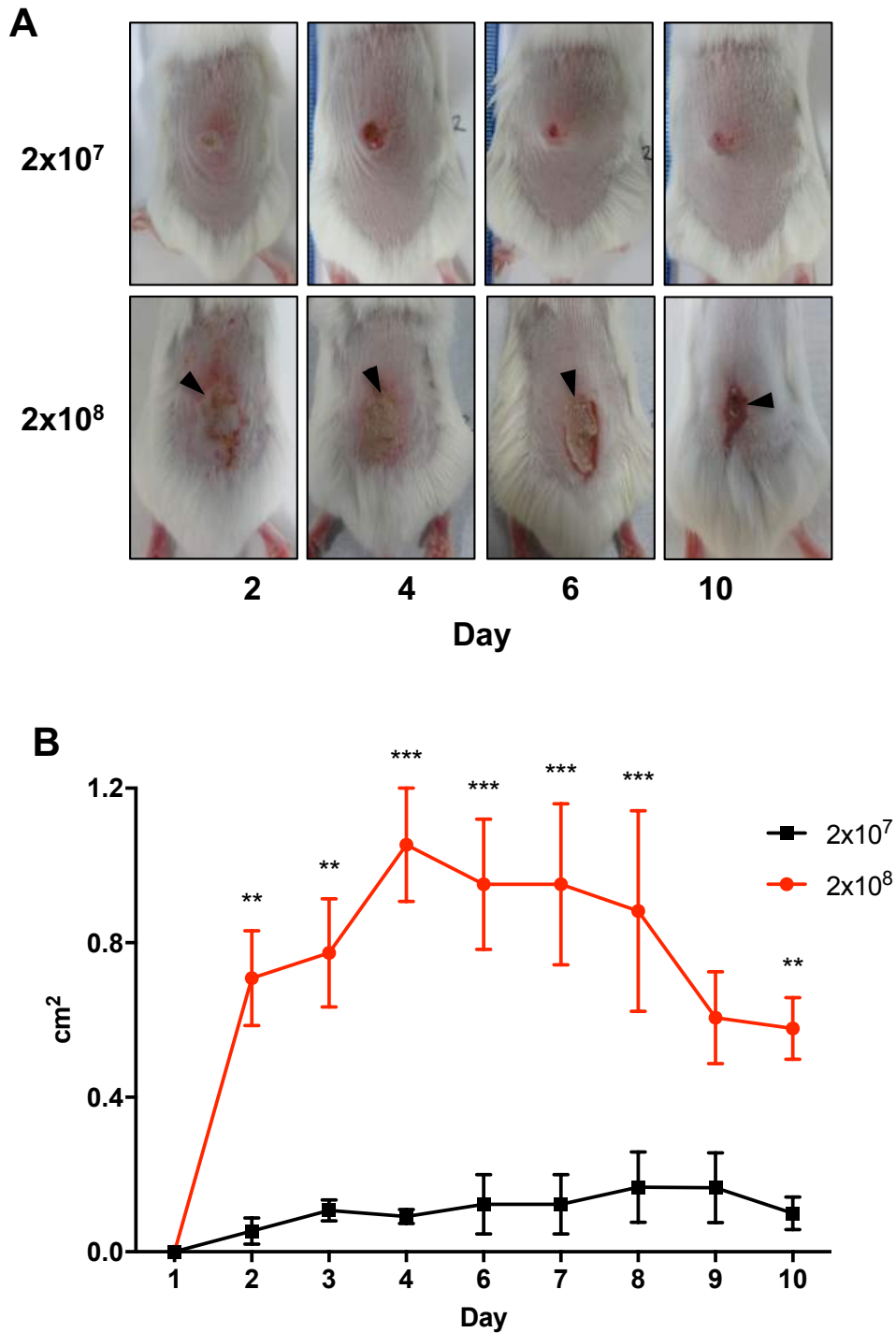


Figure 5.1. High inoculum of LAC::*lux* WT leads to increased abscess lesion area during subcutaneous abscess model. Mice were infected subcutaneously with 2×10^7 or 2×10^8 CFU LAC::*lux* WT and abscess lesion area was measured using Photon Imager. Representative lesions from each group are shown (A). Images depict the dorsal backs of mice with black arrows indicating areas of dermonecrosis. Results expressed as total lesion size (cm²) \pm SEM (B). n=5 per group. Two-way ANOVA with Bonferroni post-test was performed. ** $P < 0.01$, *** $P < 0.001$.

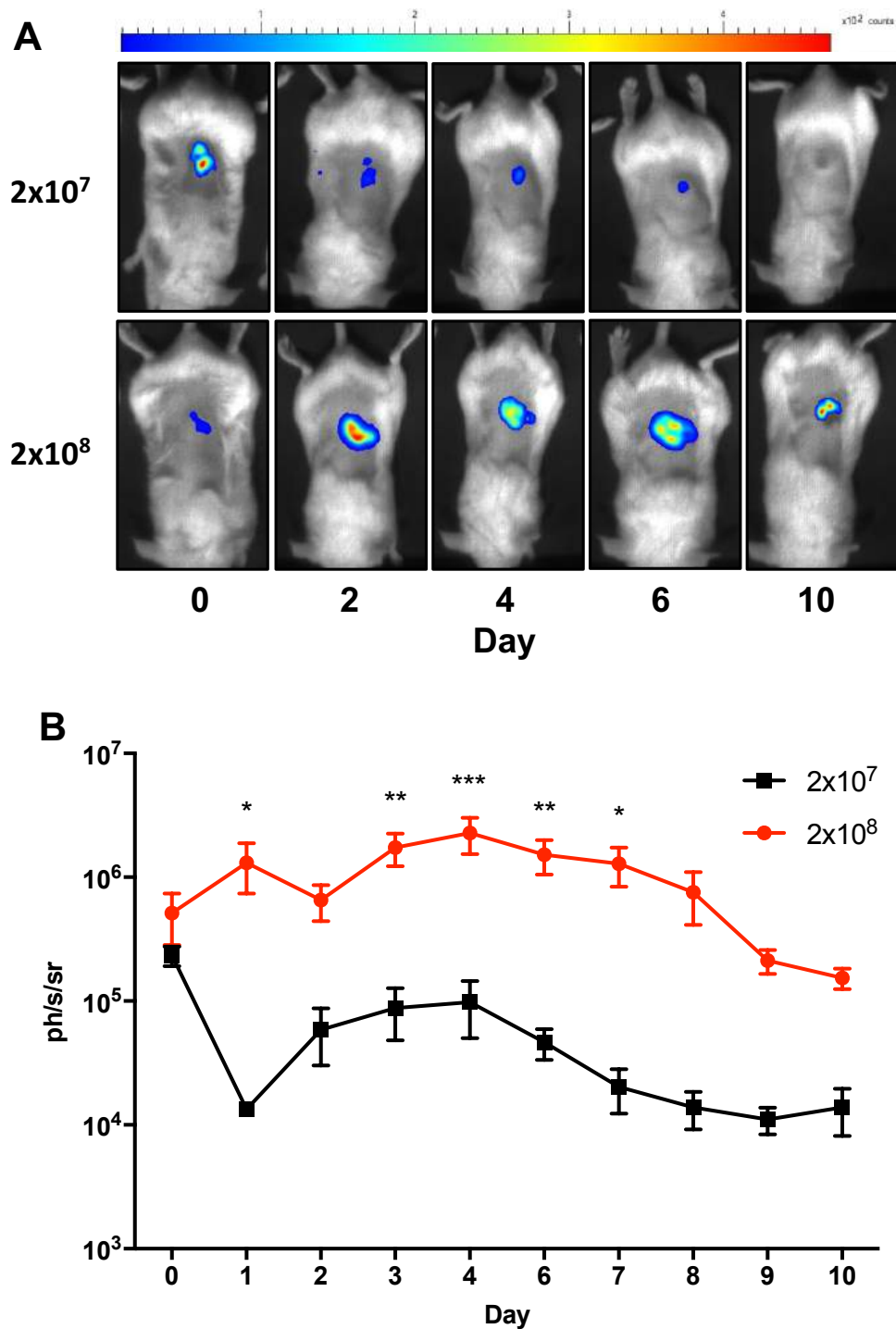


Figure 5.2. Bioluminescence imaging of *S. aureus* skin infection model. Mice were infected subcutaneously with 2×10^7 or 2×10^8 CFU LAC::*lux* WT and bioluminescence imaging was carried out using Photon Imager. Representative *in vivo* bioluminescence images from each group are shown (A). Images depict the dorsal backs of mice. Results are expressed as mean total photon flux (photons per second per steradian) \pm SEM (B). $n=5$ per group. Two-way ANOVA with Bonferroni post-test was performed. * $P < 0.05$ ** $P < 0.01$, *** $P < 0.001$.

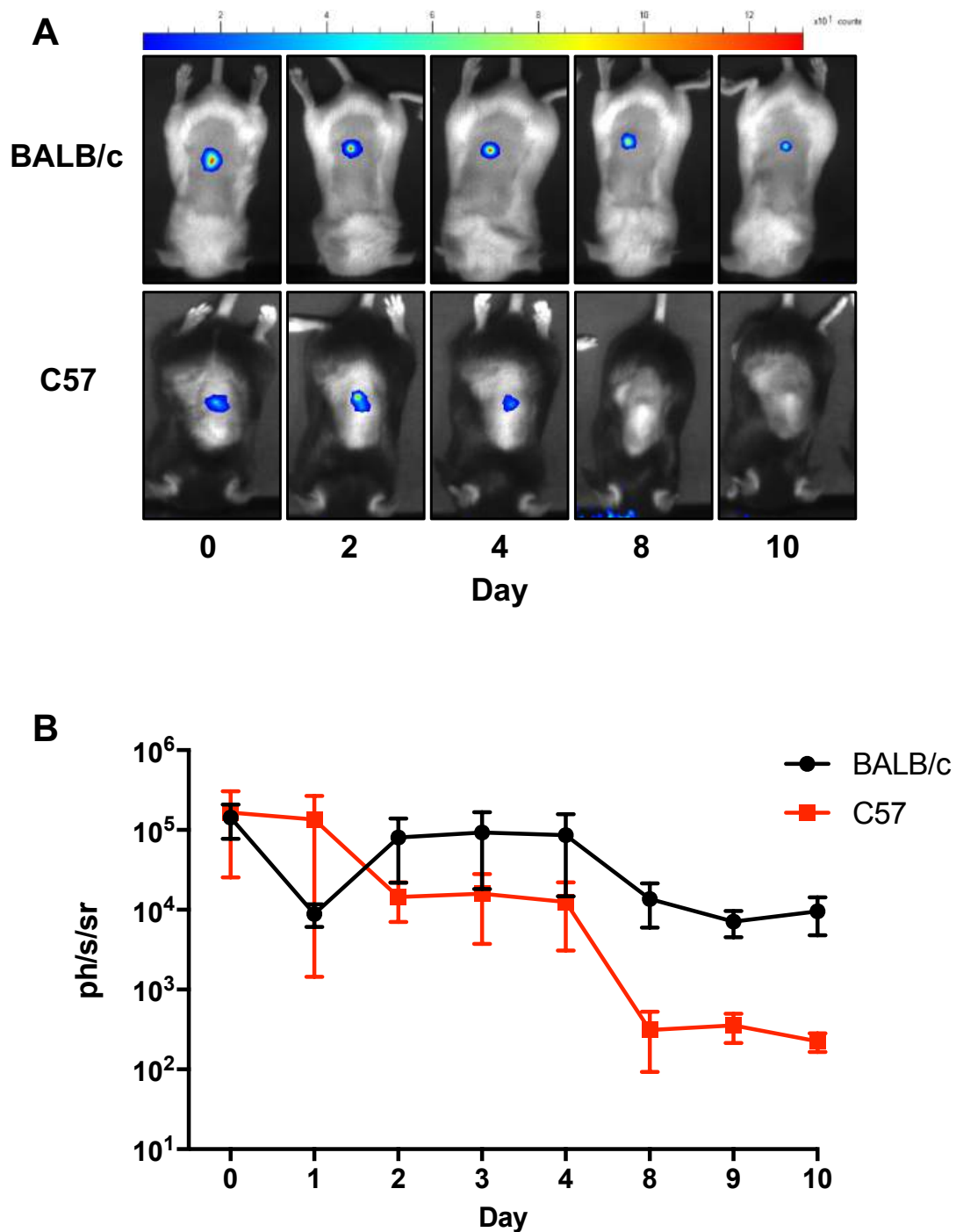


Figure 5.3. C57 mice clear *S. aureus* LAC::*lux* WT skin infection quicker than BALB/c mice. C57 or BALB/c mice were infected subcutaneously with 2×10^7 CFU LAC::*lux* WT and bioluminescence imaging was carried out using Photon Imager. Representative *in vivo* bioluminescence images from each group are shown (A). Images depict the dorsal backs of mice. Results are expressed as mean total photon flux (photons per second per steradian) \pm SEM (B). $n=5$ per group.

5.2.2 Characterising the local cellular immune response during *S. aureus* subcutaneous abscess infection

Having optimised the subcutaneous abscess model, the cells present at the infection site were investigated. Groups of BALB/c mice were given a s.c. injection of LAC::*lux* WT (2×10^7 CFU) and at 24 h post-infection, 8mm skin biopsies were excised, the tissue was digested and flow cytometry analysis was performed to analyse the cells present.

The skin abscess was mainly composed of phagocytes, of which neutrophils accounted for over 80 % of the cells present, while macrophages accounted for ~10 % of cells (Figure 5.4). This is to be expected, as it is well established that *S. aureus* abscesses are mainly composed of neutrophils [19]. The presence of T cells at the site of infection was also investigated, and CD3⁺ cells accounted for about 1 % of the cells present in the abscess tissue (Figure 5.4). When this CD3⁺ T cell population was examined in greater detail, it was found to consist of CD4⁺ T cells and $\gamma\delta$ ⁺ T cells (Figure 5.5). The presence of CD8⁺ T cells was not examined as they have not previously been demonstrated to play a role during *S. aureus* SSTIs [275]. The CD4⁺ T cells present were primarily producing IL-17 and IL-22 and a small number of cells produced IFN γ (Figure 5.6 A and B). Both IL-17 and IL-22 have previously been shown to be important for protection against *S. aureus* SSTIs [166, 192, 226]. The majority of the IL-17 and IL-22 was produced by dual producers of both cytokines, suggesting the cellular source of these cytokines was Th17 cells, while a small proportion of IL-22 was solely produced by IL-22⁺IL-17⁻ cells, indicative of Th22 cells (Figure 5.6 C and D). Similar to the CD4⁺ T cells, $\gamma\delta$ ⁺ T cells at the site of infection were primarily producing IL-17 and IL-22, while a smaller proportion of cells were producing IFN γ (Figure 5.7 A and B). The majority of the IL-22 was produced by $\gamma\delta$ ⁺ T cells dual producing IL-17 and IL-22 (Figure 5.7 C and D).

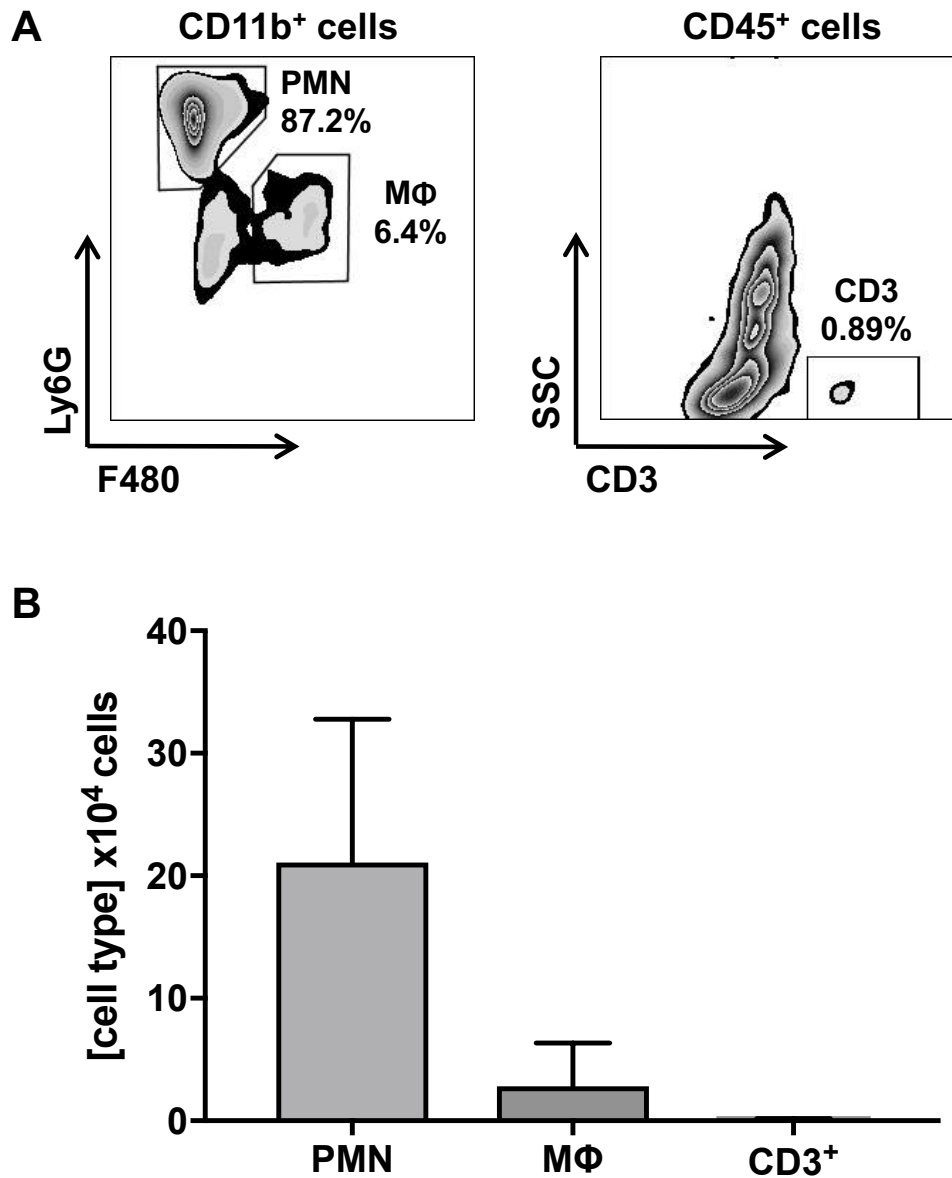


Figure 5.4. Cell types present within the skin of LAC::*lux* WT infected BALB/c mice. BALB/c mice were infected subcutaneously with 2×10^7 CFU LAC::*lux* WT. At 24h post-infection, 8mm skin biopsies were excised. Leukocytes were isolated and FACS analysis was performed to assess the number of neutrophils (Ly6G⁺F480⁻), macrophages (F480⁺Ly6G⁻) and CD3⁺ cells per skin biopsy (B). Results expressed as mean \pm SEM and representative FACS plot of CD11b⁺ and CD45⁺ cells are shown (A). n=10 per group. Data pooled from 2 independent experiments.

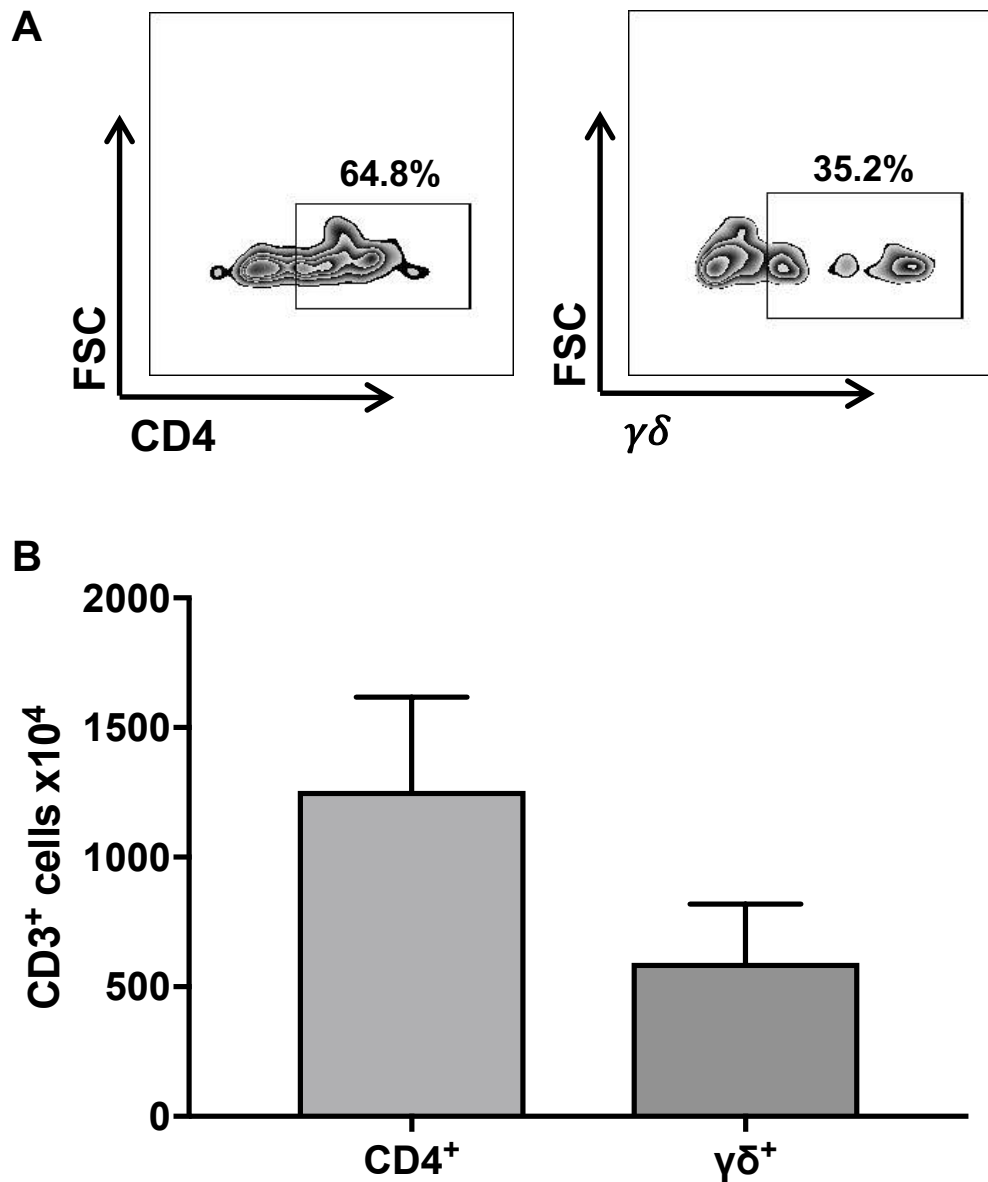


Figure 5.5. T cells present within the skin of LAC::lux WT infected BALB/c mice. BALB/c mice were infected subcutaneously with 2×10^7 CFU LAC::lux WT. At 24h post-infection, 8mm skin biopsies were excised. Leukocytes were isolated and FACS analysis was performed to assess the numbers of CD4⁺ and $\gamma\delta$ T cells per skin biopsy (B). Results expressed as mean \pm SEM and a representative FACS plots of CD3⁺ T cells are shown (A). n=10 per group. Data pooled from 2 independent experiments.

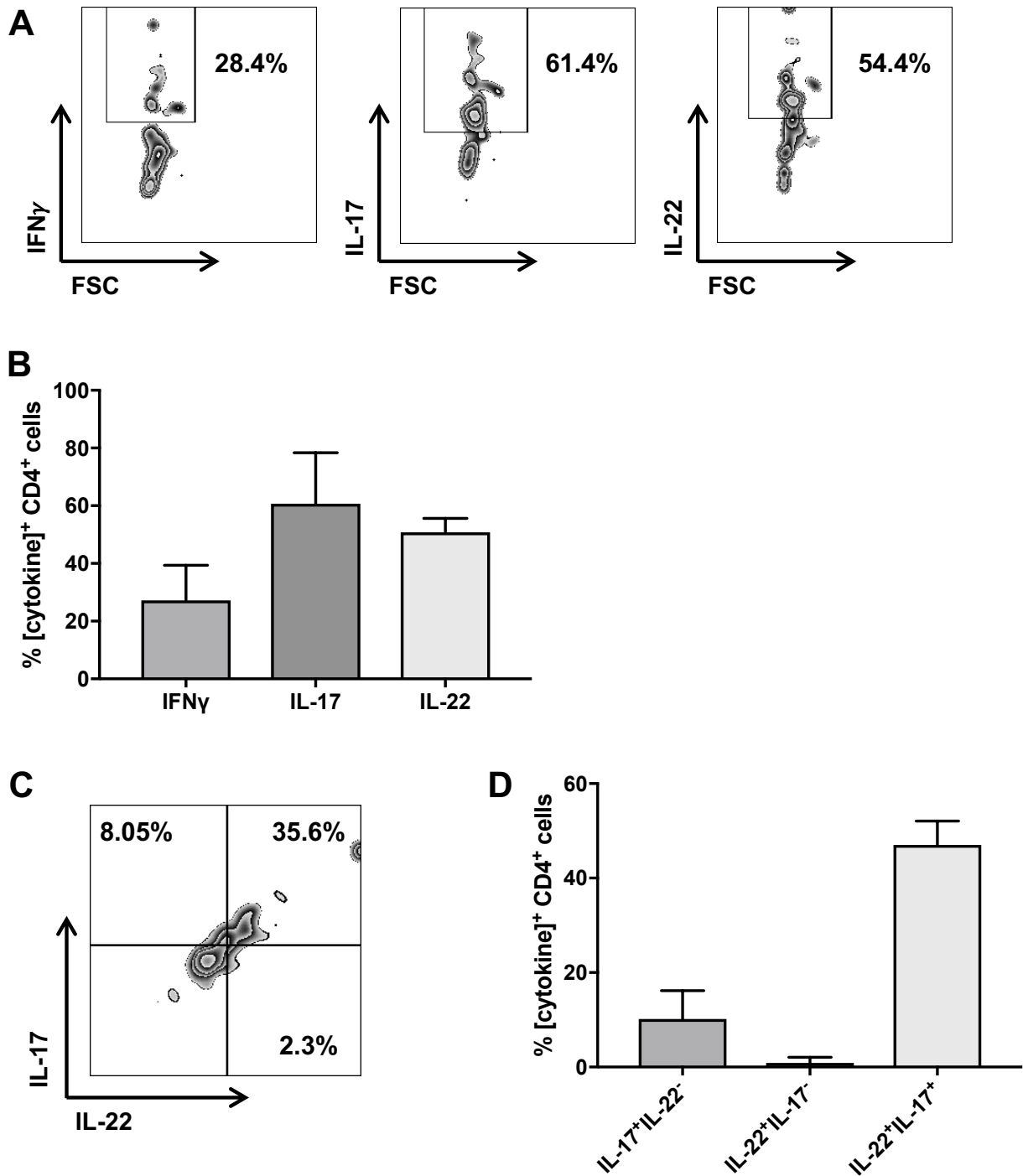


Figure 5.6. Cytokine production from CD4⁺ T cells present within the skin of LAC::*lux* WT infected mice. BALB/c mice were infected subcutaneously with 2×10^7 CFU LAC::*lux* WT. At 24h post-infection, 8mm skin biopsies were excised. Leukocytes were isolated and FACS analysis was performed to assess the percentage of IFN γ ⁺, IL-17⁺ and IL-22⁺ producing CD4⁺ T cells per skin biopsy (A, B). The percentage of dual producing IL-17⁺IL-22⁺ CD4⁺ T cells was assessed (C, D). Results expressed as mean \pm SEM and representative FACS plots of CD4⁺ T cells are shown (A, C). n=10 per group. Data pooled from 2 independent experiments.

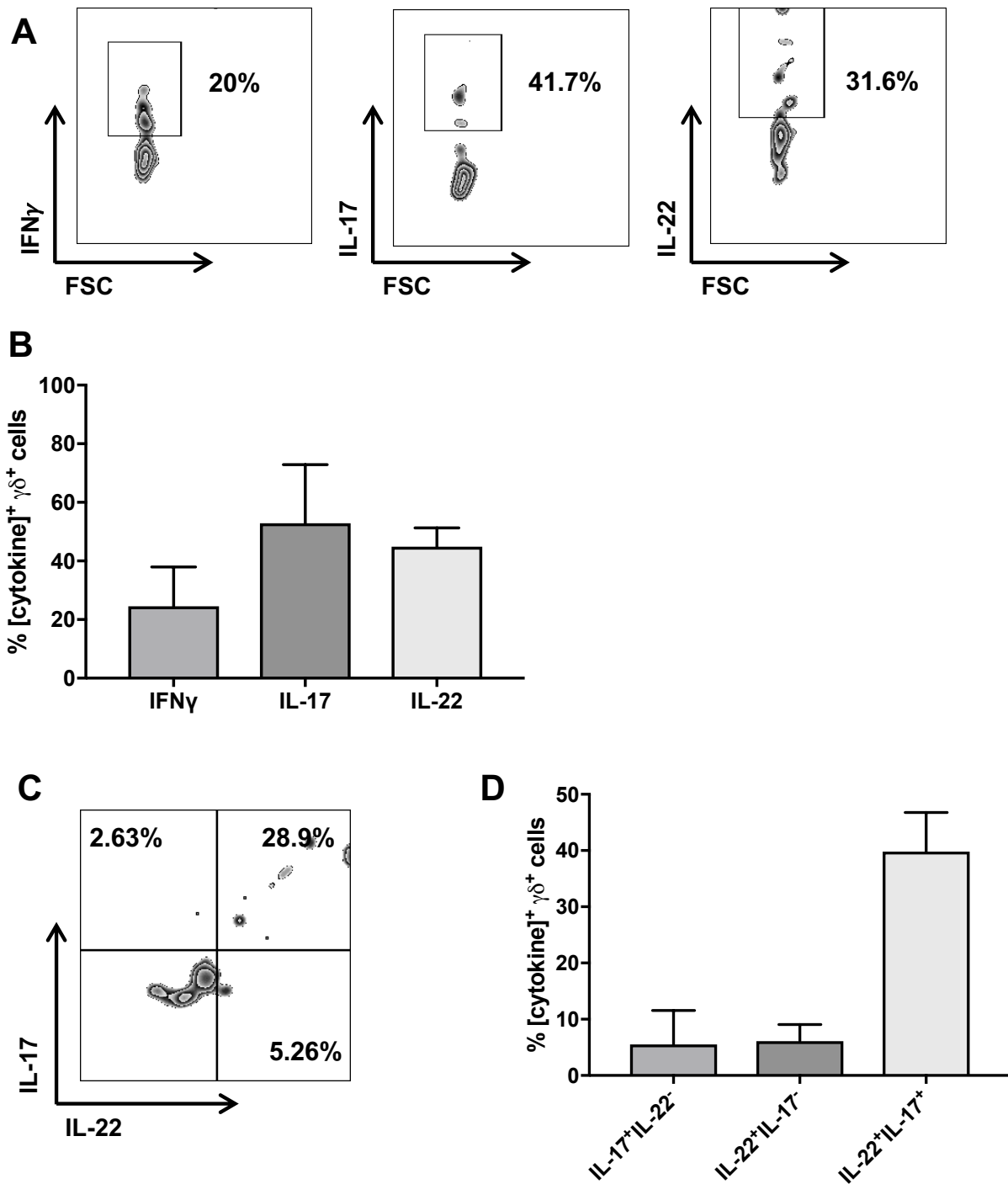


Figure 5.7. Cytokine production from $\gamma\delta^+$ T cells present within the skin of LAC::*lux* WT infected mice. BALB/c mice were infected subcutaneously with 2×10^7 CFU LAC::*lux* WT. At 24h post-infection, 8mm skin biopsies were excised. Leukocytes were isolated and FACS analysis was performed to assess the percentage of IFN γ^+ , IL-17 $^+$ and IL-22 $^+$ producing $\gamma\delta^+$ T cells per skin biopsy (A, B). The percentage of dual producing IL-17 $^+$ IL-22 $^+$ $\gamma\delta^+$ T cells was assessed (C, D). Results expressed as mean \pm SEM and representative FACS plots of $\gamma\delta^+$ T cells are shown (A, C). n=10 per group. Data pooled from 2 independent experiments.

5.2.3 LAC::*lux srtA* infected mice develop smaller abscess lesions and have reduced bacterial burden than mice infected with LAC::*lux WT*

Having optimised the model of *S. aureus* skin infection, the next step was to evaluate the role of CWA proteins during skin infection. This was carried out using the LAC::*lux srtA* mutant which was constructed (Section 3.2.1) and lacked surface bound CWA proteins.

Groups of BALB/c mice were given a s.c. injection of LAC::*lux WT* or LAC::*lux srtA* (2×10^7 CFU). Abscess lesion area and bioluminescence were monitored over a 10-day infection period. As early as day 2 post-infection, mice infected with LAC::*lux srtA* developed significantly smaller abscess lesions compared to mice infected with LAC::*lux WT* (Figure 5.8). LAC::*lux srtA* infected mice also had reduced bioluminescence up to day 6 post-infection (Figure 5.9). This decrease in bioluminescence signal corresponds with significantly reduced bacterial burden in the skin on day 3 (Figure 5.10 A) and day 6 (Figure 5.10 B) post-infection. By day 10 post-infection, most mice had cleared the bacteria from the infection site (Figure 5.10 C). Importantly, the bacteria isolated from the skin abscess at day 10 post-infection remained bioluminescent (Figure 5.11), confirming that the luciferase gene remains stably expressed throughout the infection, and that any reduction in bioluminescent signal is in fact due to a reduction in bacterial load. The abscess lesion area of LAC::*lux srtA* infected mice was reduced compared to LAC::*lux WT* up to day 10 post-infection (Figure 5.8), however, levels of bioluminescence were similar between the two groups during the last 4 days of infection (Figure 5.9). This suggests that bacterial burden and abscess lesion size are not directly linked to each other, and may be controlled by different factors.

Bacterial dissemination to the peripheral organs was assessed in this model, with minimal dissemination observed to the kidneys, liver and spleen on day 3, 6 and 10, with bacterial counts for the most part less than 2 log (Table 5.1). These results

indicate that there is no discernible systemic dissemination in this model, confirming that this is a localised skin infection model.

Taken together, these results clearly demonstrate that CWA proteins are important virulence factors during *S. aureus* SSTIs.

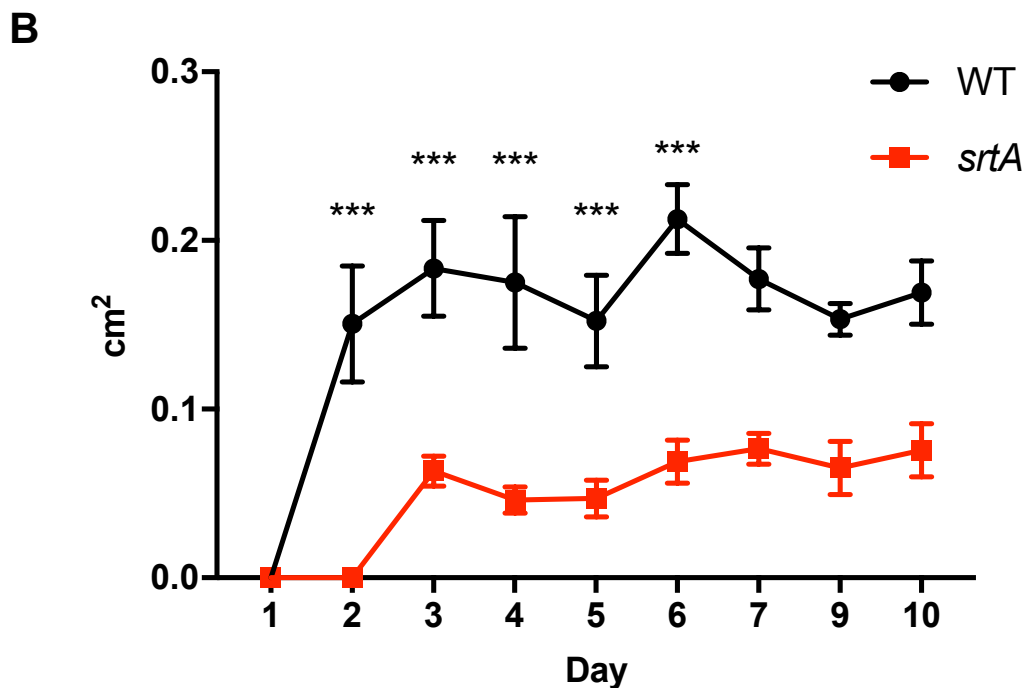
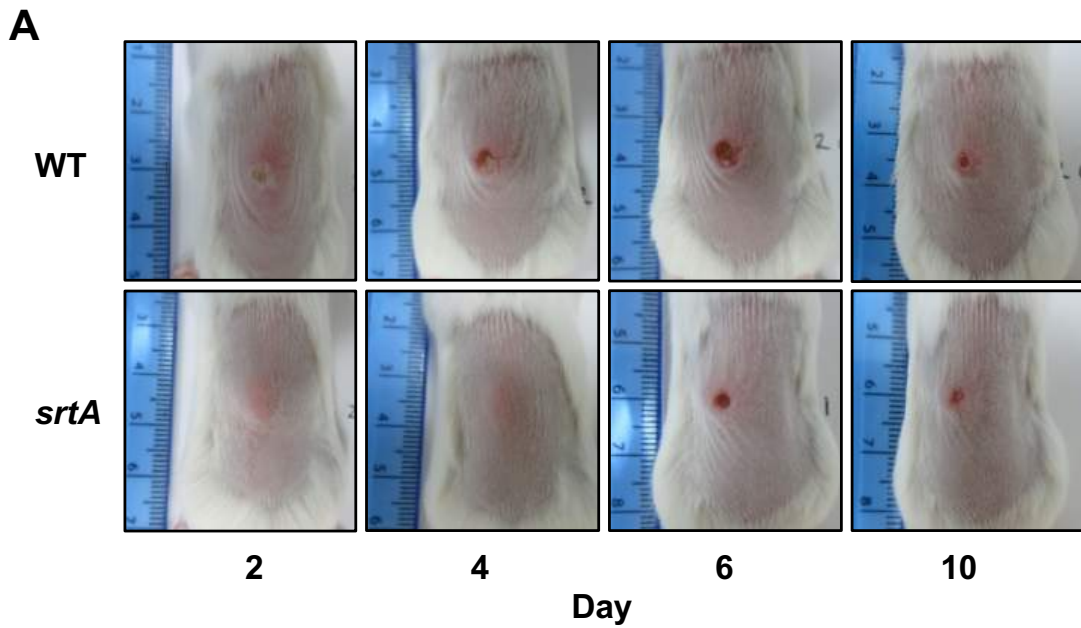


Figure 5.8. LAC::*lux srtA* infected mice develop smaller lesions than LAC::*lux* WT infected mice. BALB/c mice were infected subcutaneously with 2×10^7 CFU AC::*lux* WT and LAC::*lux srtA* and abscess lesion area was measured daily using Photon Imager. Representative lesions from each group are shown (A). Images depict the dorsal backs of mice. Results expressed as total lesion size (cm²) \pm SEM (B). n=10-14 per group. Data pooled from 2 independent experiments. Two-way ANOVA with Bonferroni post-test used for statistical analysis. *** $P < 0.001$.

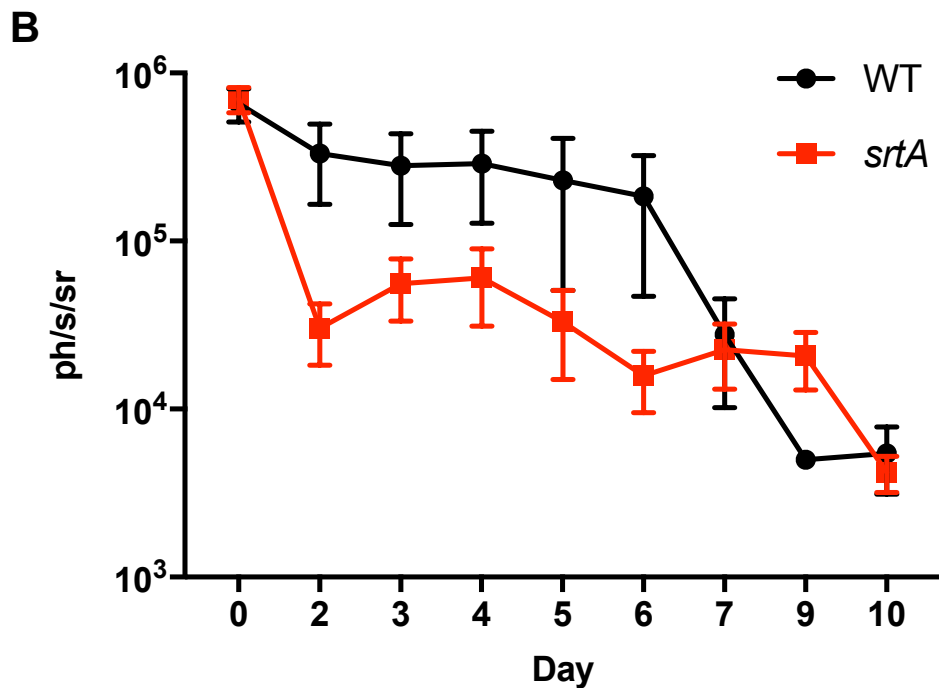
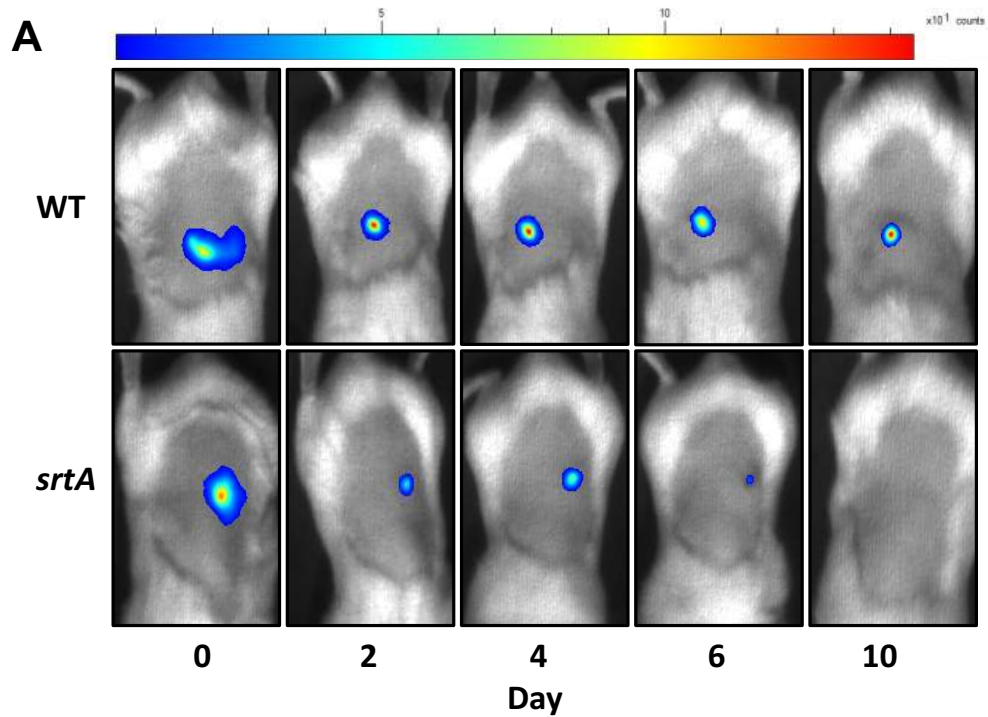


Figure 5.9. LAC::*lux srtA* infected mice have lower bacterial burden compared to LAC::*lux WT* infected mice. Mice were infected subcutaneously with 2×10^7 CFU LAC::*lux WT* and LAC::*lux srtA* and bioluminescence imaging was carried out using Photon Imager. Representative *in vivo* bioluminescence images from each group are shown (A). Images depict the dorsal backs of mice. Results are expressed as mean total photon flux (photons per second per steradian) \pm SEM (B). $n=10-14$ per group. Data pooled from 2 independent experiments.

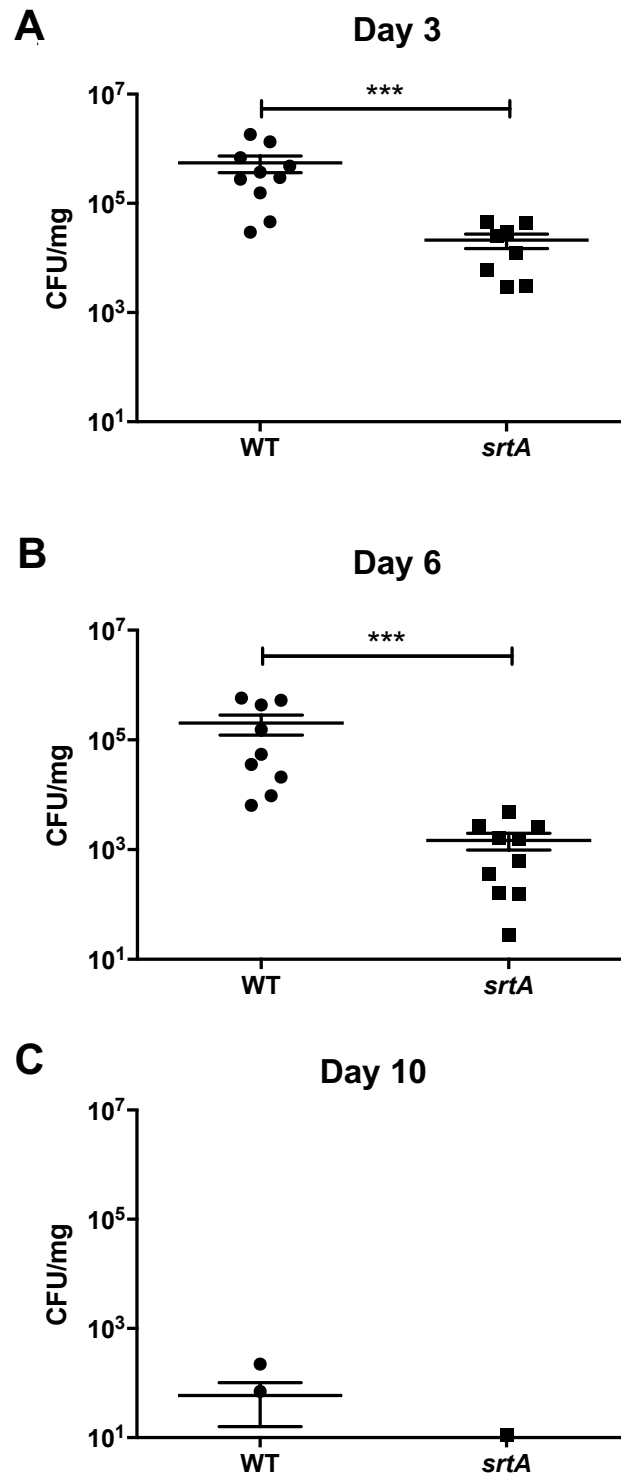


Figure 5.10. *LAC::lux srtA* infected mice have reduced bacterial burden compared to *LAC::lux* WT infected mice. Mice were infected subcutaneously with 2×10^7 CFU *LAC::lux* WT and *LAC::lux srtA*. Bacterial burden in the skin was quantified by viable counting on day 3 (A) 6 (B) and 10 (C) post-infection. Results are expressed as Log_{10} CFU/mg with means indicated by bars. Values of zero are not displayed. $n=5-10$ per group. Mann Whitney U-test used to analyse differences between groups. *** $P < 0.001$. Data pooled from 2 independent experiments.

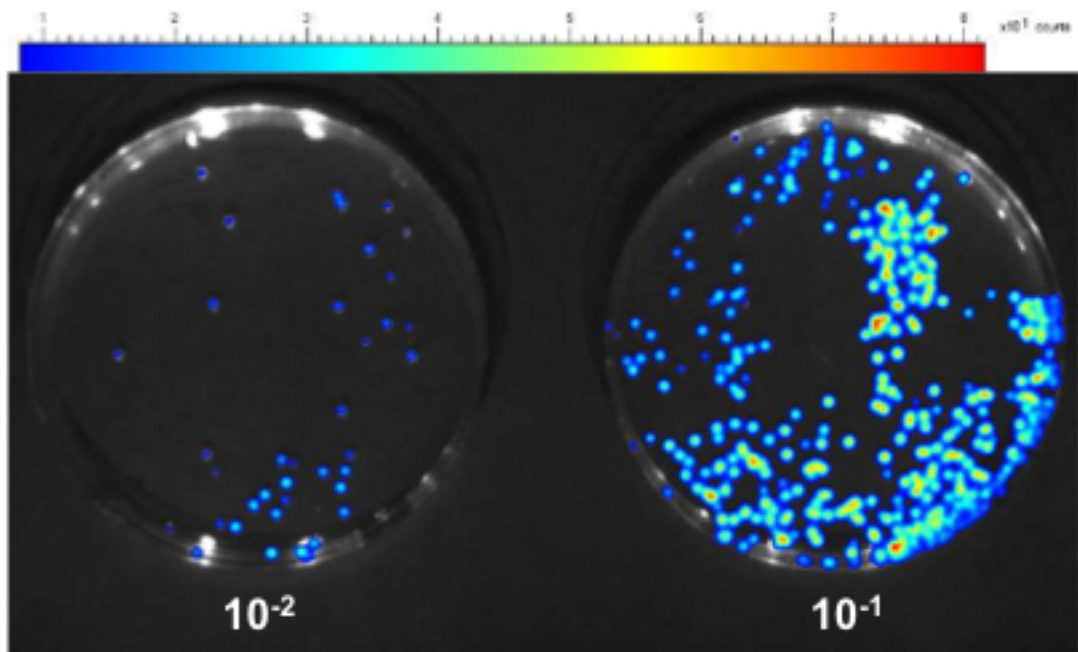


Figure 5.11. *S. aureus* isolated from infected animals remains bioluminescent. Mice were infected subcutaneously with 2×10^7 CFU LAC::*lux* WT. Bacterial burden in the skin of BALB/c mice was quantified by viable counting on day 10 and the bacteria remained bioluminescent. Photo depicts TSA plates with diluted skin homogenate (10^{-1} and 10^{-2}).

	<i>Kidneys</i>		<i>Liver</i>		<i>Spleen</i>	
	WT	<i>srtA</i>	WT	<i>srtA</i>	WT	<i>srtA</i>
Day 3	1.3	1.9	3.4	2.4	1.5	1.6
Day 6	1.9	1.5	2.13	2.3	1.2	1.1
Day 10	0	0	1.1	0	0	1.1

Table 5.1. No discernible dissemination to peripheral organs in *S. aureus* LAC::*lux* subcutaneous abscess model. Mice were infected subcutaneously with 2×10^7 CFU LAC::*lux* WT and LAC::*lux srtA*. The bacterial burden was assessed by viable counting on day 3, 6 and 10 post-infection in the kidneys, liver and spleen. Results are expressed as mean Log CFU/ml. n=5-10 per group.

5.2.4 The abscesses from LAC::*lux srtA* infected mice are smaller and less developed than LAC::*lux* WT infected mice.

Having confirmed that CWA proteins are important in determining the bacterial burden and the abscess lesion area during SSTIs, the role of these proteins in abscess development was further investigated using a histological approach. Groups of BALB/c mice were given s.c. injections of LAC::*lux* WT or LAC::*lux srtA* (2×10^7 CFU) and abscesses were excised at various time points throughout the first 96 hours of infection, embedded in paraffin wax and sectioned. Haematoxylin and eosin staining was performed on sections to examine differences in abscess structure. Skin from non-infected BALB/c mice was also stained and the skin architecture is clearly visible (Figure 5.12). A distinct abscess wall structure was observed in LAC::*lux* WT infected mice as early as 12 h post-infection, whereas defined abscess wall structures were not observed in LAC::*lux srtA* infected until 96 h post-infection (Figure 5.13). To quantify the differences between the two groups, a histology scoring system was devised which differentiated abscesses according to their architecture (Figure 2.4 M&M). Sections were scored by three independent blinded observers. The abscesses from LAC::*lux* WT infected mice are more structurally defined compared to LAC::*lux srtA* infected mice and this is seen throughout the time course, with significant differences at 48 and 96 h post-infection (Figure 4.14 A). The abscess area was also measured from each section and scored according to size (Table 2.5 M&M). The abscess area was reduced in abscesses from LAC::*lux srtA* infected mice compared to LAC::*lux* WT infected mice (Figure 4.14 B). Abscesses from LAC::*lux srtA* infected mice also have more bacteria present in the skin, not encapsulated within the abscess structure (Figure 5.13 *srtA* 24 h, 36 h). Gram stained sections further confirmed that *S. aureus* (stained Gram positive, purple) in the skin of LAC::*lux* WT infected mice is localised within the abscess structure and not present in the surrounding tissues (Figure 4.15).

Taken together, these results demonstrate that abscess architecture is disrupted and the rate of abscess formation is delayed in mice infected with LAC::*lux srtA* compared to mice infected with LAC::*lux WT*. This correlates with the reduced visible abscess lesion size in Figure 5.8.

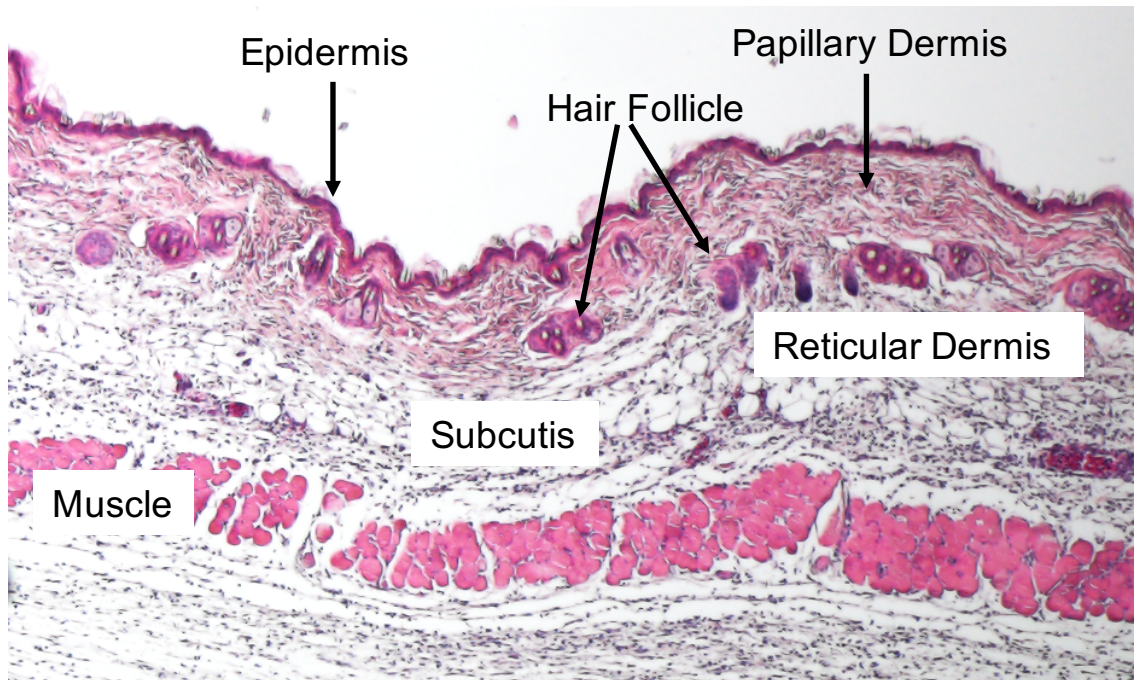
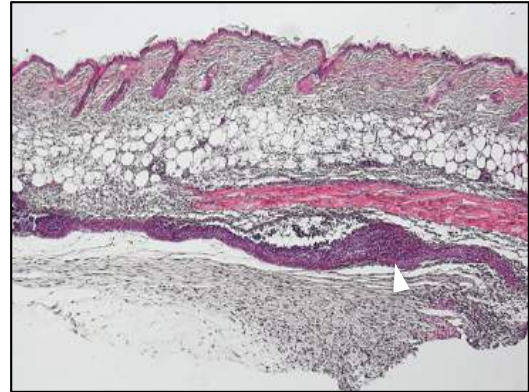
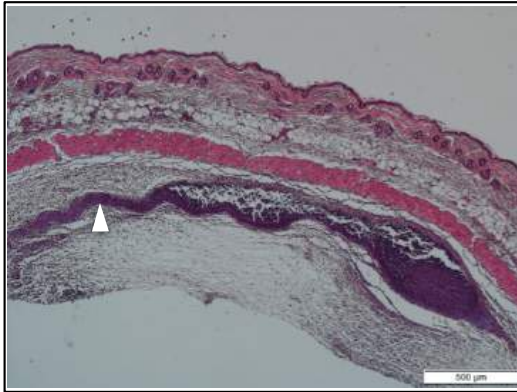


Figure 5.12. Skin structure of healthy BALB/c mice. Skin tissue was excised from BALB/c mice, fixed, embedded in paraffin wax and sectioned before haematoxylin and eosin staining was carried out. The layers of the skin are indicated.

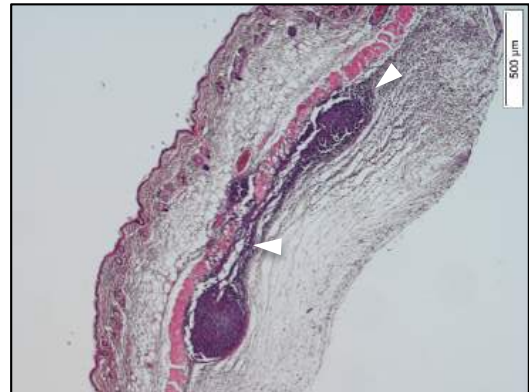
WT

srtA

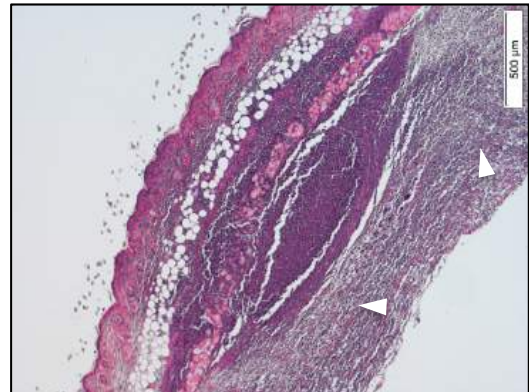
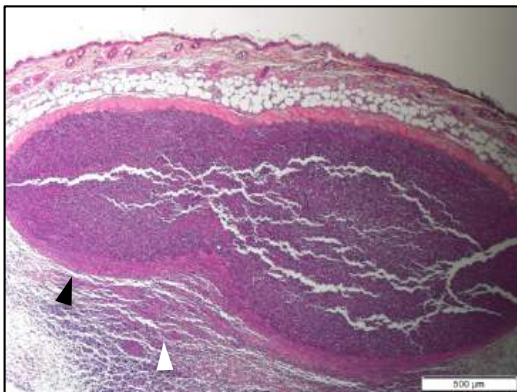
6h



12h



24h



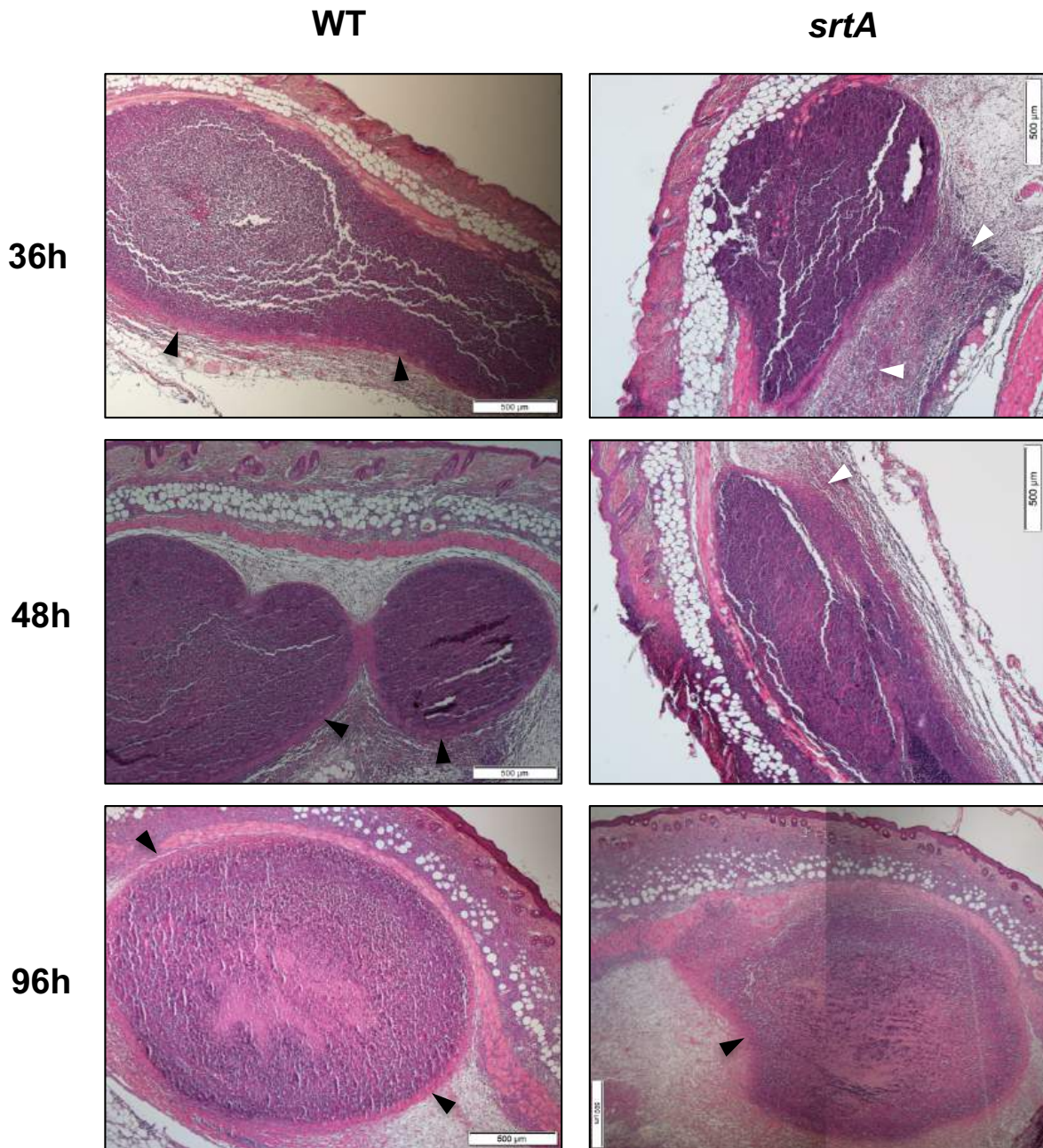


Figure 5.13. Skin abscess formation differs between LAC::*lux* WT and LAC::*lux srtA* infected mice. BALB/c mice were infected subcutaneously with 2×10^7 CFU LAC::*lux* WT or LAC::*lux srtA* and the abscess tissue was excised at 6, 12, 24, 36, 48 and 96 h post-infection. Tissue was fixed, embedded in paraffin wax and sectioned before haematoxylin and eosin staining was performed. Scale bar 500 μ m. Representative images from each group are shown. Black arrows indicate abscess wall structures. White arrows indicate bacteria present in the tissue.

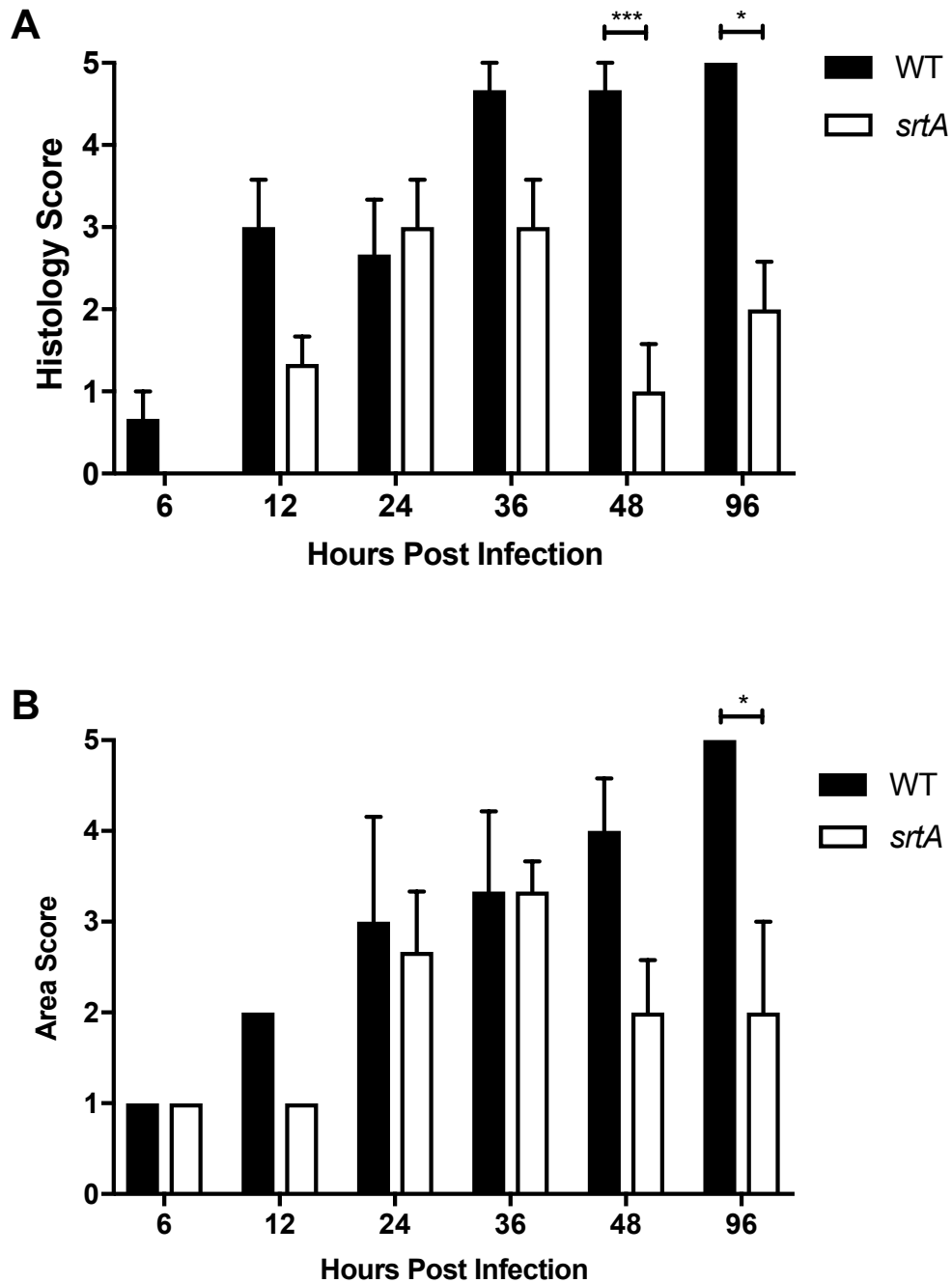


Figure 5.14. Skin abscesses from LAC::*lux srtA* infected mice are less structurally defined and smaller than LAC::*lux* WT infected mice. BALB/c mice were infected subcutaneously with 2×10^7 CFU LAC::*lux* WT or LAC::*lux srtA* and the abscess tissue was excised at 6, 12, 24, 36, 48 and 96 h post-infection. Tissue was fixed, embedded in paraffin wax and sectioned before haematoxylin and eosin staining was performed. Tissue sections were scored (double blind) by histology score (A) and area score (B). $n=6$ per group. Data pooled from two independent experiments. Mean \pm SEM. Two-way ANOVA with Bonferroni post-test used to compare variances. * $P < 0.05$, *** $P < 0.001$.

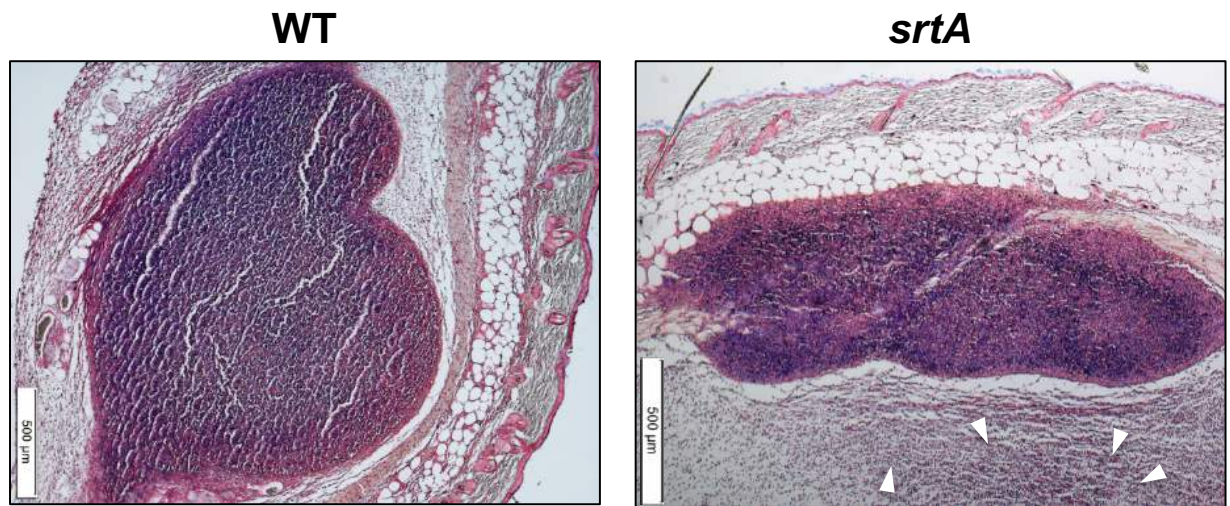


Figure 5.15. Bacteria present in the skin are localised within the skin abscess of LAC::*lux* WT infected mice. BALB/c mice were infected subcutaneously with 2×10^7 CFU LAC::*lux* WT or LAC::*lux srtA* and the abscess tissue was excised at 48 h post-infection. Tissue was fixed, embedded in paraffin wax and sectioned before Gram staining was performed. White arrows indicate bacteria present in the tissue.

5.2.5 Abscesses from LAC::*lux srtA* infected mice contain fewer neutrophils than LAC::*lux WT* infected mice.

As the size of the abscess was reduced in LAC::*lux srtA* infected mice compared to LAC::*lux WT* infected animals, we investigated the cause of this size reduction. As skin abscesses are composed of live and necrotic neutrophils [225], we examined the number of neutrophils present at the site of infection. Groups of BALB/c mice were given s.c. injections of LAC::*lux WT* or LAC::*lux srtA* (2×10^7 CFU) and abscesses were excised by 8mm biopsy punch at 24 h post-infection and neutrophil populations within the skin tissue were analysed by flow cytometry.

The number of neutrophils in the abscess tissue was significantly decreased in mice infected with LAC::*lux srtA* compared to LAC::*lux WT* infected mice (Figure 5.16 B). This decrease in neutrophils in *srtA*-infected animals was also confirmed by confocal microscopy. Immunohistochemistry staining was performed on tissue sections from LAC::*lux WT* and LAC::*lux srtA* infected animals (Figure 5.17). A reduced number of neutrophils infiltrating the area surrounding the abscess tissue are observed in LAC::*lux srtA* stained sections compared to LAC::*lux WT* at 24 h post-infection (Figure 5.17). The abscess core is not positively stained for neutrophils, presumably because the majority of neutrophils inside the abscess are necrotic.

Taken together, these results demonstrated that there are reduced numbers of neutrophils in LAC::*lux srtA* infected animals compared to LAC::*lux WT*, which correlates with the reduction in abscess area in these mice.

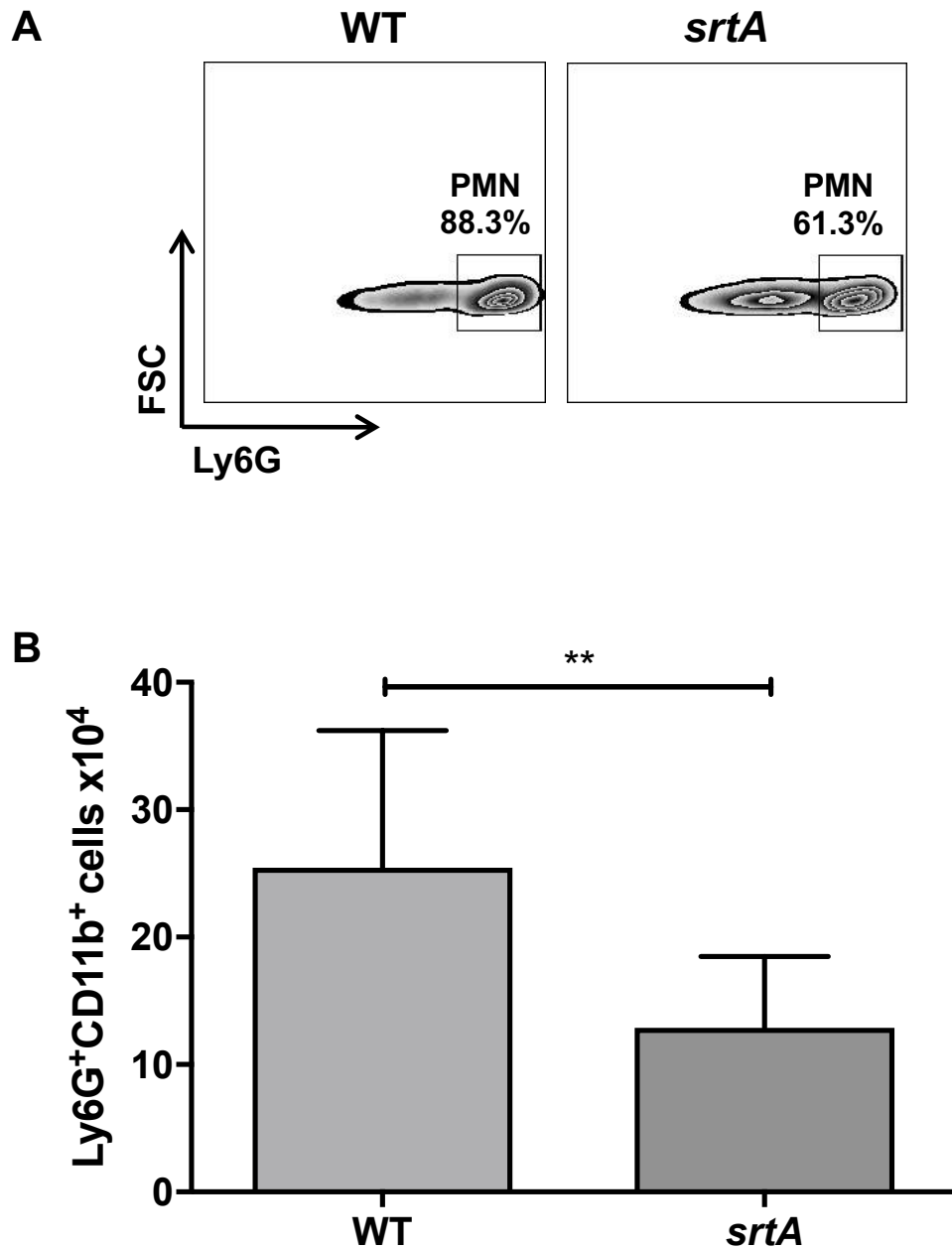
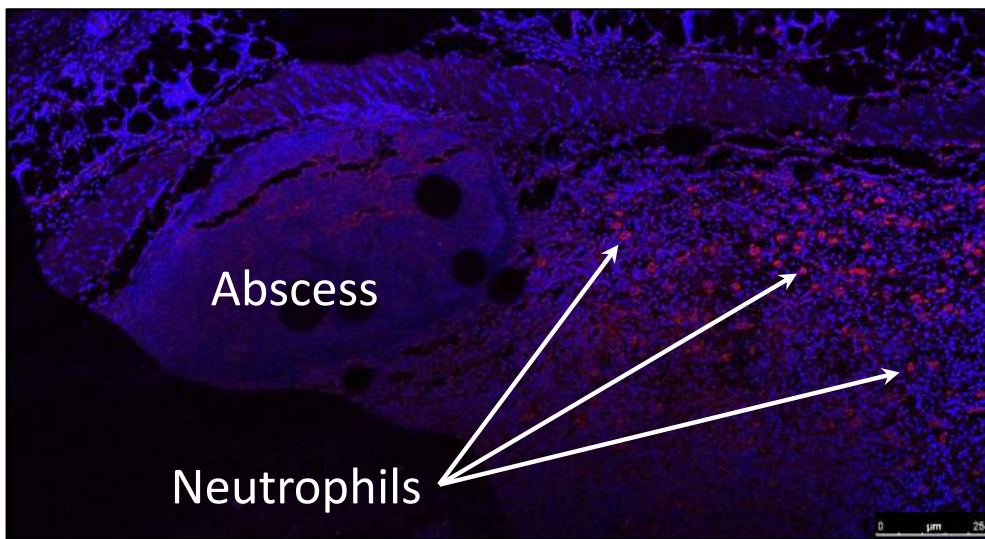


Figure 5.16. Skin abscesses from LAC::*lux srtA* infected mice contain fewer neutrophils than LAC::*lux* WT infected mice. BALB/c mice were infected subcutaneously with 2×10^7 CFU LAC::*lux* WT or LAC::*lux srtA*. At 24h post-infection, 8mm skin biopsies were excised. Leukocytes were isolated and FACS analysis was performed to assess the number of neutrophils (Ly6G⁺) per skin biopsy (B). Results expressed as mean \pm SEM and a representative FACS plots of CD11b⁺ cells are shown. n=10 per group. Data pooled from 2 independent experiments. Student's T-test used to analyse differences between groups. * $P < 0.05$, ** $P < 0.01$.

WT



srtA

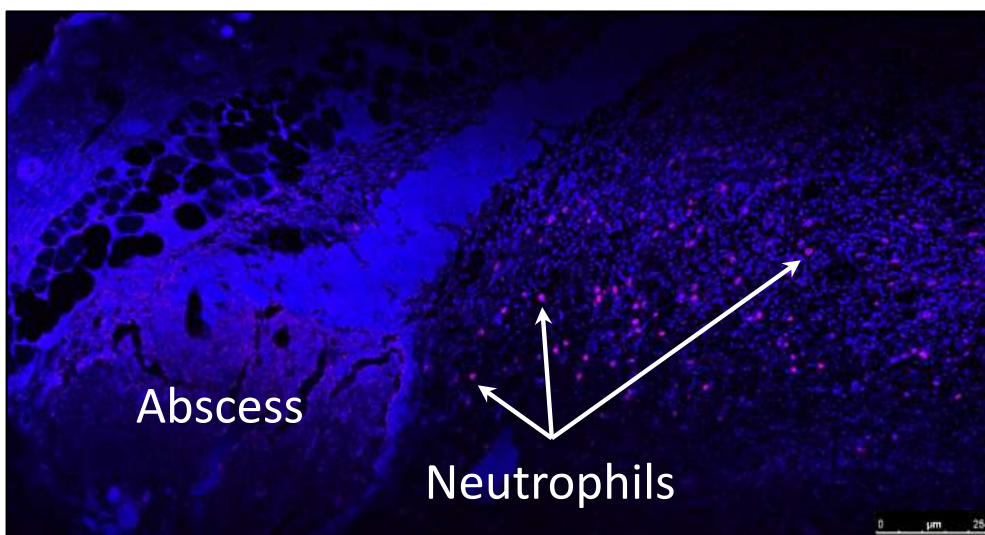


Figure 5.17. Fewer neutrophils infiltrate the surrounding tissue in LAC::lux *srtA* infected mice compared to LAC::lux WT infected mice. BALB/c mice were infected subcutaneously with 2×10^7 CFU LAC::lux WT or LAC::lux *srtA* and abscess tissue was excised at 24h post-infection. Tissue was fixed, embedded in paraffin wax and sectioned before staining for Ly6G markers on neutrophils and visualised by confocal microscopy. Red: Ly6G⁺ neutrophils. Blue: DAPI. White arrows indicate neutrophils. Abscess core is labelled. Scale bar 100 μm.

5.2.6 Mice infected with LAC::*lux* CWA protein mutants develop smaller abscess lesions and have reduced bacterial burden.

To further investigate which CWA proteins are involved in determining the abscess lesion and bacterial burden, null mutations were isolated in genes encoding ClfA, ClfB and SpA (chapter 3). LAC::*lux hla* (constructed in chapter 3) was included as a control, as it is well established that Hla is an important virulence factor involved in SSTIs [26, 35, 36]. The mutants were tested in the skin abscess model to identify if these specific CWA proteins have distinct roles during SSTIs. The infection period was shortened to 6 days, as past this point there were no significant differences in bioluminescence between LAC::*lux* WT infected mice and LAC::*lux srtA* infected mice.

Groups of BALB/c mice were given s.c. injections of 2×10^7 CFU of *S. aureus* LAC::*lux* WT, LAC::*lux clfA*, LAC::*lux clfB*, LAC::*lux spa* or LAC::*lux hla* by s.c. injection and the abscess lesion area (Figure 5.18 and 5.19) and bioluminescence (Figure 5.20 and 5.21) was monitored over a 6 day infection period. Mice infected with *clfA* (Figure 5.19 A), *clfB* (Figure 5.19 B) and *hla* (Figure 5.19 D) had significantly smaller abscess lesions on day 3-6 compared to mice infected with LAC::*lux* WT whereas LAC::*lux spa* infected mice developed abscess lesions of similar area to those infected with LAC::*lux* WT (Figure 5.19 C). The difference in abscess lesion area between the infected groups is clearly visible in the pictures of the dorsal backs of the mice on day 4 and day 6 (Figure 5.18). Interestingly, none of the mutant infected mice developed visible abscess lesions until two days post-infection.

The bioluminescence signal was also reduced in all the mutant infected groups compared to LAC::*lux* WT infected mice (Figure 5.21). The difference is clearly observed in the bioluminescent images of the mice at all time points post-infection (Figure 5.20). The reduction in bioluminescence signal in mutant infected groups was

validated by quantifying the bacterial burden in the skin on day 3 (Figure 5.22 A) and day 6 (Figure 5.22 B). The bacterial burden was reduced by $\sim 1 \text{ Log}_{10}$ in all the mutant infected groups compared to the LAC::*lux* WT group on day 3 and day 6 post-infection.

These results demonstrate that mutants of *clfA* and *clfB* cause reduced abscess lesion area and reduced bacterial burden. LAC::*lux hla* infected mice had similarly reduced lesion area and bacterial burden, which correlates with previous findings [26, 35, 36]. LAC::*lux spa* infected mice formed similar sized lesions to the LAC::*lux* WT infected mice, however, had reduced bacterial burden in the skin. This suggests that abscess formation and bacterial burden are controlled by different factors and indicates ClfA and ClfB are critical for abscess formation but that SpA may be contributing to virulence in this model by some other means.

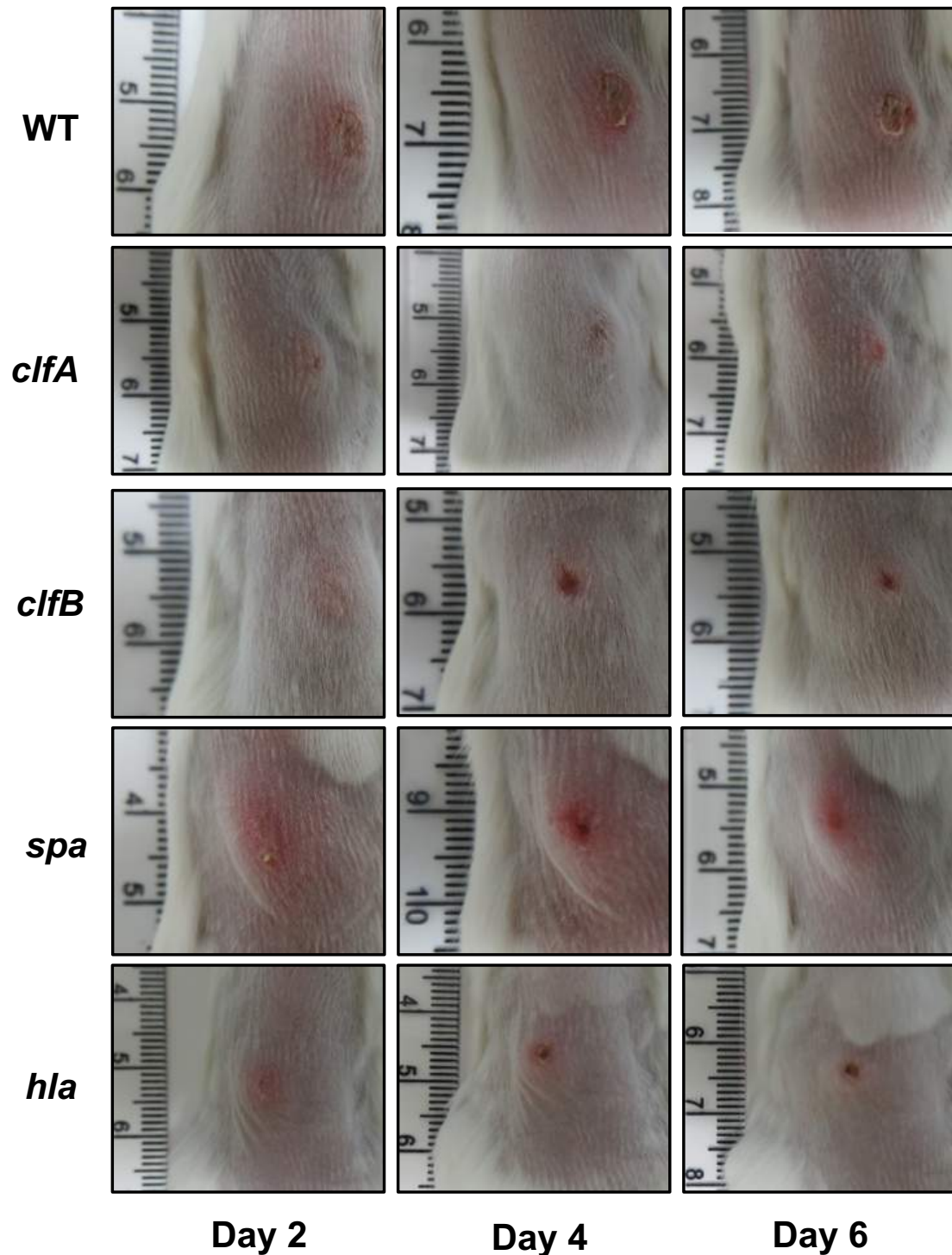


Figure 5.18. Mice infected with LAC::*lux* CWA protein mutants develop smaller abscess lesions than LAC::*lux* WT infected mice. BALB/c mice were infected subcutaneously with 2×10^7 CFU LAC::*lux* WT, LAC::*lux* *clfA*, LAC::*lux* *clfB*, LAC::*lux* *spa* or LAC::*lux* *hla* and abscess lesion size was measured daily using Photon Imager. Representative lesions from each group are shown. Images depict the dorsal backs of mice.

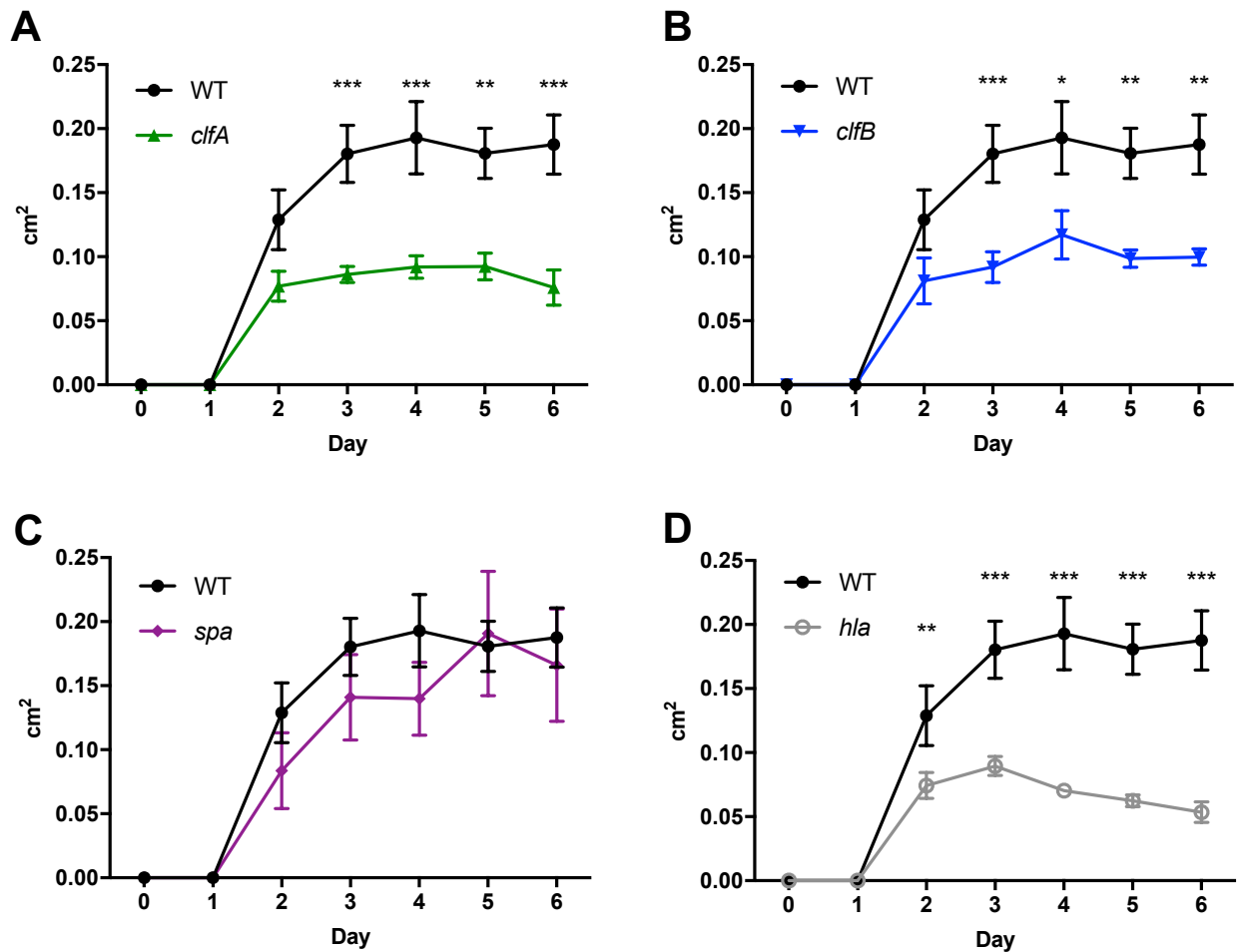


Figure 5.19. Mice infected with LAC::lux CWA protein mutants develop smaller abscess lesions compared to LAC::lux WT infected mice. BALB/c mice were infected subcutaneously with 2×10^7 CFU LAC::lux WT and LAC::lux *clfA* (A), LAC::lux *clfB* (B), LAC::lux *spa* (C) or LAC::lux *hla* (D) and abscess lesion area was measured daily using Photon Imager. Results expressed as total lesion area (cm²) \pm SEM. n=6-11 per group. Data pooled from 2 independent experiments. Two-way ANOVA with Bonferroni post-test used to analyze differences between groups. * $P < 0.05$, ** $P < 0.01$, *** $P < 0.001$.

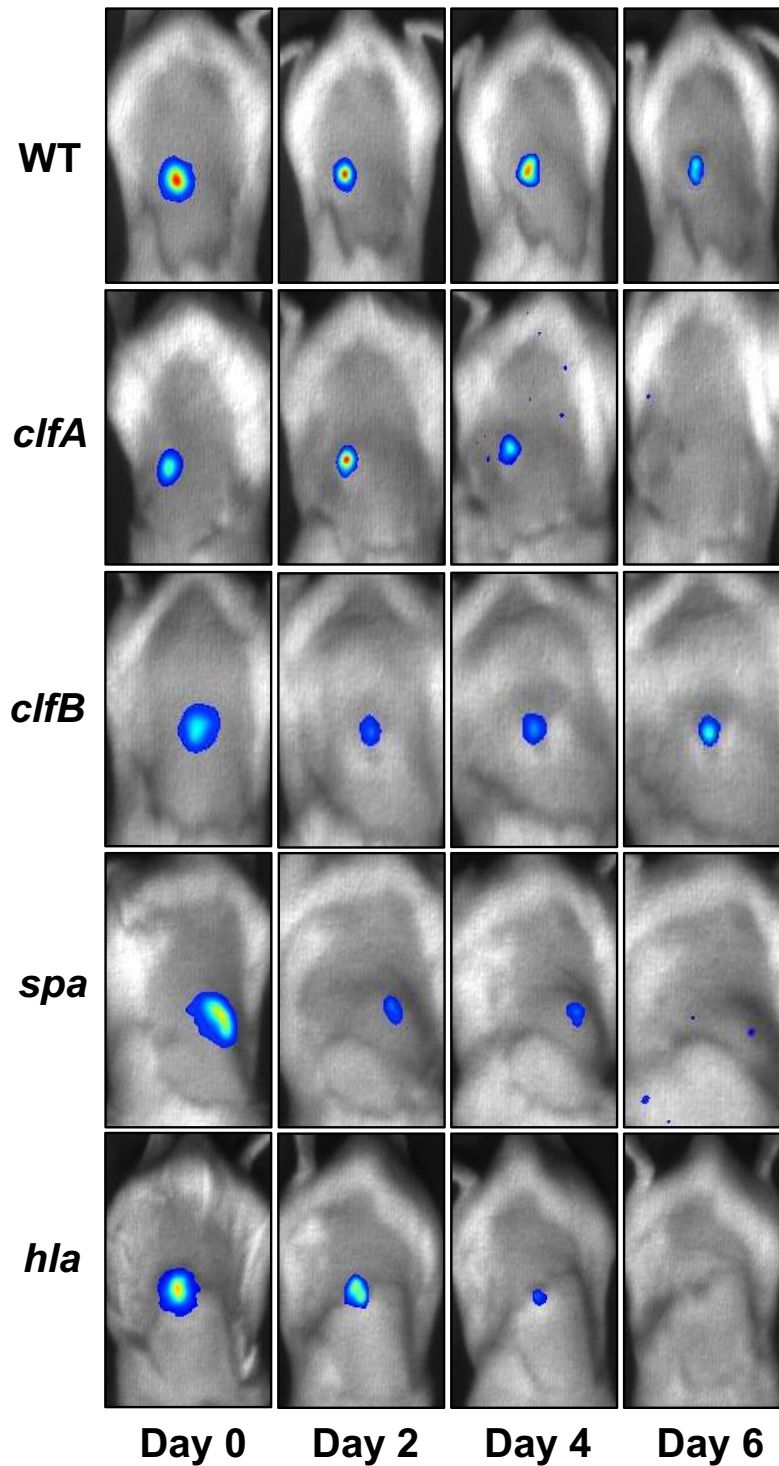


Figure 5.20. Mice infected with LAC::*lux* CWA protein mutants have decreased bioluminescence compared to LAC::*lux* WT infected mice. BALB/c mice were infected subcutaneously with 2×10^7 CFU LAC::*lux* WT, LAC::*lux* *clfA*, LAC::*lux* *clfB*, LAC::*lux* *spa* or LAC::*lux* *hla* and bioluminescence imaging was carried out using Photon Imager. Representative lesions from each group. The dorsal backs of mice are shown.

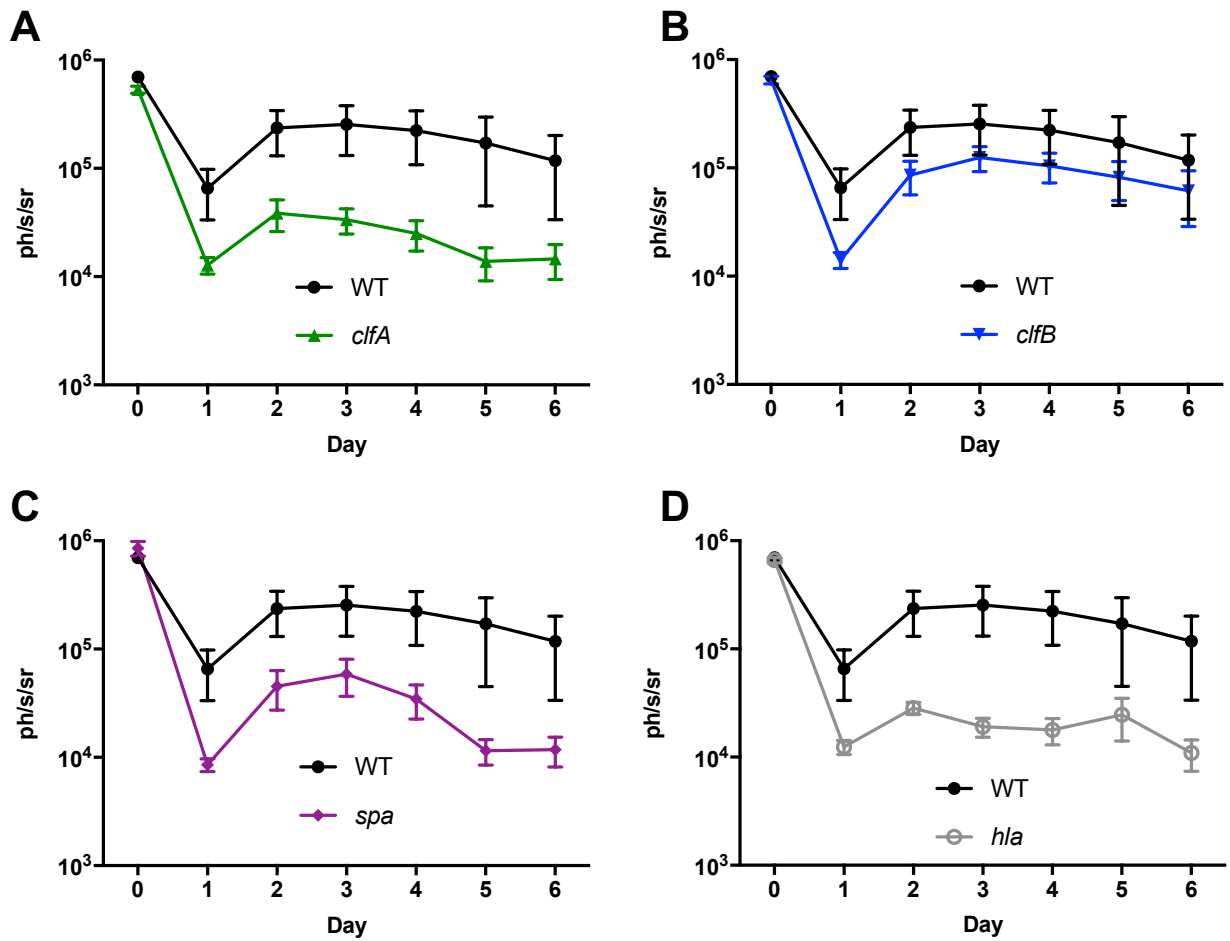


Figure 5.21. Mice infected with LAC::lux CWA protein mutants have decreased bioluminescence compared to LAC::lux WT infected mice. BALB/c mice were infected subcutaneously with 2×10^7 CFU LAC::lux WT and LAC::lux *clfA* (A), LAC::lux *clfB* (B), LAC::lux *spa* (C) or LAC::lux *hla* (D) and bioluminescence imaging was carried out using Photon Imager. Results are expressed as mean total photon flux (photons per second per steradian) \pm SEM. $n=6-11$ per group. Data pooled from 2 independent experiments.

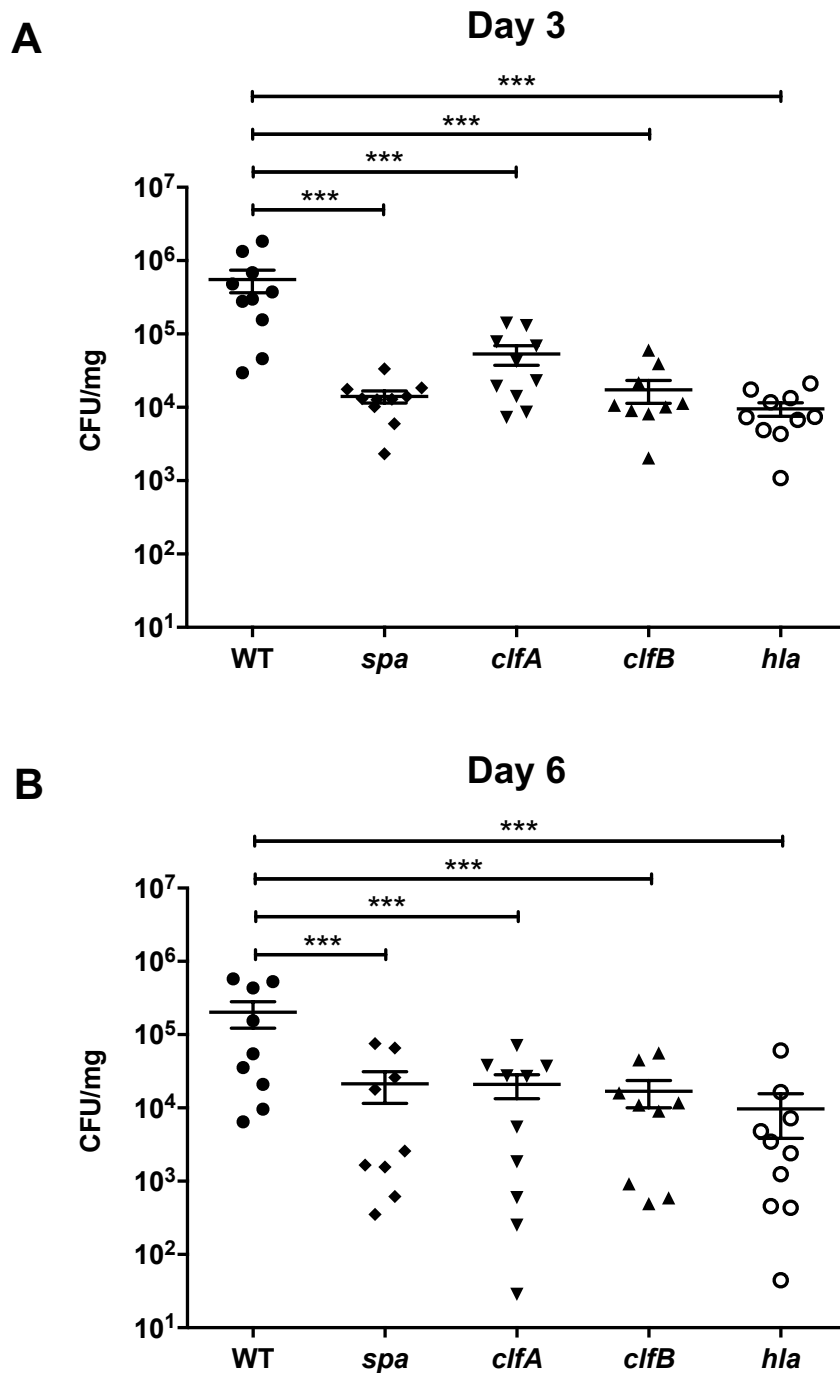


Figure 5.22. Mice infected with LAC::*lux* CWA protein mutants have decreased bacterial burden in the skin compared to LAC::*lux* WT infected mice. BALB/c mice were infected subcutaneously with 2×10^7 CFU *S. aureus* LAC::*lux* WT, LAC::*lux* *clfA*, LAC::*lux* *clfB*, LAC::*lux* *spa* or LAC::*lux* *hla*. Bacterial burden was assessed on day 3 (A) and day 6 (B) post-infection. Results are expressed as Log₁₀ CFU/mg with means indicated by bars. n=9-10. Data pooled from 2 independent experiments. One-way ANOVA with Tukey post-test used to analyse differences between groups. *** $P < 0.001$.

5.2.7 The rate of abscess formation differs between LAC::*lux* CWA protein mutants compared to LAC::*lux* WT infected mice in the first 72 hours post-infection

Having demonstrated that abscess formation appears to be delayed and disrupted in LAC::*lux srtA* infected mice compared to LAC::*lux* WT infected mice (Section 5.2.4), the individual CWA proteins were investigated for their involvement in abscess formation during the early stages of skin infection. To investigate how these CWA proteins may be involved in determining the rate of abscess formation, the abscess lesion area during the first 72 h of infection were studied (Figure 5.23). LAC::*lux srtA* was included for comparison. The rate of abscess formation appears to differ between the mutant strains compared to LAC::*lux* WT. Abscess lesions in LAC::*lux clfA*, LAC::*lux clfB*, LAC::*lux spa* and LAC::*lux hla* infected mice were visible from 48 h but formed at a decreased rate compared to LAC::*lux* WT. The abscess lesions from LAC::*lux spa* infected mice formed at a comparable rate to LAC::*lux* WT infected mice. Abscess lesion formation was the slowest to occur in mice infected with LAC::*lux srtA* where no abscess lesion was visible until 72 h post-infection. This is to be expected, as this strain lacks all surface bound CWA proteins. This suggests that some CWA proteins may be more important than others in the initial formation of the abscess during SSTIs.

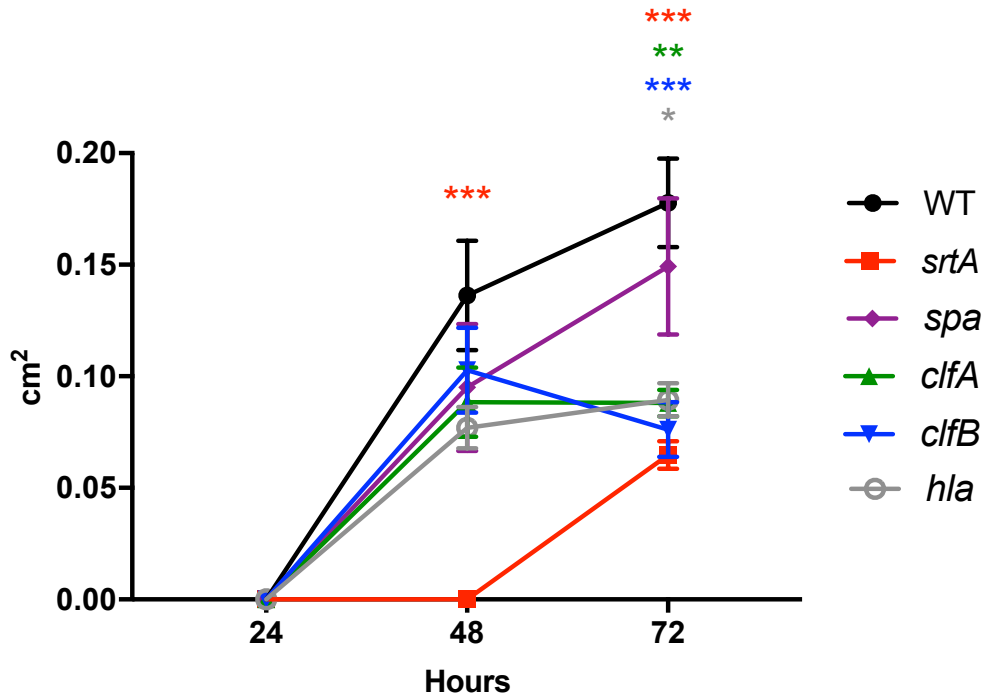


Figure 5.23. The rate of abscess formation differs between LAC::*lux* CWA protein mutants compared to LAC::*lux* WT infected mice in the first 72 hours post-infection. BALB/c mice were infected subcutaneously with 2×10^7 CFU *S. aureus* LAC::*lux* WT, LAC::*lux srtA*, LAC::*lux spa*, LAC::*lux clfA*, LAC::*lux clfB* and LAC::*lux hla* and abscess lesion area was measured using Photon Imager. Results expressed as total lesion size (cm²) \pm SEM. n=9-11 per group. Data pooled from 2 independent experiments. Two-way ANOVA with Bonferroni post-test used to analyse differences between groups. * $P < 0.05$, ** $P < 0.01$, *** $P < 0.001$.

5.2.8 Abscesses from LAC::*lux clfA*, *clfB* and *spa*-infected mice are less developed and the rate of abscess development is slower compared to LAC::*lux* WT infected mice

Initial analysis suggested that there is a difference in the rate of abscess formation in animals infected with LAC::*lux* WT compared to mice infected with LAC::*lux clfA*, *clfB*, *spa* and *hla* mutants. To further investigate this, a histological approach was used. Groups of BALB/c mice were given s.c. injections of LAC::*lux* WT, LAC::*lux clfA*, LAC::*lux clfB*, LAC::*lux spa* or LAC::*lux hla* (2×10^7 CFU) and abscesses were excised for histopathological analysis at 12, 48 and 96 h post-infection. Histological sections were examined to ascertain differences in abscess structure and size (Figure 5.24). To quantify the difference in abscess structure between the groups, sections were scored by three independent blinded observers. The abscesses from LAC::*lux clfA* (Figure 5.25 A) and LAC::*lux spa* (Figure 5.25 C) infected mice had significantly altered structure by 96 h post-infection compared to LAC::*lux* WT infected animals, suggesting these proteins are of particular importance at later stages of abscess formation. In contrast, LAC::*lux clfB* infected animals had significantly altered abscess structure compared to LAC::*lux* WT infected mice at 12 h post-infection (Figure 5.25 B), suggesting that ClfB may exert its role early in the infection process. Interestingly, there was no difference observed between abscess structure in LAC::*lux* WT and LAC::*lux hla*-infected mice (Figure 5.25 D), implying that Hla does not impact upon abscess formation. The abscess area was also measured from each section and scored according to size (Table 2.5 M&M). The abscess area was reduced in abscesses from LAC::*lux clfA* (Figure 5.26 A), *clfB* (Figure 5.26 B) and *spa* (Figure 5.26 C) infected mice compared to LAC::*lux* WT infected mice at all time points. Abscesses from LAC::*lux hla* infected mice were the same size as the WT abscesses (Figure 5.28 E), again suggesting that secreted toxins do not play a role in abscess formation. Taken together, these results demonstrate that ClfA, ClfB and SpA affect abscess architecture and the rate of abscess formation, however they

may assert their effects at different stages in the infection process. Crucially, these results have demonstrated for the first time that ClfB has an important function during *S. aureus* SSTIs and it may exert its effect early in the infection process.

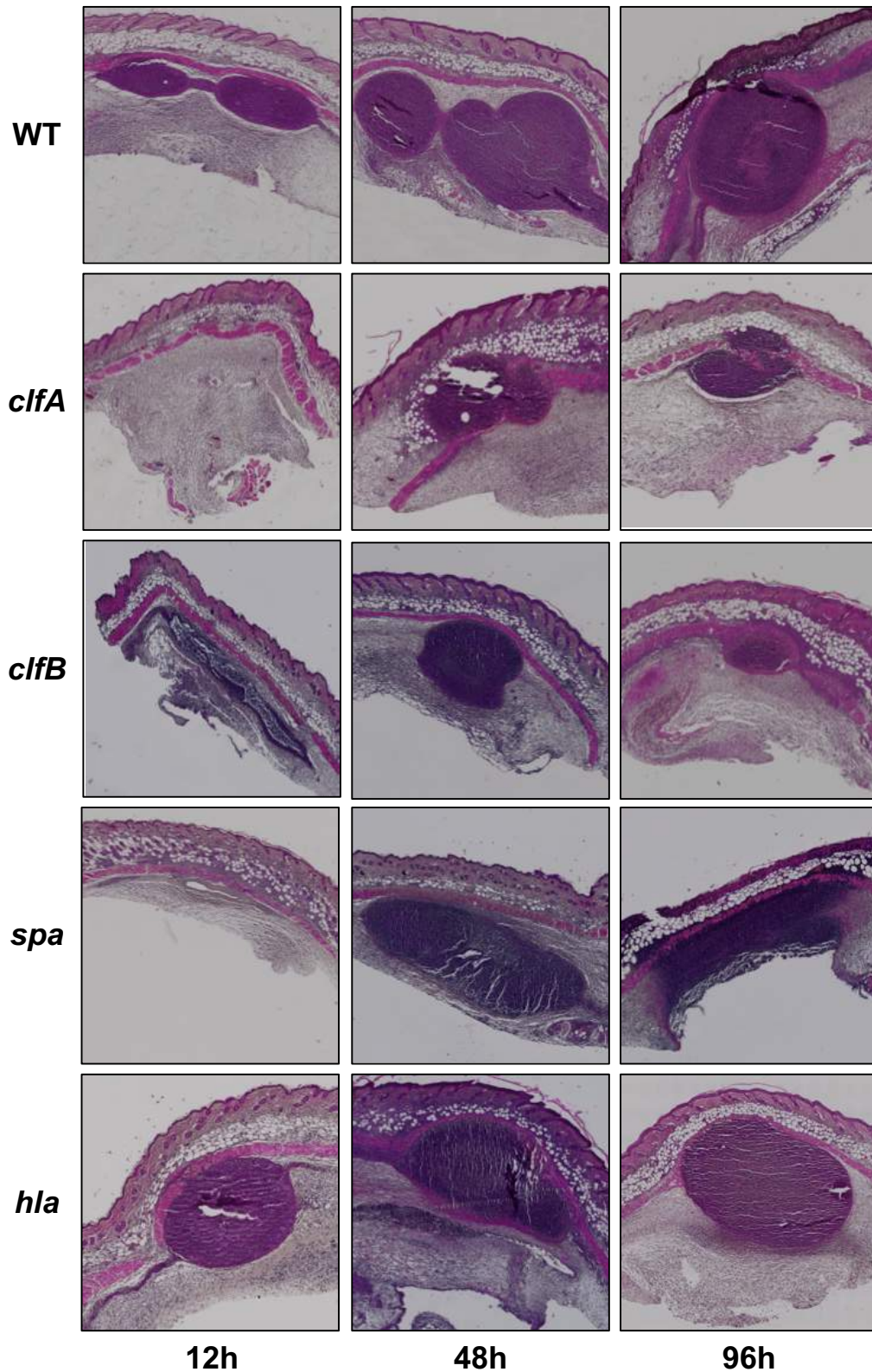


Figure 5.24. Time course of *S. aureus* skin abscess formation. BALB/c mice were infected subcutaneously with 2×10^7 CFU *S. aureus* LAC::*lux* WT, LAC::*lux clfA*, LAC::*lux clfB*, LAC::*lux spa*, and LAC::*lux hla* and the abscess tissue was excised at 12, 48 and 96 hours post-infection. Tissue was sectioned and haematoxylin and eosin staining was performed. Representative images from each group are shown.

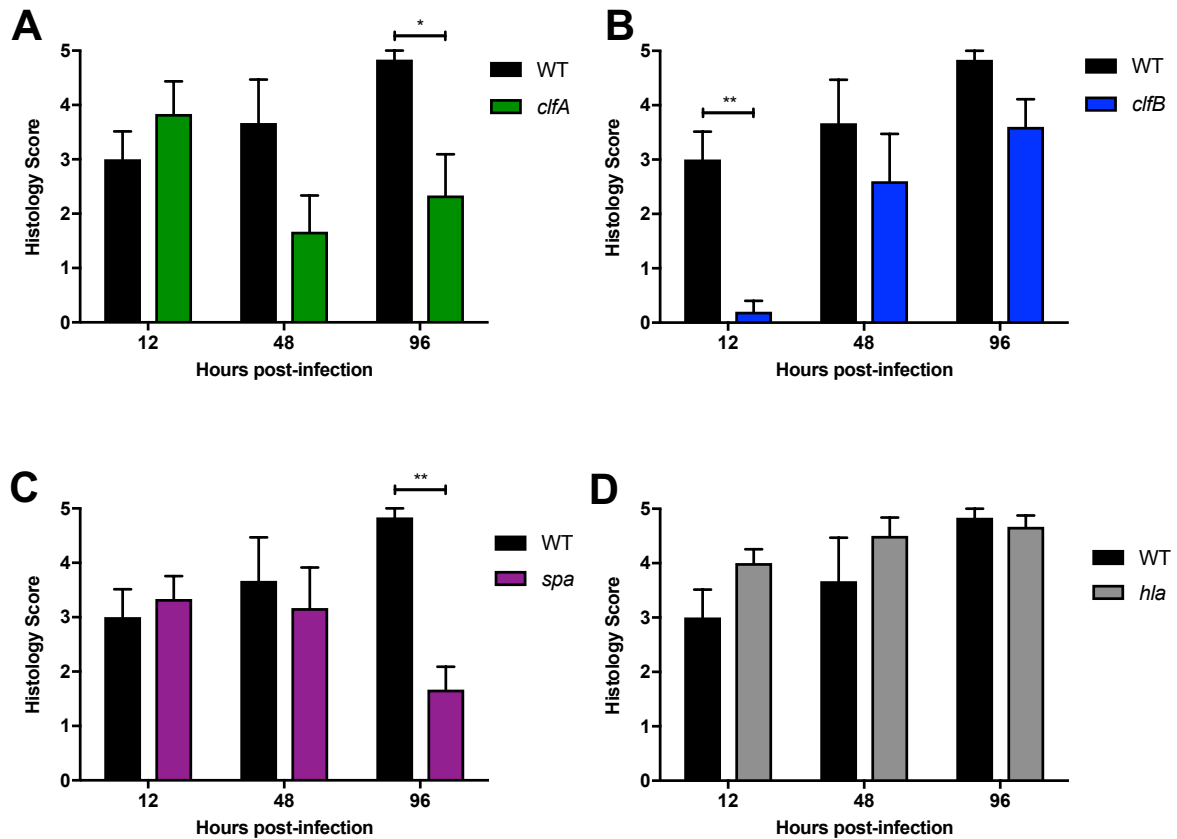


Figure 5.25. Abscesses formed by LAC::*lux* WT are more structurally defined than those of LAC::*lux* CWA protein mutants. BALB/c mice were infected subcutaneously with 2×10^7 CFU LAC::*lux* WT and LAC::*lux* *clfA* (A), LAC::*lux* *clfB* (B) LAC::*lux* *spa* (C) or LAC::*lux* *hla* (D) and the abscess tissue was excised at various time points (12, 48, 96 hours). Tissue was fixed, embedded in paraffin wax and sectioned before haematoxylin and eosin staining was performed. Tissue sections were scored (double blind) for histology score. Results expressed as mean score \pm SEM. $n=6$ per group. Data pooled from 2 independent experiments. Two-way ANOVA with Bonferroni post-test used to analyse differences between groups. * $P < 0.05$, ** $P < 0.01$.

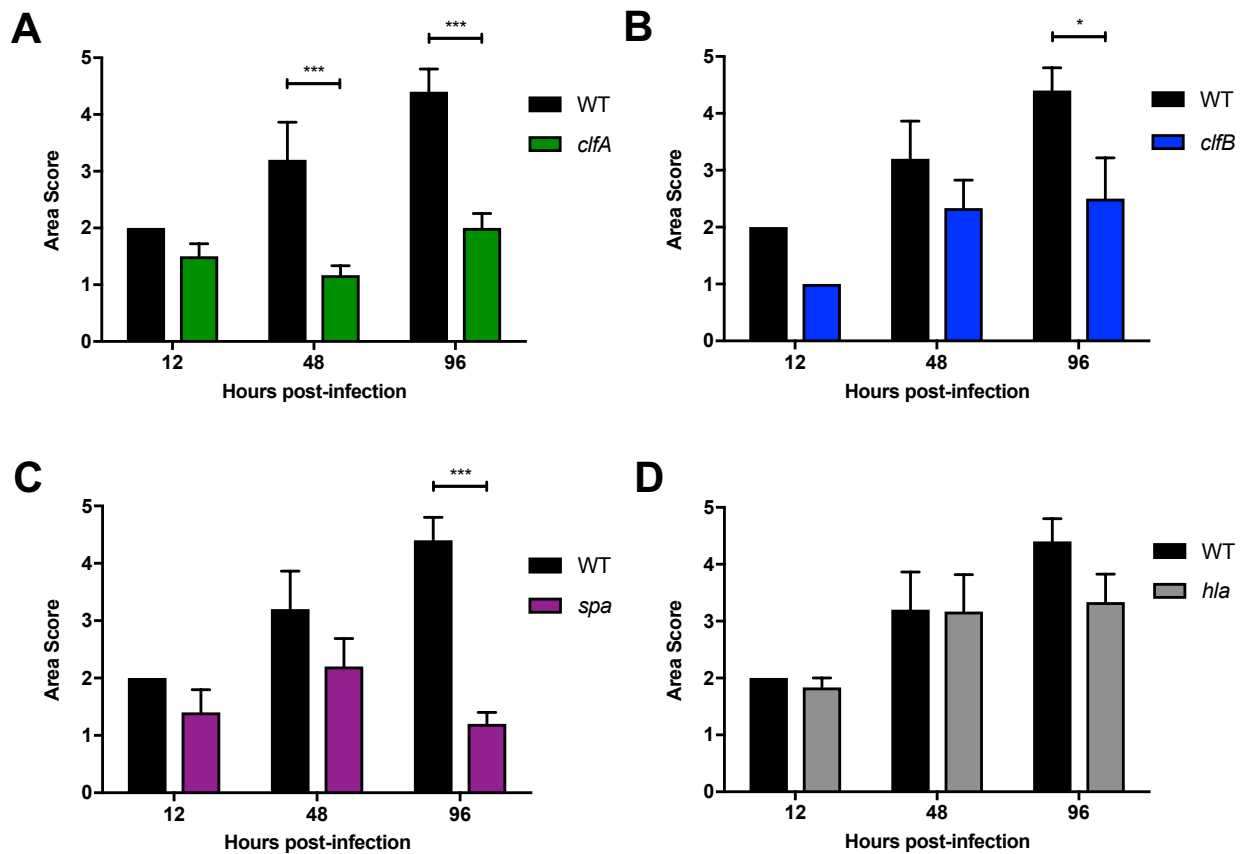


Figure 5.26. Abscesses formed by LAC::*lux* CWA protein mutants form smaller abscesses compared to LAC::*lux* WT. BALB/c mice were infected subcutaneously with 2×10^7 CFU LAC::*lux* WT and LAC::*lux* *clfA* (A), LAC::*lux* *clfB* (B) LAC::*lux* *spa* (C) or LAC::*lux* *hla* (D) and the abscess tissue was excised at various time points (12, 48, 96 hours). Tissue was fixed, embedded in paraffin wax and sectioned before haematoxylin and eosin staining was performed. Abscess area was computed using ImageJ software and the areas were scored accordingly. Results expressed as mean score \pm SEM. $n=6$ per group. Data pooled from 2 independent experiments. Two-way ANOVA with Bonferroni post-test used to analyse differences between groups. * $P < 0.05$, *** $P < 0.001$.

5.2.9 The ClfB ligand loricrin is expressed within the skin abscess tissue in LAC::*lux* WT infected mice.

Having observed a novel role for ClfB, its function during SSTIs was further investigated. *S. aureus* is known to bind to the squamous epithelium of the anterior nares via its interaction between ClfB and loricrin to promote nasal colonisation [50]. To investigate whether the binding of loricrin by ClfB may be important during SSTIs, loricrin expression was investigated within the tissue during *S. aureus* subcutaneous abscess formation. Skin abscess tissue sections were prepared at 48 h post-infection and stained for the presence of loricrin (Figure 5.27). High power magnification indicates that Loricrin is clearly present in the epidermal layer (Figure 5.27 B) which is to be expected as it is a major component of the cornified envelope. Low power magnification indicated that loricrin is also present surrounding the abscess structure (Figure 5.27 A) and under high power magnification appears to be present at the abscess wall structure, as evident by the dark brown staining surrounding the abscess (Figure 5.29 C).

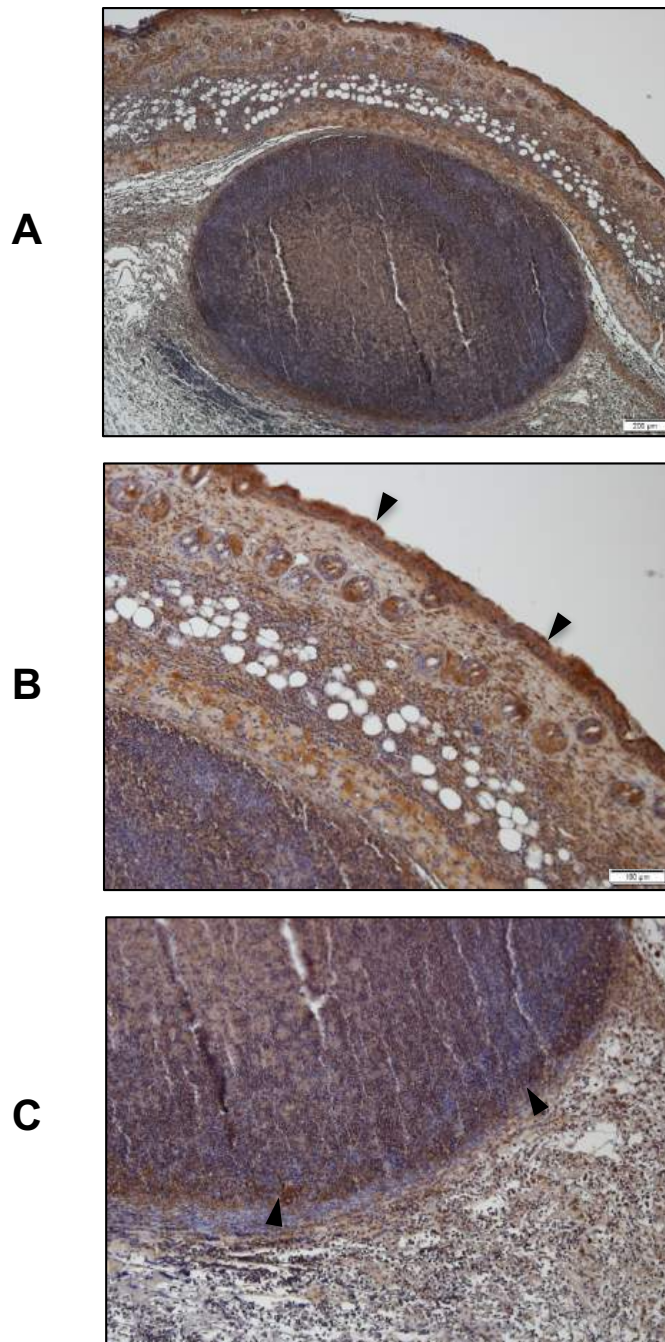


Figure 5.27. Loricrin is present within the skin abscess tissue of LAC::*lux* WT infected animals. BALB/c mice were infected subcutaneously with 2×10^7 CFU LAC::*lux* WT and abscess tissue was excised at 48h post-infection. Tissue was fixed, embedded in paraffin wax and sectioned before staining with rabbit anti-murine loricrin IgG followed by an anti-rabbit IgG-HRP secondary antibody. Loricrin staining was developed using DAB substrate (dark brown). Low power field of the entire abscess structure is shown (A). Relative tissue sections are shown in high power fields: skin epidermal layer (B) and abscess wall (C). Black arrows indicate the presence of loricrin. Representative images of n=3 stained sections.

5.2.10 The ClfB-loricrin interaction is important for virulence during *S. aureus* SSTIs

To investigate if the ClfB-loricrin interaction is specifically required for virulence during *S. aureus* SSTIs, recombinant loricrin loop L2v was used to block the interaction between ClfB and native loricrin. LAC::*lux* WT (2×10^7 CFU) was pre-incubated with loricrin L2v-GST or PBS prior to s.c. injection. To account for the presence of GST, a separate group of mice were challenged with LAC::*lux* WT pre-incubated with recombinant GST. The abscess lesion area was measured at 72 h post-infection and mice that received loricrin L2v had reduced abscess lesion area compared to either PBS or GST groups (Figure 5.28). Bioluminescence imaging was also performed throughout the 72-h infection period. A decrease in bioluminescence was observed throughout the infection period in the presence of loricrin L2v, compared to mice injected with GST or PBS (Figure 5.29). This reduction was confirmed with a significant decrease in the bacterial burden in the skin at 72 h post-infection in mice that received LAC::*lux* WT with loricrin L2v compared to mice that received LAC::*lux* WT with PBS or GST (Figure 5.30).

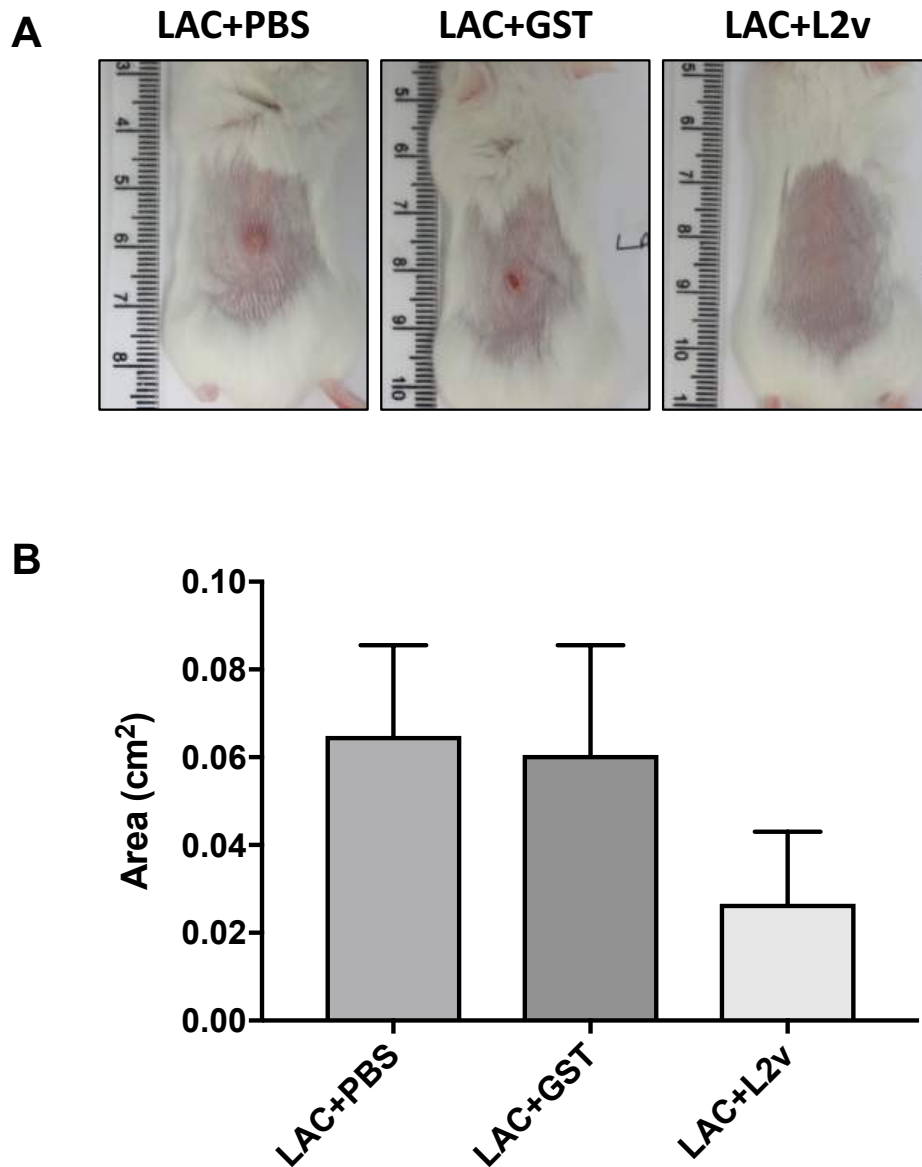


Figure 5.28. Blocking of the ClfB-loricrin interaction *in vivo* results in reduced abscess lesion area during subcutaneous abscess model. LAC::*lux* WT (2×10^7 CFU) was pre-incubated with PBS, GST or recombinant loricrin L2v-GST (24 μ M) for 30 min before subcutaneous inoculation. Abscess lesion area was measured at 72h post-infection. Representative lesions from each group are shown (A). Images depict the dorsal backs of mice. Results expressed as total lesion area (cm²) \pm SEM (B). n=5. One-way ANOVA with Tukey post-test used to analyse differences between groups.

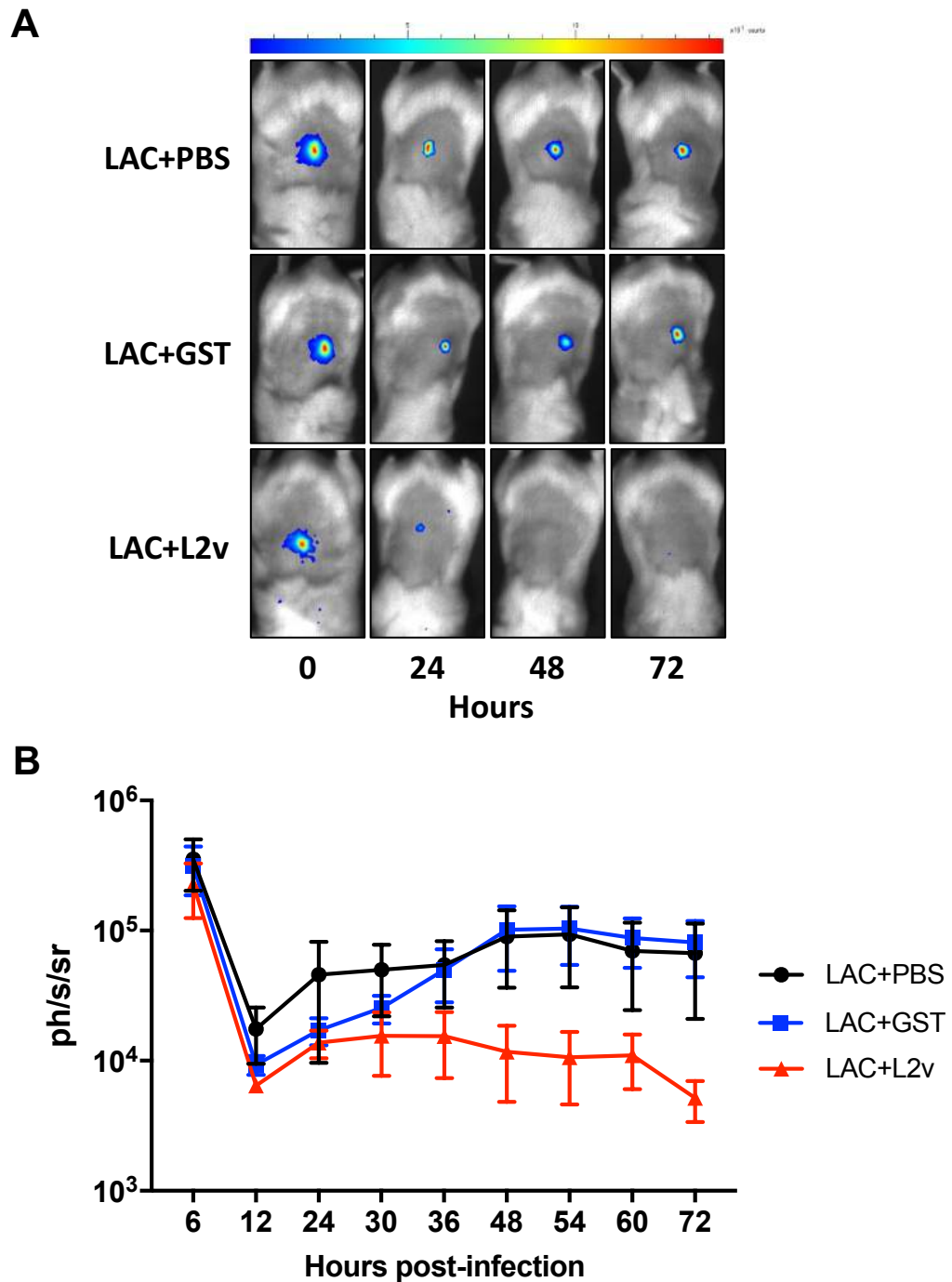


Figure 5.29. Blocking of the ClfB-loricrin interaction *in vivo* results in reduced bioluminescence during subcutaneous abscess model. LAC::*lux* WT (2×10^7 CFU) was pre-incubated with PBS, GST or recombinant loricrin L2v-GST (24 μ M) for 30 min before subcutaneous injection. Bioluminescence imaging was carried out over 72 h using Photon Imager. Representative *in vivo* bioluminescence images from each group are shown (A). Images depict the dorsal backs of mice. Results are expressed as mean total photon flux (photons per second per steradian) \pm SEM (B). $n=5$ per group.

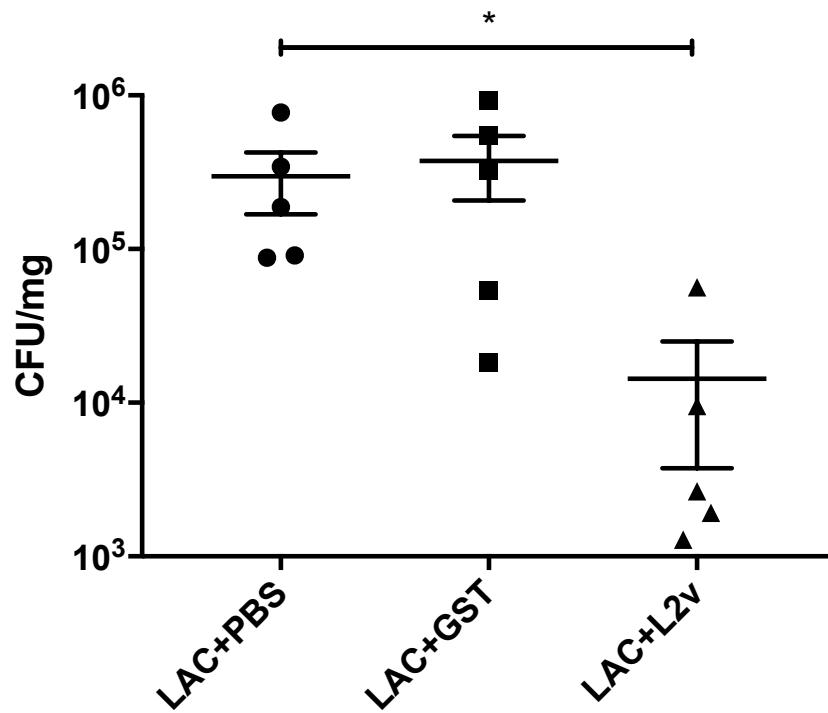


Figure 5.30. Blocking of the CifB-loricrin interaction *in vivo* results in reduced bacterial burden during subcutaneous abscess model. LAC::*lux* WT (2×10^7 CFU) was pre-incubated with PBS, GST or recombinant loricrin L2v-GST (24 μ M) for 30 min before subcutaneous inoculation. Bacterial burden was assessed at 72h post-infection. Results are expressed as Log₁₀ CFU/mg with means indicated by bars. n=5. One-way ANOVA with Tukey post-test used to analyse differences between groups. * $P < 0.05$.

5.2.11 Model vaccines comprising ClfB and ClfA induce antigen-specific humoral responses

Having discovered a novel role for ClfB during skin infection, the use of ClfB as a vaccine antigen targeted against SSTIs was investigated. A model vaccine containing ClfB was formulated with CpG, as this has previously been demonstrated to help drive protective immune responses against systemic infection when combined with ClfA (Chapter 4). ClfB was also combined with the widely used and licensed adjuvant, aluminium potassium sulfate (alum). For comparison, mice were also vaccinated with ClfA in combination with either CpG or alum.

Groups of naïve BALB/c mice were vaccinated via the s.c. route with alum (0.5 mg/ml) or CpG (50 µg/mouse) alone or in combination with ClfB or ClfA (5 µg/mouse) on d 0, 14 and 28. On d 42 (2 weeks after final immunisation) humoral immune responses were measured in these vaccinated mice. Sera were isolated and antibody titres assessed by ELISA. Anti-ClfB IgG titres were measured in control groups and groups that received ClfB (i.e. CpG+ClfB and Alum+ClfB) (Figure 5.31 A) and anti-ClfA IgG titres were measured in control groups and groups that received ClfA (i.e. CpG+ClfA and Alum+ClfA) (Figure 5.31 B). Vaccination with ClfB induced significantly elevated ClfB-specific IgG titres in mice compared to control groups regardless of the adjuvant used (Figure 5.31 A). ClfA also induced significant levels of ClfA-specific antibodies compared to adjuvant alone groups and this was irrespective of which adjuvant was used (Figure 5.31 B). Interestingly, ClfA induced ~3 Log₁₀ increase in antibody titres compared to ClfB, suggesting that ClfA is a more potent inducer of humoral immune responses in mice.

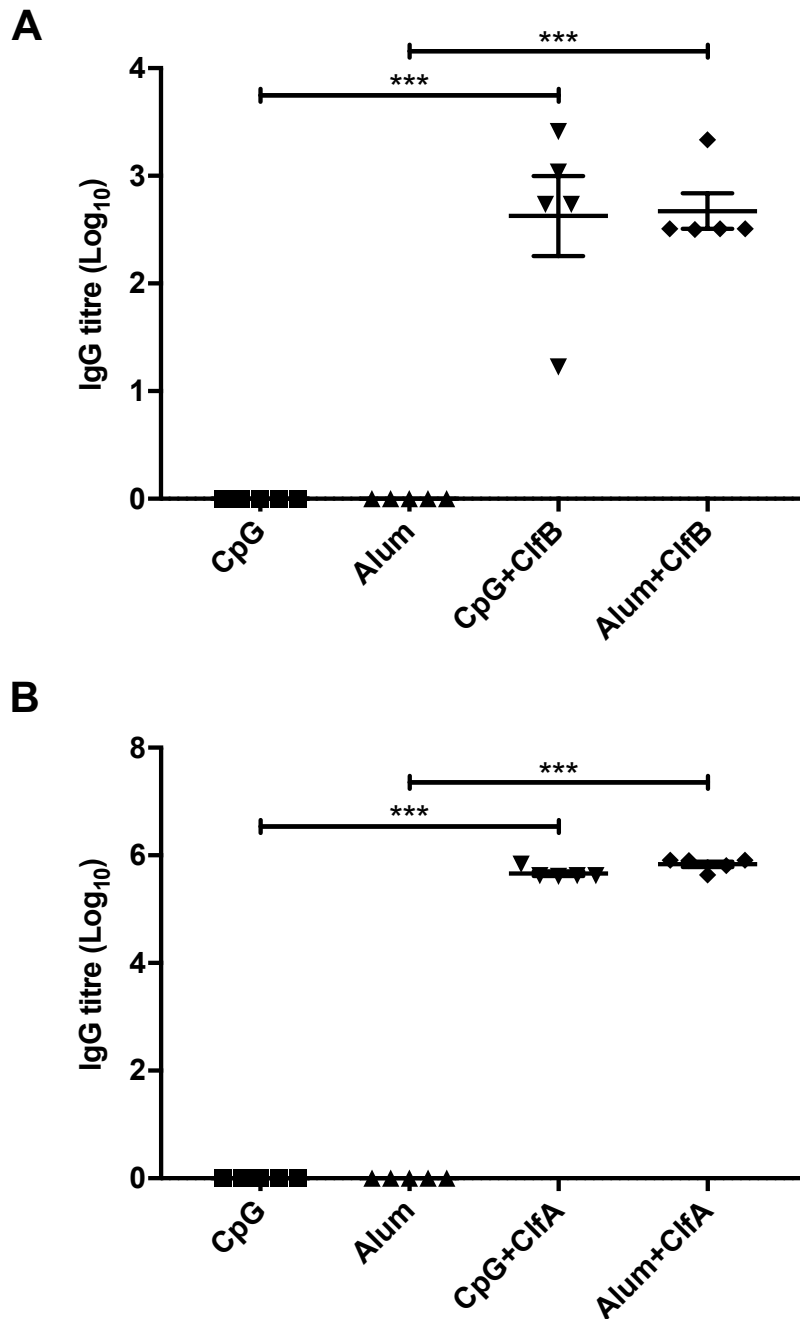


Figure 5.31. Model vaccines comprising ClfB and ClfA induce antigen-specific humoral immune responses. BALB/c mice were vaccinated with CpG (50 μ g/mouse) or alum (0.5 mg/mouse) alone or combined with ClfB or ClfA (5 μ g/mouse) via s.c. injection on d 0, 14, 28. On d 42 sera was collected from vaccinated mice. ClfB-specific (A) or ClfA-specific (B) IgG titres were determined using ELISA. Results expressed as mean \pm SEM. n=5 per group. One-way ANOVA with Tukey post-test was performed to compare variances. *** $p < 0.001$.

5.2.12 Model vaccines comprising ClfB and ClfA induces antigen-specific cellular responses

Having confirmed that vaccination could induce humoral immunity, cellular immune responses were also measured in these vaccinated mice. The ILN, which is the local draining lymph node to the site of vaccination, and spleens were isolated from vaccinated mice. Total isolated cells were stimulated *in vitro* with ClfB (5 µg/ml), ClfA (5 µg/ml) or anti-CD3 and PMA as a positive control. Cell supernatants were collected 72 h post-stimulation for analysis of secreted cytokines by ELISA to assess antigen-specific cellular responses.

Vaccination with ClfB combined with CpG resulted in elevated IFN γ and IL-17 production from ILN (Figure 5.32 A) and spleen (Figure 5.32 B) cells compared to mice vaccinated with CpG alone. Similarly, IFN γ and IL-17 levels were elevated, for the most part, from mice vaccinated with ClfB in combination with alum compared to adjuvant alone groups from ILN cells (5.32 C) or splenocytes (5.32 D). These results demonstrate that vaccination with ClfB is capable of activating cellular responses in mice.

Vaccination with ClfA in combination with CpG (Figure 5.33 A, B) or alum (Figure 5.33 B, C) also induced elevated levels of IFN γ and IL-17 production from cells isolated from the ILN (Figure 5.33 A, C) and spleen (Figure 5.33 B, D) compared to adjuvant alone groups.

Overall, the levels of cytokine detected using this assay were low, however they do indicate that these vaccine formulations can induce antigen specific responses in vaccinated animals.

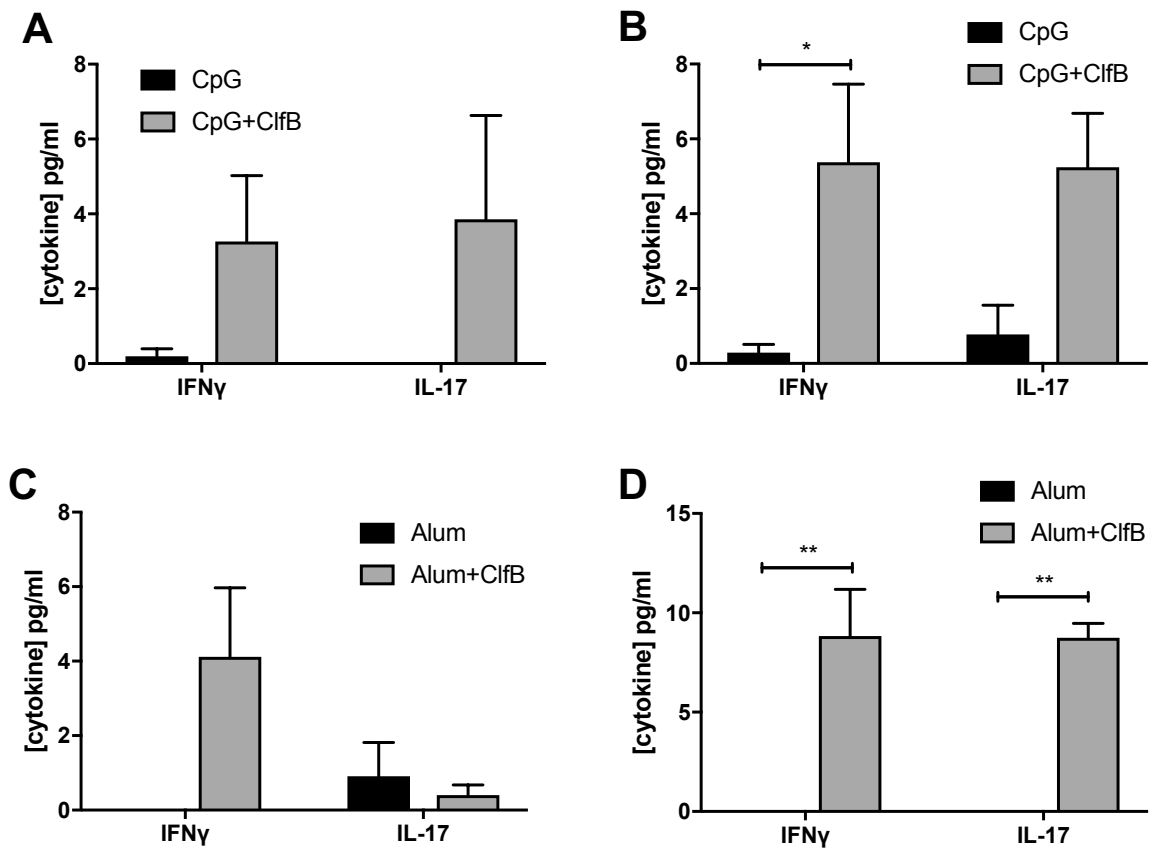


Figure 5.32. Model vaccines comprising ClfB induce cellular immune responses. BALB/c mice were vaccinated with CpG (50 μ g/mouse) or alum (0.5 mg/mouse) alone or combined with ClfB (5 μ g/mouse) via s.c. injection on d 0, 14, 28. Antigen-specific responses by cells isolated from the inguinal lymph nodes (A, C) and spleen (B, D) were determined on d 42, by *ex vivo* stimulation with media or ClfB (5 μ g/ml) for 72 h, and subsequent ELISA to determine levels of IFN γ and IL-17. Media only responses were subtracted from responses to antigens. Results expressed as mean \pm SEM. n=5 per group. Two-way ANOVA with Bonferroni post-test was performed to compare variances. * $p < 0.05$, ** $p < 0.005$.

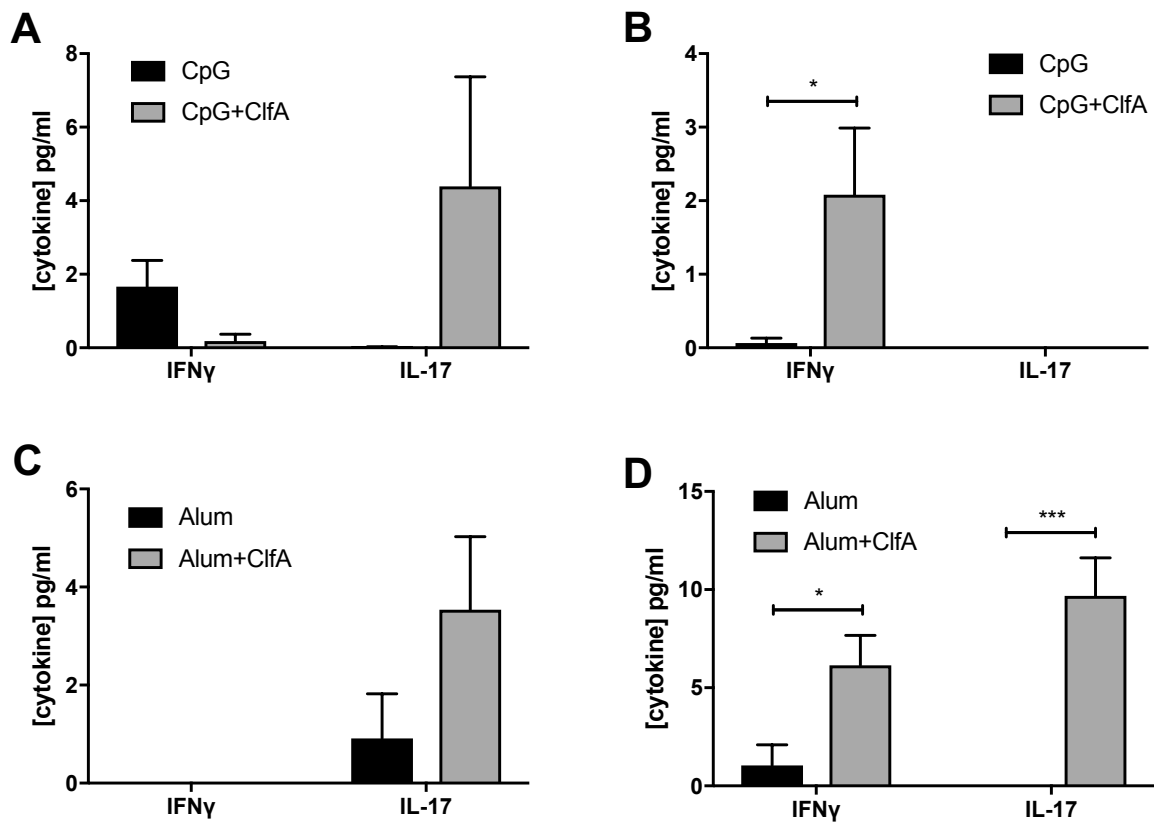


Figure 5.33. Model vaccines comprising ClfA induce cellular immune responses. BALB/c mice were vaccinated with CpG (50 μ g/mouse) or alum (0.5 mg/mouse) alone or combined with ClfA (5 μ g/mouse) via s.c. injection on d 0, 14, 28. Antigen-specific responses by cells isolated from the inguinal lymph nodes (A, C) and spleen (B, D) were determined on d 42, by *ex vivo* stimulation with media or ClfA (5 μ g/ml) for 72 h, and subsequent ELISA to determine levels of IFN γ and IL-17. Media only responses were subtracted from responses to antigens. Results expressed as mean \pm SEM. n=5 per group. Two-way ANOVA with Bonferroni post-test was performed to compare variances. * $p < 0.05$, *** $p < 0.001$.

5.2.13 Model vaccines comprising ClfB and ClfA protect against subsequent *S. aureus* skin infection

Having demonstrated that immunisation with ClfB and ClfA in combination with CpG or alum could induce both cellular and humoral immune responses, the ability of these vaccines to offer protection against *S. aureus* SSTIs was assessed. Groups of BALB/c mice were vaccinated via the s.c. route with alum (0.5 mg/ml) or CpG (50 µg/mouse) alone or in combination with ClfB or ClfA (5 µg/mouse) on d 0, 14 and 28. On d 42 (2 weeks after final immunisation), mice were given a s.c. injection of LAC::*lux* WT (2×10^7 CFU) and *in vivo* bioluminescent imaging was performed to monitor the infection over a 6-day period.

Mice vaccinated with ClfB in combination with CpG or alum developed significantly smaller abscess lesions throughout the 6-day infection period compared to those vaccinated with adjuvant alone (Figure 5.34). A significant reduction in abscess lesion area was also observed in mice vaccinated with ClfA combined with CpG or alum (Figure 5.35). The bacterial burden in the skin of CpG+ClfB and alum+ClfB vaccinated mice was decreased throughout the course of infection as measured by bioluminescence (Figure 5.36). This reduction in bacterial burden was confirmed by viable counting on d 6 post-infection, with significant decreases in CFUs in ClfB vaccinated mice compared to their relevant adjuvant alone control (Figure 5.37). Mice vaccinated with ClfA in combination with either adjuvant also had significantly reduced bioluminescence during the infection period (Figure 5.38). The bacterial burden in the skin on d 6 was also significantly lower in mice vaccinated with CpG or alum in combination with ClfA compared to adjuvant alone vaccinated animals (Figure 5.39).

Taken together, these results indicate that ClfB and ClfA are successful vaccine antigens that can lead to the production of humoral and cellular immune responses, which ultimately lead to the protection against subsequent *S. aureus* SSTIs.

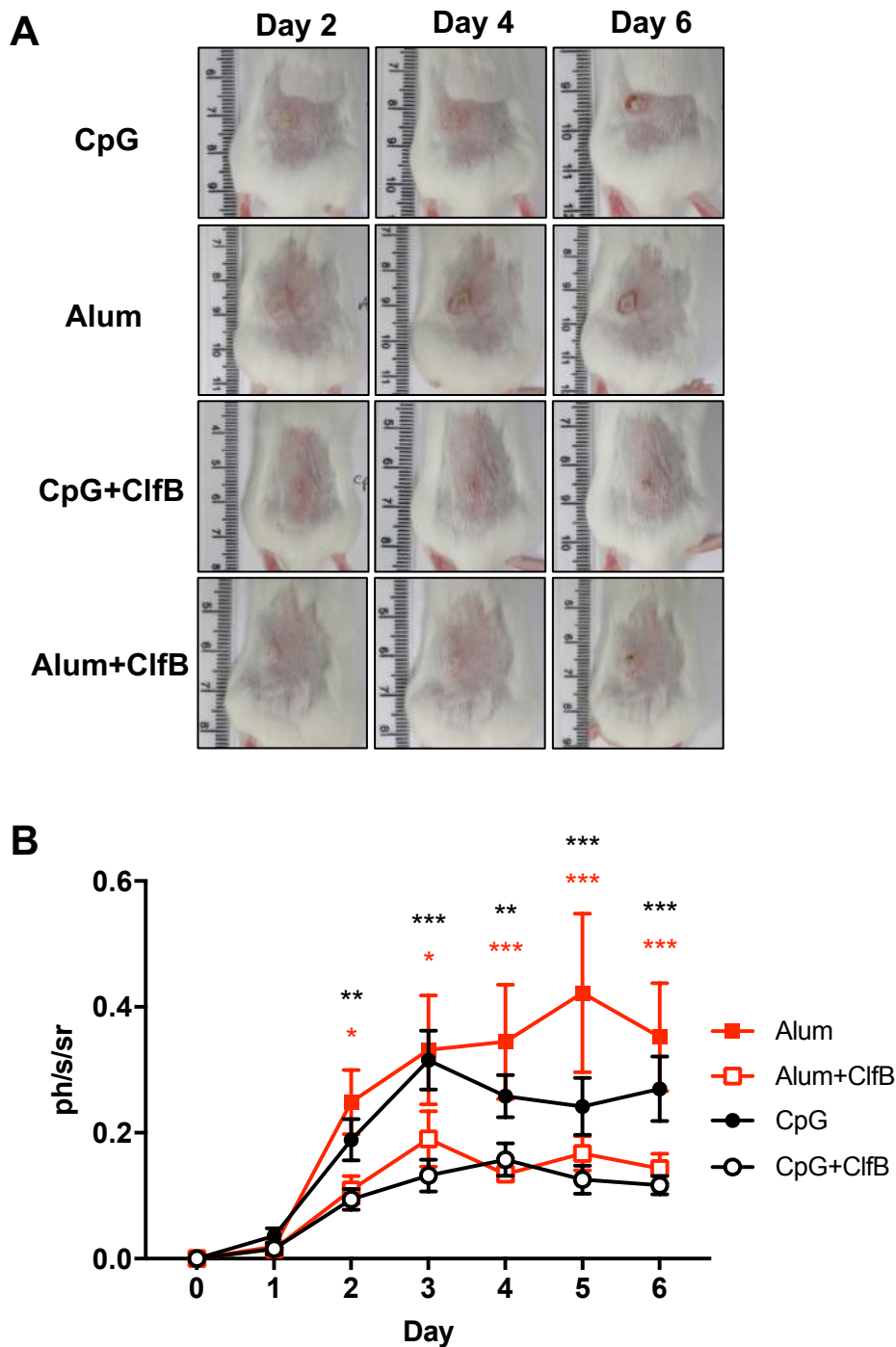


Figure 5.34. Model vaccines comprising ClfB in combination with CpG or alum reduces abscess lesion area. Mice were vaccinated with CpG (50 $\mu\text{g}/\text{mouse}$) or alum (0.5 mg/mouse) alone or combined with ClfB (5 $\mu\text{g}/\text{mouse}$) via s.c. injection on d 0, 14, 28. On d 42, mice were infected subcutaneously with 2×10^7 CFU LAC::*lux* WT and abscess lesion size was measured daily using Photon Imager. Representative images from each group are shown (A). Results expressed as total lesion size (cm^2) \pm SEM (B). $n=10$ per group. Data pooled from 2 independent experiments. Two-way ANOVA with Bonferroni post-test used to analyze differences between groups. * $p < 0.05$, ** $p < 0.005$, *** $P < 0.001$.

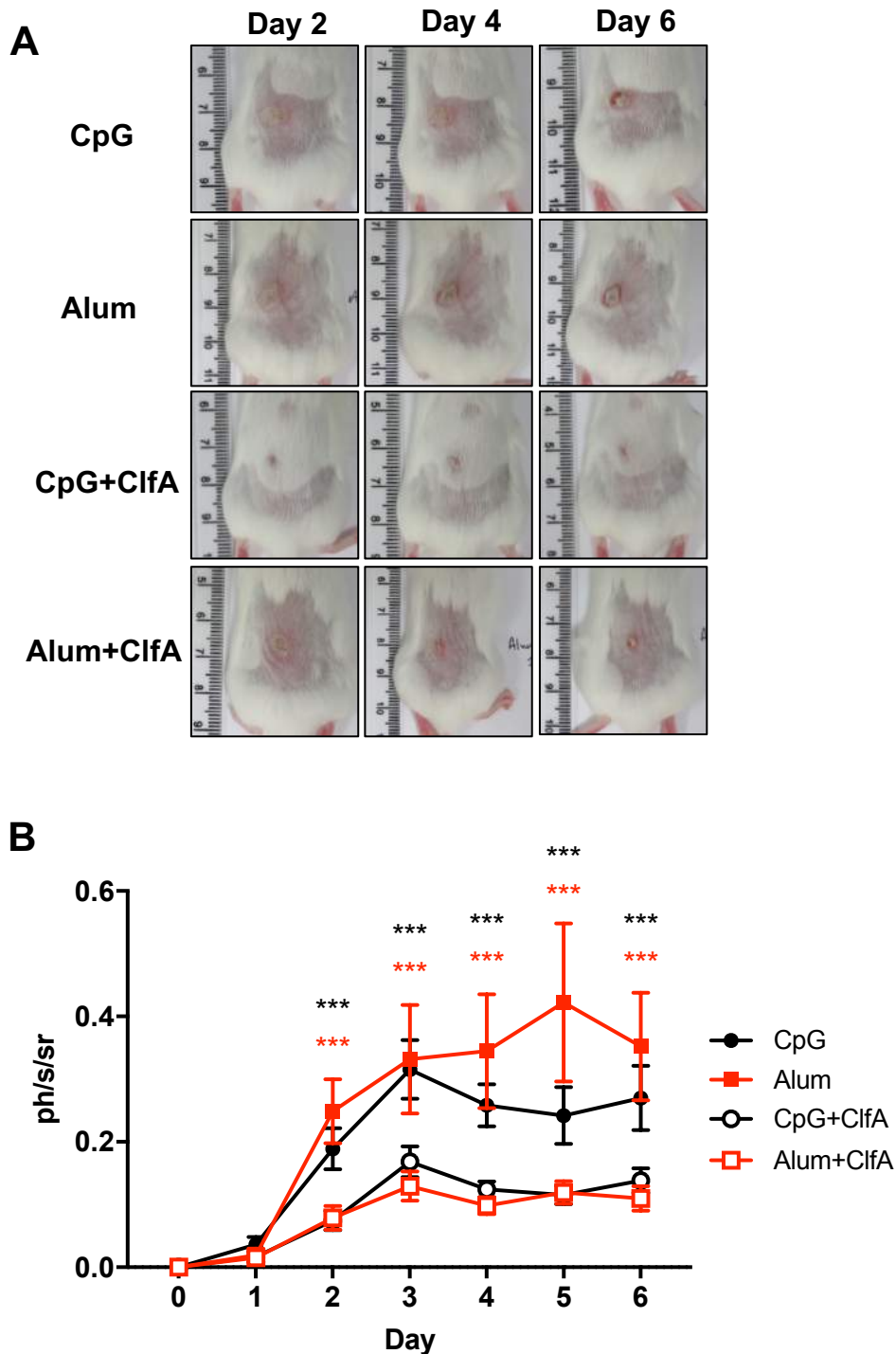


Figure 5.35. Model vaccines comprising CifA in combination with CpG or alum reduces abscess lesion area. BALB/c mice were vaccinated with CpG (50 $\mu\text{g}/\text{mouse}$) or alum (0.5 mg/mouse) alone or combined with CifA (5 $\mu\text{g}/\text{mouse}$) via s.c. injection on d 0, 14, 28. On d 42, mice were infected subcutaneously with 2×10^7 CFU LAC::*lux* WT and abscess lesion size was measured daily using Photon Imager. Representative images from each group are shown (A). Results expressed as total lesion size (cm^2) \pm SEM (B). $n=10$ per group. Data pooled from 2 independent experiments. Two-way ANOVA with Bonferroni post-test used to analyze differences between groups. *** $P < 0.001$.

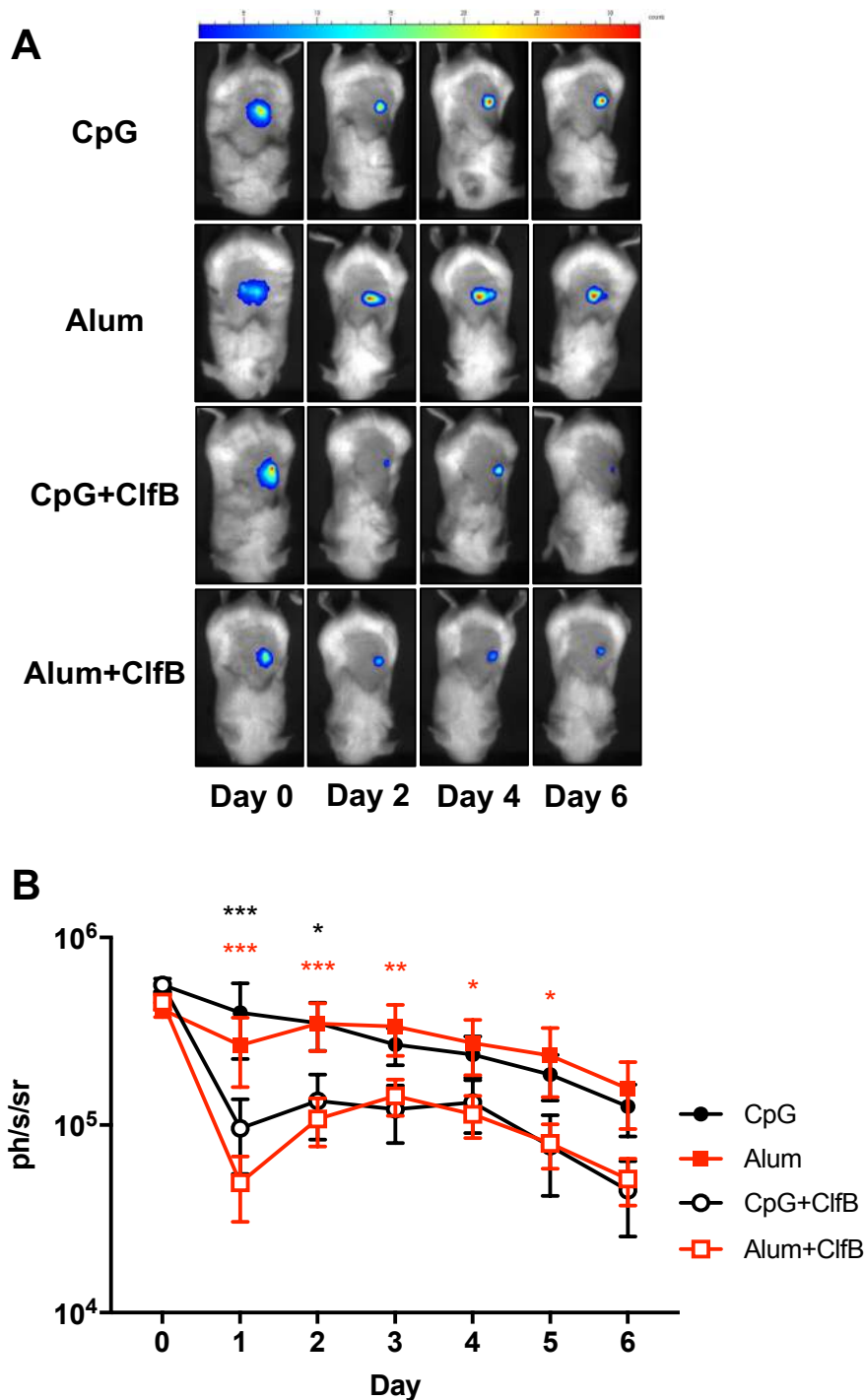


Figure 5.36. Model vaccines comprising ClfB in combination with CpG or alum reduces bioluminescence. BALB/c mice were vaccinated with CpG (50 $\mu\text{g}/\text{mouse}$) or alum (0.5 mg/mouse) alone or combined with ClfB (5 $\mu\text{g}/\text{mouse}$) via s.c. injection on d 0, 14, 28. On d 42, mice were infected s.c. with 2×10^7 CFU LAC::*lux* WT and bioluminescence imaging was carried out using Photon Imager. Representative *in vivo* bioluminescence images from each group are shown (A). Results are expressed as mean total photon flux (photons per second per steradian) \pm SEM (B). n=10 per group. Data pooled from 2 independent experiments. Two-way ANOVA with Bonferroni post-test was performed. * $P < 0.05$, ** $P < 0.01$, *** $P < 0.001$.

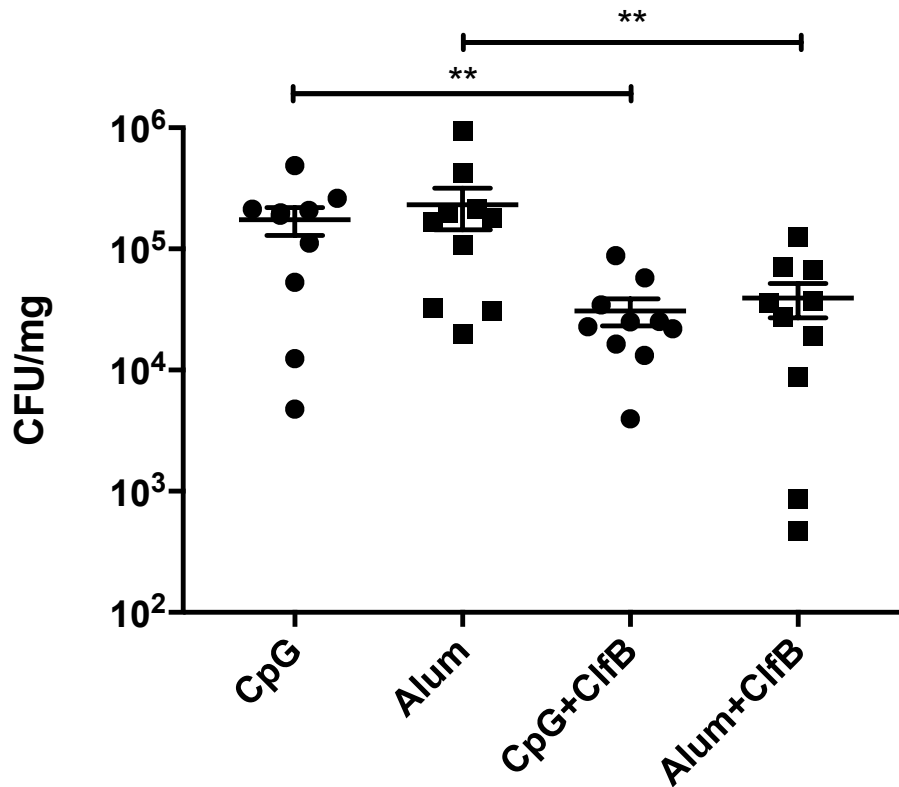


Figure 5.37. Model vaccines comprising CifB in combination with CpG or alum leads to a reduction in bacterial burden in the skin. Mice were vaccinated with CpG (50 $\mu\text{g}/\text{mouse}$) or alum (0.5 mg/mouse) alone or combined with CifB (5 $\mu\text{g}/\text{mouse}$) via s.c. injection on d 0, 14, 28. On d 42, mice were infected s.c. with 2×10^7 CFU *S. aureus* LAC::*lux* WT and bacterial burden was measured on d 49 by viable counting. Results are expressed as mean total photon flux (photons per second per steradian) \pm SEM. n=10 per group. Data pooled from 2 independent experiments. One ANOVA with Tukey post-test used to analyze differences between groups. ** $P < 0.01$.

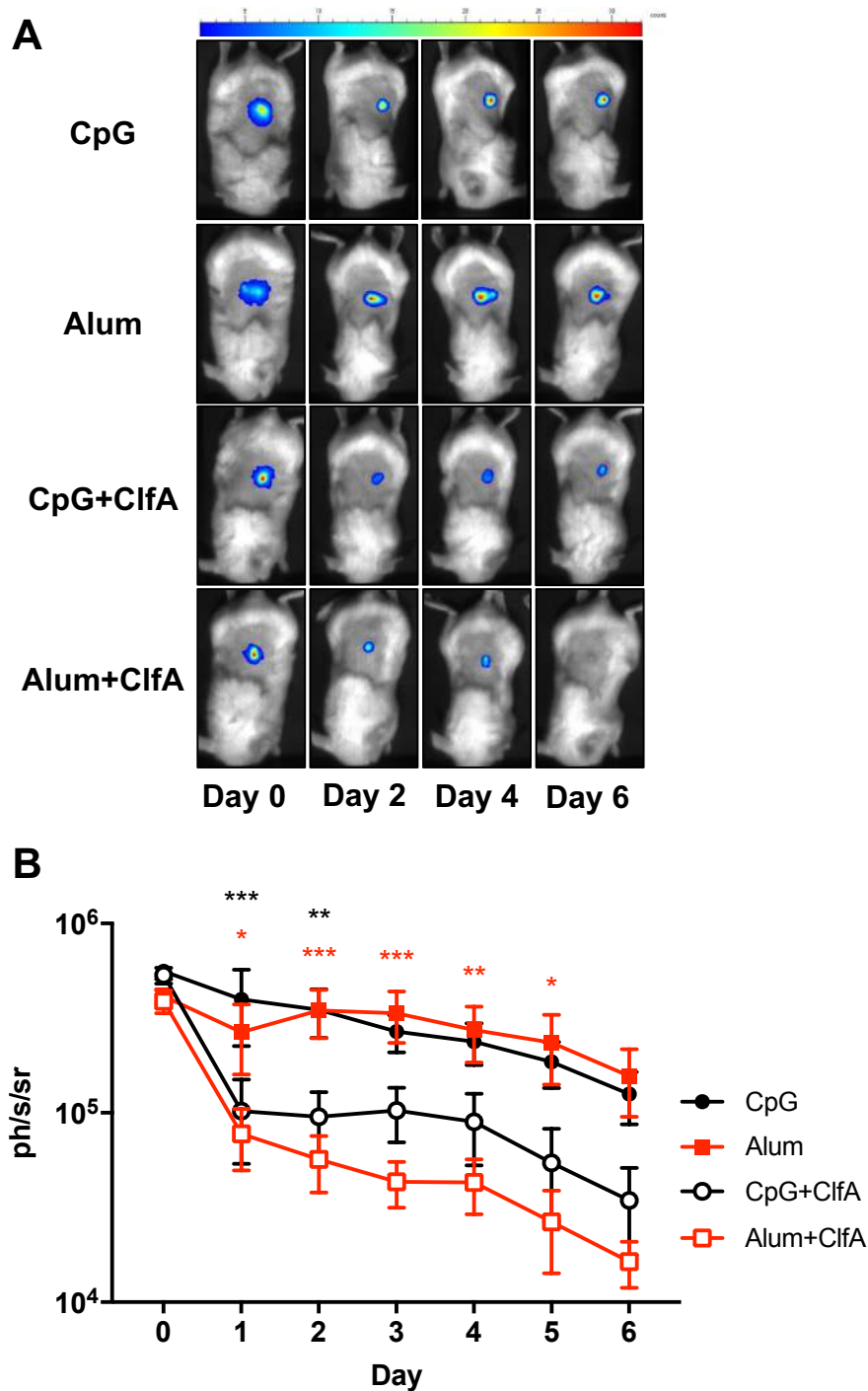


Figure 5.38. Model vaccines comprising ClfA in combination with CpG or alum reduces bioluminescence. BALB/c mice were vaccinated with CpG (50 μ g/mouse) or alum (0.5 mg/mouse) alone or combined with ClfB (5 μ g/mouse) via s.c. injection on d 0, 14, 28. On d 42, mice were infected s.c. with 2×10^7 CFU LAC::*lux* WT and bioluminescence imaging was carried out using Photon Imager. Representative *in vivo* bioluminescence images from each group are shown (A). Results are expressed as mean total photon flux (photons per second per steradian) \pm SEM (B). n=10 per group. Data pooled from 2 independent experiments. Two-way ANOVA with Bonferroni post-test was performed. * $P < 0.5$, ** $P < 0.01$, *** $P < 0.001$.

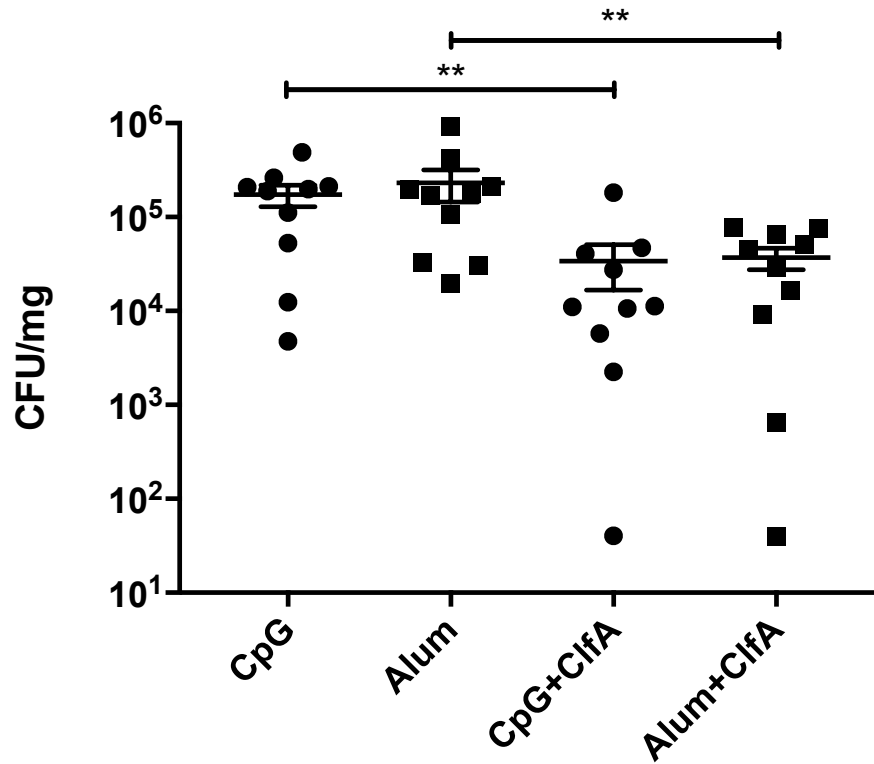


Figure 5.39. Model vaccines comprising CifA leads to a reduction in bacterial burden in the skin. Mice were vaccinated with CpG (50 μ g/mouse) or alum (0.5 mg/mouse) alone or combined with CifB (5 μ g/mouse) via s.c. injection on d 0, 14, 28. On d 42, mice were infected subcutaneously with 2×10^7 CFU LAC::*lux* WT and bacterial burden was measured on d 49 by viable counting. Results are expressed as mean total photon flux (photons per second per steradian) \pm SEM. n=10 per group. Data pooled from 2 independent experiments. One ANOVA with Tukey post-test used to analyze differences between groups. ** $P < 0.01$.

5.3 Discussion

To date, only one study has examined the contribution of multiple individual CWA proteins to virulence during skin infection in a murine model [45]. The study examined the contribution to pathogenesis of the surface proteins, SpA, fibronectin binding proteins (FnBPs), SasF and ClfA by exclusively measuring bacterial burden in the skin. The mutants used in the study however were generated in a number of different strain backgrounds, none of which were clinically relevant strains, making it almost impossible to draw clear conclusions about their roles during SSTIs. The majority of research into the virulence potential of CWA proteins has been carried out using systemic invasive models of infection and there is a paucity of information regarding the specific roles played by individual surface proteins during SSTI.

To address this, a murine model of *S. aureus* skin infection was optimized for this study. A moderate inoculum (2×10^7 CFU) was chosen, as it did not cause visible amounts of dermonecrosis, which is known to be primarily caused by secreted toxins [21]. There was no discernible bacterial dissemination to the peripheral organs in this model of infection, indicating that this is a localised skin infection model. The immune cells present at the site of infection were also characterised. The skin abscess was mainly composed of neutrophils, which correlates with previous findings [292]. The presence of IL-17 and IL-22 producing CD4⁺ and $\gamma\delta^+$ T cells at the site of infection is to be expected, as these cells are known to be important components of the protective immune response during *S. aureus* SSTIs [21, 225]. Interestingly there was a small number of Th1 cells present in the skin abscess tissue. Their function during SSTIs is currently unknown, but previously in a surgical wound infection, Th1 cells were found to be detrimental and resulted in increased bacterial burden at the infection site [275]. The role of these cells during this subcutaneous abscess model remains to be further investigated.

Initial studies using the LAC::*lux srtA* mutant in the murine subcutaneous abscess model of *S. aureus* skin infection confirmed that CWA proteins are important virulence factors during SSTI. Smaller abscess lesions with reduced bacterial burden form when CWA proteins are absent from the infecting strain of bacteria. Histopathology analysis was also carried out which highlighted the importance of CWA proteins during the initial development of the skin abscess, as when these are absent as in LAC::*lux srtA*, the abscesses form at a much slower rate compared to LAC::*lux* WT infected animals and lack much of the structural definition that is typical of an abscess. The reduction in abscess size in LAC::*lux srtA* infected animals was associated with a reduced number of neutrophils at the site of infection. This suggests that CWA proteins are capable of inducing neutrophil recruitment to the site of infection, presumably by T cell activation. This correlates with findings from Chapter 4, which reveal that CWA proteins are capable of activating CD4⁺ T cells and inducing the production of IL-17, which is known to drive neutrophil recruitment [173-177].

To further probe which specific surface proteins may be involved during SSTIs, CWA protein null mutants of ClfA, ClfB and SpA were constructed and investigated in this murine infection model. Mice infected with LAC::*lux clfA* formed significantly smaller abscess lesions compared to LAC::*lux* WT infected mice and bacterial burden in the skin was significantly reduced on day 3 and 6 post-infection. The bacterial burden results mirrors what was seen before in the Kwiecinski *et al.* study on day two in mice infected with a *clfA*-deficient strain of *S. aureus* Newman [45]. A recent study however, using a rabbit skin infection model saw no reduction in bacterial burden in mice infected with a *clfA*-deficient strain of Newman [105]. It is possible that differences in animal species (mouse versus rabbit) and infection models employed account for the differences in results with bacterial burden.

Bacterial burden was also reduced in mice infected with LAC::*lux spa*, however the abscess lesion area was not greatly affected. This suggests that an increase in bacterial clearance does not directly affect the size of the abscess lesion on the dorsal backs of the mice. The abscess structure is disrupted in LAC::*lux spa* infected mice compared to LAC::*lux* WT infected animals. SpA has previously been demonstrated to be an important factor in determining the number of kidney abscesses during i.v. infection [44]. This study also correlates with findings that SpA exerts its effect later in the infection process (after ~48 h) during kidney abscess formation [44]. This study has demonstrated that in the context of SSTI SpA is not important in determining the rate of abscess lesion formation, but is involved to some degree in determining the abscess structure and bacterial burden.

Mice infected with LAC::*lux hla* had reduced bacterial burden in the skin and also formed smaller abscess lesions compared to LAC::*lux* WT infected mice. This correlates with previous reports on the role of Hla during SSTIs [26, 35, 36]. However, the structure and the overall size of the skin abscess was not altered in LAC::*lux hla* infected animals compared to LAC::*lux* WT. This suggests that Hla and possibly other secreted proteins are not primarily involved in determining abscess structure at the site of infection but are likely the primary driver of dermonecrosis during SSTIs as has been previously shown [33, 35, 37, 293].

One of the most striking findings from this study is that ClfB appears to play a very important role during SSTIs, affecting both lesion size, bacterial burden and abscess structure. ClfB has never previously been examined in a skin infection model, and its main role was thought to be involved in *S. aureus* colonisation of the anterior nares [50]. These data now suggest however, that ClfB may have a crucial role during skin infection. ClfB appears to be particularly important at the very early stages of infection, in contrast to ClfA and SpA, which were found to affect abscess formation at later time points. ClfB is known to bind to squames in the nasal cavity via

interactions with both loricrin and cytokeratin 10 and it is also capable of adhering to fibrinogen and cytokeratin 8 [52, 109, 114]. This suggests that it may be capable of binding at other anatomical locations that contain these ligands, thus facilitating initial attachment of the bacteria. Immunohistochemistry analysis has revealed that loricrin, as expected was present in the outermost layer of the skin, the corneal layer. Interestingly, loricrin also appears to be associated with the wall of the skin abscess structure of LAC::*lux* WT infected mice. Although loricrin is normally confined to the granular and corneal layers of the skin [294, 295], the expression and localisation of loricrin is disrupted during wound healing [296, 297]. This may account for the presence of loricrin in the subcutaneous tissue, which may facilitate the binding of *S. aureus* via ClfB and the subsequent formation of the abscess wall. To investigate this proposed ClfB-loricrin interaction in the skin, the interaction between LAC::*lux* WT and loricrin *in vivo* was blocked using recombinant loricrin loop L2v. Pre-incubation with recombinant loricrin L2v abolishes the ability of ClfB to bind to native ligands in the skin, as L2v will be bound in the binding trench of ClfB. Throughout the 3-day infection period, mice infected with LAC::*lux* WT pre-incubated with L2v had reduced bacterial burden and abscess lesion size compared to control groups. These data reveal that ClfB is using its ligand binding ability to contribute to pathogenesis during skin infection. It is possible that ClfB is binding to an alternative ligand in the skin, such as fibrinogen or keratin, and that this interaction is being blocked when pre-incubated with recombinant loricrin. To confirm these interactions are loricrin specific, future experiments will use loricrin-deficient mice to investigate the ClfB-loricrin interaction during SSTIs.

Having uncovered a novel role for ClfB during *S. aureus* skin infection, the ability of a vaccine containing ClfB to offer protection against SSTIs was investigated. ClfB has never previously been investigated as a vaccine antigen targeted against *S. aureus* skin infection and the only previous vaccines to use ClfB were targeted against nasal

colonisation [112] and i.v. infection [298]. A model vaccine was formulated with ClfB in combination with the adjuvant CpG which was used as an adjuvant in Chapter 4 and previously by Browne *et al.* [156] and others [286, 287, 290]. Although CpG has successfully driven Th1 and Th17 responses in this study (Chapter 4) and in other vaccine studies [156, 287, 299], it is not currently licensed for human use, although it is currently in phase III clinical trials [300]. Alum, on the other hand, is one of five adjuvants currently licensed for use in humans [300]. ClfB was also combined with alum and the ability of these vaccines to induce cellular and humoral immune responses was investigated. Model vaccines containing ClfA in combination with CpG and alum were also formulated as a comparison, as ClfA combined with CpG has been demonstrated to drive Th1 and Th17-mediated protection against systemic *S. aureus* infection (chapter 4) [156, 299].

Vaccination with ClfB activated humoral immune responses by inducing significant levels of antigen-specific antibody titres compared to adjuvant alone controls, regardless of the adjuvant used. Vaccination with ClfB was also capable of inducing IFN γ and IL-17 responses from ILN and spleen cells. The levels of IFN γ detected were low in mice vaccinated with ClfB in combination with CpG. However, this is unsurprising as although CpG is known to polarise Th responses to Th1 away from Th2 responses, the vaccine was administered in BALB/c mice which are Th2 dominant. Similarly, alum is known to drive a Th2/Th17 immune response, which may explain the low IFN γ responses detected in these groups. Notwithstanding the low levels of cytokine detected, it is clear that antigen-specific cellular immune responses are being generated by this vaccination strategy. This correlates with findings from Chapter 4 which demonstrates ClfB is capable of inducing antigen-specific T cell responses in human CD4⁺ T cells by inducing the activation of Th1 and Th17 cells [299]. Vaccination with ClfA in combination with CpG or alum also resulted in the induction of both cellular and humoral immune responses.

Immunisation with ClfB led to a substantial reduction in the severity of the subsequent *S. aureus* LAC::*lux* WT skin infection, with reduced bacterial burden throughout the course of infection and a significant reduction in the abscess lesion area when compared to adjuvant alone control groups. The protection offered by these vaccines is presumably mediated by the induction of humoral responses, while at the same time activating T cell responses. The induction of ClfB-specific antibodies is likely to aid protection against subsequent infection by inhibiting the binding of ClfB to ligands present within the skin (i.e. loricrin, cytokeratin10 and fibrinogen), and thus having a detrimental impact upon the ability of the bacteria to establish within the skin. A robust cellular response would be essential for the recruitment and activation of phagocytes, primarily neutrophils, to clear the bacteria during *S. aureus* SSTIs. Interestingly, the choice of adjuvant did not affect the outcome of infection, highlighting that ClfB represents a promising vaccine antigen, capable of offering protection against *S. aureus* SSTIs regardless of what it is adjuvanted with. Infection only controls were not included in this experiment, as the effect of LAC::*lux* WT infection in naïve BALB/c mice had previously been determined (Figure 5.20 and 5.21). The adjuvant alone groups are very similar in both area and bioluminescence to LAC::*lux* WT infected naïve mice. However, the inclusion of an infection only control group would further enhance these results.

Similar protection against skin infection was observed in mice vaccinated with ClfA in combination with CpG or alum. This further indicates that ClfA is a favourable vaccine antigen, as it is capable of inducing protective immune responses against both systemic and localised infections. Future studies using a vaccine composed of both ClfA and ClfB could be carried out to investigate whether greater protection against SSTIs could be achieved when combined or if they are offering protection in a redundant manner.

Taken together, the results of this study highlight the importance of CWA proteins as virulence determinants during *S. aureus* SSTIs which play a role in determining the bacterial burden at the site of infection but most importantly identifies for the first time how these proteins also affect the structure and formation of the skin abscess. Of particular importance is the novel role discovered for ClfB during skin infections. ClfB exerts its effect in the early stage of infection and its interaction with loricrin appears to play a role during pathogenesis. These data support the targeting of ClfB in future vaccine studies to offer protection against *S. aureus* SSTIs and perhaps ClfB in combination with ClfA could offer even greater protection in model anti-*S. aureus* vaccines against SSTIs specifically.

Chapter 6

General Discussion

S. aureus SSTIs are occurring more frequently and treatment of these infections is becoming increasingly difficult due to the pathogen's propensity to develop antibiotic resistance. Thus, there is an urgent need to develop alternative treatments, and vaccines that prevent or lessen the severity of *S. aureus* SSTIs may offer a potential solution. Substantial efforts have already been employed to develop anti-*S. aureus* vaccines, however all passive and active immunisation strategies thus far have failed to show efficacy in human trials [205, 220]. In the past, *S. aureus* vaccines were designed to induce neutralising and opsonising antibodies [219], and although these vaccines produced robust humoral immunity, and proved efficacious in pre-clinical models, they did not prevent or attenuate infection in clinical trials [220]. It is now accepted that the development of anti-staphylococcal strategies will need to target adaptive cellular immune responses, in particular T cells. New anti-*S. aureus* vaccine therapies should therefore have the ability to activate both cellular and humoral responses. However, a universal anti-*S. aureus* vaccine may never be realised [224], as numerous studies have implicated the importance of differing immune responses depending on the site of infection [21, 156, 182, 183]. Instead, a vaccine targeting specific clinical manifestations may be more realistic. A prophylactic vaccine targeted against SSTIs would be of great benefit, as although skin infections do not have a high mortality rate, they represent the most frequent site of *S. aureus* infection and are a significant burden on healthcare systems and management and treatment costs can be substantial [225, 301].

Before particular T cell subsets can be targeted by vaccination, staphylococcal T cell antigens have to be identified. The CWA proteins of *S. aureus* are in direct contact with the host immune system, as they are surface exposed, and thus their ability to induce immune responses should be considered. However, there is a dearth of information on the ability of these CWA proteins to act as T cell antigens. This thesis examined the specific role of CWA proteins during *S. aureus* skin infection and

investigated their potential to activate T cells, with the ultimate aim of developing a model vaccine targeted against *S. aureus* SSTIs.

Initially, studies using *in vitro* human T cell cultures investigated the potential of CWA proteins to activate T cells, as any future anti-*S. aureus* vaccine, regardless of infection site, will need to activate cellular immune responses. This project clearly identifies CWA proteins as potent activators of human CD4⁺ T cells and highlights their potential as an important pool of T cell antigens that have not previously been thoroughly investigated. The individual CWA proteins; ClfA, ClfB and SdrC, were all capable of inducing antigen-specific Th1 and Th17 cell responses, albeit to differing extents. Of the proteins tested in this study, ClfA was the most capable of inducing T cell responses and further research was carried out to decipher which subdomain of the protein was responsible for its antigenic ability. Interestingly, ClfA N123 and N23 were potent Th1 and Th17 antigens, whereas the N1 domain was exclusively able to activate Th1 cells. This suggests that the Th17-activating region of ClfA is located within the N23 domain, whereas there is redundancy in the part of ClfA that can activate Th1 cells. The ability of these subdomains to activate T cells *in vivo*, and the downstream effect of this to offer protection against systemic infection was investigated. Vaccination with all of the subdomains in combination with the adjuvant, CpG, led to T cell and antibody mediated protection against systemic *S. aureus* dissemination. However, taken together with the human T cell data, it is clear that ClfA N123 led to the greatest Th1 and Th17 activation compared to the individual subdomains, thus our data supports the use of ClfA N123 as an antigen in anti-*S. aureus* vaccines. This is critical information for the field as ClfA is included as an antigen in two multivalent vaccines currently in development [280, 281, 284].

Overall these studies support the need for a systematic screen of all CWA proteins of *S. aureus* for their T cell activating ability and in particular this study has highlighted that T cell epitopes may be located within specific domains of a protein. As the

healthy population possess circulating *S. aureus*-specific T cells [272], the use of healthy human blood to screen for potential antigens is an approach that could be utilised in advance of clinical trials to identify T cell activating capacity. Approaches like this are promising when antigens have already been selected, however, high-throughput T cell assays are costly and time-consuming. Thus, *in silico* methods of epitope discovery present a potential alternative. T cell epitope prediction offers the ability to identify candidate cell epitopes that are predicted to bind to MHCs. Algorithms have been developed to test the potential capacity of a given peptide to bind to a predetermined MHC allele [302]. Numerous studies have predicted CD4⁺ T cell epitopes through *in silico* T cell epitope mapping and used these as candidate vaccine epitopes against a range of microorganisms, including *Chlamydia* [303], HIV [304, 305], *Plasmodium vivax* [306] and *Schistosoma mansoni* [307]. T cell epitope mapping is a valuable tool which has thus far been underutilised in *S. aureus* vaccine development and there is a paucity of information regarding this technique, with the exception of one computational study which predicted fibronectin binding protein A (FnbpA), seine-rich adhesin for platelets (SraP), collagen adhesion (Cna) and elastin binding proteins (EbpS) as containing suitable T cell epitopes [308], however no follow up *in vitro* or *in vivo* characterisation was carried out to support these findings. Importantly, this study predicted CWA proteins (FnbpA and Cna) as potential T cell antigens, which supports the data presented in this thesis. This study also predicted ClfA and ClfB to contain B cell epitopes, which correlates with findings in this thesis, as both of these proteins induced antibody production when used as vaccine antigens.

As previously mentioned, it is likely that a universal anti-*S. aureus* vaccine will never be realised, and therefore a vaccine against *S. aureus* SSTI would be of great benefit. In order to develop new therapies against *S. aureus* SSTIs, a greater understanding of the virulence factors involved in skin infection is needed, as until

now there has been a paucity of information regarding their roles. This thesis aimed to elucidate the role of CWA proteins during SSTIs and specifically investigate their contribution to abscess formation. The clinically relevant CA-MRSA USA300 strain, LAC::*lux*, was used to create isogenic null mutations to investigate the contribution of CWA proteins to SSTIs. The USA300 lineage is responsible for most CA-MRSA SSTIs [17], making it a very relevant strain to examine in a skin infection model.

This study confirms that CWA proteins are required for virulence during SSTIs, and in particular, has identified ClfA, ClfB and SpA as important factors in determining the formation and structure of the skin abscess, which in turn impacts upon bacterial burden. The most striking finding from this study however, is the role of ClfB during SSTIs. Previous to this study, ClfB's main role has been attributed to *S. aureus* nasal colonisation where it binds to host ligands loricrin and cytokeratin 10 in the anterior nares to facilitate colonisation [50, 112, 113]. Its contribution to skin infection had never previously been demonstrated. This study now identifies ClfB as a novel CWA protein involved in the pathogenesis of SSTIs. ClfB is involved in determining the formation and structure of the abscess and as a result bacterial burden. In contrast to other CWA, ClfB appears to exert its effect early during the infection process. The interaction between ClfB and loricrin within the skin appears to be important for virulence during SSTIs, as when this interaction is blocked *in vivo*, there is a reduction in the severity of the skin infection, however further work is needed to fully characterise this interaction occurring in the skin.

Having identified an important role for ClfB during skin infection, the ability of ClfB to induce protective immune responses against SSTIs was investigated. Vaccination with ClfB has previously been shown to reduce murine nasal colonisation [112], and vaccination with ClfB in combination with Freund's adjuvant reduced bacterial burden in the kidneys of i.v. infected mice [298]. However, vaccination with ClfB has never previously been investigated against skin infection. In fact, only a handful of studies

have previously attempted to vaccinate against *S. aureus* skin infection. These have included vaccination with ClfA [277], Als3p [226] and adenosine synthase A [309] in combination with alum and SasX combined with Freund's adjuvant [310]. The ability of a vaccine containing ClfB to protect against *S. aureus* SSTI was investigated in this study. ClfB induced antigen-specific Th1 and Th17 activation in human T cells (Chapter 4), and induced IL-17 and IFN γ responses in mice following vaccination when adjuvanted with CpG or alum (Chapter 5). ClfB-specific antibodies were also induced with these vaccine formulations, proving that ClfB can activate the humoral and cellular arms of the immune system. This immune activation resulted in reduced pathology during subsequent *S. aureus* skin infection. Thus, this study identified ClfB as novel virulence determinant during SSTIs which has the ability to offer protection against SSTIs when used as a vaccine antigen. In addition, this study also demonstrated the potential for ClfA to be used in a SSTI vaccine. Vaccination with ClfA combined with alum and sigma adjuvant system (SAS) has previously failed to offer protection against *S. aureus* skin infection [277]. However, only a single time point (day 2 post-infection) was investigated and the study used C57 mice [277], as opposed to BALB/c mice used in this study, which may account for the discrepancies. A vaccine combining ClfA and ClfB may be an ideal vaccine against *S. aureus* SSTIs and this should be investigated in the future. A successful anti-*S. aureus* vaccine will likely comprise multiple antigens, which enable the induction of humoral immunity and specific T cell responses, which would act in concert to protect against a broad array of staphylococcal strains.

Future work is needed to further understand the skin immune response to *S. aureus* infection, which may uncover new strategies of vaccination. In a previous study, *S. aureus* SSTIs in BALB/c mice elicited protective immunity against subsequent *S. aureus* SSTIs, and this protection was mediated by antibody and IL-17 responses [311]. This suggests that a skin specific immune response may be resulting in

protection against subsequent infection. It would be interesting to investigate whether a systemic challenge would also result in subsequent protection against *S. aureus* SSTIs. It has been previously demonstrated that T cells can accumulate and persist in skin following herpes simplex virus (HSV) infection [312, 313], and cutaneous T cell lymphoma [314] where they can provide enhanced immunity compared to their circulating counterparts, suggesting a skin specific immune response. After an infection, pathogen-specific tissue resident memory T (Trm) cells persist in non-lymphoid tissue to provide a first line of defence against infection at mucocutaneous surfaces [315]. A recent study has identified CD4⁺ Trm cell accumulation in the lungs during *B. pertussis* infection, and these CD4⁺ Trm cells mediated rapid protection against subsequent infection [316]. Thus, vaccination strategies that create Trm cell pools at sites of pathogen entry may represent attractive options for future anti-*S. aureus* vaccines. A simian immunodeficiency virus (SIV) vaccine induced high-frequency SIV-specific CD8⁺ Trm cells in rhesus macaques resulting in control of intrarectal infection from highly pathogenic SIV [317]. Similarly, vaccination with an attenuated strain of HSV generated CD4⁺ Trm cells leading to enhanced protection from subsequent intravaginal HSV infection [318]. A newly developed malaria vaccine, PfSPZ, had promising efficacy in human clinical trials, however protected patients exhibited low levels of T cells and vaccine-specific antibodies within blood [319]. Further studies found the frequency of Trm cells within the liver (the relevant site for T cell-mediated protection against malaria) to be 100-fold higher [319]. Taken together, these studies provide evidence that Trm cells are capable of providing robust and rapid immune protection at critical barrier sites. There is currently no information on the existence of Trm cells during *S. aureus* infection, however, due to their presence during other viral and bacterial infections, it is likely these cells exist after *S. aureus* SSTIs and targeting these cells may lead to greater vaccine efficacy.

In summary, this thesis significantly advances the understanding of the role of CWA proteins during *S. aureus* SSTIs. ClfB, ClfA and SpA were identified as specific factors involved in determining the structure and formation of the abscess, which in turn impacts upon the bacterial burden (Figure 6.1 A). It is likely that other CWA proteins, not examined in this study, may be involved in these processes too. This work has also identified CWA proteins as a promising pool of T cell antigens, capable of inducing antigen-specific Th1 and Th17 cell responses both in mice and in humans (Figure 6.1 B). Using this information, model vaccines comprising of ClfB or ClfA were found to induce both cellular and humoral immune responses in mice. This vaccine-induced cellular response is likely to comprise of CD4⁺ and $\gamma\delta$ ⁺ T cells (Figure 6.1 C). Vaccine induced CD8⁺ T cells may also aid in the clearance of intracellularly infected cells, eliminating a survival niche exploited by staphylococci [146, 195, 197, 198], although this remains to be investigated. The induction of T cells leads to production of cytokines such as IFN γ , IL-17 and IL-22, which can promote phagocyte activation and recruitment to the site of infection, leading to clearance of the bacteria. ClfB and ClfA-specific humoral responses are likely inhibiting the function of ClfB and ClfA and also contributing to opsonification. Ultimately, vaccination with these CWA proteins leads to protection against *S. aureus* SSTIs.

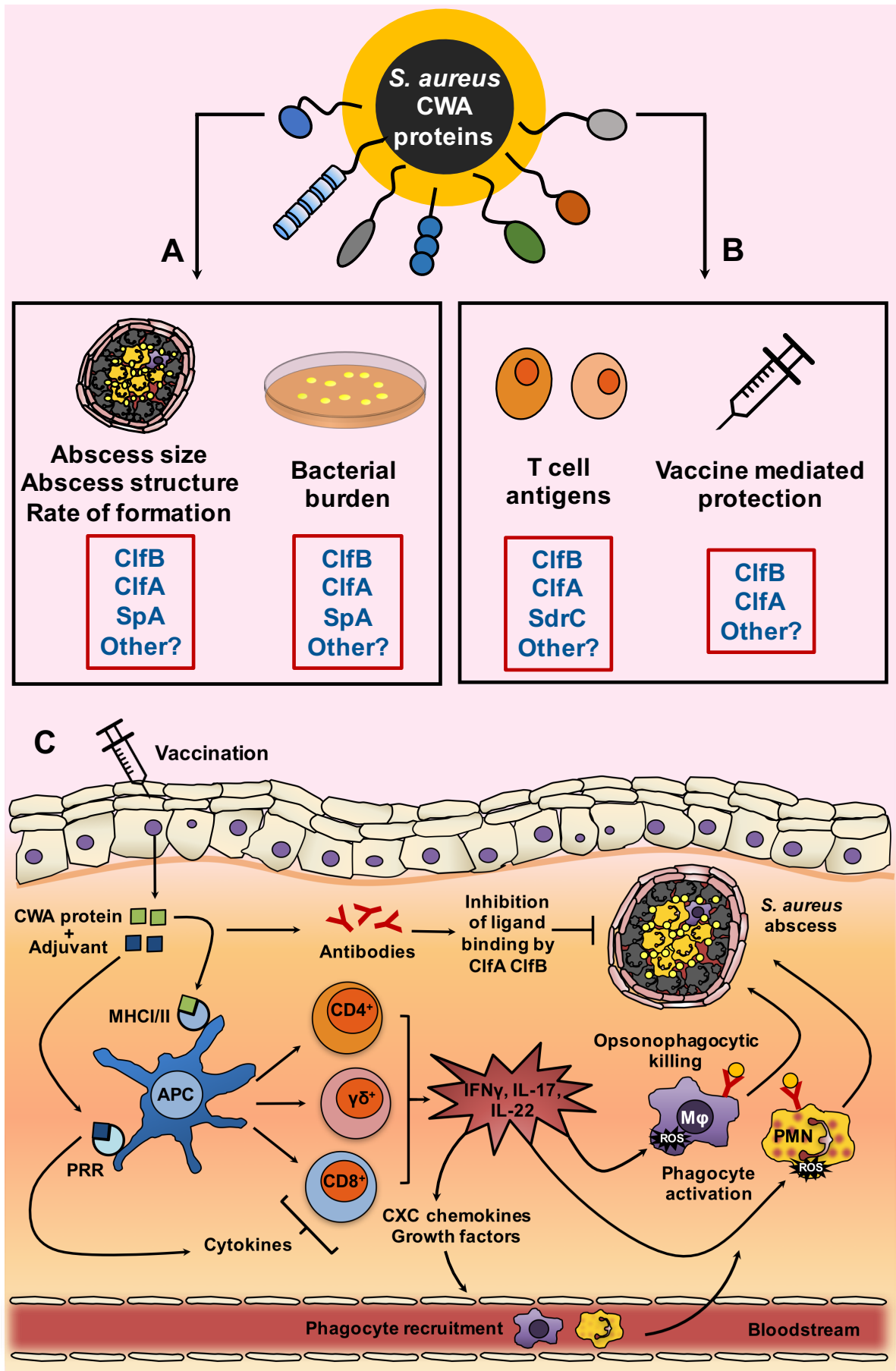


Figure 6.1. *S. aureus* cell wall-anchored (CWA) proteins are prime vaccine candidates for anti-*S. aureus* SSTI vaccines. *S. aureus* CWA proteins determine the structure and formation of the skin abscess, which in turn impacts upon the bacterial burden during SSTIs (A). CWA proteins are capable of activating T cells and inducing protective immunity when used as vaccine antigens (B). Red boxes contain specific factors involved in these processes. Vaccination with CWA proteins in combination with an adjuvant leads to cellular and humoral immune responses (C). Induction of cellular immunity can allow for the generation of CD4⁺, CD8⁺ and $\gamma\delta^+$ T cells, specific for the selected staphylococcal antigens. Upon infection, vaccine induced T cells produce effector cytokines (such as IFN γ , IL-17 and IL-22), the downstream effects of which promote phagocyte activation and recruitment to the infection site. Antigen-specific antibody responses, can neutralise virulence factors and in the presence of activated phagocytes mediate opsonophagocytic killing of the invading staphylococci. Therefore, induction of both arms of immunity leads to efficient clearance of invading staphylococci.

Chapter 7

References

1. Lowy, F.D., *Staphylococcus aureus* infections. N Engl J Med, 1998. **339**(8): p. 520-32.
2. Boucher, H.W. and G.R. Corey, *Epidemiology of methicillin-resistant Staphylococcus aureus*. Clin Infect Dis, 2008. **46 Suppl 5**: p. S344-9.
3. Klevens, R.M., et al., *Invasive methicillin-resistant Staphylococcus aureus infections in the United States*. JAMA, 2007. **298**(15): p. 1763-71.
4. Voyich, J.M., et al., *Insights into mechanisms used by Staphylococcus aureus to avoid destruction by human neutrophils*. J Immunol, 2005. **175**(6): p. 3907-19.
5. Voyich, J.M., et al., *Is Panton-Valentine leukocidin the major virulence determinant in community-associated methicillin-resistant Staphylococcus aureus disease?* J Infect Dis, 2006. **194**(12): p. 1761-70.
6. Aiello, A.E., et al., *Meticillin-resistant Staphylococcus aureus among US prisoners and military personnel: review and recommendations for future studies*. Lancet Infect Dis, 2006. **6**(6): p. 335-41.
7. DeLeo, F.R., et al., *Community-associated methicillin-resistant Staphylococcus aureus*. Lancet, 2010. **375**(9725): p. 1557-68.
8. Kock, R., et al., *Methicillin-resistant Staphylococcus aureus (MRSA): burden of disease and control challenges in Europe*. Euro Surveill, 2010. **15**(41): p. 19688.
9. Ki, V. and C. Rotstein, *Bacterial skin and soft tissue infections in adults: A review of their epidemiology, pathogenesis, diagnosis, treatment and site of care*. Can J Infect Dis Med Microbiol, 2008. **19**(2): p. 173-84.
10. Barr, B., M. Felkner, and P.M. Diamond, *High school athletic departments as sentinel surveillance sites for community-associated methicillin-resistant staphylococcal infections*. Tex Med, 2006. **102**(4): p. 56-61.
11. Campbell, K.M., et al., *Risk factors for community-associated methicillin-resistant Staphylococcus aureus infections in an outbreak of disease among military trainees in San Diego, California, in 2002*. J Clin Microbiol, 2004. **42**(9): p. 4050-3.
12. Ellis, M.W., et al., *Presence and molecular epidemiology of virulence factors in methicillin-resistant Staphylococcus aureus strains colonizing and infecting soldiers*. J Clin Microbiol, 2009. **47**(4): p. 940-5.
13. Kazakova, S.V., et al., *A clone of methicillin-resistant Staphylococcus aureus among professional football players*. N Engl J Med, 2005. **352**(5): p. 468-75.
14. Hersh, A.L., et al., *National trends in ambulatory visits and antibiotic prescribing for skin and soft-tissue infections*. Arch Intern Med, 2008. **168**(14): p. 1585-91.
15. Bassetti, M., et al., *European perspective and update on the management of complicated skin and soft tissue infections due to methicillin-resistant Staphylococcus aureus after more than 10 years of experience with linezolid*. Clin Microbiol Infect, 2014. **20 Suppl 4**: p. 3-18.
16. Otto, M., *Basis of virulence in community-associated methicillin-resistant Staphylococcus aureus*. Annu Rev Microbiol, 2010. **64**: p. 143-62.
17. Moran, G.J., et al., *Methicillin-resistant S. aureus infections among patients in the emergency department*. N Engl J Med, 2006. **355**(7): p. 666-74.
18. Bae, I.G., et al., *Presence of genes encoding the panton-valentine leukocidin exotoxin is not the primary determinant of outcome in patients with complicated skin and skin structure infections due to methicillin-resistant Staphylococcus aureus: results of a multinational trial*. J Clin Microbiol, 2009. **47**(12): p. 3952-7.
19. Kobayashi, S.D., N. Malachowa, and F.R. DeLeo, *Pathogenesis of Staphylococcus aureus abscesses*. Am J Pathol, 2015. **185**(6): p. 1518-27.
20. Men, S., O. Akhan, and M. Koroglu, *Percutaneous drainage of abdominal abscess*. Eur J Radiol, 2002. **43**(3): p. 204-18.

21. Lacey, K.A., J.A. Geoghegan, and R.M. McLoughlin, *The Role of Staphylococcus aureus Virulence Factors in Skin Infection and Their Potential as Vaccine Antigens*. Pathogens, 2016. **5**(1).
22. Spaan, A.N., et al., *The staphylococcal toxin Panton-Valentine Leukocidin targets human C5a receptors*. Cell Host Microbe, 2013. **13**(5): p. 584-94.
23. Spaan, A.N., J.A.G. van Strijp, and V.J. Torres, *Leukocidins: staphylococcal bi-component pore-forming toxins find their receptors*. Nat Rev Microbiol, 2017. **15**(7): p. 435-447.
24. Malachowa, N., et al., *Staphylococcus aureus leukotoxin GH promotes inflammation*. J Infect Dis, 2012. **206**(8): p. 1185-93.
25. Morinaga, N., Y. Kaihou, and M. Noda, *Purification, cloning and characterization of variant LukE-LukD with strong leukocidal activity of staphylococcal bi-component leukotoxin family*. Microbiol Immunol, 2003. **47**(1): p. 81-90.
26. Kobayashi, S.D., et al., *Comparative analysis of USA300 virulence determinants in a rabbit model of skin and soft tissue infection*. J Infect Dis, 2011. **204**(6): p. 937-41.
27. Lipinska, U., et al., *Panton-Valentine leukocidin does play a role in the early stage of Staphylococcus aureus skin infections: a rabbit model*. PLoS One, 2011. **6**(8): p. e22864.
28. Malachowa, N., et al., *Insights into the Staphylococcus aureus-Host Interface: Global Changes in Host and Pathogen Gene Expression in a Rabbit Skin Infection Model*. PLoS One, 2015. **10**(2): p. e0117713.
29. Ezepchuk, Y.V., et al., *Staphylococcal toxins and protein A differentially induce cytotoxicity and release of tumor necrosis factor-alpha from human keratinocytes*. J Invest Dermatol, 1996. **107**(4): p. 603-9.
30. Hocke, A.C., et al., *Perturbation of endothelial junction proteins by Staphylococcus aureus alpha-toxin: inhibition of endothelial gap formation by adrenomedullin*. Histochem Cell Biol, 2006. **126**(3): p. 305-16.
31. Thelestam, M., R. Mollby, and T. Wadstrom, *Effects of staphylococcal alpha-, beta-, delta-, and gamma-hemolysins on human diploid fibroblasts and HeLa cells: evaluation of a new quantitative assay for measuring cell damage*. Infect Immun, 1973. **8**(6): p. 938-46.
32. Walev, I., et al., *Staphylococcal alpha-toxin kills human keratinocytes by permeabilizing the plasma membrane for monovalent ions*. Infect Immun, 1993. **61**(12): p. 4972-9.
33. Wilke, G.A. and J. Bubeck-Wardenburg, *Role of a disintegrin and metalloprotease 10 in Staphylococcus aureus alpha-hemolysin-mediated cellular injury*. Proc Natl Acad Sci U S A, 2010. **107**(30): p. 13473-8.
34. Ebsen, H., et al., *Differential Surface Expression of ADAM10 and ADAM17 on Human T Lymphocytes and Tumor Cells*. PLoS ONE, 2013. **8**(10): p. e76853.
35. Kennedy, A.D., et al., *Targeting of alpha-hemolysin by active or passive immunization decreases severity of USA300 skin infection in a mouse model*. J Infect Dis, 2010. **202**(7): p. 1050-8.
36. Chua, K.Y., et al., *Hyperexpression of alpha-hemolysin explains enhanced virulence of sequence type 93 community-associated methicillin-resistant Staphylococcus aureus*. BMC Microbiol, 2014. **14**: p. 31.
37. Tkaczyk, C., et al., *Identification of anti-alpha toxin monoclonal antibodies that reduce the severity of Staphylococcus aureus dermonecrosis and exhibit a correlation between affinity and potency*. Clin Vaccine Immunol, 2012. **19**(3): p. 377-85.
38. Otto, M., *Staphylococcus aureus toxins*. Current Opinion in Microbiology, 2014. **17**(0): p. 32-37.

39. Surewaard, B.G., et al., *Staphylococcal alpha-phenol soluble modulins contribute to neutrophil lysis after phagocytosis*. Cell Microbiol, 2013. **15**(8): p. 1427-37.
40. Geiger, T., et al., *The stringent response of Staphylococcus aureus and its impact on survival after phagocytosis through the induction of intracellular PSMs expression*. PLoS Pathog, 2012. **8**(11): p. e1003016.
41. Wang, R., et al., *Identification of novel cytolytic peptides as key virulence determinants for community-associated MRSA*. Nat Med, 2007. **13**(12): p. 1510-4.
42. Hendrickx, A.P., et al., *Architects at the bacterial surface - sortases and the assembly of pili with isopeptide bonds*. Nat Rev Microbiol, 2011. **9**(3): p. 166-76.
43. Mazmanian, S.K., et al., *Staphylococcus aureus sortase mutants defective in the display of surface proteins and in the pathogenesis of animal infections*. Proc Natl Acad Sci U S A, 2000. **97**(10): p. 5510-5.
44. Cheng, A.G., et al., *Genetic requirements for Staphylococcus aureus abscess formation and persistence in host tissues*. Faseb j, 2009. **23**(10): p. 3393-404.
45. Kwiecinski, J., T. Jin, and E. Josefsson, *Surface proteins of Staphylococcus aureus play an important role in experimental skin infection*. Apmis, 2014.
46. Deivanayagam, C.C., et al., *A novel variant of the immunoglobulin fold in surface adhesins of Staphylococcus aureus: crystal structure of the fibrinogen-binding MSCRAMM, clumping factor A*. Embo j, 2002. **21**(24): p. 6660-72.
47. Ganesh, V.K., et al., *A structural model of the Staphylococcus aureus ClfA-fibrinogen interaction opens new avenues for the design of anti-staphylococcal therapeutics*. PLoS Pathog, 2008. **4**(11): p. e1000226.
48. Hair, P.S., et al., *Staphylococcus aureus clumping factor A binds to complement regulator factor I and increases factor I cleavage of C3b*. J Infect Dis, 2008. **198**(1): p. 125-33.
49. Hair, P.S., et al., *Clumping factor A interaction with complement factor I increases C3b cleavage on the bacterial surface of Staphylococcus aureus and decreases complement-mediated phagocytosis*. Infect Immun, 2010. **78**(4): p. 1717-27.
50. Mulcahy, M.E., et al., *Nasal colonisation by Staphylococcus aureus depends upon clumping factor B binding to the squamous epithelial cell envelope protein loricrin*. PLoS Pathog, 2012. **8**(12): p. e1003092.
51. Ganesh, V.K., et al., *Structural and biochemical characterization of Staphylococcus aureus clumping factor B/ligand interactions*. J Biol Chem, 2011. **286**(29): p. 25963-72.
52. Walsh, E.J., et al., *Clumping factor B, a fibrinogen-binding MSCRAMM (microbial surface components recognizing adhesive matrix molecules) adhesin of Staphylococcus aureus, also binds to the tail region of type I cytokeratin 10*. J Biol Chem, 2004. **279**(49): p. 50691-9.
53. Xiang, H., et al., *Crystal structures reveal the multi-ligand binding mechanism of Staphylococcus aureus ClfB*. PLoS Pathog, 2012. **8**(6): p. e1002751.
54. Abraham, N.M. and K.K. Jefferson, *Staphylococcus aureus clumping factor B mediates biofilm formation in the absence of calcium*. Microbiology, 2012. **158**(Pt 6): p. 1504-12.
55. Barbu, E.M., et al., *SdrC induces staphylococcal biofilm formation through a homophilic interaction*. Mol Microbiol, 2014. **94**(1): p. 172-85.
56. Barbu, E.M., et al., *beta-Neurexin is a ligand for the Staphylococcus aureus MSCRAMM SdrC*. PLoS Pathog, 2010. **6**(1): p. e1000726.
57. Corrigan, R.M., H. Miajlovic, and T.J. Foster, *Surface proteins that promote adherence of Staphylococcus aureus to human desquamated nasal epithelial cells*. BMC Microbiol, 2009. **9**: p. 22.

58. Sharp, J.A., et al., *Staphylococcus aureus* surface protein SdrE binds complement regulator factor H as an immune evasion tactic. *PLoS One*, 2012. **7**(5): p. e38407.
59. Vazquez, V., et al., *Fibrinogen is a ligand for the Staphylococcus aureus microbial surface components recognizing adhesive matrix molecules (MSCRAMM) bone sialoprotein-binding protein (Bbp)*. *J Biol Chem*, 2011. **286**(34): p. 29797-805.
60. Keane, F.M., et al., *Fibrinogen and elastin bind to the same region within the A domain of fibronectin binding protein A, an MSCRAMM of Staphylococcus aureus*. *Mol Microbiol*, 2007. **63**(3): p. 711-23.
61. Sinha, B., et al., *Heterologously expressed Staphylococcus aureus fibronectin-binding proteins are sufficient for invasion of host cells*. *Infect Immun*, 2000. **68**(12): p. 6871-8.
62. Peacock, S.J., et al., *Bacterial fibronectin-binding proteins and endothelial cell surface fibronectin mediate adherence of Staphylococcus aureus to resting human endothelial cells*. *Microbiology*, 1999. **145 (Pt 12)**: p. 3477-86.
63. Burke, F.M., et al., *The A domain of fibronectin-binding protein B of Staphylococcus aureus contains a novel fibronectin binding site*. *FEBS J*, 2011. **278**(13): p. 2359-71.
64. Zong, Y., et al., *A 'Collagen Hug' model for Staphylococcus aureus CNA binding to collagen*. *EMBO J*, 2005. **24**(24): p. 4224-36.
65. Kang, M., et al., *Collagen-binding microbial surface components recognizing adhesive matrix molecule (MSCRAMM) of Gram-positive bacteria inhibit complement activation via the classical pathway*. *J Biol Chem*, 2013. **288**(28): p. 20520-31.
66. Clarke, S.R., et al., *Identification of in vivo-expressed antigens of Staphylococcus aureus and their use in vaccinations for protection against nasal carriage*. *J Infect Dis*, 2006. **193**(8): p. 1098-108.
67. Clarke, S.R., et al., *Iron-regulated surface determinant protein A mediates adherence of Staphylococcus aureus to human corneocyte envelope proteins*. *Infect Immun*, 2009. **77**(6): p. 2408-16.
68. Clarke, S.R. and S.J. Foster, *IsdA protects Staphylococcus aureus against the bactericidal protease activity of apolactoferrin*. *Infect Immun*, 2008. **76**(4): p. 1518-26.
69. Clarke, S.R., et al., *The Staphylococcus aureus surface protein IsdA mediates resistance to innate defenses of human skin*. *Cell Host Microbe*, 2007. **1**(3): p. 199-212.
70. Pilpa, R.M., et al., *Functionally distinct NEAT (NEAr Transporter) domains within the Staphylococcus aureus IsdH/HarA protein extract heme from methemoglobin*. *J Biol Chem*, 2009. **284**(2): p. 1166-76.
71. Grigg, J.C., et al., *Structural biology of heme binding in the Staphylococcus aureus Isd system*. *J Inorg Biochem*, 2010. **104**(3): p. 341-8.
72. Zapotoczna, M., et al., *Iron-regulated surface determinant B (IsdB) promotes Staphylococcus aureus adherence to and internalization by non-phagocytic human cells*. *Cell Microbiol*, 2013. **15**(6): p. 1026-41.
73. Visai, L., et al., *Immune evasion by Staphylococcus aureus conferred by iron-regulated surface determinant protein IsdH*. *Microbiology*, 2009. **155**(Pt 3): p. 667-79.
74. Deisenhofer, J., *Crystallographic refinement and atomic models of a human Fc fragment and its complex with fragment B of protein A from Staphylococcus aureus at 2.9- and 2.8-Å resolution*. *Biochemistry*, 1981. **20**(9): p. 2361-70.
75. Cedergren, L., et al., *Mutational analysis of the interaction between staphylococcal protein A and human IgG1*. *Protein Eng*, 1993. **6**(4): p. 441-8.

76. Silverman, G.J. and C.S. Goodyear, *Confounding B-cell defences: lessons from a staphylococcal superantigen*. Nat Rev Immunol, 2006. **6**(6): p. 465-75.
77. Gomez, M.I., et al., *Staphylococcus aureus protein A induces airway epithelial inflammatory responses by activating TNFR1*. Nat Med, 2004. **10**(8): p. 842-8.
78. Graille, M., et al., *Crystal structure of a Staphylococcus aureus protein A domain complexed with the Fab fragment of a human IgM antibody: structural basis for recognition of B-cell receptors and superantigen activity*. Proc Natl Acad Sci U S A, 2000. **97**(10): p. 5399-404.
79. O'Seaghdha, M., et al., *Staphylococcus aureus protein A binding to von Willebrand factor A1 domain is mediated by conserved IgG binding regions*. Febs j, 2006. **273**(21): p. 4831-41.
80. Martin, F.J., et al., *Staphylococcus aureus activates type I IFN signaling in mice and humans through the Xr repeated sequences of protein A*. J Clin Invest, 2009. **119**(7): p. 1931-9.
81. Roche, F.M., M. Meehan, and T.J. Foster, *The Staphylococcus aureus surface protein SasG and its homologues promote bacterial adherence to human desquamated nasal epithelial cells*. Microbiology, 2003. **149**(Pt 10): p. 2759-67.
82. Geoghegan, J.A., et al., *Role of surface protein SasG in biofilm formation by Staphylococcus aureus*. J Bacteriol, 2010. **192**(21): p. 5663-73.
83. Kukita, K., et al., *Staphylococcus aureus SasA is responsible for binding to the salivary agglutinin gp340, derived from human saliva*. Infect Immun, 2013. **81**(6): p. 1870-9.
84. Siboo, I.R., H.F. Chambers, and P.M. Sullam, *Role of SraP, a Serine-Rich Surface Protein of Staphylococcus aureus, in binding to human platelets*. Infect Immun, 2005. **73**(4): p. 2273-80.
85. Yang, Y.H., et al., *Structural insights into SraP-mediated Staphylococcus aureus adhesion to host cells*. PLoS Pathog, 2014. **10**(6): p. e1004169.
86. Thammavongsa, V., O. Schneewind, and D.M. Missiakas, *Enzymatic properties of Staphylococcus aureus adenosine synthase (AdsA)*. BMC Biochem, 2011. **12**: p. 56.
87. Thammavongsa, V., et al., *Staphylococcus aureus synthesizes adenosine to escape host immune responses*. J Exp Med, 2009. **206**(11): p. 2417-27.
88. Thammavongsa, V., D.M. Missiakas, and O. Schneewind, *Staphylococcus aureus degrades neutrophil extracellular traps to promote immune cell death*. Science, 2013. **342**(6160): p. 863-6.
89. Li, M., et al., *MRSA epidemic linked to a quickly spreading colonization and virulence determinant*. Nat Med, 2012. **18**(5): p. 816-9.
90. Schroeder, K., et al., *Molecular characterization of a novel Staphylococcus aureus surface protein (SasC) involved in cell aggregation and biofilm accumulation*. PLoS One, 2009. **4**(10): p. e7567.
91. Roche, F.M., et al., *Characterization of novel LPXTG-containing proteins of Staphylococcus aureus identified from genome sequences*. Microbiology, 2003. **149**(Pt 3): p. 643-54.
92. Valle, J., et al., *Bap, a biofilm matrix protein of Staphylococcus aureus prevents cellular internalization through binding to GP96 host receptor*. PLoS Pathog, 2012. **8**(8): p. e1002843.
93. Cucarella, C., et al., *Bap, a Staphylococcus aureus surface protein involved in biofilm formation*. J Bacteriol, 2001. **183**(9): p. 2888-96.
94. McDevitt, D., et al., *Characterization of the interaction between the Staphylococcus aureus clumping factor (ClfA) and fibrinogen*. Eur J Biochem, 1997. **247**(1): p. 416-24.
95. Foster, T.J., et al., *Adhesion, invasion and evasion: the many functions of the surface proteins of Staphylococcus aureus*. Nat Rev Microbiol, 2014. **12**(1): p. 49-62.

96. O'Connell, D.P., et al., *The fibrinogen-binding MSCRAMM (clumping factor) of Staphylococcus aureus has a Ca²⁺-dependent inhibitory site*. J Biol Chem, 1998. **273**(12): p. 6821-9.
97. McCormack, N., T.J. Foster, and J.A. Geoghegan, *A short sequence within subdomain N1 of region A of the Staphylococcus aureus MSCRAMM clumping factor A is required for export and surface display*. Microbiology, 2014. **160**(Pt 4): p. 659-70.
98. Farrell, D.H., et al., *Role of fibrinogen alpha and gamma chain sites in platelet aggregation*. Proceedings of the National Academy of Sciences of the United States of America, 1992. **89**(22): p. 10729-10732.
99. Hettasch, J.M., M.G. Bolyard, and S.T. Lord, *The residues AGDV of recombinant gamma chains of human fibrinogen must be carboxy-terminal to support human platelet aggregation*. Thromb Haemost, 1992. **68**(6): p. 701-6.
100. Loughman, A., et al., *Roles for fibrinogen, immunoglobulin and complement in platelet activation promoted by Staphylococcus aureus clumping factor A*. Mol Microbiol, 2005. **57**(3): p. 804-18.
101. Josefsson, E., et al., *Protection against experimental Staphylococcus aureus arthritis by vaccination with clumping factor A, a novel virulence determinant*. J Infect Dis, 2001. **184**(12): p. 1572-80.
102. McAdow, M., et al., *Preventing Staphylococcus aureus sepsis through the inhibition of its agglutination in blood*. PLoS Pathog, 2011. **7**(10): p. e1002307.
103. Moreillon, P., et al., *Role of Staphylococcus aureus coagulase and clumping factor in pathogenesis of experimental endocarditis*. Infect Immun, 1995. **63**(12): p. 4738-43.
104. Flick, M.J., et al., *Genetic elimination of the binding motif on fibrinogen for the S. aureus virulence factor ClfA improves host survival in septicemia*. Blood, 2013. **121**(10): p. 1783-94.
105. Malachowa, N., et al., *Contribution of Staphylococcus aureus Coagulases and Clumping Factor A to Abscess Formation in a Rabbit Model of Skin and Soft Tissue Infection*. PLoS One, 2016. **11**(6): p. e0158293.
106. Ni Eidhin, D., et al., *Clumping factor B (ClfB), a new surface-located fibrinogen-binding adhesin of Staphylococcus aureus*. Mol Microbiol, 1998. **30**(2): p. 245-57.
107. Perkins, S., et al., *Structural organization of the fibrinogen-binding region of the clumping factor B MSCRAMM of Staphylococcus aureus*. J Biol Chem, 2001. **276**(48): p. 44721-8.
108. McAleese, F.M., et al., *Loss of clumping factor B fibrinogen binding activity by Staphylococcus aureus involves cessation of transcription, shedding and cleavage by metalloprotease*. J Biol Chem, 2001. **276**(32): p. 29969-78.
109. Walsh, E.J., et al., *Identification of the Staphylococcus aureus MSCRAMM clumping factor B (ClfB) binding site in the alphaC-domain of human fibrinogen*. Microbiology, 2008. **154**(Pt 2): p. 550-8.
110. Entenza, J.M., et al., *Contribution of clumping factor B to pathogenesis of experimental endocarditis due to Staphylococcus aureus*. Infect Immun, 2000. **68**(9): p. 5443-6.
111. Rindi, S., et al., *Antibody response in patients with endocarditis caused by Staphylococcus aureus*. Eur J Clin Invest, 2006. **36**(8): p. 536-43.
112. Schaffer, A.C., et al., *Immunization with Staphylococcus aureus clumping factor B, a major determinant in nasal carriage, reduces nasal colonization in a murine model*. Infect Immun, 2006. **74**(4): p. 2145-53.
113. Wertheim, H.F., et al., *Key role for clumping factor B in Staphylococcus aureus nasal colonization of humans*. PLoS Med, 2008. **5**(1): p. e17.

114. Steven, A.C. and P.M. Steinert, *Protein composition of cornified cell envelopes of epidermal keratinocytes*. J Cell Sci, 1994. **107 (Pt 2)**: p. 693-700.
115. Forsgren, A. and K. Nordstrom, *Protein A from Staphylococcus aureus: the biological significance of its reaction with IgG*. Ann N Y Acad Sci, 1974. **236(0)**: p. 252-66.
116. Oeding, P., A. Grov, and B. Myklestad, *IMMUNOCHEMICAL STUDIES ON ANTIGEN PREPARATIONS FROM STAPHYLOCOCCUS AUREUS. 2. PRECIPITATING AND ERYTHROCYTE-SENSITIZING PROPERTIES OF PROTEIN A (ANTIGEN A) AND RELATED SUBSTANCES*. Acta Pathol Microbiol Scand, 1964. **62**: p. 117-27.
117. Hillson, J.L., et al., *The structural basis of germline-encoded VH3 immunoglobulin binding to staphylococcal protein A*. J Exp Med, 1993. **178(1)**: p. 331-6.
118. Hartleib, J., et al., *Protein A is the von Willebrand factor binding protein on Staphylococcus aureus*. Blood, 2000. **96(6)**: p. 2149-56.
119. Moks, T., et al., *Staphylococcal protein A consists of five IgG-binding domains*. Eur J Biochem, 1986. **156(3)**: p. 637-43.
120. Foster, T.J., *Immune evasion by staphylococci*. Nat Rev Microbiol, 2005. **3(12)**: p. 948-58.
121. Lindmark, R., K. Thoren-Tolling, and J. Sjoquist, *Binding of immunoglobulins to protein A and immunoglobulin levels in mammalian sera*. J Immunol Methods, 1983. **62(1)**: p. 1-13.
122. Goodyear, C.S. and G.J. Silverman, *Death by a B cell superantigen: In vivo VH-targeted apoptotic supraclonal B cell deletion by a Staphylococcal Toxin*. J Exp Med, 2003. **197(9)**: p. 1125-39.
123. Kim, H.K., et al., *Identifying protective antigens of Staphylococcus aureus, a pathogen that suppresses host immune responses*. Faseb j, 2011. **25(10)**: p. 3605-12.
124. Classen, A., et al., *TNF receptor I on human keratinocytes is a binding partner for staphylococcal protein A resulting in the activation of NF kappa B, AP-1, and downstream gene transcription*. Exp Dermatol, 2011. **20(1)**: p. 48-52.
125. Sutton, C.E., et al., *Interleukin-1 and IL-23 induce innate IL-17 production from gammadelta T cells, amplifying Th17 responses and autoimmunity*. Immunity, 2009. **31(2)**: p. 331-41.
126. Zeng, X., et al., *gammadelta T cells recognize a microbial encoded B cell antigen to initiate a rapid antigen-specific interleukin-17 response*. Immunity, 2012. **37(3)**: p. 524-34.
127. Martin, B., et al., *Interleukin-17-producing gammadelta T cells selectively expand in response to pathogen products and environmental signals*. Immunity, 2009. **31(2)**: p. 321-30.
128. Murphy, K., et al., *Janeway's immunobiology*. 2012, New York: Garland Science.
129. Murphy, A.G., *Characterization of T cell responses during S. aureus infection, in Biochemistry and Immunology*. 2014, Trinity College Dublin: Trinity College Dublin Library.
130. Hermos, C.R., P. Yoong, and G.B. Pier, *High levels of antibody to panton-valentine leukocidin are not associated with resistance to Staphylococcus aureus-associated skin and soft-tissue infection*. Clin Infect Dis, 2010. **51(10)**: p. 1138-46.
131. Verkaik, N.J., et al., *Anti-staphylococcal humoral immune response in persistent nasal carriers and noncarriers of Staphylococcus aureus*. J Infect Dis, 2009. **199(5)**: p. 625-32.

132. Mohamed, N., et al., *Inhibition of Staphylococcus aureus adherence to collagen under dynamic conditions*. Infect Immun, 1999. **67**(2): p. 589-94.
133. Verbrugh, H.A., et al., *Staphylococcus aureus opsonization mediated via the classical and alternative complement pathways. A kinetic study using MgEGTA chelated serum and human sera deficient in IgG and complement factors C1s and C2*. Immunology, 1979. **36**(3): p. 391-7.
134. Spellberg, B., et al., *The antifungal vaccine derived from the recombinant N terminus of Als3p protects mice against the bacterium Staphylococcus aureus*. Infect Immun, 2008. **76**(10): p. 4574-80.
135. Holtfreter, S., J. Kolata, and B.M. Broker, *Towards the immune proteome of Staphylococcus aureus - The anti-S. aureus antibody response*. Int J Med Microbiol, 2010. **300**(2-3): p. 176-92.
136. Yi, J., et al., *Serum capacity to neutralize superantigens does not affect the outcome of Staphylococcus aureus bacteremia*. Eur J Clin Microbiol Infect Dis, 2012.
137. David, M.Z., et al., *Predominance of methicillin-resistant Staphylococcus aureus among pathogens causing skin and soft tissue infections in a large urban jail: risk factors and recurrence rates*. J Clin Microbiol, 2008. **46**(10): p. 3222-7.
138. Huang, S.S. and R. Platt, *Risk of methicillin-resistant Staphylococcus aureus infection after previous infection or colonization*. Clin Infect Dis, 2003. **36**(3): p. 281-5.
139. Song, E., et al., *Chronic granulomatous disease: a review of the infectious and inflammatory complications*. Clin Mol Allergy, 2011. **9**(1): p. 10.
140. Anwar, S., et al., *The rise and rise of Staphylococcus aureus: laughing in the face of granulocytes*. Clin Exp Immunol, 2009. **157**(2): p. 216-24.
141. Robertson, C.M., et al., *Neutrophil depletion causes a fatal defect in murine pulmonary Staphylococcus aureus clearance*. J Surg Res, 2008. **150**(2): p. 278-85.
142. Soell, M., et al., *Capsular polysaccharide types 5 and 8 of Staphylococcus aureus bind specifically to human epithelial (KB) cells, endothelial cells, and monocytes and induce release of cytokines*. Infect Immun, 1995. **63**(4): p. 1380-6.
143. Standiford, T.J., et al., *Lipoteichoic acid induces secretion of interleukin-8 from human blood monocytes: a cellular and molecular analysis*. Infect Immun, 1994. **62**(1): p. 119-25.
144. Krakauer, T., *Interleukin-8 production by human monocytic cells in response to staphylococcal exotoxins is direct and independent of interleukin-1 and tumor necrosis factor-alpha*. J Infect Dis, 1998. **178**(2): p. 573-7.
145. Spaan, A.N., et al., *Neutrophils versus Staphylococcus aureus: a biological tug of war*. Annu Rev Microbiol, 2013. **67**: p. 629-50.
146. Gresham, H.D., et al., *Survival of Staphylococcus aureus inside neutrophils contributes to infection*. J Immunol, 2000. **164**(7): p. 3713-22.
147. McLoughlin, R.M., et al., *IFN-gamma regulated chemokine production determines the outcome of Staphylococcus aureus infection*. J Immunol, 2008. **181**(2): p. 1323-32.
148. Thwaites, G.E. and V. Gant, *Are bloodstream leukocytes Trojan Horses for the metastasis of Staphylococcus aureus?* Nat Rev Microbiol, 2011. **9**(3): p. 215-22.
149. Flannagan, R.S., B. Heit, and D.E. Heinrichs, *Antimicrobial Mechanisms of Macrophages and the Immune Evasion Strategies of Staphylococcus aureus*. Pathogens, 2015. **4**(4): p. 826-68.
150. Deshmane, S.L., et al., *Monocyte chemoattractant protein-1 (MCP-1): an overview*. J Interferon Cytokine Res, 2009. **29**(6): p. 313-26.

151. Shi, C. and E.G. Pamer, *Monocyte recruitment during infection and inflammation*. Nat Rev Immunol, 2011. **11**(11): p. 762-74.
152. Gordon, S., *Pattern recognition receptors: doubling up for the innate immune response*. Cell, 2002. **111**(7): p. 927-30.
153. van der Laan, L.J., et al., *Regulation and functional involvement of macrophage scavenger receptor MARCO in clearance of bacteria in vivo*. J Immunol, 1999. **162**(2): p. 939-47.
154. van Lookeren Campagne, M., C. Wiesmann, and E.J. Brown, *Macrophage complement receptors and pathogen clearance*. Cell Microbiol, 2007. **9**(9): p. 2095-102.
155. Verbrugh, H.A., et al., *Opsonization of encapsulated Staphylococcus aureus: the role of specific antibody and complement*. J Immunol, 1982. **129**(4): p. 1681-7.
156. Brown, A.F., et al., *Memory Th1 Cells Are Protective in Invasive Staphylococcus aureus Infection*. PLoS Pathog, 2015. **11**(11): p. e1005226.
157. Sakiniene, E., T. Bremell, and A. Tarkowski, *Inhibition of nitric oxide synthase (NOS) aggravates Staphylococcus aureus septicaemia and septic arthritis*. Clin Exp Immunol, 1997. **110**(3): p. 370-7.
158. Aaronson, D.S. and C.M. Horvath, *A road map for those who don't know JAK-STAT*. Science, 2002. **296**(5573): p. 1653-5.
159. Hsieh, C.S., et al., *Development of TH1 CD4+ T cells through IL-12 produced by Listeria-induced macrophages*. Science, 1993. **260**(5107): p. 547-9.
160. Stout, R.D. and K. Bottomly, *Antigen-specific activation of effector macrophages by IFN-gamma producing (TH1) T cell clones. Failure of IL-4-producing (TH2) T cell clones to activate effector function in macrophages*. J Immunol, 1989. **142**(3): p. 760-5.
161. Cassatella, M.A., et al., *Molecular basis of interferon-gamma and lipopolysaccharide enhancement of phagocyte respiratory burst capability. Studies on the gene expression of several NADPH oxidase components*. J Biol Chem, 1990. **265**(33): p. 20241-6.
162. Erwig, L.P., et al., *Initial cytokine exposure determines function of macrophages and renders them unresponsive to other cytokines*. J Immunol, 1998. **161**(4): p. 1983-8.
163. MacMicking, J., Q.W. Xie, and C. Nathan, *Nitric oxide and macrophage function*. Annu Rev Immunol, 1997. **15**: p. 323-50.
164. Erbe, D.V., et al., *The effect of cytokines on the expression and function of Fc receptors for IgG on human myeloid cells*. Mol Immunol, 1990. **27**(1): p. 57-67.
165. Ellis, T.N. and B.L. Beaman, *Interferon-gamma activation of polymorphonuclear neutrophil function*. Immunology, 2004. **112**(1): p. 2-12.
166. Cho, J.S., et al., *IL-17 is essential for host defense against cutaneous Staphylococcus aureus infection in mice*. J Clin Invest, 2010. **120**(5): p. 1762-73.
167. Zhao, Y.X., I.M. Nilsson, and A. Tarkowski, *The dual role of interferon-gamma in experimental Staphylococcus aureus septicaemia versus arthritis*. Immunology, 1998. **93**(1): p. 80-5.
168. Hirota, K., et al., *Plasticity of Th17 cells in Peyer's patches is responsible for the induction of T cell-dependent IgA responses*. Nat Immunol, 2013. **14**(4): p. 372-9.
169. Bettelli, E., et al., *Reciprocal developmental pathways for the generation of pathogenic effector TH17 and regulatory T cells*. Nature, 2006. **441**(7090): p. 235-8.
170. Harrington, L.E., et al., *Interleukin 17-producing CD4+ effector T cells develop via a lineage distinct from the T helper type 1 and 2 lineages*. Nat Immunol, 2005. **6**(11): p. 1123-32.

171. Wei, L., et al., *IL-21 is produced by Th17 cells and drives IL-17 production in a STAT3-dependent manner*. J Biol Chem, 2007. **282**(48): p. 34605-10.
172. Zhou, L., et al., *IL-6 programs T(H)-17 cell differentiation by promoting sequential engagement of the IL-21 and IL-23 pathways*. Nat Immunol, 2007. **8**(9): p. 967-74.
173. Andreassen, C., D.A. Powell, and N.H. Carbonetti, *Pertussis toxin stimulates IL-17 production in response to Bordetella pertussis infection in mice*. PLoS One, 2009. **4**(9): p. e7079.
174. Fossiez, F., et al., *T cell interleukin-17 induces stromal cells to produce proinflammatory and hematopoietic cytokines*. J Exp Med, 1996. **183**(6): p. 2593-603.
175. Schwarzenberger, P., et al., *Requirement of endogenous stem cell factor and granulocyte-colony-stimulating factor for IL-17-mediated granulopoiesis*. J Immunol, 2000. **164**(9): p. 4783-9.
176. Ye, P., et al., *Interleukin-17 and lung host defense against Klebsiella pneumoniae infection*. Am J Respir Cell Mol Biol, 2001. **25**(3): p. 335-40.
177. Albanesi, C., A. Cavani, and G. Girolomoni, *IL-17 is produced by nickel-specific T lymphocytes and regulates ICAM-1 expression and chemokine production in human keratinocytes: synergistic or antagonist effects with IFN-gamma and TNF-alpha*. J Immunol, 1999. **162**(1): p. 494-502.
178. Lu, Y.J., et al., *Interleukin-17A mediates acquired immunity to pneumococcal colonization*. PLoS Pathog, 2008. **4**(9): p. e1000159.
179. Kao, C.Y., et al., *IL-17 markedly up-regulates beta-defensin-2 expression in human airway epithelium via JAK and NF-kappaB signaling pathways*. J Immunol, 2004. **173**(5): p. 3482-91.
180. Liang, S.C., et al., *Interleukin (IL)-22 and IL-17 are coexpressed by Th17 cells and cooperatively enhance expression of antimicrobial peptides*. J Exp Med, 2006. **203**(10): p. 2271-9.
181. Holland, S.M., et al., *STAT3 mutations in the hyper-IgE syndrome*. N Engl J Med, 2007. **357**(16): p. 1608-19.
182. Milner, J.D., et al., *Impaired T(H)17 cell differentiation in subjects with autosomal dominant hyper-IgE syndrome*. Nature, 2008. **452**(7188): p. 773-6.
183. Ishigame, H., et al., *Differential roles of interleukin-17A and -17F in host defense against mucoepithelial bacterial infection and allergic responses*. Immunity, 2009. **30**(1): p. 108-19.
184. Maher, B.M., et al., *Nlrp-3-driven interleukin 17 production by gammadeltaT cells controls infection outcomes during Staphylococcus aureus surgical site infection*. Infect Immun, 2013. **81**(12): p. 4478-89.
185. Duhon, T., et al., *Production of interleukin 22 but not interleukin 17 by a subset of human skin-homing memory T cells*. Nat Immunol, 2009. **10**(8): p. 857-63.
186. Trifari, S., et al., *Identification of a human helper T cell population that has abundant production of interleukin 22 and is distinct from T(H)-17, T(H)1 and T(H)2 cells*. Nat Immunol, 2009. **10**(8): p. 864-71.
187. Aujla, S.J., et al., *IL-22 mediates mucosal host defense against Gram-negative bacterial pneumonia*. Nat Med, 2008. **14**(3): p. 275-81.
188. Zheng, Y., et al., *Interleukin-22 mediates early host defense against attaching and effacing bacterial pathogens*. Nat Med, 2008. **14**(3): p. 282-9.
189. Boniface, K., et al., *IL-22 inhibits epidermal differentiation and induces proinflammatory gene expression and migration of human keratinocytes*. J Immunol, 2005. **174**(6): p. 3695-702.
190. Eyerich, S., et al., *Th22 cells represent a distinct human T cell subset involved in epidermal immunity and remodeling*. J Clin Invest, 2009. **119**(12): p. 3573-85.

191. Gauguet, S., et al., *Intestinal Microbiota of Mice Influences Resistance to Staphylococcus aureus Pneumonia*. *Infect Immun*, 2015. **83**(10): p. 4003-14.
192. Chan, L.C., et al., *Non-Redundant Roles of IL-17A and IL-22 in Murine Host Defense Against Cutaneous and Hematogenous Infection Due to Methicillin-Resistant Staphylococcus aureus*. *Infect Immun*, 2015.
193. Murphy, A.G., et al., *Staphylococcus aureus infection of mice expands a population of memory gammadelta T cells that are protective against subsequent infection*. *J Immunol*, 2014. **192**(8): p. 3697-708.
194. Malhotra, N., et al., *IL-22 derived from gammadelta T cells restricts Staphylococcus aureus infection of mechanically injured skin*. *J Allergy Clin Immunol*, 2016. **138**(4): p. 1098-1107.e3.
195. Garzoni, C. and W.L. Kelley, *Staphylococcus aureus: new evidence for intracellular persistence*. *Trends Microbiol*, 2009. **17**(2): p. 59-65.
196. Koziel, J., et al., *Phagocytosis of Staphylococcus aureus by macrophages exerts cytoprotective effects manifested by the upregulation of antiapoptotic factors*. *PLoS One*, 2009. **4**(4): p. e5210.
197. Kubica, M., et al., *A potential new pathway for Staphylococcus aureus dissemination: the silent survival of S. aureus phagocytosed by human monocyte-derived macrophages*. *PLoS One*, 2008. **3**(1): p. e1409.
198. O'Keefe, K.M., et al., *Manipulation of Autophagy in Phagocytes Facilitates Staphylococcus aureus Bloodstream Infection*. *Infect Immun*, 2015. **83**(9): p. 3445-57.
199. Manz, R.A., et al., *Maintenance of serum antibody levels*. *Annu Rev Immunol*, 2005. **23**: p. 367-86.
200. Plotkin, S.A., *Vaccines: past, present and future*. *Nat Med*, 2005. **11**(4 Suppl): p. S5-11.
201. Greco, D., et al., *A controlled trial of two acellular vaccines and one whole-cell vaccine against pertussis. Progetto Pertosse Working Group*. *N Engl J Med*, 1996. **334**(6): p. 341-8.
202. Girard, M.P., et al., *A review of vaccine research and development: meningococcal disease*. *Vaccine*, 2006. **24**(22): p. 4692-700.
203. Posfay-Barbe, K.M. and E.R. Wald, *Pneumococcal vaccines: do they prevent infection and how?* *Curr Opin Infect Dis*, 2004. **17**(3): p. 177-84.
204. Pizza, M., et al., *Identification of vaccine candidates against serogroup B meningococcus by whole-genome sequencing*. *Science*, 2000. **287**(5459): p. 1816-20.
205. Daum, R.S. and B. Spellberg, *Progress toward a Staphylococcus aureus vaccine*. *Clin Infect Dis*, 2012. **54**(4): p. 560-7.
206. Hiramatsu, K., *Vancomycin-resistant Staphylococcus aureus: a new model of antibiotic resistance*. *Lancet Infect Dis*, 2001. **1**(3): p. 147-55.
207. Sanchez Garcia, M., et al., *Clinical outbreak of linezolid-resistant Staphylococcus aureus in an intensive care unit*. *JAMA*, 2010. **303**(22): p. 2260-4.
208. Marty, F.M., et al., *Emergence of a clinical daptomycin-resistant Staphylococcus aureus isolate during treatment of methicillin-resistant Staphylococcus aureus bacteremia and osteomyelitis*. *J Clin Microbiol*, 2006. **44**(2): p. 595-7.
209. Fattom, A., et al., *Safety and immunogenicity of a booster dose of Staphylococcus aureus types 5 and 8 capsular polysaccharide conjugate vaccine (StaphVAX) in hemodialysis patients*. *Vaccine*, 2004. **23**(5): p. 656-63.
210. Release, P., *Nabi pharmaceuticals announces the results of StaphVAX(R) confirmatory phase III clinical trial*<http://www.prnewswire.com/news-releases/nabi-biopharmaceuticals-announces-results-of-staphvaxr-confirmatory-phase-iii-clinical-trial-55039197.html>. 2005

211. Trivier, D., et al., *Influence of iron depletion on growth kinetics, siderophore production, and protein expression of Staphylococcus aureus*. FEMS Microbiol Lett, 1995. **127**(3): p. 195-9.
212. Kuklin, N.A., et al., *A novel Staphylococcus aureus vaccine: iron surface determinant B induces rapid antibody responses in rhesus macaques and specific increased survival in a murine S. aureus sepsis model*. Infect Immun, 2006. **74**(4): p. 2215-23.
213. Harro, C., et al., *Safety and immunogenicity of a novel Staphylococcus aureus vaccine: results from the first study of the vaccine dose range in humans*. Clin Vaccine Immunol, 2010. **17**(12): p. 1868-74.
214. Inc, I., *Inhibtiex reports favourable results from Aurexis phase II trial for the treatment of staphylococcal bloodstream infections*. 2005.
215. Release, P., *PR Newswire. Inhibitiex Reports Top-Line Results in Phase III Study of Veronate(R)*. <http://www.prnewswire.com/cgi-bin/stories.pl?ACCT=104&STORY=/www/story/04-03-2006/0004331599&EDATE=>. April 3, 2006
216. Weisman, L.E., *Antibody for the prevention of neonatal nosocomial staphylococcal infection: a review of the literature*. Arch Pediatr, 2007. **14 Suppl 1**: p. S31-4.
217. Creech, C.B., 2nd, et al., *Vaccination as infection control: a pilot study to determine the impact of Staphylococcus aureus vaccination on nasal carriage*. Vaccine, 2009. **28**(1): p. 256-60.
218. Prevaes, S.M., et al., *Nasopharyngeal colonization elicits antibody responses to staphylococcal and pneumococcal proteins that are not associated with a reduced risk of subsequent carriage*. Infect Immun, 2012. **80**(6): p. 2186-93.
219. Proctor, R.A., *Challenges for a universal Staphylococcus aureus vaccine*. Clin Infect Dis, 2012. **54**(8): p. 1179-86.
220. Fowler, V.G., Jr. and R.A. Proctor, *Where does a Staphylococcus aureus vaccine stand?* Clin Microbiol Infect, 2014. **20 Suppl 5**: p. 66-75.
221. Zhao, Y.X., I.M. Nilsson, and A. Tarkowski, *The dual role of interferon-gamma in experimental Staphylococcus aureus septicaemia versus arthritis*. Immunology, 1998. **93**(1): p. 80-5.
222. Misstear, K., et al., *Targeted nasal vaccination provides antibody-independent protection against Staphylococcus aureus*. J Infect Dis, 2014. **209**(9): p. 1479-84.
223. Lin, L., et al., *Th1-Th17 cells mediate protective adaptive immunity against Staphylococcus aureus and Candida albicans infection in mice*. PLoS Pathog, 2009. **5**(12): p. e1000703.
224. Pier, G.B., *Will there ever be a universal Staphylococcus aureus vaccine?* Hum Vaccin Immunother, 2013. **9**(9): p. 1865-76.
225. Miller, L.S. and J.S. Cho, *Immunity against Staphylococcus aureus cutaneous infections*. Nat Rev Immunol, 2011. **11**(8): p. 505-18.
226. Yeaman, M.R., et al., *Mechanisms of NDV-3 vaccine efficacy in MRSA skin versus invasive infection*. Proc Natl Acad Sci U S A, 2014. **111**(51): p. E5555-63.
227. Krishna, S. and L.S. Miller, *Host-pathogen interactions between the skin and Staphylococcus aureus*. Curr Opin Microbiol, 2012. **15**(1): p. 28-35.
228. Nestle, F.O., et al., *Skin immune sentinels in health and disease*. Nat Rev Immunol, 2009. **9**(10): p. 679-91.
229. Candi, E., R. Schmidt, and G. Melino, *The cornified envelope: a model of cell death in the skin*. Nat Rev Mol Cell Biol, 2005. **6**(4): p. 328-40.
230. Moran, G.J., et al., *Acute Bacterial Skin Infections: Developments Since the 2005 Infectious Diseases Society of America (IDSA) Guidelines*. The Journal of Emergency Medicine, 2013. **44**(6): p. e397-e412.

231. Kupper, T.S. and R.C. Fuhlbrigge, *Immune surveillance in the skin: mechanisms and clinical consequences*. Nat Rev Immunol, 2004. **4**(3): p. 211-22.
232. Miller, L.S., *Toll-like receptors in skin*. Adv Dermatol, 2008. **24**: p. 71-87.
233. von Bernuth, H., et al., *Pyogenic bacterial infections in humans with MyD88 deficiency*. Science, 2008. **321**(5889): p. 691-6.
234. Picard, C., et al., *Pyogenic bacterial infections in humans with IRAK-4 deficiency*. Science, 2003. **299**(5615): p. 2076-9.
235. Miller, L.S., et al., *MyD88 mediates neutrophil recruitment initiated by IL-1R but not TLR2 activation in immunity against Staphylococcus aureus*. Immunity, 2006. **24**(1): p. 79-91.
236. Ku, C.L., et al., *Selective predisposition to bacterial infections in IRAK-4-deficient children: IRAK-4-dependent TLRs are otherwise redundant in protective immunity*. J Exp Med, 2007. **204**(10): p. 2407-22.
237. Cua, D.J. and C.M. Tato, *Innate IL-17-producing cells: the sentinels of the immune system*. Nat Rev Immunol, 2010. **10**(7): p. 479-89.
238. Korn, T., et al., *IL-17 and Th17 Cells*. Annu Rev Immunol, 2009. **27**: p. 485-517.
239. Li, M.Z. and S.J. Elledge, *SLIC: a method for sequence- and ligation-independent cloning*. Methods Mol Biol, 2012. **852**: p. 51-9.
240. Monk, I.R., et al., *Transforming the untransformable: application of direct transformation to manipulate genetically Staphylococcus aureus and Staphylococcus epidermidis*. MBio, 2012. **3**(2).
241. Lofblom, J., et al., *Optimization of electroporation-mediated transformation: Staphylococcus carnosus as model organism*. J Appl Microbiol, 2007. **102**(3): p. 736-47.
242. Monk, I.R., et al., *Transforming the untransformable: application of direct transformation to manipulate genetically Staphylococcus aureus and Staphylococcus epidermidis*. MBio, 2012. **3**(2): p. e00277-11.
243. Novick, R.P., *Genetic systems in staphylococci*. Methods Enzymol, 1991. **204**: p. 587-636.
244. Mazmanian, S.K., et al., *Staphylococcus aureus sortase mutants defective in the display of surface proteins and in the pathogenesis of animal infections*. Proceedings of the National Academy of Sciences of the United States of America, 2000. **97**(10): p. 5510-5515.
245. Bramley, A.J., et al., *Roles of alpha-toxin and beta-toxin in virulence of Staphylococcus aureus for the mouse mammary gland*. Infect Immun, 1989. **57**(8): p. 2489-94.
246. Richardson, M.P., et al., *A simple flow cytometry assay using dihydrorhodamine for the measurement of the neutrophil respiratory burst in whole blood: comparison with the quantitative nitrobluetetrazolium test*. J Immunol Methods, 1998. **219**(1-2): p. 187-93.
247. Diep, B.A., et al., *Complete genome sequence of USA300, an epidemic clone of community-acquired methicillin-resistant Staphylococcus aureus*. Lancet, 2006. **367**(9512): p. 731-9.
248. Thurlow, L.R., et al., *Staphylococcus aureus biofilms prevent macrophage phagocytosis and attenuate inflammation in vivo*. J Immunol, 2011. **186**(11): p. 6585-96.
249. Kreiswirth, B.N., et al., *The toxic shock syndrome exotoxin structural gene is not detectably transmitted by a prophage*. Nature, 1983. **305**(5936): p. 709-12.
250. Tzianabos, A.O., J.Y. Wang, and J.C. Lee, *Structural rationale for the modulation of abscess formation by Staphylococcus aureus capsular polysaccharides*. Proc Natl Acad Sci U S A, 2001. **98**(16): p. 9365-70.

251. Monk, I.R. and T.J. Foster, *Genetic manipulation of Staphylococci-breaking through the barrier*. Front Cell Infect Microbiol, 2012. **2**: p. 49.
252. Monk, I.R., et al., *Complete Bypass of Restriction Systems for Major Staphylococcus aureus Lineages*. MBio, 2015. **6**(3): p. e00308-15.
253. Dajcs, J.J., et al., *Corneal Pathogenesis of Staphylococcus aureus Strain Newman*. Investigative Ophthalmology & Visual Science, 2002. **43**(4): p. 1109-1115.
254. Horinouchi, S. and B. Weisblum, *Nucleotide sequence and functional map of pC194, a plasmid that specifies inducible chloramphenicol resistance*. J Bacteriol, 1982. **150**(2): p. 815-25.
255. Khan, S.A. and R.P. Novick, *Complete nucleotide sequence of pT181, a tetracycline-resistance plasmid from Staphylococcus aureus*. Plasmid, 1983. **10**(3): p. 251-9.
256. Biswas, I., et al., *High-efficiency gene inactivation and replacement system for gram-positive bacteria*. J Bacteriol, 1993. **175**(11): p. 3628-35.
257. Bae, T. and O. Schneewind, *Allelic replacement in Staphylococcus aureus with inducible counter-selection*. Plasmid, 2006. **55**(1): p. 58-63.
258. Manting, E.H. and A.J. Driessen, *Escherichia coli translocase: the unravelling of a molecular machine*. Mol Microbiol, 2000. **37**(2): p. 226-38.
259. Ji, Y., et al., *Identification of critical staphylococcal genes using conditional phenotypes generated by antisense RNA*. Science, 2001. **293**(5538): p. 2266-9.
260. Monk, I.R., et al., *Development of multiple strain competitive index assays for Listeria monocytogenes using pIMC; a new site-specific integrative vector*. BMC Microbiol, 2008. **8**: p. 96.
261. Maguin, E., et al., *New thermosensitive plasmid for gram-positive bacteria*. J Bacteriol, 1992. **174**(17): p. 5633-8.
262. Corvaglia, A.R., et al., *A type III-like restriction endonuclease functions as a major barrier to horizontal gene transfer in clinical Staphylococcus aureus strains*. Proc Natl Acad Sci U S A, 2010. **107**(26): p. 11954-8.
263. Veiga, H. and M.G. Pinho, *Inactivation of the Saul type I restriction-modification system is not sufficient to generate Staphylococcus aureus strains capable of efficiently accepting foreign DNA*. Appl Environ Microbiol, 2009. **75**(10): p. 3034-8.
264. Waldron, D.E. and J.A. Lindsay, *Sau1: a novel lineage-specific type I restriction-modification system that blocks horizontal gene transfer into Staphylococcus aureus and between S. aureus isolates of different lineages*. J Bacteriol, 2006. **188**(15): p. 5578-85.
265. Xu, S.Y., et al., *A type IV modification-dependent restriction enzyme SauUSI from Staphylococcus aureus subsp. aureus USA300*. Nucleic Acids Res, 2011. **39**(13): p. 5597-610.
266. Traber, K. and R. Novick, *A slipped-mispairing mutation in AgrA of laboratory strains and clinical isolates results in delayed activation of agr and failure to translate delta- and alpha-haemolysins*. Mol Microbiol, 2006. **59**(5): p. 1519-30.
267. Traber, K.E., et al., *agr function in clinical Staphylococcus aureus isolates*. Microbiology, 2008. **154**(Pt 8): p. 2265-74.
268. Tegmark, K., A. Karlsson, and S. Arvidson, *Identification and characterization of SarH1, a new global regulator of virulence gene expression in Staphylococcus aureus*. Mol Microbiol, 2000. **37**(2): p. 398-409.
269. Berube, B.J. and J. Bubeck Wardenburg, *Staphylococcus aureus alpha-toxin: nearly a century of intrigue*. Toxins (Basel), 2013. **5**(6): p. 1140-66.
270. Novick, R.P., et al., *The agr P2 operon: an autocatalytic sensory transduction system in Staphylococcus aureus*. Mol Gen Genet, 1995. **248**(4): p. 446-58.

271. Novick, R.P., et al., *Synthesis of staphylococcal virulence factors is controlled by a regulatory RNA molecule*. EMBO J, 1993. **12**(10): p. 3967-75.
272. Kolata, J.B., et al., *The Fall of a Dogma? Unexpected High T-Cell Memory Response to Staphylococcus aureus in Humans*. J Infect Dis, 2015. **212**(5): p. 830-8.
273. Kalka-Moll, W.M., et al., *Zwitterionic polysaccharides stimulate T cells by MHC class II-dependent interactions*. J Immunol, 2002. **169**(11): p. 6149-53.
274. Weidenmaier, C., R.M. McLoughlin, and J.C. Lee, *The zwitterionic cell wall teichoic acid of Staphylococcus aureus provokes skin abscesses in mice by a novel CD4+ T-cell-dependent mechanism*. PLoS One, 2010. **5**(10): p. e13227.
275. McLoughlin, R.M., et al., *CD4+ T cells and CXC chemokines modulate the pathogenesis of Staphylococcus aureus wound infections*. Proc Natl Acad Sci U S A, 2006. **103**(27): p. 10408-13.
276. Hawkins, J., et al., *A recombinant clumping factor A-containing vaccine induces functional antibodies to Staphylococcus aureus that are not observed after natural exposure*. Clin Vaccine Immunol, 2012. **19**(10): p. 1641-50.
277. Li, X., et al., *Preclinical Efficacy of Clumping Factor A in Prevention of Staphylococcus aureus Infection*. MBio, 2016. **7**(1): p. e02232-15.
278. Veloso, T.R., et al., *Vaccination against Staphylococcus aureus experimental endocarditis using recombinant Lactococcus lactis expressing ClfA or FnbpA*. Vaccine, 2015. **33**(30): p. 3512-7.
279. Begier, E., et al., *SA4Ag, a 4-antigen Staphylococcus aureus vaccine, rapidly induces high levels of bacteria-killing antibodies*. Vaccine, 2017. **35**(8): p. 1132-1139.
280. Frenck, R.W., Jr., et al., *Safety, tolerability, and immunogenicity of a 4-antigen Staphylococcus aureus vaccine (SA4Ag): Results from a first-in-human randomised, placebo-controlled phase 1/2 study*. Vaccine, 2017. **35**(2): p. 375-384.
281. Levy, J., et al., *Safety and immunogenicity of an investigational 4-component Staphylococcus aureus vaccine with or without AS03B adjuvant: Results of a randomized phase I trial*. Hum Vaccin Immunother, 2015. **11**(3): p. 620-31.
282. Monaci, E., et al., *MF59- and Al(OH)₃-Adjuvanted Staphylococcus aureus (4C-Staph) Vaccines Induce Sustained Protective Humoral and Cellular Immune Responses, with a Critical Role for Effector CD4 T Cells at Low Antibody Titers*. Front Immunol, 2015. **6**: p. 439.
283. Nissen, M., et al., *A randomized phase I study of the safety and immunogenicity of three ascending dose levels of a 3-antigen Staphylococcus aureus vaccine (SA3Ag) in healthy adults*. Vaccine, 2015. **33**(15): p. 1846-1854.
284. Creech, C.B., et al., *Safety, tolerability, and immunogenicity of a single dose 4-antigen or 3-antigen Staphylococcus aureus vaccine in healthy older adults: Results of a randomised trial*. Vaccine, 2017. **35**(2): p. 385-394.
285. Schmidt, C.S., et al., *NDV-3, a recombinant alum-adjuvanted vaccine for Candida and Staphylococcus aureus, is safe and immunogenic in healthy adults*. Vaccine, 2012. **30**(52): p. 7594-600.
286. Hemmi, H., et al., *A Toll-like receptor recognizes bacterial DNA*. Nature, 2000. **408**(6813): p. 740-5.
287. Ross, P.J., et al., *Relative contribution of Th1 and Th17 cells in adaptive immunity to Bordetella pertussis: towards the rational design of an improved acellular pertussis vaccine*. PLoS Pathog, 2013. **9**(4): p. e1003264.
288. Reimer, L.G., M.L. Wilson, and M.P. Weinstein, *Update on detection of bacteremia and fungemia*. Clinical Microbiology Reviews, 1997. **10**(3): p. 444-465.

289. Beeson, P.B., E.S. Brannon, and J.V. Warren, *OBSERVATIONS ON THE SITES OF REMOVAL OF BACTERIA FROM THE BLOOD IN PATIENTS WITH BACTERIAL ENDOCARDITIS*. J Exp Med, 1945. **81**(1): p. 9-23.
290. Mori, A., et al., *The vaccine adjuvant alum inhibits IL-12 by promoting PI3 kinase signaling while chitosan does not inhibit IL-12 and enhances Th1 and Th17 responses*. Eur J Immunol, 2012. **42**(10): p. 2709-19.
291. Hsu, S.C., et al., *Mesenchymal stem cells promote neutrophil activation by inducing IL-17 production in CD4+ CD45RO+ T cells*. Immunobiology, 2013. **218**(1): p. 90-5.
292. Molne, L., M. Verdrengh, and A. Tarkowski, *Role of neutrophil leukocytes in cutaneous infection caused by Staphylococcus aureus*. Infect Immun, 2000. **68**(11): p. 6162-7.
293. Tkaczyk, C., et al., *Staphylococcus aureus alpha toxin suppresses effective innate and adaptive immune responses in a murine dermonecrosis model*. PLoS One, 2013. **8**(10): p. e75103.
294. Lopez, O., et al., *New arrangement of proteins and lipids in the stratum corneum cornified envelope*. Biochim Biophys Acta, 2007. **1768**(3): p. 521-9.
295. Mehrel, T., et al., *Identification of a major keratinocyte cell envelope protein, loricrin*. Cell, 1990. **61**(6): p. 1103-12.
296. Escámez, M.J., et al., *An In Vivo Model of Wound Healing in Genetically Modified Skin-Humanized Mice*. Journal of Investigative Dermatology, 2004. **123**(6): p. 1182-1191.
297. Inada, R., et al., *Facilitated wound healing by activation of the Transglutaminase 1 gene*. Am J Pathol, 2000. **157**(6): p. 1875-82.
298. Stranger-Jones, Y.K., T. Bae, and O. Schneewind, *Vaccine assembly from surface proteins of Staphylococcus aureus*. Proc Natl Acad Sci U S A, 2006. **103**(45): p. 16942-7.
299. Lacey, K.A., et al., *The Staphylococcus aureus cell wall-anchored protein clumping factor A is an important T cell antigen*. Infect Immun, 2017.
300. Lee, S. and M.T. Nguyen, *Recent Advances of Vaccine Adjuvants for Infectious Diseases*. Immune Network, 2015. **15**(2): p. 51-57.
301. Suaya, J.A., et al., *Incidence and cost of hospitalizations associated with Staphylococcus aureus skin and soft tissue infections in the United States from 2001 through 2009*. BMC Infectious Diseases, 2014. **14**: p. 296-296.
302. Li Pira, G., et al., *High throughput T epitope mapping and vaccine development*. J Biomed Biotechnol, 2010. **2010**: p. 325720.
303. Barker, C.J., et al., *In silico identification and in vivo analysis of a novel T-cell antigen from Chlamydia, NrdB*. Vaccine, 2008. **26**(10): p. 1285-96.
304. De Groot, A.S., et al., *HIV vaccine development by computer assisted design: the GAIA vaccine*. Vaccine, 2005. **23**(17-18): p. 2136-48.
305. Rosa, D.S., S.P. Ribeiro, and E. Cunha-Neto, *CD4+ T cell epitope discovery and rational vaccine design*. Arch Immunol Ther Exp (Warsz), 2010. **58**(2): p. 121-30.
306. Rosa, D.S., et al., *Immunogenicity of a recombinant protein containing the Plasmodium vivax vaccine candidate MSP119 and two human CD4+ T-cell epitopes administered to non-human primates (Callithrix jacchus jacchus)*. Microbes and Infection, 2006. **8**(8): p. 2130-2137.
307. Garcia, T.C., et al., *Peptides containing T cell epitopes, derived from Sm14, but not from paramyosin, induce a Th1 type of immune response, reduction in liver pathology and partial protection against Schistosoma mansoni infection in mice*. Acta Trop, 2008. **106**(3): p. 162-7.
308. Oprea, M. and F. Antohe, *Reverse-vaccinology strategy for designing T-cell epitope candidates for Staphylococcus aureus endocarditis vaccine*. Biologicals, 2013. **41**(3): p. 148-53.

309. Zhang, B.Z., et al., *Immunotherapy Targeting Adenosine Synthase A Decreases Severity of Staphylococcus aureus Infection in Mouse Model*. J Infect Dis, 2017. **216**(2): p. 245-253.
310. Liu, Q., et al., *Targeting surface protein SasX by active and passive vaccination to reduce Staphylococcus aureus colonization and infection*. Infect Immun, 2015. **83**(5): p. 2168-74.
311. Montgomery, C.P., et al., *Protective immunity against recurrent Staphylococcus aureus skin infection requires antibody and interleukin-17A*. Infect Immun, 2014. **82**(5): p. 2125-34.
312. Gebhardt, T., et al., *Memory T cells in nonlymphoid tissue that provide enhanced local immunity during infection with herpes simplex virus*. Nat Immunol, 2009. **10**(5): p. 524-30.
313. Gebhardt, T., et al., *Different patterns of peripheral migration by memory CD4+ and CD8+ T cells*. Nature, 2011. **477**(7363): p. 216-9.
314. Clark, R.A., et al., *Skin effector memory T cells do not recirculate and provide immune protection in alemtuzumab-treated CTCL patients*. Sci Transl Med, 2012. **4**(117): p. 117ra7.
315. Ariotti, S., et al., *T cell memory. Skin-resident memory CD8(+) T cells trigger a state of tissue-wide pathogen alert*. Science, 2014. **346**(6205): p. 101-5.
316. Wilk, M.M., et al., *Lung CD4 Tissue-Resident Memory T Cells Mediate Adaptive Immunity Induced by Previous Infection of Mice with Bordetella pertussis*. J Immunol, 2017. **199**(1): p. 233-243.
317. Hansen, S.G., et al., *Profound early control of highly pathogenic SIV by an effector memory T-cell vaccine*. Nature, 2011. **473**(7348): p. 523-7.
318. Iijima, N. and A. Iwasaki, *T cell memory. A local macrophage chemokine network sustains protective tissue-resident memory CD4 T cells*. Science, 2014. **346**(6205): p. 93-8.
319. Ishizuka, A.S., et al., *Protection against malaria at 1 year and immune correlates following PfSPZ vaccination*. Nat Med, 2016. **22**(6): p. 614-23.